Universidade de Brasília

Instituto de Geociências

Proveniência de sedimentos dos grupos Canastra, Ibiá, Vazante e Bambuí – Um estudo de zircões detríticos e Idades Modelo Sm-Nd

Joseneusa Brilhante Rodrigues

Tese de Doutorado

Nº 90

2008

Joseneusa Brilhante Rodrigues

Proveniência de sedimentos dos grupos Canastra, Ibiá, Vazante e Bambuí – Um estudo de zircões detríticos e Idades Modelo Sm-Nd

Banca Examinadora:

Márcio Martins Pimentel – UnB

(orientador)

Roberto Ventura Santos – UnB

Luiz Carlos da Silva – UnB/CPRM

Aroldo Misi – UFBA

Marli Babinski – USP

Reinhardt Adolfo Fuck – UnB (suplente)

À meus pais, filhos e marido.

AGRADECIMENTOS

Várias instituições e pessoas contribuíram de forma significativa para o desenvolvimento e conclusão desta tese. Assim gostaria de agradecer:

- À compreensão e carinho de minha família;

- À CPRM pelo incentivo, principalmente na pessoa de meu chefe imediato, Luiz Carlos da Silva e nos meus colegas e amigos Thiers, Jaime e Mylène;

- Ao Instituto de Geociências pela acolhida e apoio;

- Ao CNPq pelo indispensável apoio financeiro;

- Ao Laboratório de Geocronologia da Universidade de Brasília, que nos últimos tempos tornou-se meu segundo lar;

- À Companhia Mineira de Metais pelo grande apoio nas etapas de campo;

- À meu orientador pelo apoio nos momentos em que foi necessário nortear meu caminho, palavras de incentivo e pela grande paciência...

- Às amigas químicas, Bárbara, Jeanne, Sandrine e Hariadne, pela imensa ajuda durante as análises;

- Aos amigos do laboratório Sérgio, Emília, Natália, Cristiano, Dani, Mari, Carol, Denílson, Jaqueline, Alcino e Anderson;

- Aos professores que sempre se mostraram dispostos a ajudar, em especial Elton, Mássimo, Benhard e Fuck;

- Aos queridos motoristas Zilberto e Correia;

- Enfim, a todos aqueles que de alguma forma contribuíram na construção do trabalho, meu obrigado...

Índice

Índice de Figuras

Índice de Tabelas

RESUMO

Esta tese visa investigar a origem dos detritos dos grupos Canastra, Vazante, Ibiá e Bambuí além da Formação Jequitaí. Análises integradas de U-Pb em zircões detríticos via SHRIMP e LAM-ICP-MS e Sm-Nd em rocha total permitiram determinar limites deposicionais, indicar possíveis fontes de sedimentos e fornecer elementos para interpretações tectônicas.

O Grupo Canastra constitui uma seqüência regressiva de margem passiva, composta principalmente por rochas metapelíticas e metapsamíticas metamorfizadas em fácies xisto verde incluindo filito, metarritmito, quartzito e restritas intercalações de calcário e filito carbonático. O Grupo Vazante representa uma seqüência detrito-carbonática constituída principalmente por quartzitos, ardósias, conglomerado, siltito e dolomitos estromatolíticos. O Grupo Ibiá apresenta localmente um diamictito basal recoberto por filitos e calci-xistos, que são os principais constituintes do grupo. A Formação Jequitaí é uma unidade glacial, representada principalmente por diamictitos, que ocorre cobrindo vastas áreas do Cráton São Francisco e com algumas exposições na Faixa Brasília. Suas rochas são recobertas por carbonatos do Grupo Bambuí, o qual representa uma seqüência carbonática-siliciclástica com crescente componente detrítico para o topo.

Os dados U-Pb em zircão permitiram identificar as populações ou grãos detríticos mais jovens das unidades e estabelecer os limites máximos para deposição que são de 1030, 935, 640, 880 e 610 Ma para os Grupos Canastra, Vazante, Ibiá, Formação Jequitaí e Grupo Bambuí, respectivamente.

De maneira geral foi observada pouca contribuição de terrenos arqueanos nos sedimentos estudados. O Cráton São Francisco-Congo revelou-se um importante fornecedor de detritos, especialmente para os grupos Canastra e Vazante. Já os dados dos grupos Ibiá e Bambuí evidenciaram a considerável presença de rochas da Faixa Brasília no suprimento de sedimentos. Dentre as amostras analisadas para U-Pb, somente as do Grupo Canastra não apresentaram grãos Neoproterozóicos.

O espectro de idades dos grãos detríticos apresentados pelo Grupo Canastra inclui um largo intervalo de idades (1030-2996 Ma), com significativo componente Paleoproterozóico (~1,8 e ~2,1 Ga) e uma importante fonte Mesoproterozóica (1,1-1,2 Ga) para a Formação Paracatu. Estes resultados associados aos dados Sm-Nd, que forneceram T_{DM} superiores a 1,9 Ga, são consistentes com o ambiente de uma margem continental passiva para o Grupo Canastra.

As formações do Grupo Vazante forneceram padrões variados de idade U-Pb de zircões detríticos em um intervalo de 935 a 3520 Ma, porém de maneira geral terrenos de ~2,1 Ga constituem a principal fonte de sedimentos de boa parte das formações. A população mais jovem (~950 Ma) ocorre apenas nas unidades basais do Grupo Vazante, sugerindo que esta fonte foi isolada ou recoberta durante a evolução da bacia. No entanto, dados Sm-Nd revelam a participação de terrenos jovens em praticamente em todo o grupo, em especial na Formação Lapa (T_{DM} de 1,67 a 2,00 Ga). A Formação Serra do Garrote apresentou predominância de fontes Paleoproterozóicas, tanto nas análises Sm-Nd como nas U-Pb. O topo do grupo é marcado por uma significativa mudança de fontes. Nas formações Morro do Calcário e Lapa um forte pico de idades entre 1,1-1,2 Ga representa a principal fonte, seguido por pequenas contribuições Paleoproterozóicas. Terrenos do Cráton São Francisco-Congo são considerados as principais fontes dos sedimentos do Grupo Vazante, que pode ser interpretado como uma seqüência associada a uma margem continental passiva. Os dados Sm-Nd da Formação Lapa não são totalmente compatíveis com esta interpretação e podem indicar a aproximação de terrenos significativamente mais jovens, tais como o Arco Magmático de Goiás.

Os zircões do diamictito do Grupo Ibiá apresentaram idades entre 936 e 2500 Ma. Em contraste, os calcifilitos que sobrepõem os diamictitos revelam a dominante proveniência de fontes Neoproterozóicas, com importantes picos em 665, 740 e 850 Ma. Os dados Sm-Nd apresentam comportamento bimodal, com intervalos de T_{DM} de 1,16-1,46 e 1,58-2.01 Ga.

Terrenos do Cráton São Franciso e Arco Magmático de Goiás são as mais prováveis fontes do grupo, que possivelmente representa uma seqüência do tipo *fore-arc*.

A distribuição de idades dos zircões detríticos dos diamictitos da Formação Jequitaí indicam fontes Paleoproterozóicas dominantes (2,0-2,2 Ga) assim como fontes Mesoproterozóicas e Neoproterozóicas (~880 Ma). Estes dados sugerem detritos provavelmente derivados dos Cráton São Francisco-Congo. Os dados Sm-Nd e U-Pb de grãos detríticos do Grupo Bambuí demonstraram grande variação longitudinal e temporal em suas fontes. Os padrões de idades de zircão e monazitas do Conglomerado Carrancas são idênticos aos encontrados em rochas do Complexo Belo Horizonte, o que indica que os sedimentos derivam de uma fonte local. As análises U-Pb de amostras da região da Serra de São Domingos revelaram a principal contribuição de fontes Paleoproterozóicas assim como importante aporte de material Neoproterozóico e um pequeno componente arqueano. As amostras do segmento sul do grupo apresentaram padrão simples de idades, com a dominante presença de zircões Neoproterozóicos (principalmente ~640 Ma). Os dados Sm-Nd apontam a crescente contribuição de material juvenil para o topo do grupo, com idades modelo variando de ~2,5 Ga para a Formação Sete Lagoas a ~1,5 Ga para Formação Três Marias. O conjunto de dados corrobora a interpretação de que o Grupo Bambuí representa uma bacia *foreland*, com sedimentos originais derivados principalmente de rochas da Faixa Brasília e subordinamente do Cráton São Francisco-Congo. As idades dos zircões detríticos da seqüência superior da Formação Sete Lagoas (com importante componente de 610-640 Ma) em associação a dados previamente publicados de Pb-Pb de ca. 740 Ma da seqüência inferior, reforçam a sugestão baseada em dados geofísicos de que a seqüência inferior não pertença ao Grupo Bambuí.

ABSTRACT

Meso- to Neoproterozoic sedimentary/metasedimentary units of southern Brasília Belt and São Francisco-Congo Craton had their provenance investigated in this thesis. The Canastra, Vazante, Ibiá and Bambuí groups and the Jequitaí Formation were studied. Integrated whole-rock Sm-Nd models ages and in situ (LAM-ICPMS and SHRIMP) U-Pb zircon analyses allowed the determination of depositional limits, pointed out possible sources and furnished elements for tectonic interpretation.

The Canastra Group constitutes a regressive sedimentary sequence composed mainly of metapelitic and metapsammitic greenschist-facies rocks. These include phyllite, metarhythmite and quartzite with minor intercalations of limestone as well as carbonaceous and carbonatic phyllite. The Vazante Group comprises a marine detrital-carbonatic sequence composed mainly of quartzite, slate, conglomerate, metasiltstone and dolomite with abundant stromatolitic structures. The Ibiá Group is formed by a basal diamictite followed upwards by metapelitic rocks (phyllites and calc-schists). The Jequitaí Formation is a glacial unit covering large areas of the São Francisco Craton and is also exposed within the Brasília Belt. It is overlain by the carbonatic Sete Lagoas Formation, the basal unit of the Bambuí Group which represents a carbonate-siliciclastic sequence with upward increase of the detritic component.

The U-Pb zircon data allow the identification of the youngest detrital grains of the studied unit and the establishment of the maximum depositional ages. These are 1030, 925, 640, 610 and 880 Ma for the Canastra, Vazante, Ibiá and Bambuí groups and the Jequitaí Formation, respectively.

Few contributions of Archean terrains were observed. The São Francisco-Congo Craton was identified as an important supplier of detritus, in particular for the Canastra and Vazante groups. Conversely, data from the Ibiá and Bambuí groups emphasise the strong contribution from the Brasília Belt. The Canastra Group was the only unit that did not show Neoproterozoic grains.

The provenance signature of the Canastra Group comprises a wide range of detrital zircon ages (1030-2996 Ma) with a significant Paleoproterozoic component (~1.8 and ~2.1 Ga) and an important Mesoproterozoic source (1.1- 1.2 Ga), specially for the Paracatu Formation. This is consistent with a passive margin setting for the deposition of the Canastra sediments.

The U-Pb detrital zircon signatures vary significantly among the formations (925-3520 Ma) but, in general, 2.1 Gy terrains (Gy pra years e Ga para years ago…) constitute the main source in most formations (sugestão: in general, the main source of these formations comprise 2.1 Ga terrains). The youngest population (ca. 950 Ma) only occurs at the lowest stratigraphic units of the Vazante Group. However Sm-Nd data reveals the contribution of young terrains in all groups, in particular in the Lapa Formation (T_{DM} of 1.67-2.00 Ga). The Sm-Nd and U-Pb data for the Serra do Garrote Formation showed predominance of the Paleoproterozoic source. The top of the group is marked by significant change of sources; the pattern found in the Morro do Calcário and Lapa formations show a main age peak at 1.1-1.2 Ga and other small Paleoproterozoic contributions. The results suggest that Paleo- and Mesoproterozoic terrains within the São Francisco-Congo Craton represent the main sources of detrital sediments for the Vazante Group. Therefore, it may be interpreted as a passive margin sequence developed along the western margin of that continent. Slightly younger model ages in the upper Lapa Formation, however, are not entirely consistent with derivation solely from the craton and may indicate contribution from younger sources such as the Neoproterozoic Goiás Magmatic Arc to the west.

Zircon grains from the diamictite of the Ibiá Group present ages raging from 936 to 2500 Ma. In contrast, the overlying calciphyllite of the Rio Verde Formation reveals a dominant Neoproterozoic provenance pattern with important peaks at 665, 740 and 850 Ma. The Sm-Nd data show a bimodal behaviour with intervals at 1.16-1.46 and 1.58-2.01 Ga. The São

Francisco-Congo Cranton and Goiás Magmatic Arc are, most probably, the two main source regions for the Ibiá Group which may represent, therefore, a former fore-arc sedimentary sequence.

The age distribution of the detrital zircon grains of the Jequitaí rocks indicates a dominant Paleoproterozoic source (2.0-2.2 Ga) as well as minor Mesoproterozoic and early Neoproterozoic (~880 Ma) components. These are all probably derived from the São Francisco Craton. The Sm-Nd and detrital zircon for the Bambuí Group demonstrate longitudinal and temporal variation of the source areas. The patterns observed in zircon and monazite from Carrancas Conglomerate are identical to those found in the Belo Horizonte Complex which indicates a local source. Rocks exposed in the northern area showed major contribution from Paleoproterozoic sources as well as an important component from Neoproterozoic ages and a small Archean population. Samples from the southern part of the group show a simple age pattern with the dominant presence of Neoproterozoic zircons (mainly ca. 640 My). The Sm-Nd data show an increasing contribution derived from younger materials upward in the stratigraphic sequence. T_{DM} ages vary from ca. 2.5 Ga at the bottom to values around 1.5 Ga at the top. The data reinforce the interpretation that the Bambuí Group represents a foreland basin with the original sediments being derived mainly from the Brasília Belt, to the west. However, some contribution from the São Francisco Craton is not discarded. The detrital zircon age of the upper sequence (with 610-640 Ma population) associated with the previously published Pb-Pb isochronic ages of ca. 740 Ma of the lower sequence reinforce the suggestion, based on geophysical data, that the lower sequence does not belong to Bambuí Group.

Capítulo 1 - INTRODUÇÃO

1.1 – APRESENTAÇÃO E LOCALIZAÇÃO

A presente tese buscou investigar a fonte de sedimentos de unidades litoestratigráficas integrantes da Faixa Brasília e o seu significado geotectônico na evolução tectônica do orógeno. A ausência de associações ígneas e o limitado conteúdo fossilífero têm levado ao estabelecimento de intervalos amplos de deposição para estas rochas, o que associado aos freqüentes contatos tectônicos têm dificultado o estabelecimento de uma estratigrafia e evolução tectônica definitiva. Buscando minimizar este problema, o foco desta tese foi o estudo de proveniência, por meios isotópicos, em especial através de análise U-Pb em zircões detríticos via LAM-ICPMS e idades modelo Sm-Nd de rochas pertencentes aos grupos Vazante, Canastra, Ibiá e Bambuí, além da Formação Jequitaí. Foram selecionadas amostras representativas das unidades nas imediações das cidades de Unaí, Cristalina, Paracatu, Vazante, Coromandel, Sete Lagoas, Três Maria, Santa Fé de Minas e oeste de Formoso, na Serra de São Domingos (Figura 1.1).

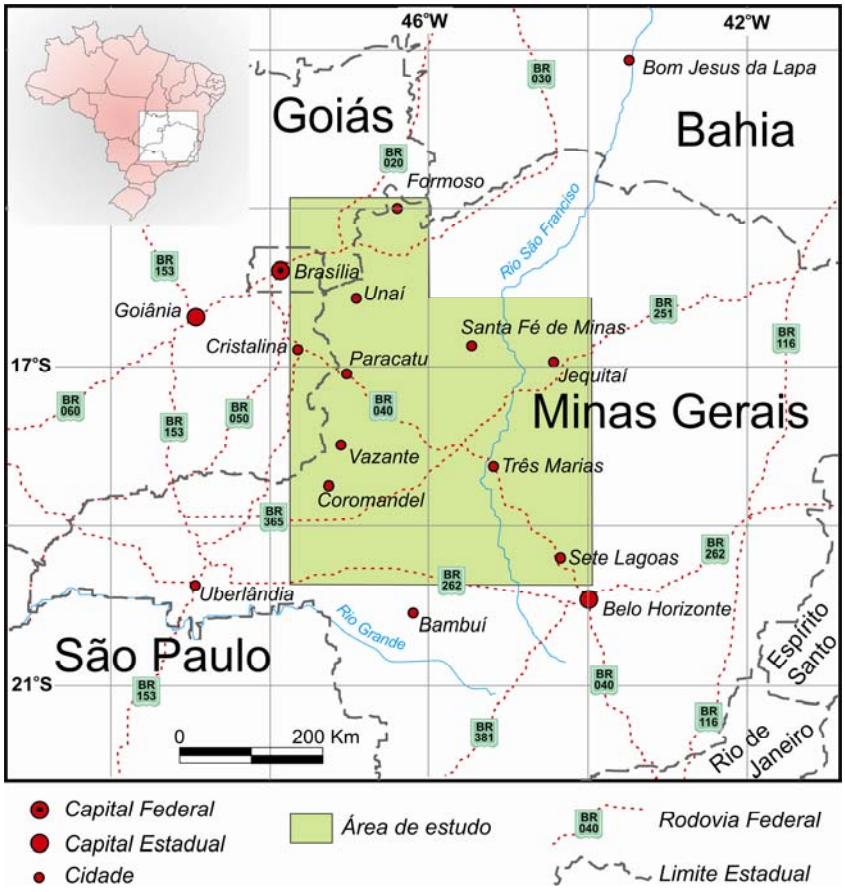

Figura 1.1 – Localização geográfica da área estudada.

A tese está estruturada em seis capítulos, sendo que os capítulos 3, 4 e 5 estão dispostos no formato de artigos e apresentam os dados gerados para os grupos Vazante, Canastra-Ibiá, e Bambui-Formação Jequitaí, respectivamente.

1.2 - OBJETIVOS

O objetivo desta tese é contribuir no entendimento dos processos evolutivos da Faixa Brasília, no que se refere à dinâmica de aporte de sedimentos, e assim ajudar a reconstruir parte de sua história geológica. Este objetivo global foi almejado em etapas que incluem:

- Estabelecer padrões de idade das fontes dos sedimentos estudados;
- Identificar ou restringir suas idades de sedimentação;
- Fornecer elementos que auxiliem no entendimento de suas relações com as unidades vizinhas;
- Determinar quando houve inversão da margem passiva e deposição do Grupo Bambuí, e;
- Procurar identificar a influência de fontes juvenis como as do Arco Magmático de Goiás nos sedimentos da faixa.

1.3 -METODOLOGIA

Quatro etapas de campo foram realizadas, durante as quais foram coletadas amostras representativas das unidades estudadas. Buscou-se coletar pelo menos uma amostra de cada formação para análises U-Pb em zircão e um número maior para Sm-Nd. Adicionalmente, carbonatos da Formação Sete Lagoas foram coletados para análise de isótopos de estrôncio. O estudo pelo método SHRIMP foi realizado na Australian National University em Canberra, Austrália. As demais análises foram efetuadas no Laboratório de Geocronologia da Universidade de Brasília, integrado à Rede Geochronos.

1.3.1 – U-Pb via LAM-ICP-MS e SHRIMP

A separação de concentrados de zircão e monazita foi realizada conforme o procedimento padrão do laboratório, no qual a amostra é reduzida via britador e extraída a fração inferior a 500 μm. A partir do material recolhido são concentrados os minerais pesados com uso de bateia. O concentrado é passado pelo separador isodinâmico Frantz e finalmente o zircão e/ou monazita são separados manualmente em lupa binocular. Para a confecção dos

mounts não foi realizado nenhum processo de seleção dos zircões, visando uma amostragem randômica das populações existentes nos sedimentos. Os *mounts* foram confeccionados com resina epóxi (a frio), desgastados e polidos para exposição do interior dos grãos.

1.3.1.1 – LAM-ICP-MS

As determinações realizadas no LAM-ICP-MS seguiram o procedimento apresentado por Buhn *et al* (*in press*). Para a limpeza dos *mounts* foi utilizado banho com ácido nítrico diluído (3%), água Nanopure® em ultrassom e por último em acetona para extração de qualquer resíduo de umidade.

As análises isotópicas foram realizadas no LAM-MC-ICP-MS Neptune (Thermo-Finnigan) acoplado ao Nd-YAG (λ=213nm) Laser Ablation System (New Wave Research, USA). A ablação dos grãos foi realizada em *spots* 25-40 μm, em modo *raster*, com freqüência de 9-13 Hz e intensidade de 0.19 a 1.02 J/cm^2. O material pulverizado foi carreado por um fluxo de He (~0.40 L/min) e Ar (~0.90 L/min). Em todas as análises foi utilizado o padrão internacional GJ-1 para a correção da deriva do equipamento, assim como o fracionamento entre os isótopos de U e Pb. Para a verificação da acurácia foram realizadas análises no padrão FC-1.

Os dados foram adquiridos em 40 ciclos de 1 segundo. O procedimento de coletada de dados seguiu a seqüência de leitura: - 1 branco, 1 padrão, 3 amostras, 1 banco e 1 padrão. Em cada leitura são determinadas as intensidades das massas ^{202}Hg, ^{204} (Pb+Hg), ^{206}Pb, ^{207}Pb, ^{208}Pb e ^{238}U.

A redução dos dados brutos, que inclui as correções para branco, deriva do equipamento e chumbo comum, foram realizadas em planilha EXCEL, confeccionada no próprio laboratório. As incertezas associadas às razões apresentadas nas tabelas são de 1σ, em porcentagem. As idades foram calculadas utilizando o ISOPLOT 3.0 (Ludwig, 2003).

1.3.1.2 – SHRIMP

As análises SHRIMP foram realizadas utilizando as microssondas iônicas SHRIMP I e II, nas quais foram determinadas as razões entre as massas Zr^20^+, $^{204}Pb^+$, $^{206}Pb^+$, $^{207}Pb^+$, $^{208}Pb^+$, $^{238}U^+$, $^{232}Th^{16}O^+$, $^{238}U^{16}O^+$. Uma análise é composta em média por seis leituras em cada massa em cada ponto, perfazendo um total de 20 a 25 minutos por ponto analisado. A cada 3 grãos analisados uma análise do padrão é efetuada. Os dados são reduzidos no

programa SQUID (Ludwig, 2000) e as incertezas associadas às razões são de 1 σ. As idades calculadas utilizando o ISOPLOT 3.0 (Ludwig, 2003).

1.3.2 – Método Sm-Nd

As análises isotópicas de Sm-Nd seguiram o método descrito por Gioia & Pimentel (2000). Neste procedimento cerca de 50 mg de amostra pulverizada é misturada a uma solução traçadora de ^{149}Sm e ^{150}Nd. A amostra é dissolvida em cápsulas Savillex® por meio de sucessivos ataques ácidos em HF, HNO_3 e HCl. Os conteúdos de Sm e Nd são extraídos através de colunas de trocas catiônicas, confeccionadas em Teflon e preenchidas com resina LN-Spec. Os sais de Sm e Nd são depositados em filamentos de rênio com ácido nítrico e evaporados. As leituras das razões foram realizadas no espectrômetro de massas multicoletor, modelo Finnigan MAT 262 em modo estático. As incertezas para as razões de Sm/Nd e $^{143}Nd/^{144}Nd$ são inferiores a ±0.5% (2σ) e ±0.005% (2σ), respectivamente, baseados em repetidas análises nos padrões internacionais BHVO-1 e BCR-1. A razão $^{143}Nd/^{144}Nd$ foi normalizada em função da razão $^{146}Nd/^{144}Nd$ de 0,7219. Os valores de T_{DM} foram calculados usando o modelo de De Paolo (1981).

1.3.3 – Método Sr-Sr

Para a determinação da razão $^{87}Sr/^{86}Sr$ em carbonato foi seguido procedimento apresentado por Gioia *et al.* (1999), no qual cerca de 50 mg de rocha total pulverizada é pesada e adicionado 1 ml de ácido acético (0,5N). Este material é centrifugado e o sobrenadante evaporado. O resíduo é dissolvido em 1 ml de HCl (6N) e a solução passa por coluna de troca catiônica para a extração do Sr. A coluna é preenchida pela resina Sr-spec (Dt Bu CH18-C6 em 1-octanol). O sal de Sr é depositado em filamento e as leituras realizadas em processo idêntico ao método Sm-Nd, descrito acima.

Capítulo 2 – CONTEXTO GEOLÓGICO

A Faixa Brasília possui estrutura aproximadamente norte-sul (Figura 2.1), margeia os limites ocidentais do Cráton São Francisco, sendo disposta em um complexo conjunto de dobramentos e lascas de empurrão com vergência para o cráton. Tanto o metamorfismo quanto a deformação são progressivamente mais intensos a oeste, o que levou à sua divisão em duas zonas: - Externa, margeando o cráton, e a Interna, a oeste (Fuck *et al*., 1994).

Inicialmente considerava-se que a Faixa Brasília fosse constituída pelos grupos Paranoá e Bambuí (Marini *et al*., 1984a.) enquanto que os grupos Araxá, Ibiá e Serra da Mesa eram incluídos na Faixa Uruaçu, supostamente mais antiga. Entretanto, a evolução do conhecimento revelou a íntima relação entre as unidades vizinhas, o que levou a inserção das últimas na Faixa Brasília. Estudos de detalhe, dados estruturais, geoquímicos, geofísicos e datações mais precisas indicaram que boa porção do material possui idade Meso-Neoproterozóica e que várias associações litológicas tiveram origem e evolução conjunta. Parte da área considerada como pertencente ao Maciço Mediano de Goiás mostrou-se mais jovem, assim como as unidades tidas como Uruaçuanas. Isso desencadeou uma série de estudos que resultou em um novo entendimento da evolução da Província Tocantins. Dentro desta nova concepção a Faixa Brasília tornou-se mais abrangente, incluindo a Faixa Uruaçu e o Maciço de Goiás (Dardenne, 2000). Seus principais constituintes são (Pimentel *et al.* 2001): a) Bloco continental exótico composto por unidades arqueanas (Região Crixás-Goiás); b) Embasamento siálico de idade paleoproterozóica, interpretado como parte do Cráton São Francisco, envolvida durante a tectônica Brasiliana (especialmente exposta na região de Almas-Cavalcante e Anápolis); c) Espessos pacotes sedimentares de natureza diversa, metamorfisados em diferentes graus, incluídos nos grupos Araí, Paranoá, Serra da Mesa, Araxá, Ibiá, Vazante, Canastra e Bambuí; d) Arco Magmático de Goiás, formado por seqüências vulcano-sedimentares, do tipo arco de ilha, associadas a rochas tonalíticas/granodioríticas.

Na região central da Faixa Brasília, destaca-se uma mega-estrutura, organizada em uma expressiva associação de formas curvas, orientadas aproximadamente no sentido WNW-ESE, denominada Sintaxe dos Pirineus (Araújo Filho, 2000). A Sintaxe dos Pirineus divide a Faixa Brasília em dois segmentos com características estruturais e metamórficas distintas.

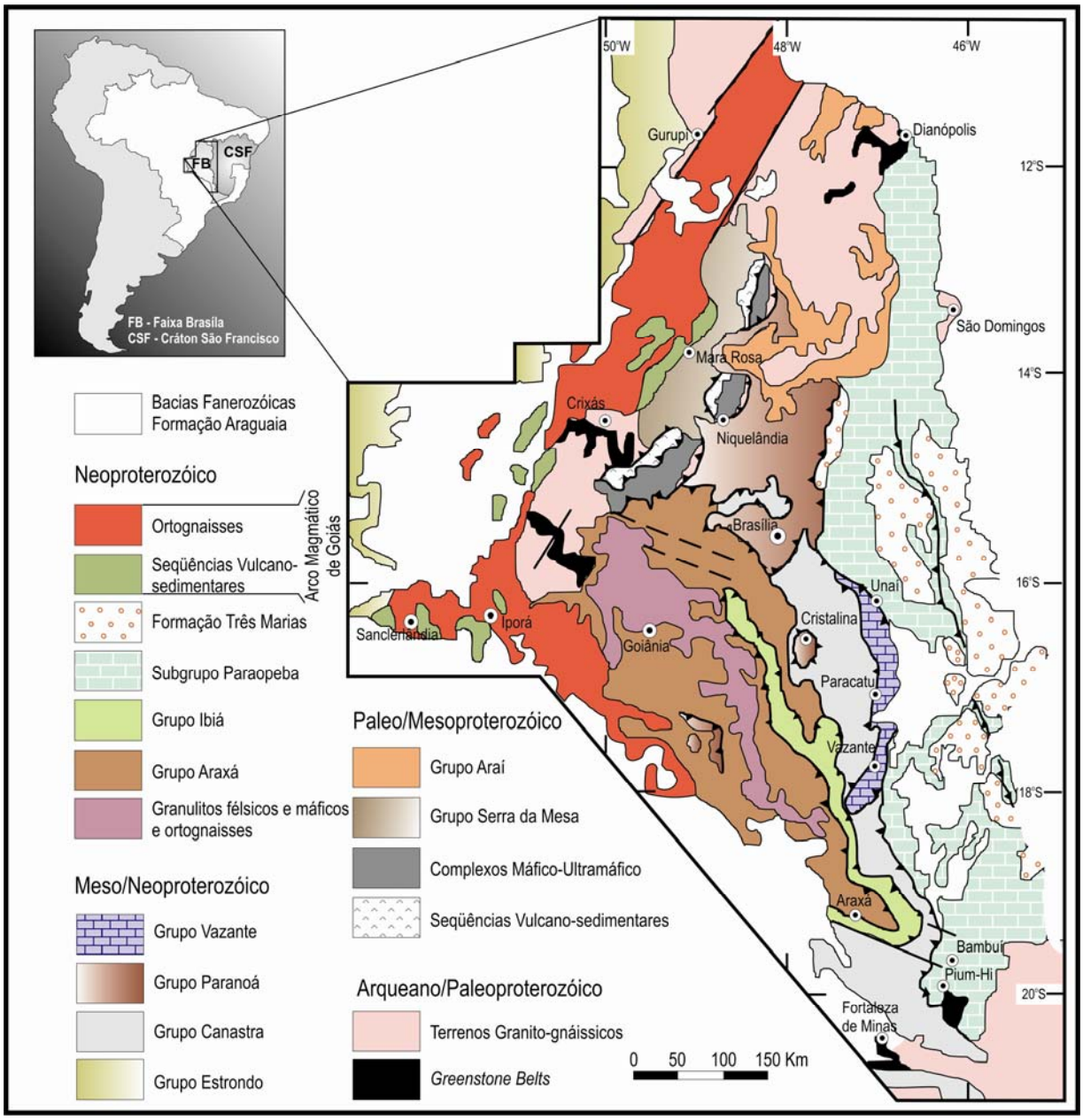

Figura 2.1 – Unidades Tectônicas da Faixa Brasília (Modificado de Dardenne, 2000).

As rochas sedimentares localizadas a norte da estrutura apresentam metamorfismo e deformação menos intensos e preservam, em grande parte, as relações estratigráficas; já no segmento a sul, metamorfismo e deformação são mais intensos, com significativo transporte tectônico de material, dificultando o estabelecimento das relações estratigráficas entre as diferentes unidades (Pimentel *et al.*, 2001).

2.1 – UNIDADES METASSEDIMENTARES

A determinação precisa da idade de deposição destes grupos tem sido dificultada pela limitada presença de unidades vulcânicas. Datações de rochas intrusivas, relações de campo e estudos fossilíferos indicam que sua sedimentação é dominantemente meso-neoproterozóica. A seguir são apresentadas descrições sucintas das unidades estudadas na presente tese:

2.1.1 – Grupo Vazante

O Grupo Vazante ocorre como uma estreita faixa de rochas orientadas aproximadamente no sentido N-S, que se estende por cerca de 250 Km, nas proximidades das cidades mineiras de Coromandel, Vazante, Lagamar, Paracatu e Unaí (Fig. 2.2). Seus contatos dão-se por meio de falhas, tanto a oeste com o Grupo Canastra quanto a leste com o Grupo Bambuí. A unidade consiste em um conjunto de filitos, ardósias, quartzitos, metassiltitos, raros calcários e abundantes dolomitos de origem algal (Marini *et al.*, 1984b). A presença de importantes depósitos minerais de Zn, Pb e P alojados em rochas do Grupo Vazante o tornaram alvo de diversos estudos.

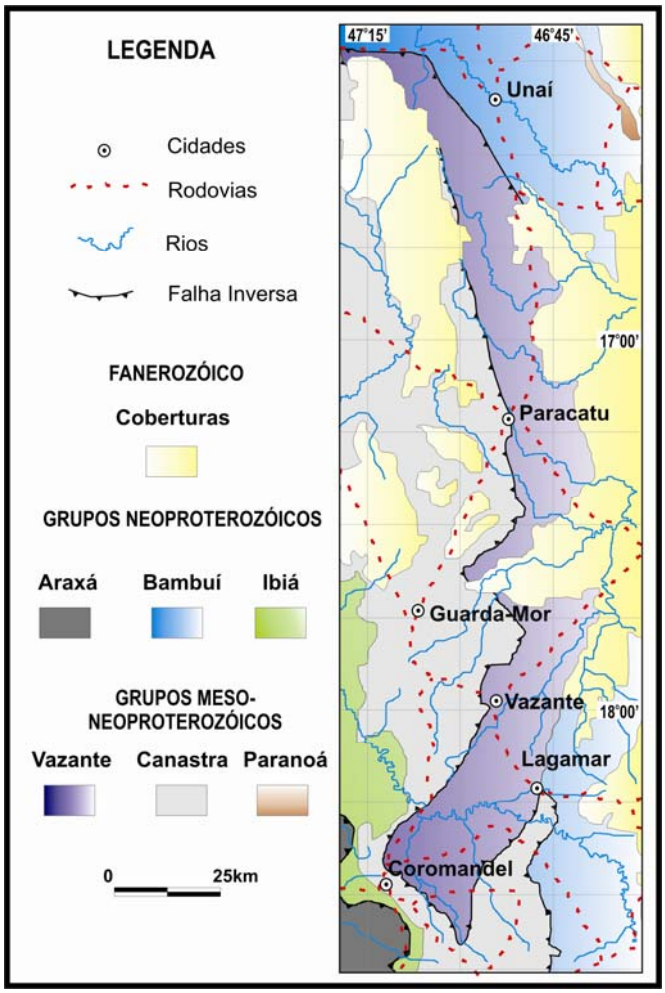

Figura 2.2 – Situação geológica do Grupo Vazante (Modificado de Bizzi *et al.* (2001)).

Inicialmente incluída no Grupo Bambuí, a unidade só foi individualizada por Dardenne (1978), quando recebeu o nome de Formação Vazante. Estudos posteriores voltaram a correlacioná-la ao Bambuí (Madalosso, 1980) e outras unidades como os grupos Canastra (Campos Neto, 1984) e Paranoá (Rigobello *et al.*, 1988). Entretanto o aprimoramento do conhecimento geológico (Madalosso & Valle, 1978; Pinho, 1990;

Nogueira, 1993; Dardenne *et al*, 1997 e 1998, Souza, 1997, entre outros) permitiu que a unidade fosse elevada ao *status* de Grupo, composto por sete formações (Fig. 2.3) (Dardenne, 2000), da base para topo:

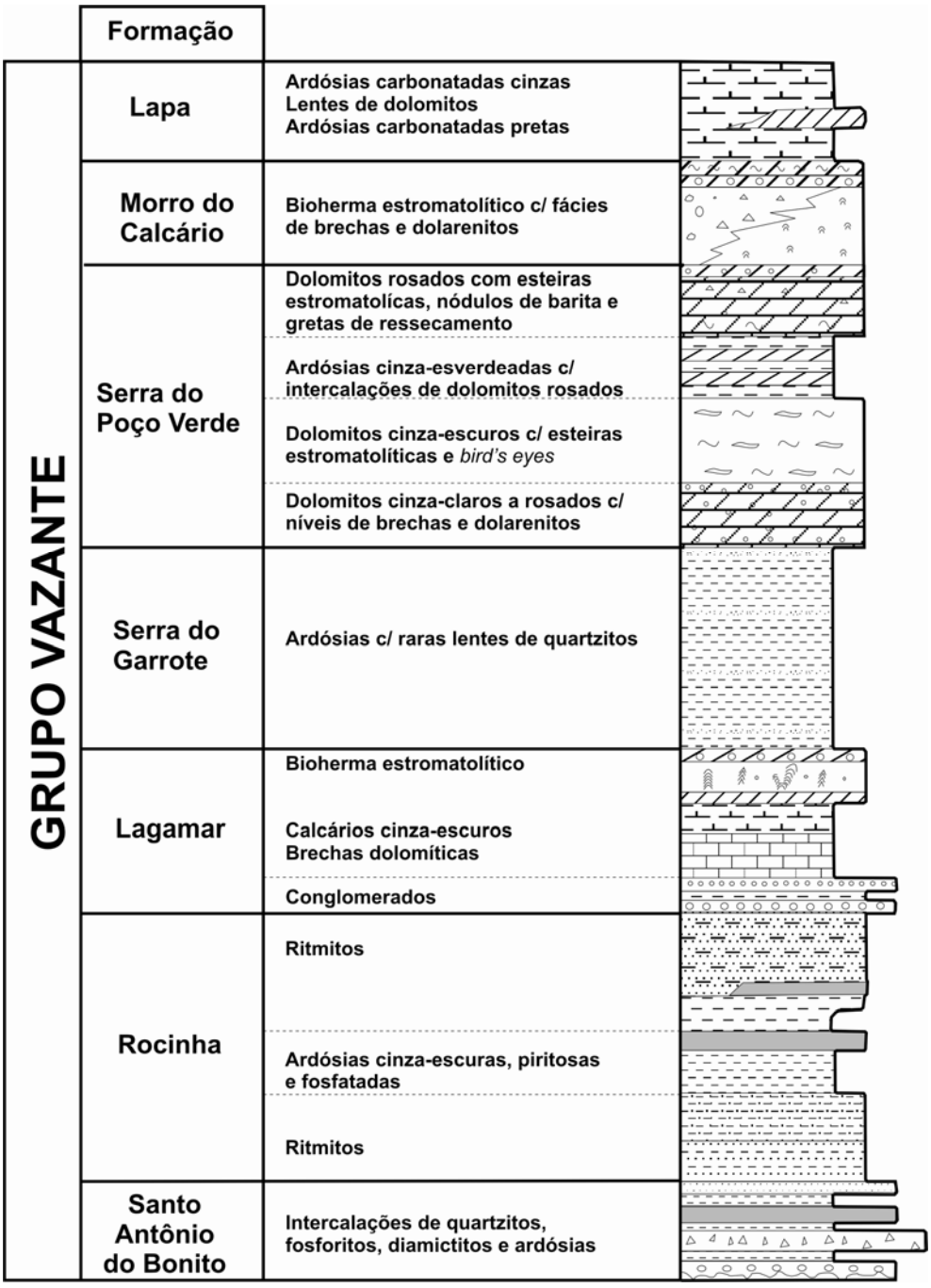

Figura 2.3 – Coluna estratigráfica do Grupo Vazante (Dardenne, 2000).

• Formação Retiro/Santo Antônio do Bonito: Consiste de níveis métricos de quartzito branco, localmente conglomerático, intercalado com níveis ardosianos. Horizontes

restritos de diamictitos podem ser localizados (rios Rios Santo Antônio do Bonito e Santo Inácio), neles estão presentes seixos de quartzitos, calcários, dolomitos, metassiltitos e rochas graníticas em matriz pelítica, por vezes fosfatada;

• Formação Rocinha: Sua porção basal é representada por seqüência rítmica areno-pelítica, recoberta por espesso pacote de ardósias e metassiltitos regularmente intercalados. Segue-se um pacote de ardósias cinza escuras, carbonáticas e piritosas, com finas laminações fosfáticas, que transicionam para um intervalo de fosfarenitos ricos em intraclastos e pellets, que constituem o depósito de Rocinha (Souza, 1997 e Dardenne *et al,* 1998). Nos ritmitos do topo da formação (siltito e quartizito) são encontrados níveis fosfaneníticos que originaram o depósito de Lagamar (Nogueira, 1993);

• Formação Lagamar: Conglomerados, quartzitos, metassiltitos e ardósias formam a base da unidade, sendo sobrepostos por brechas intraformacionais dolomíticas, recobertas por calcários cinza escuros, bem estratificados, com intercalações de brechas lamelares. No topo da unidade são localizados dolomitos estromatolíticos bihermais do gênero *Conophyton* (Cloud & Dardenne, 1973), lateralmente esses biohermas interdigitam-se com metassiltitos carbonáticos e metapelitos ardosianos;

• Formação Serra do Garrote: Unidade formada por espesso pacote de ardósias cinza escura a cinza esverdeada, às vezes rítmicas, carbonosas e piritosas, com finas intercalações de quartzitos (Madalosso & Vale, 1978, Madalosso, 1980, Dardenne, 1978; Campos Neto, 1984; Dardenne *et al*., 1997, 1998);

• Formação Serra do Poço Verde: Da base para o topo, esta formação é representada por dolomitos laminados cinza a rosa, ardósias cinza a esverdeada, sericita filito, dolomitos cinza escuro com *bird eyes,* margas e filitos carbonos a pirita (Babinski *et al*., 2005);

• Formação Morro do Calcário: Seqüência dominantemente dolomítica constituída por biostromos e biohermas com laminações convexas, doloruditos, dolarenitos oolíticos e oncolíticos. Na porção norte (Paracatu-Unaí) o pacote chega a atingir 900 m. Nesta área concentram-se doloruditos, possivelmente resultado do retrabalhamento dos bihermas estromatolíticos. Dardenne (2000) sugere que esta espessura anormal represente uma deposição contínua das formações Morro do Calcário e Serra do Poço Verde, não permitindo as individualizações, como ocorre em Vazante;

• Formação Lapa: A formação de topo apresenta-se de forma distinta nas regiões de Vazante e Unaí. Na primeira ela ocorre como uma seqüência de filitos carbonosos, metassiltitos carbonáticos, lentes de dolomitos (esteiras de cianobactérias, estromatólitos colunares e brechas intraformacionais) e níveis de quartzitos. Já na região de Unaí é composta por arenitos e conglomerados líticos intercalados com ardósias escuras. Um nível diamictítico recentemente descrito na interfácie das formações Morro do Calcário e Lapa (Brody *et al.*, 2004) associado a valores negativos de $\delta^{13}C$ levaram Asmy *et al.* (2006) a interpretar os carbonatos da formação como um depósito do tipo *cap carbonate*.

Segundo Dardenne (1981) as rochas do Grupo Vazante correspondem a um megaciclo regressivo, resultado de sedimentação inicialmente em ambiente marinho sublitorâneo, passando a perilitorâneo carbonatado, seguido por um conjunto recifal litorâneo e finalmente a um ambiente de planície de maré.

Apesar de já ter sido alvo de estudos paleontológicos e isotópicos, a idade do grupo ainda é controversa. A presença do estromatólito *Conophyton* indica um período de deposição entre 1,35 a 0,9 Ga, o que torna a unidade correlacionável ao Grupo Paranoá, porém a presença do conglomerado basal muito similar ao da Formação Jequitaí permite correlacioná-lo ao Grupo Bambuí. As análises de isótopos de oxigênio, carbono e estrôncio levaram Azmy *et al.* (2001) a sugerir que a deposição do topo do Grupo Vazante seja sincrônica à fase glacial Sturtiana, embora os autores ressaltem que os padrões isotópicos do Pré-Cambriano ainda estejam pobremente definidos.

Pimentel *et al.* (2001) apresentam idades modelo Sm-Nd variando entre 2,1 a 1,7 Ga, que são valores intermediários entre os obtidos para o Grupo Paranoá (2,3-2,0 Ga) e Grupo Bambuí (1,9-1,3 Ma), levando os autores a sugerirem uma idade também intermediária para a deposição das rochas do Grupo Vazante. Idades U-Pb de zircões de conglomerados da base do grupo foram apresentadas por Dardenne *et al.* (2003), os quais forneceram idades de 2081±35 Ma (seixo granítico da Fm Santo Antônio do Bonito) e 2,18-1,85 Ga (idades $^{207}Pb/^{206}Pb$ de grãos detríticos do conglomerado Arrependido).

Estudos isotópicos realizados por Asmy *et al.* (2006) no recém interpretado nível diamictítico da Fm Lapa resultaram em dados fortemente negativos de $\delta^{13}C$, levando os autores a comparar o Grupo Vazante ao Grupo Otavi (Congo), sugerindo que o diamictito da Formação Santo Antônio do Bonito represente uma discreta e precoce deposição Sturtiana.

Babinski *et al.* (2005) realizaram análises isotópicas por diversos métodos em um dique de rocha metabásica alojada na Formação Serra do Poço Verde. As T_{DM} obtidas giram em torno de 1,0 Ga. Já a análise morfológica e as idades U-Pb dos zircões (cerca de 2,0 Ga) levaram os autores a interpretá-los como xenocristais, provavelmente absorvidos da encaixante. Titanitas também foram estudadas e revelaram alta concentração de Pb comum e baixos teores de U (razão U/Pb=0,001). Suas idades modelo $^{207}Pb/^{206}Pb$ (Stacey & Kramers, 1975) variaram entre 780 a 870 Ma.

2.1.2 – Grupo Canastra

O termo Formação Canastra foi utilizado primeiramente por Barbosa (1955) na serra homônima, incluindo na unidade sedimentos psamíticos e pelíticos. Estudos posteriores (Barbosa *et al.*, 1970, Marini *et al.*, 1984a, Bizzi *et al.*, 2001, entre outros) expandiram seus limites e, atualmente, este grupo inclui áreas no oeste de Minas Gerais, além de porções em Goiás e Distrito Federal (Figura 2.4). Apesar das inúmeras pesquisas realizadas, sua litoestratigrafia ainda não está plenamente definida, principalmente em função dos freqüentes contatos tectônicos e repetições de seqüências.

O histórico do conhecimento sobre o Grupo Canastra (que foi elevado a tal categoria por Barbosa *et al.*, 1970) tem íntima relação com a do Grupo Araxá, uma vez que já foram considerados como partes de uma mesma unidade e individualizados diversas vezes. Entretanto nos últimos anos parece haver consenso que se tratam de unidades diferentes, embora haja semelhanças entre suas rochas (Seer, 1999; Valeriano *et al.*, 2004a, b; Dardenne, 2000). Similaridades litológicas, tais como abundância em níveis psamíticos, presença rítmica de pelitos e níveis com associações carbonáticas, têm levado muitos autores a correlacionar os grupos Canastra e Paranoá (Dardenne, 1979; Pereira, 1992; Campos Neto, 1984; Freitas-Silva, 1991). A maioria de suas rochas está metamorfisada em fácies xisto verde, podendo alcançar fácies anfibolito na região de Tapira (Silva, 2003).

Estudos de detalhe na região de Paracatu-Coromandel (Campos Neto, 1984; Freitas Silva, 1991; Pereira, 1992) levaram Freitas-Silva & Dardenne (1994) a identificar o ordenamento estratigráfico para o Grupo Canastra, aplicável à porção noroeste de Minas Gerais, na qual o grupo é dividido em três formações (Figura 2.5):

- Formação Serra do Landim: Esta unidade foi definida por Madalloso & Valle (1978) como parte da Formação Vazante, só sendo integrada ao Grupo Canastra por Freitas-Silva & Dardenne (1994). A porção basal da unidade é constituída por margas e lentes

de calcário, que gradam para níveis de calci-filitos/calci-xistos, que são os principais constituintes da unidade. No topo aparecem ocasionais lentes de quartzitos finos. O contato com a Fm Paracatu é tectônico, onde é comum encontrar nódulos de pseudo-chert;

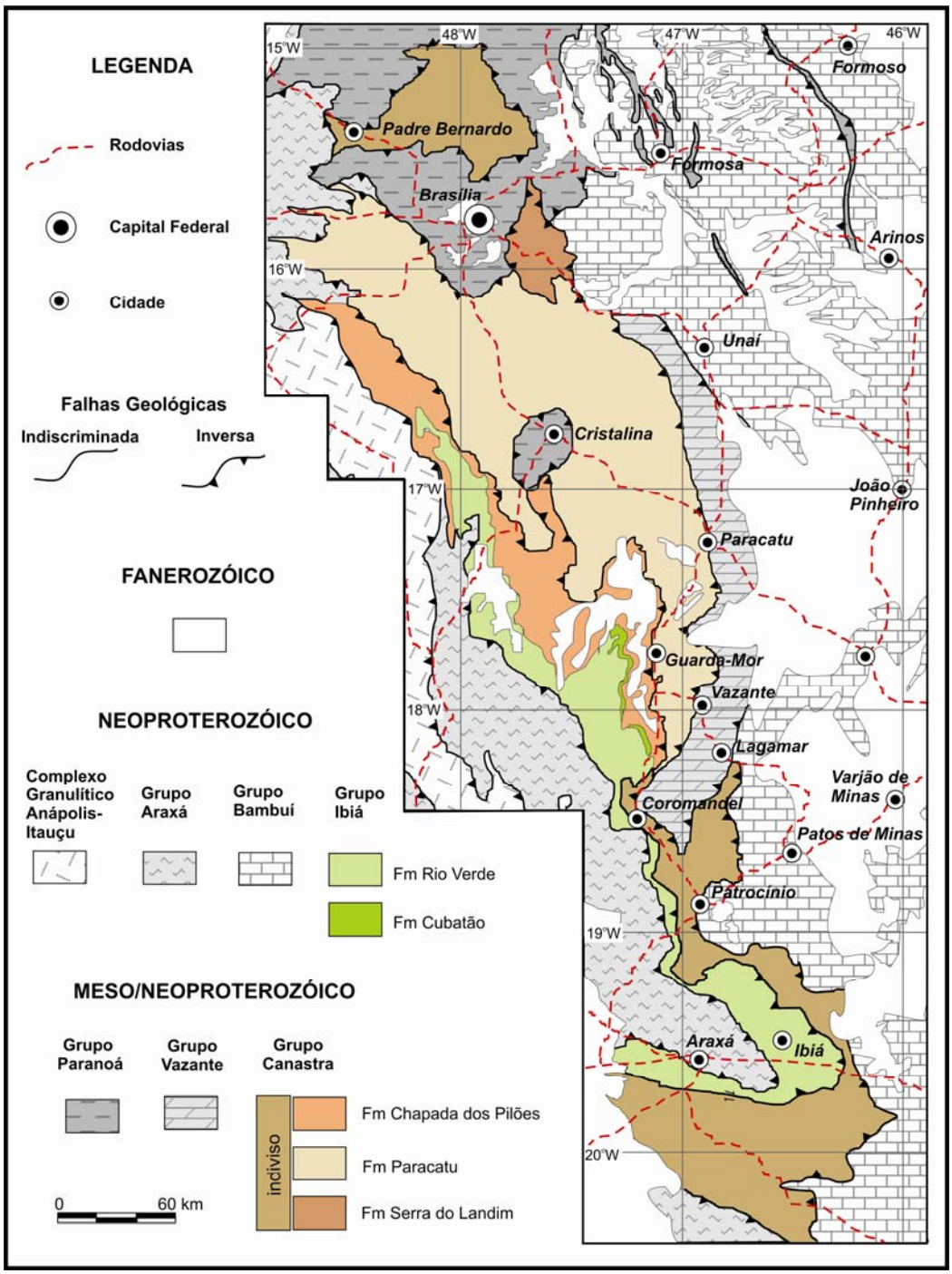

Figura 2.4 – Mapa geológico da porção sudoeste da Faixa Brasília, trazendo em destaque os grupos Canastra e Ibiá (modificado de Bizzi *et al.*, 2001).

• Formação Paracatu: Freitas-Silva & Dardenne (1994) individualizaram dois membros que compõem a Fm Paracatu, inicialmente definida por Almeida (1969). O membro basal, denominado Morro do Ouro, inclui filitos carbonosos escuros com intercalações variadas de quartzitos finos, que podem alcançar 100 metros de espessura. O Membro Serra da Anta é representado por espesso pacote de sericita filitos, com intercalações de filito carbonoso e quartzitos finos. Os contatos entre os membros, assim como com as demais formações são tectônicos;

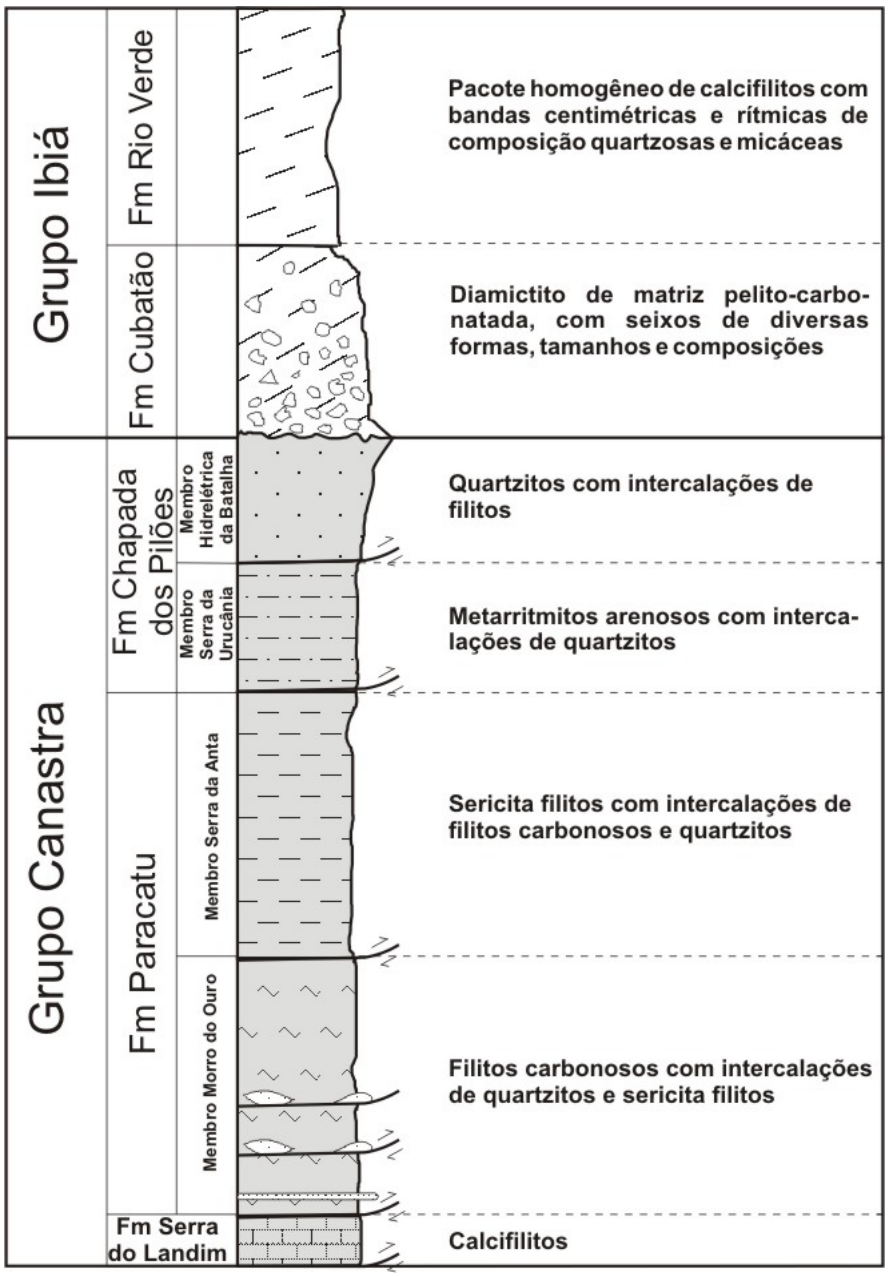

Figura 2.5 – Coluna estratigráfica dos grupos Canastra e Ibiá (modificado de Dardenne, 2000 e Pereira, 1992).

• Formação Chapada dos Pilões: A unidade ocorre a oeste de Paracatu e Vazante e também é constituída de dois membros. O pacote basal de metarritmitos arenosos com níveis de quartzito representa o Membro Serra da Urucânia, já o pacote superior, predominantemente quartzítico com finos níveis de filitos é denominado Membro Hidroelétrica Batalha.

Na área em questão o Grupo Canastra apresenta uma sucessão de rochas que caracteriza um megaciclo regressivo (Dardenne, 2000), a base rica em matéria orgânica e piritas diagenéticas são interpretadas como depósitos de águas profundas; estas passam para níveis turbidíticos, com presença de correntes de gravidade. Os sedimentos gradam para fácies plataformais dominadas pela ação de correntes de tempestade, e finalmente no topo ocorrem sedimentos de plataforma rasa, dominados por correntes de maré, indicando transporte de leste para oeste.

Poucos estudos isotópicos foram realizados na unidade. Idades T_{DM} obtidas por Pimentel *et al.* (2001) estão próximas a 2,2 Ga, sugerindo fontes paleoproterozóicas para os sedimentos. Valeriano *et al.* (2004a) analisaram zircões de um quartzito coletado na *Nappe* de Araxá e estes apresentaram idades diversas, entre 1226 e 2875 Ma, sem definição de nenhuma moda. A idade de 1226 Ma é tida como a idade máxima para a deposição dos sedimentos originais.

2.1.3 – Grupo Ibiá

Barbosa *et al.* (1970) definiram a Formação Ibiá, na qual incluíram os calcixistos que ocorrem na vizinhança da cidade homônima (MG). Rochas similares foram incluídas na unidade, estendendo seus limites até o estado de Goiás (Fig. 2.1). Estudos de detalhe na região de Coromandel-Guarda Mor permitiram que Pereira (1992) individualizasse duas formações (Fig. 2.4 e 2.5) elevando a unidade Ibiá ao *status* de grupo:

• Formação Cubatão: É a unidade basal que repousa em discordância erosiva sobre o Grupo Canastra. Trata-se de um pacote de rochas de abundante matriz pelito-carbonatada, na qual flutuam seixos de diferentes tamanhos, formas e composições. Em direção ao topo, ocorre diminuição no tamanho e quantidade de seixos;

• Formação Rio Verde: Homogêneo pacote de calcixistos e calcifilitos com finos níveis quartzíticos, às vezes micáceo. Composicionalmente muito similar à matriz dos

diamictitos da Formação Cubatão. Não são observadas estruturas sedimentares reliquiares.

A posição estratigráfica do Grupo Ibiá ainda carece definição precisa. Algumas correlações com unidades vizinhas são sugeridas, especialmente no que se refere à relação entre os diamictitos da Formação Cubatão e a Formação Jequitaí (Pereira, 1992). Os poucos dados isotópicos disponíveis para a unidade não são conclusivos. Estes dados restringem-se a estudos de idades modelo Sm-Nd (Pimentel *et al.*, 2001), que variam de 1,1 a 1,3 Ga, indicando uma fonte relativamente juvenil para estas rochas e as idades $^{207}Pb/^{206}Pb$ de 2133±24 – 2101±14 Ma obtidas em zircões extraídos de um seixo granítico da Formação Cubatão (Dardenne *et al*., 2003).

2.1.4 - Grupo Bambuí

A denominação Bambuí foi introduzida por Rimann (1917) para a extensa associação de rochas pelito-carbonatadas que recobrem diversas unidades da Faixa Brasília e do Cráton São Francisco (Fig. 2.6), porém Costa & Branco (1961) foram os primeiros a apresentar uma divisão litoestratigráfica, em grande parte adotada até os dias de hoje. Os autores individualizaram da base para o topo as seguintes formações: Carrancas, Sete Lagoas e Rio Paraopeba (Membros Santa Helena, Lagoa do Jacaré, Três Marias, e Serra da Saudade).

Diversos estudos que se sucederam (Oliveira, 1967, Braun, 1968, Costa *et al,* 1970; Dardenne 1978; Alvarenga, 1978; Barbosa *et al.*, 70, Dardenne., 79) resultaram na apresentação de várias colunas e subdivisões estratigráficas. Entretanto a proposta de Dardenne (2000), que retoma a organização estratigráfica proposta por Costa & Branco (1961) será parcialmente adotada neste trabalho. Nela o grupo é organizado em cinco formações que se encontram mais ou menos constantes nos estados de Goiás, Minas Gerais e Bahia:

• Formação Sete Lagoas: Trata-se de uma unidade essencialmente carbonática, com dolomitos, finos níveis argilosos, dolomitos laminados, estromatolíticos, brechas intraformacionais, dolarenitos e calcários oolíticos. Seu contato basal é discordante. Em sua área tipo, Vieira *et al.* (2007) identificaram duas seqüências deposicionais. A primeira é representada por calcário cinza claro e a segunda é composta na base por alternância de níveis carbonáticos e restritos níveis pelito-carbonatados, seguidos por um espesso pacote de calcário negro, às vezes estromatolítico.

• Formação Serra de Santa Helena: É constituída predominantemente por folhelhos e siltitos laminados. Localmente ocorrem níveis de arenitos muito finos. São encontradas estruturas sedimentares do tipo estratificações cruzadas e plano-paralela;

• Formação Lagoa do Jacaré: Trata-se de siltitos esverdeados calcíferos e margosos com intercalações finas de calcários, laminações argilosas e bancos de calcários oolíticos e pisolíticos;

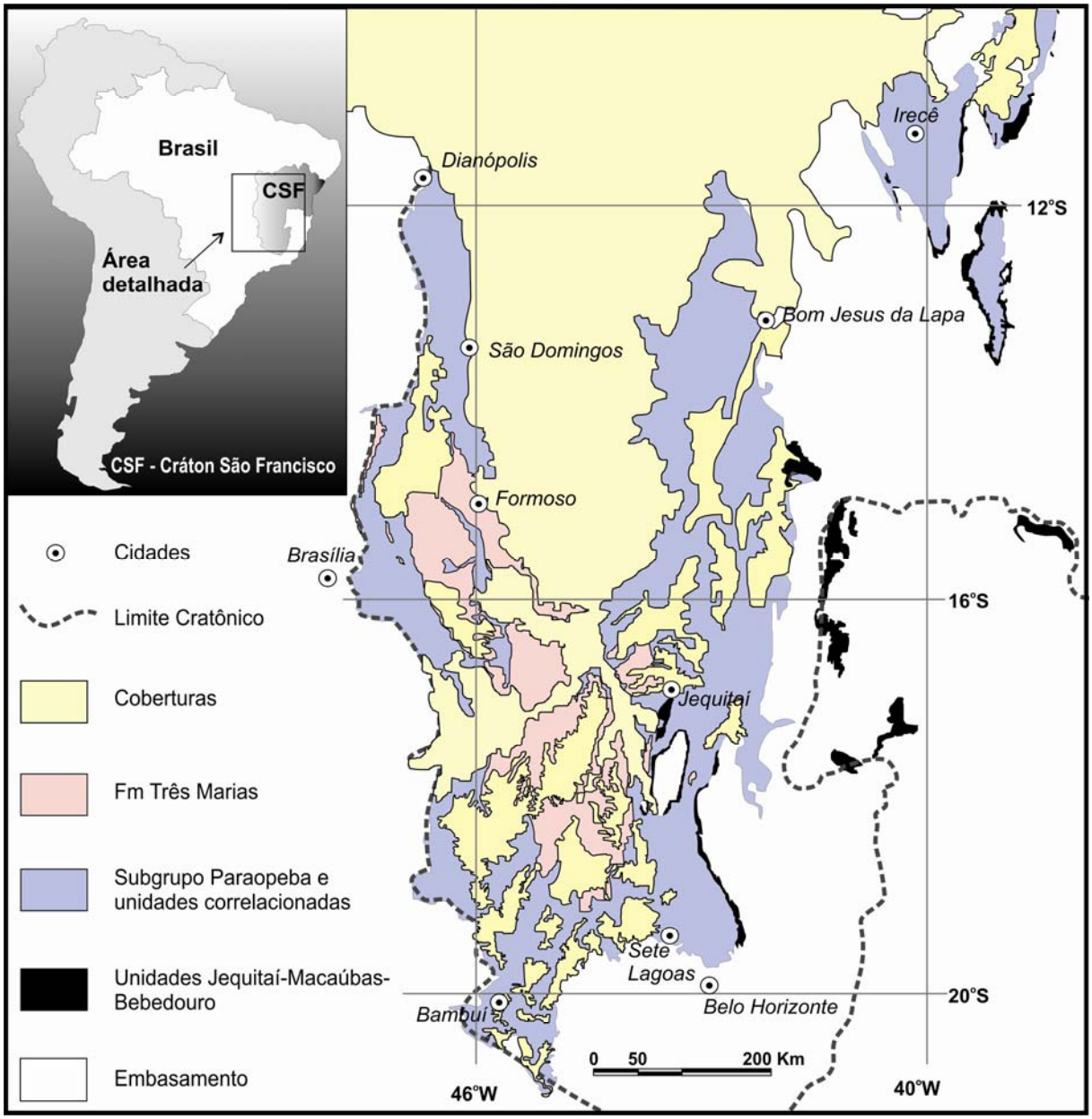

Figura 2.6 – Mapa de ocorrência do Grupo Bambuí e das unidades glaciogênicas Jequitaí-Macaúbas e Bebedouro (Modificado de Bizzi *et al.*, 2002).

• Formação Serra da Saudade: É composta por folhelhos, argilitos, siltitos argilosos verdes e raras lentes de calcário cinza claro.

• Formação Três Marias: Predominam arcóseos finos e siltitos arcoseanos de cor verde escuro, geralmente com estratificação plano-paralela e abundantes marcas de ondas. Foliações esferoidais podem ser observadas.

Os sedimentos do Grupo Bambuí foram depositados em uma plataforma epicontinental, inicialmente em um ambiente de mar raso, evoluindo para recifal e finalmente foi instaurado um sistema aluvial (Marini *et al.*, 1984a, Dardenne, 2000, D'Agrella-Filho *et al.*, 2000). A seqüência *shallowing upward* foi estabelecida em três megaciclos regressivos (Dardenne, 2000). O primeiro megaciclo é representado pela Formação Sete Lagoas, o segundo pelas formações Serra de Santa Helena e Lagoa do Jacaré e por fim o último composto pelas formações Serra da Saudade e Três Marias.

Guimarães (1997) estudando a região de Bezerra-Cabeceiras-GO identificou composições distintas entre os argilo-minerais das unidades basais e os das formações Serra da Saudade e Três Marias. Nas unidades de topo predominam argilo-minerais quimicamente imaturos, o que não ocorre nas demais. A autora interpreta que a associação química e mineralógica da seqüência seja típica de margem continental ativa.

Diversos estudos isotópicos realizados nas rochas do Grupo Bambuí não conseguiram determinar com precisão o período de sua sedimentação. Análises Rb-Sr (Bonhomme *et al.*, 1982; Parenti Couto *et al.*, 1981; Thomaz Filho *et al.*, 1998, Chang, 1997) forneceram idades de cerca de 560-690 Ma, interpretadas como idades mínimas para a deposição.

Embora diversas análises isotópicas de chumbo tenham sido realizadas em rochas do grupo (Babinski *et al.*, 1993, Iyer *et al*, 1995, Iyer & Babinski, 1995, Babinski *et al.*, 1999, D'Agrella-Filho *et al.*, 2000), somente Babinski *et al.* (2007) apresentam uma isócrona Pb-Pb bem ajustada e confeccionada com dados de rochas da Formação Sete Lagoas aparentemente bem preservas isotopicamente. A idade obtida, 740±20 Ma e MSWD de 0,62, é interpretada pelos autores como a melhor estimativa de idade de deposição para as rochas da formação.

As idades modelo Sm-Nd obtidas para amostras deste grupo (Pimentel *et al.*, 2001 e Silva *et al.*, 2006) indicam rochas proterozóicas como fonte dos sedimentos (T_{DM} variam de 1,3 a 2,0 Ga). Idades de zircões detríticos do conglomerado Samburá (Subgrupo Paraopeba) são reportados por Dardenne *et al.* (2003) e apresentam idades entre 1,8 e 0,65 Ga, indicando

a presença de fontes brasilianas (Arco Magmático de Goiás?). Coelho *et al.* (2007) analisaram amostras do Subgrupo Paraopeba, coletadas na região de Unaí-MG. Os resultados revelaram fontes com idades entre 1,44 e 2,66 Ga, com contribuição predominante de terrenos com 2,1 Ga.

Dados isotópicos de carbono da Fm Sete Lagoas (Chang *et al,* 1993, Iyer & Babinski, 1995, Martins, 1999, Santos *et al.*, 2000 e 2004, Misi *et al.*, 2005 e Babinski *et al,* 2007) revelam valores negativos de $\delta^{13}C‰_{(PDB)}$ para a base da unidade (~-5), tornando-se fortemente positivo no topo (~+15), comportamento similar ao de carbonatos de período pós-glacial, levando-os a serem correlacionados a depósitos Sturtianos. As razões isotópicas de $^{87}Sr/^{86}Sr$ dos carbonatos apresentam valores de 0,70734 a 0,70810 (Chang *et al.*, 1993, Iyer *et al.*, 1995, Misi *et al.*, 2007, Babinski *et al.,* 2007), que são valores comparáveis à composição da água do mar durante o intervalo de aproximadamente 660-600 Ma, segundo Halverson *et al.* (2007).

2.1.5 – Formação Jequitaí

A Formação Jequitaí é um depósito glacio-marinho (Uhlein *et al.,* 1994, 1998, Cukrov, 1999) que ocorre na região homônima (MG) e nas bordas do Domo de Cristalina (GO) (Fig. 2.6). A unidade é formada por diamictitos maciços com raras intercalações de arenitos e argilitos. Os clastos são compostos principalmente por fragmentos de rochas graníticas, gnáissicas, calcários e quartzitos. A matriz é pelítica, por vezes arenosa, sendo comum o tom esverdeado e a presença de carbonatos. Na região de Jequitái a unidade repousa em discordância sobre os quartzitos e metassiltitos do Supergrupo Espinhaço.

Semelhanças têm levado vários autores a considerar a Formção Jequitaí correlata dos depósitos glaciais do Grupo Macaúbas (Uhlein *et al.*, 1994, 1998 D'Agrella-Filho *et al.*, 2000, Babinski & Kaufman, 2003, Santos *et al.,* 2004, entre outros), embora a associação ao Grupo Bambuí já tenha sido também considerada.

Zircões detríticos da Formação Jequitaí foram analisados por Pimentel *et al.* (2002). As idades obtidas agrupam-se em três modas, a mais jovem (0,9-1,2 Ga) identificada em uma amostra da região de Jequitaí (MG), uma intermediária (1,55-1,75 Ga) apresentada pela amostra coletada próximo a Cristalina (GO) e a mais antiga (1,9-2,2 Ga) encontrada em ambas as amostras.

Capítulo 3 – GRUPO VAZANTE

Este capítulo é destinado à apresentação e discussão dos dados isotópicos relacionados ao Grupo Vazante. A primeira parte do capítulo tem como foco o estudo de proveniência das rochas (meta)sedimentares. Este item está estruturado na forma de artigo, ainda a ser submetido, com o título: "Provenance of the Vazante Group: new Sm-Nd and U-Pb (LAM-ICPMS and SHRIMP) isotopic data and implications for the tectonic evolution of the Brasília Belt". Na segunda parte são apresentadas as análises relacionadas a duas rochas ígneas associadas à unidade.

Provenance of the Vazante Group: new Sm-Nd and U-Pb (LAM-ICPMS and SHRIMP) isotopic data and implications for the tectonic evolution of the Brasília Belt

Rodrigues, J.B., [a,b,*], Pimentel, M.M.[b]; Buhn, B.[b], Dardenne, M. A. [b], Alvarenga, C.J.S. [b], Armstrong,R.A.[c]

a - Companhia de Pesquisa de Recursos Minerais, b- Universidade de Brasília, c – Australian National University, * corresponding author

ABSTRACT

The Vazante Group is one of the main lithostratigraphic units of the Neoproterozoic Brasília Belt, in central Brazil. Its age, tectonic significance and stratigraphic relationships with adjacent units, however, are still poorly understood. These issues are considered to be instrumental for the better understanding of the tectonic evolution of the orogen. The Vazante Group comprises a marine detrital-carbonatic sequence made mainly of quartzite, slate, conglomerate, metasiltstone and dolomite with abundant stromatolitic structures, comprising seven lithostratigraphic units. From base to top these are: Santo Antônio do Bonito, Rocinha, Lagamar, Serra do Garrote, Serra do Poço Verde, Morro do Calcário and Lapa formations.

Whole-rock Sm-Nd models ages (19 samples) as well as in situ (LAM-ICPMS and SHRIMP) U-Pb zircon data (9 samples) for sedimentary rocks of the different stratigraphic units of the Vazante Group are presented in this study, and their significance is discussed.

Detrital zircon grains from the basal Santo Antônio do Bonito Formation indicated ages varying from 1.0 to 1.85 Ga. One quartzite sample from the overlying Rocinha Formation shows a slightly broader age distribution, with major peaks at 0.94 and 2.2 Ga, and minor peaks at 1.2, 1.6 and 1.8 Ga. The youngest population of 0.94 Ga determine the maximum depositional age of the group. The Arrependido conglomerate of the Lagamar Formation shows a very homogeneous Paleoproterozoic population with $^{207}Pb/^{206}Pb$ ages forming a major peak between 2.1 and 2.2 Ga. Granite pebbles from this conglomerate show the same age. Two samples from the northern segment of the Serra do Garrote Formation also present a very simple provenance pattern with a single peak at 2.2 Ga, suggesting provenance from the sialic basement of the São Francisco Craton. On the other hand, the sample from the southern segment of this formation shows a larger age dispersion towards ages as young as ca. 1.3 Ga. Quartzite and sandstone samples from the upper Morro do Calcário and Lapa formations show important contribution from Mesoproterozoic (ca. 1.2 Ga) sources and much less important input from Paleoproterozoic sources, compared with the other formations. Sm-Nd data also indicate important input from younger sources in rocks of the Lapa Formation (T_{DM} from 1.67 to 2.0 Ga), whereas rocks of the Serra do Garrote Formation present the oldest pattern, with T_{DM} values ranging from 2.03 to 2.76 Ga.

The results suggest that Paleo- and Mesoproterozoic terrains within the São Francisco-Congo Craton represent the main sources of detrital sediments of the Vazante Group and that it may be interpreted as a passive margin sequence developed along the western margin of that continent. Slightly younger model ages in the upper Lapa Formation, however, are not entirely consistent with derivation solely from the craton and may indicate contribution from younger sources, such as the Neoproterozoic Goiás Magmatic Arc, to the west.

3.1 - INTRODUCTION

The Vazante Group is one of the main and lithostratigraphic units of the Neoproterozoic Brasilia Belt, an orogenic belt developed along the western margin of the São Francisco Craton (Fig. 3.1). The belt represents the result of ocean closure between the São

Francisco and Amazon continents during the Brasiliano Orogeny and displays tectonic vergence and decreasing metamorphic polarity towards the east. Several lithostratigraphic units formed by sedimentary sequences constitute the eastern part of the belt. Deformation and metamorphism increase towards the west, reaching granulite facies conditions in the central part of the belt. The absence of volcanic rocks, the tectonic contacts between the different stratigraphic units, and the poor fossil record have contributed to the controversy concerning the age and tectonic significance of these supracrustal sequences. Previous provenance work have suggested that some of the units represent passive margin sequences (e.g the Paranoá Group), others are fore- or back-arc syn-orogenic successions (e.g. the Araxá Group), and one (the Bambuí Group) may represent the post-inversion foreland basin (Pimentel et al. 2001). The significance of the Vazante Group, however, remained controversial.

The main objectives of this study are: (i) to investigate the provenance pattern of the original sediments of the Vazante Group using LAM-ICPMS U-Pb ages of detrital zircons coupled with Sm-Nd model ages, (ii) to constrain the depositional age of the Vazante Group, and (iii) to contribute to a better understanding of the geological evolution of the Brasília Belt.

3.2 - GEOLOGIC SETTING

The Vazante Group is a thick sedimentary unit, exposed as a narrow and continuous belt (about 40x250Km) comprising a pelite-carbonate sequence, presenting fault contacts with the Canastra Group to the west and with the Bambuí Group to the east (Fig. 3.1). It is made of phyllite, slate, quartzite, metasiltstone, algal dolomite and minor limestone. The original sediments were deposited on a shallow marine platform during a regressive cycle (Dardenne, 1981 and 2000), starting with a coastal setting, passing to a coastal reef and finally ending in a tidal plain deposit. The majority of its mineral deposits (Zn, Pb and P) is hosted by dolomitic rocks.

The several field studies carried out in the southern part of the group (Madalosso,1980 Campos Neto, 1984, Rigobello *et al.*, 1988, Madalosso & Valle, 1978; Pinho, 1990; Nogueira, 1993; Dardenne et al, 1997 e 1998, Souza, 1997) resulted in the stratigraphic column summarized by Dardenne (2000). The group may be divided into the following formations, from base to top:

- **Retiro/Santo Antônio do Bonito Formation:** This is formed mainly by layers of white quartzite, locally conglomeratic, intercalated with slate beds. Some diamictite

beds are also identified along the Santo Antônio do Bonito and Santo Inácio rivers, consisting of pebbles of quartzite, limestone, dolomite, metasiltstone and granite supported by a pelitic-carbonatic-phosphatic matrix;

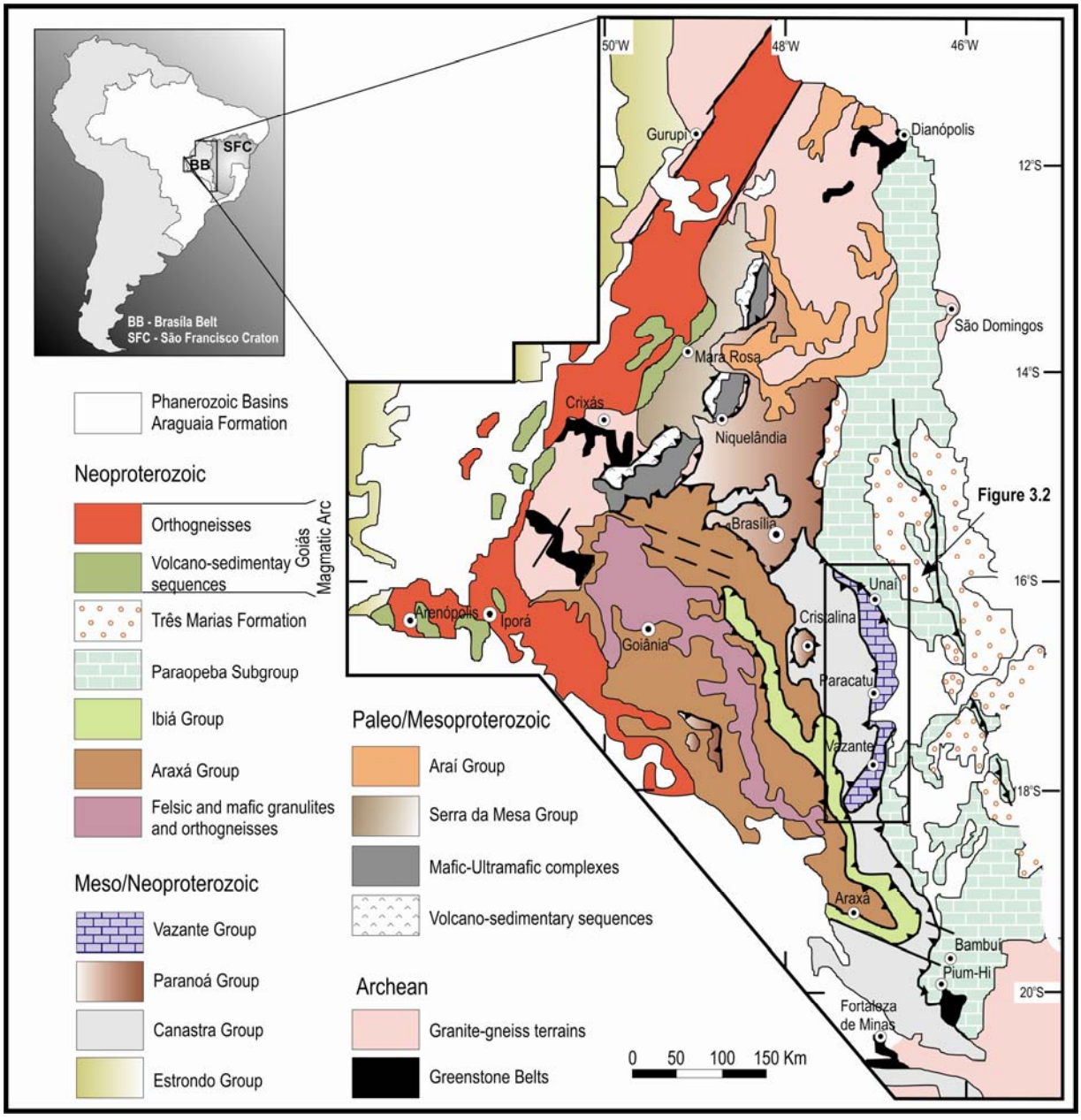

Figure 3.1. Simplified geological map of Brasília Belt (based on Dardenne, 2000).

- **Rocinha Formation:** The basal part of this formation consists of a rhythmic psamo-pelitic sequence, covered by a thick and also rhythmic succession of slate and metasiltstone, which are, in turn, covered by a layer of pyrite-bearing dark slate with phosphatic lamination that grades into intraclast- and pellet-rich phospharenite. The

upper portion is composed essentially of phospharenite. This unit hosts two major phosphate deposits: Rocinha and Lagamar.

- **Lagamar Formation:** Conglomerate, quartzite, metasiltstone and slate form the base of this unit. They are covered by dolomitic intrafomational breccia, grading into dark grey, well-stratified limestone layers with intercalations of lamellar breccia. At the top, the dolomitic stromatolitic bioherms made of *Conophyton* and *Jacutophyton* dominate the sequence. Laterally and vertically these bioherms interdigitate with carbonate-bearing metasiltstone and slate.

- **Serra do Garrote Formation:** This unit is formed by thick beds of carbonaceous and pyrite-bearing dark grey-greenish slate, occasionally rhythmic, intercalated with fine quartzite layers (Madaloso & Vale, 1978; Madalosso, 1980; Dardenne, 1978; Campos Neto, 1984; Dardenne et al., 1997,1998).

- **Serra do Poço Verde Formation:** This formation is made up of grey-pink laminated dolomites, grey to greenish slate, sericite phyllite, dark grey dolomites with bird eyes, marble, carbonaceous phyllite with pyrite (Babinski et al., 2005).

- **Morro do Calcário Formation:** This sequence is formed mainly by dolomite with biostromes and bioherms presenting convex lamination, dolorudite, oolitic dolarenite, oncolits and rare quartzite. An unconformity marks the top of the sequence (Misi et al., 2005). At the northern portion (between Paracatu and Unaí), this unit may reach thicknesses of approximately 900 m. In this area dolorudite is common, indicating reworking of the stromatolitic bioherms. Dardenne (2000) suggested that deposition of the Morro do Calcário and Serra do Poço Verde formations was continuous, without a noticeable distinction between them.

- **Lapa Formation:** This unit presents different characteristics in the southern and northern areas of exposure of the Vazante Group. In the Vazante region it includes carbonaceous phyllite, metasiltstone, carbonate-bearing metasiltstone, dolomitic lenses (cyanobacteria mats, columnar stromatolites and intrafomational breccia), as well as quartzite beds (Madalloso and Valle, 1978; Madalosso, 1980). In the Unaí area, lithic sandstone and conglomerate intercalate with beds of dark slate (Laranjeira, 1992).

The recently described layer of diamictite (Brody et al, 2004, Olcott et al, 2005, Azmy et al., 2006) at the upper part of the Morro do Calcário Formation is still under discussion, including its stratigraphic position. Nevertheless, the presence of this diamiticte

layer associated with C and O isotopic data led Azmy et al (2006) to interpret the Lapa Formation as a cap carbonate unit.

Despite the paleontologic and isotopic studies carried out in rocks of the Vazante Group, its sedimentation age, remains a controversial issue. Different lithological, isotopic and paleontological features have been used to establish correlations with other sedimentary units of the Brasília Belt, such as the Bambuí, Paranoá and Canastra groups. The presence of *Conophyton* stromatolites led Cloud and Dardenne (1973) to suggest a depositional age between 1.35 Ga and 0.9 Ga. Its basal diamictite, however, has been correlated with the Jequitaí Formation, of probable Sturtian age (Dardenne, 1979, Karfunkl & Hoppe, 1988, Azmy et al. 2001, 2006).

Pimentel et al. (2001) presented Sm-Nd model ages ranging from 2.1 Ga to 1.7 Ga for the pelitic rocks of the Vazante Group, which are intermediate between those of the Paranoá (2.3-2.0 Ga) and of the Bambuí groups (1.9-1.3 Ga). U-Pb zircon ages obtained by Dardenne et al. (2003) for granite pebbles of the Santo Antônio do Bonito Formation and for the Arrependido conglomerate are, respectively, 2081±35 Ma and 2.18-1.85 Ga.

Sr isotopic data available for carbonates range from 0.7061 to 0.7522 (Serra do Garrote, Morro do Calcário and Lapa formations). The higher values suggest that the dolomitization process may have disturbed the original composition (Azmy et al., 2005). The study of the relation between Sr, Rb and Mn concentrations led Azmy et al. (2001) and Misi et al. (2005) to consider the values between 0.7061 and 0.7069, found in Serra do Garrote and Lapa formations, as the best value for the $^{87}Sr/^{86}Sr$, which probably represents the depositional conditions. However recent data for the Serra do Garrote Formation show $^{87}Sr/^{86}Sr$ values which are considerably higher, ranging between 0.70760 and 0.70791 for samples with low Mn/Sr ratios (Misi et al., 2007).

Azmy et al. (2005, 2006), based on the recently described glacial layer at the upper part of the group and the strongly negative $\delta^{13}C$ anomaly of the Lapa Formation, suggested a comparison between the Vazante Group and the Otavi Group of Namibia (Hoffman et al, 2004, Halverson et al, 2005), indicating that the Santo Antônio do Bonito basal diamictite might represent a discrete earlier Sturtian deposit. However, recent Re-Os dating gave ages of 993 ± 46 and 1100 ± 77 Ma for organic-rich shale samples from layers immediately above the uppermost diamictite (Azmy et al., 2008). This is not coherent with the maximum depositional ages for the Santo Antônio do Bonito Formation and the diamictite of the Morro

do Calcário Formation given by detrital zircon U-Pb ages of 988±15 and 1000±25 Ma, respectively.

A mafic dike emplaced into the Serra do Poço Verde Formation was studied by Babinski et al. (2005) by different isotopic methods. They present Sm-Nd T_{DM} values of ca. 1.0 Ga and zircon grains extracted from them represent xenocrysts, with ID-TIMS ages of ca. 2.0 Ga. Titanites were also analysed and presented high content of common lead, $^{207}Pb/^{206}Pb$ model ages vary between 780 and 870 Ma.

3.3 - ANALYTICAL PROCEDURES

For LAM-MC-ICP-MS and SHRIMP samples were crushed with a jaw crusher and powdered to approximately 500 μm. Heavy mineral concentrates were obtained by panning and were subsequently purified using a Frantz isodynamic separator. Zircon grains were selected from the least magnetic fraction. The grains were set in epoxy resin mounts, without selection and their surface were then polished to expose the grains interiors.

The U-Pb analyses by LAM-ICP-MS were carried out using the Finnigan Neptune coupled to a Nd-YAG laser (λ=213nm) ablation system (New Wave Research, USA) at the Geochronology Laboratory of the Universidade de Brasília. The analytical procedures follow those outlined in Buhn et al. (in press), where the mounts were cleaned in a HNO_3 solution (3%) and ultraclean water bath. The ablation was done with spot size of 25-30μm in raster mode, at frequency of 9-13 Hz and intensity of 0.19-1.02 J/cm^2. The ablated material was carried by Ar (~0.90 L/min) and He (~0.40 L/min) in analyses of 40 cycles of 1 second. Unknown were bracketed by measurements of the international standard GJ-1 following the sequence 1 blank, 1 standard, 3 unknown, 1 blank and 1 standard. The accuracy was controlled using the standard FC-1. Raw data were reduced using a home made spreadsheet and corrections were done for background, instrumental mass-bias drift and common Pb. The ages were calculated using ISOPLOT 3.0 (Ludwig, 2003).

The SHRIMP samples were mounted with standard zircon crystals SL13+FC1, and the mount was photographed at 150× magnification in reflected and transmitted light. Cathodoluminescence (CL) images were obtained in order to reveal internal structures of the zircon grains. Ion microprobe analyses were carried out using SHRIMP I and II at the Research School of Earth Sciences, Australian National University, Canberra, Australia. SHRIMP analytical methods and data treatment follow those described by Williams (1998) and Williams and Meyer (1998). The ion microprobe primary beam in both equipments

typically produce spots with diameter between 20–30 μm. Uncertainties reported in tables and figures are given at 1σ level, and final ages are quoted at the 95% confidence level. The data have been processed using SQUID and ISOPLOT 3.0 (Ludwig, 2003).

Sm-Nd isotopic measurements were carried out on a multi-collector Finnigan MAT 262 mass spectrometer in static mode and followed the method described by Gioia and Pimentel (2000). Whole-rock powders (ca. 50 mg) were mixed with a ^{149}Sm–^{150}Nd spike solution and disolved in HF, HNO_3 and HCl in Savillex capsules. Sm and Nd extraction of whole-rock samples was done by cation exchange techniques, using Teflon columns containing LN-Spec resin (HDEHP—di-ethylhexil phosphoric acid supported on PTFE powder). Sm and Nd samples were loaded onto Re evaporation filaments of a double filament assembly. Uncertainties for Sm/Nd and ^{143}Nd/^{144}Nd ratios are better than ±0.5% (2σ) and ±0.005% (2σ), respectively, based on repeated analyses of international rock standards BHVO-1 and BCR-1. ^{143}Nd/^{144}Nd ratios were normalised to ^{146}Nd/^{144}Nd of 0.7219. T_{DM} values were calculated using De Paolo's (1981) model.

3.4- RESULTS

3.4.1 – LAM-MC-ICP-MS Zircon Provenance Patterns

Eight samples collected from three distinct areas of the Vazante Group (Fig. 3.2) belonging to five formations, were selected for LAM-ICPMS analyses. The main characteristics of the analysed samples and their zircon grains are summarized in Table 3.1. The probability density plot used ^{207}Pb/^{206}Pb ages of concordant data (better than 90% of concordance) with low common lead contents. The complete analytical data set is in the Appendix A.

3.4.1.1 – Santo Antônio do Bonito/Retiro Formation

The sample from the Santo Antônio do Bonito/Retiro Formation (STO-3) is a diamictite with pebbles of limestone, quartzite and granite set in a fine-grained matrix (Fig. 3.2). Zircon grains were extracted preferably from the matrix however only a few grains were obtained. No diagram is presented for this sample since only fifteen grains were analysed. Age results for the 9 concordant analyses range between 997 and 1907 Ma (Appendix A).

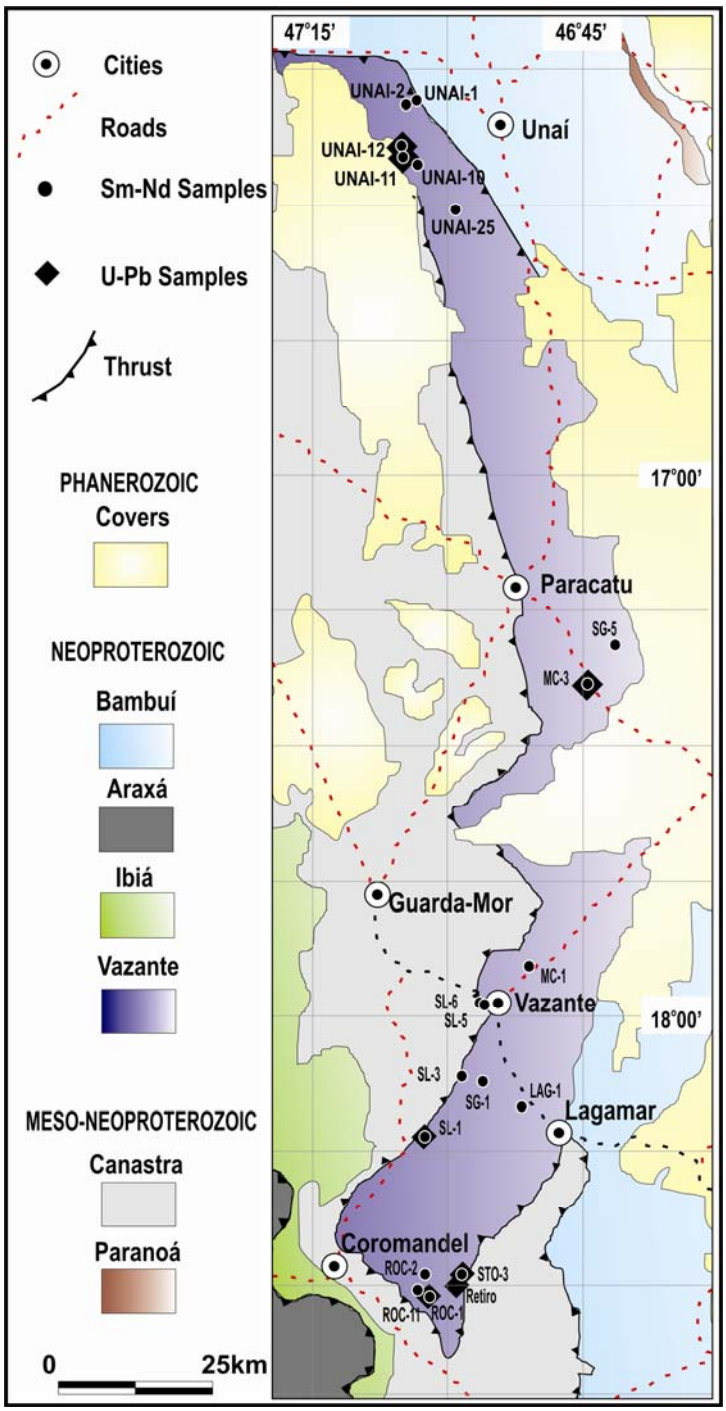

Figure 3.2. Simplified geological map of the Vazante Group with samples locations (modified from Bizzi et al, 2004).

3.4.1.2 – Rocinha Formation

Sample ROC-1 is a medium-grained quartzite from the Coromandel area (Fig. 3.2). The detrital zircon exhibit typical transport features. They comprise colourless rounded prisms to spherical grains. One hundred one grains were analysed and ninety nine produced concordant data. The Rocinha Formation sample (ROC-1) defines a scattered pattern (Fig.3.3),

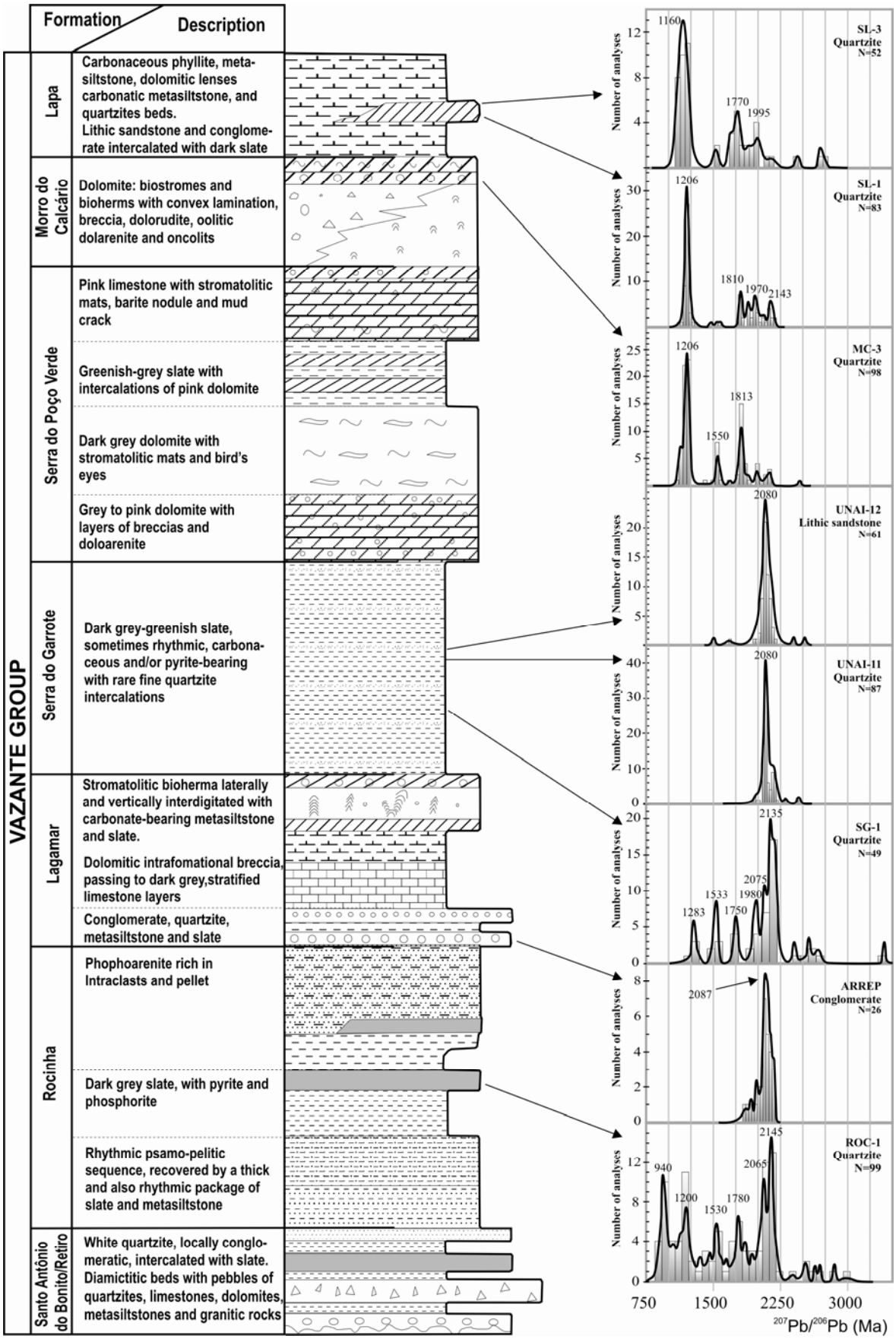

Figure 3.3 – Stratigraphic column of Vazante Group (Dardenne, 2000) and relative probability distribution diagram of $^{207}Pb/^{206}Pb$ zircon ages of the analysed samples.

in which three main peaks are pointed out, at ~2.15, 1.20 and 0.94 Ga. Other subordinate sources are represented by age peaks from 1.1 Ga to 2.99 Ga. The neoproterozoic population is formed by 14 concordant zircon analyses (Fig. 3.4). The youngest concordant age of 935 ± 14 Ma (zircon 53) represents the maximum depositional age of the unit.

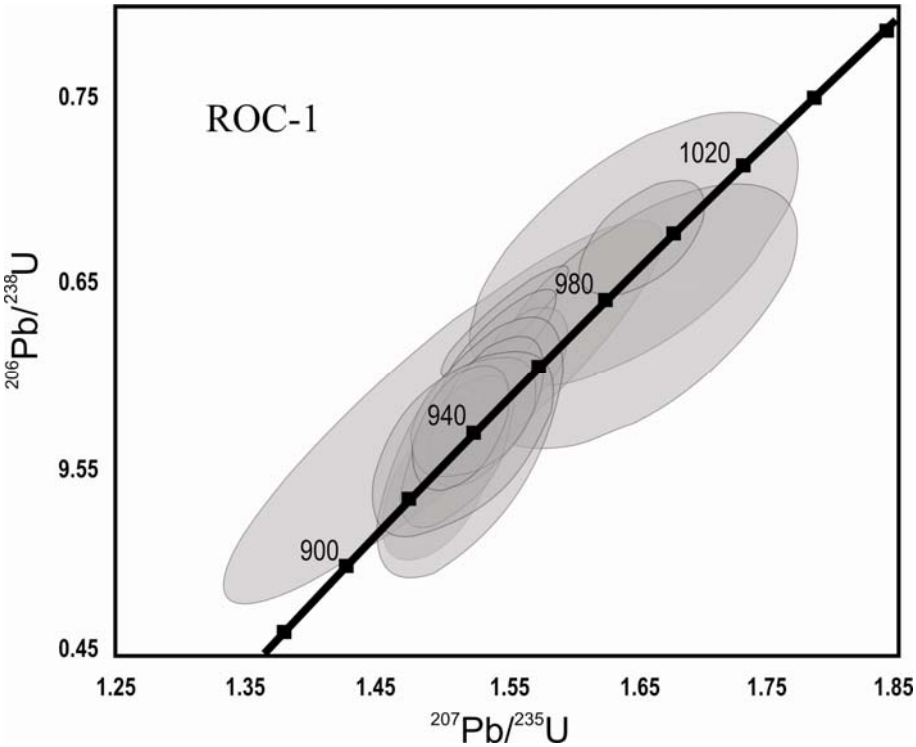

Figure 3.4 – Concordia diagram of the neoproterozoic zircon population of ROC-1.

3.4.1.3 – Serra do Garrote Formation

Three samples of the Serra do Garrote Formation were analysed. Two of them were collected from the Unai region, in the north (UNAI-11 and 12), and a third one (SG-1) from the south (Fig. 3.2). Both in the northern and southern areas of the Vazante Group, these rocks are overlain by a dolomitic unit, which is strikingly continuous along the entire extension of the Vazante Group, from south to north. The provenance patterns for the samples in the northern part of the Vazante Group are very similar and indicate a main Paleoproterozoic (age peak at 2.08 Ga) source (Fig. 3.3). In the southern sample, however, other age peaks are identified (at ca. 1.28, 1.53 and 1.75 Ga). The youngest concordant grain identified in the unit (grain 10) has the age of 1296 ± 13 Ma.

Formation	Sample	Rock	Zircon	Age Peaks (Ga)		Youngest Concordant Age (Ma)
				Main	Minor	
Lapa	SL-1 S 18º 13' 22" W 47º 02' 43"	Massive quartzite	Colorless to light brown, clear, large rounded prisms (83/88)	1.21	1.81, 1.97, 2.14	1164±11 (z59)
	SL-3 S 18º 08' 56" W 46º 58' 55"	Massive quartzite	Colorless to lightly brown, clear, large rounded prisms (52/59)	1.16	1.77, 1.99	1082±14 (z38)
Morro do Calcário	MC-3 S 17º 23' 24" W 46º 44' 30"	Coarse quartzite with carbonaceous matrix	Large, very rounded, clear and colourless (98/100)	1.21	1.55, 1.81	1137±8 (z30)
Serra do Garrote	UNAI-12 S 16º 23' 30" W 47º 05' 03"	Lithic sandstone	Small prismatic, rounded, clear (61/63)	2.08		1944±86 (z33)
	UNAI-11 S 16º 24' 30" W 47º 05' 00"	Coarse quartzite	Large, rounded, clear (87/87)	2.08		1963±16 (z62)
	SG-1 S 18º 09' 46" W 47º 56' 40",	Fine quartzite	Euhedric, rounded, light yellow to brown with some inclusions (49/52)	2.13	1.53, 1.98, 2.07	1296±13 (z10)
Rocinha	ROC-1 S 18º 31' 33" W 47º 02' 03"	Quartzite	Prismatic, spherical, colourless, pink, brownish, yellowish (99/101)	0.94, 2.15	1.20, 1.78, 2.06	935±14 (z53)
Santo Antônio do Bonito	STO-3 S 18º 29' 40" W 46º 58' 10"	Diamictite, with pebbles of mudstone, siltstone and quartzite	Rounded, prismatic, colourless, yellowish (10/15)	-	-	997±29 (z20)

Table 3.1. The main characteristics of the analysed samples. In the Zircon column the numbers represent the used data from the total of analysed grains.

3.4.1.4 – Morro do Calcário Formation

One sample of the Morro do Calcário Formation (MC-3) was analyzed. This is a coarse quartzite with carbonaceous matrix from the Paracatu region. Their zircon grains are large, very rounded, clear and colorless. The probability density plot (Fig. 3.3) shows a main age peak at 1.25 Ga and a minor population at 1.8 Ga. The youngest concordant age observed is 1137±8 Ma (zircon 30).

3.4.1.5 – Lapa Formation

Two quartzite samples of the Lapa Formation (Fig. 3.2) were studied and both (SL-1 and SL-3) show provenance patterns identical to the Morro do Calcário (Fig. 3.3). Sample SL-1 had 88 zircons analyzed, of which, 83 produced concordant data. Fifty nine zircon grains from SL-3 were analyzed and fifty two were concordant. The zircon grains are large, clear, rounded, light brown or colorless. The youngest grains found have the ages of 1084±14 and 1164±11 for SL-3 and SL-1, respectively.

3.4.2 – SHRIMP Zircon Provenance Patterns

The SHRIMP analyses were carried out in one samples of the Arrependido Conglomerate (Lagamar Formation) and pebbles of the basal diamictite (Retiro/Santo Antônio do Bonito Formation).

3.4.2.1 – Santo Antônio do Bonito/Retiro Formation

Thirteen zircon grains were extracted from several small pebbles of the diamictite of the Retiro region (Fig. 3.2). The results are shown in Fig. 3.5 and the complete analytical data set is in the Appendix A.

The analytical points form a poorly defined discordia line indicating the upper intercept of 2081±35 and MSWD =11.2. The paleoproterozoic age of the pebbles is compatible with the pattern obtained by LAM-ICP-MS data for the source of the Vazante Group.

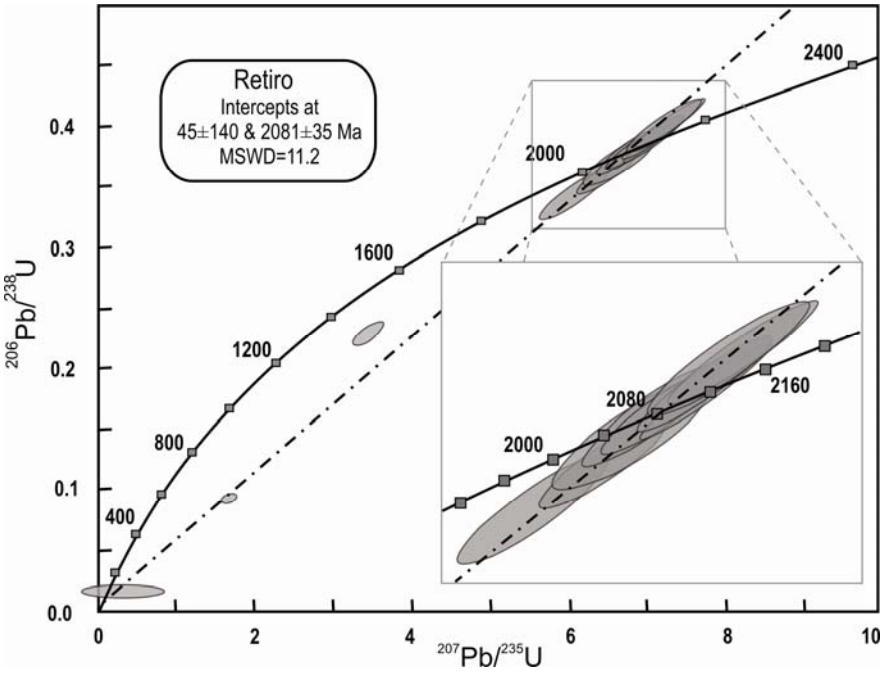

Figure 3.5 – Concordia Diagram for pebbles of the Santo Antônio do Bonito/Retiro Formation.

3.4.2.2 – Lagamar Formation

The Arrependido conglomerate occurs at the base of the Lagamar Formation. Thirty one grains were analyzed and twenty six yielded concordant data and present a main age peak at 2.08 Ga and a minor at 1.98 Ga. The provenance pattern (Fig. 3.3) is very similar to that of the Serra do Garrote samples, suggesting a similar source area for both formations.

3.4.3 – Sm-Nd Results

Nineteen samples from the Vazante Group had their Sm-Nd composition investigated. The isotopic results are presented in Table 3.2, together with data published by Pimentel et al (2001). The analysed samples show a large range in Sm and Nd concentrations (0.78-12.61 ppm and 4.17-73.55 ppm, respectively), with $^{147}Sm/^{144}Nd$ ratios ranging in the interval between 0.097 and 0.138.

Sample	Rock	GPS data		Sm	Nd	$^{143}Nd/^{144}Nd$	$^{147}Sm/^{144}Nd$	T_{DM}
		Latitude	Longitude	(ppm)	(ppm)			(Ga)
LAPA FORMATION								
SL-1	quartzite	-18.222820	-47.045310	0.79	4.96	0.511752±18	0.097	1.67
SL-3	quartzite	-18.148920	-46.981860	1.32	6.95	0.511749±20	0.115	1.98
SL-5	quartzite	-17.980540	-46.921910	6.82	38.21	0.511643±21	0.108	2.00
SL-6pel	rhythmite	-17.994220	-46.927910	9.07	48.28	0.511909±15	0.113	1.71
MGV-8*				6.33	33.14	0.511888±05	0.115	1.78
MGV-7*				7.64	43.61	0.511678±06	0.106	1.91
KJF41-6*				9.85	55.31	0.511825±08	0.108	1.72
CX-100*				5.24	25.57	0.511933±09	0.124	1.87
CX-50*				4.74	22.34	0.511959±03	0.128	1.87
PALMITAL*				4.09	20.22	0.511998±04	0.122	1.70
MORRO DO CALCÁRIO FORMATION								
MC-1	marble	-17.972190	-46.891808	4.9	27.46	0.511521±28	0.108	2.18
MC-3	quartzite	-17.389906	-46.741733	3.72	20.17	0.511619±11	0.112	2.11
SERRA DO POÇO VERDE FORMATION								
VAZ-1B*				6.5	36.41	0.511566±05	0.108	2.10
VAZ-1ª*				6.08	35.03	0.511649±05	0.105	1.94
VAZ-1C*				5.43	30.66	0.51158±04	0.107	2.07
M-244-6*				2.41	16.54	0.51145±03	0.088	1.92
M-244-4*				4.52	38.81	0.511321±03	0.070	1.82
SERRA DO GARROTE FORMATION								
UNAI-10B	quartzite	-16.406350	-47.082110	4.24	22.78	0.511555±20	0.112	2.23
UNAI-11	quartzite	-16.408200	-47.083330	2.48	12.4	0.511362±16	0.121	2.76
UNAI-25B	slate	-16.467920	-47.031880	7.16	43.21	0.511159±19	0.100	2.52
SG-1	quartzite	-18.161440	-46.944420	0.78	4.17	0.511566±20	0.113	2.22
SG-5	fine rhythmite	-17.365032	-46.679000	6.08	26.71	0.511851±17	0.138	2.38
BT-48	Lithic sandstone			1.71	8.77	0.511623±10	0.118	2.24
K-44-13*				5.62	30.78	0.511626±06	0.111	2.03
K-44-20*				4.67	24.57	0.511715±05	0.116	2.05
LAGAMAR FORMATION								
LAG-1	slate	-18.176859	-46.858604	4.68	25.14	0.511765±19	0.117	1.91
ROCINHA FORMATION								
UNAI-1pel	rhythmite	-16.264011	-47.073519	10.91	61.21	0.511628±15	0.107	2.02
UNAI-2pel	rhythmite	-16.275326	-47.077753	7.86	45.31	0.511594±06	0.105	2.02
UNAI-1	siltstone	-16.264011	-47.073519	3.46	17.67	0.511605±07	0.118	2.29
ROC-1	quartzite	-18.525892	-47.034313	2.57	15.08	0.511645±19	0.103	1.91
ROC-2	quartzite	-18.495627	-47.052077	1.12	6.38	0.511274±11	0.107	2.51
ROC-3	slate	-18.518259	-47.048407	12.61	73.55	0.511683±10	0.104	1.87

Table 3.2. Sm-Nd data for samples of Vazante Group, (*) samples from Pimentel et al (2001).

Although all formations present some variation in the T_{DM} values, the results may be divided into three groups: a) the youngest group, composed by samples of the Lapa Formation, b) the oldest group, represented by the Serra do Garrote Formation, and c) The intermediate group, comprising all others units (Fig. 3.6).

The most striking feature of the Nd isotopic data is the clearly younger T_{DM} values (as low as 1.67 Ga) for samples of the Lapa Formation (Figure 3.6). Some of these young values are not compatible with sediment derivation from Paleoproterozoic terrains of the São Francisco Craton and require the contribution from younger sources.

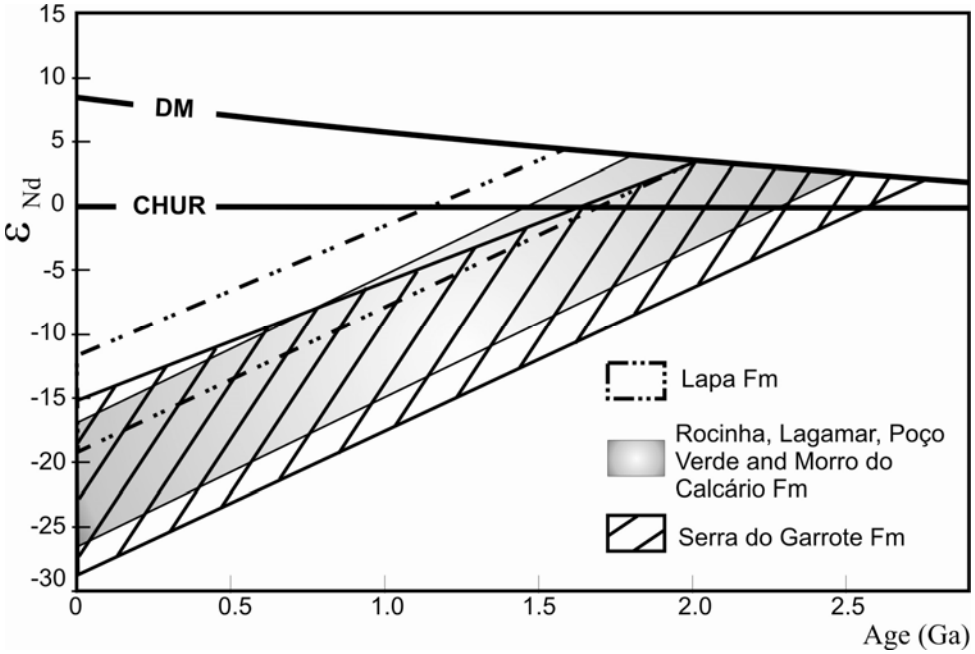

Figure 3.6 – Nd evolution diagram for the Vazante Group.

3.5- DISCUSSION

3.5.1 Depositional Age

Previous studies pointed out that the depositional age of the Vazante Group remains poorly constrained, with values ranging between 1.35 and 0.63 Ga. The LAM-ICP-MS U-Pb data presented here allowed to better constrain this interval. The youngest concordant zircon grain was identified in the Rocinha Formation and its age of 935±14 Ma is taken here as the maximum depositional age for the Vazante Group, what led to interpret the Vazante Group as a Neoproterozoic deposit. The minimum depositional age is given by the metamorphic peak of the Brasília Belt of 630 Ma (Pimentel et al., 1999).

The detrital zircon age pattern of the Rocinha Formation is not coherent with the isochron Re-Os age (Azmy et al., 2008) for rocks from the Lapa Formation (~1.0 Ga).

3.5.2 Source Region and Tectonic Implications

U-Pb zircon ages show that the detrital zircon signatures vary significantly along the deposition history of Vazante Group. The basal sample of the Vazante Group (STO-3) did not yield sufficient zircon grains to allow a solid statistical assessment about its source. Nevertheless the data present some similarity with the Rocinha sample. Zircon ages of the conglomerate of the Lagamar Formation, on the other hand, present a rather different pattern; the neoproterozoic population is not observed and paleoproterozoic rocks represent the main sediment source. The Serra do Garrote Fm sample from the Vazante area presents a broader age distribution, however without the neoproterozoic population. Samples collected in the northern part of the area (Unaí region – Figure 3.2) display very different characteristics: - UNAI-11 is a coarse quartzite, with large rounded zircon grains and UNAI-12 is a lithic sandstone with small prismatic zircons. Despite the differences in shape and size of the zircon grains, both samples present a simple provenance pattern with a single peak at 2.15 Ga (Fig. 3.3)

The Sm-Nd model ages of rocks of the Rocinha and Lagamar formations denote some contribution of younger sources, they furnished T_{DM} values of ~1.91 Ga, what is not observed in samples of the Serra do Garrote Formation, which consistently show T_{DM} values older than 2.2 Ga (Tab. 3.3 and Fig. 3.6). Both U-Pb and Sm-Nd data suggest that sources younger than Paleoproterozoic were not involved in the provenance of the Serra do Garrote sediments.

Although an unconformity is identified between the Morro do Calcário and Lapa formations (Misi et al., 2005), these units display similar provenance patterns, indicating significant contribution from 1.2 Ga old sources and minor contributions of 1.6-2.15 Ga areas. The majority of T_{DM} ages of these rocks are younger than 2.0 Ga suggesting the participation of younger and maybe distal (Meso- or Neoproterozoic) sources.

The combined U-Pb data for the Vazante Group (565 valid analyses) indicate that paleoproterozoic terrains (1.7-2.3 Ga) represents the major sediment suppliers to the Vazante basin (Fig. 3.7). The second major source is represented by Mesoproterozoic grains (ca. 1.15-1.30) Ga.

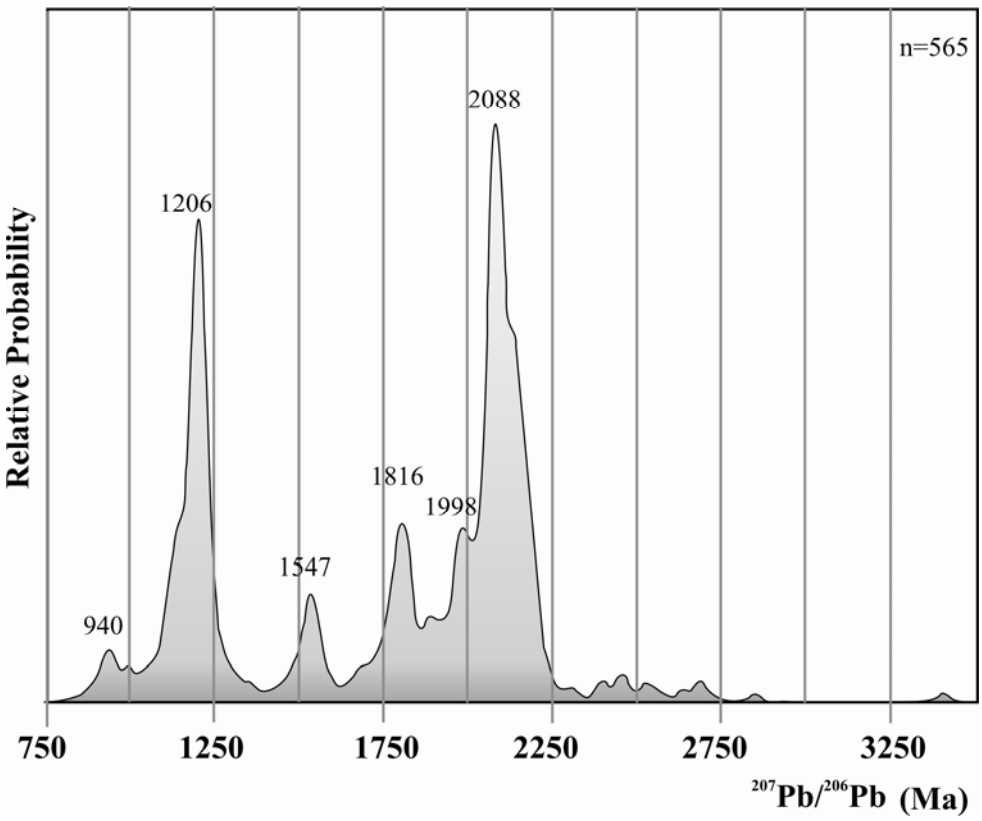

Figure 3.7 - $^{207}Pb/^{206}Pb$ age histogram for all detrital zircon grains from the Vazante Group.

3.6 - CONCLUSIONS

Several paleoproterozoic terrains identified within the São Francisco-Craton (Oliveira et al., 1999, Silva et al, 2002a,b, D'el Rey Silva et al, 2007, Rios et al, 2007, Noce et al., 2007, among others) may represent the main source areas of the detrital sediments of the Vazante Group. The origin of the other main source (1.15-1.25 Ga) is not obvious. A ca. 1.2 Ga old magmatic arc recently identified in the southwest segment of the Brasília Belt (Klein, 2008) might have been probably source for zircons, but mesoproterozoic terrains of the São Francisco-Congo Craton with similar age (Hanson et al., 1988, Tack et al., 1994, Ring et al., 1999) can not discarded.

The youngest (ca. 940 Ma) population (2.5% of zircons) only occurs at the lowest stratigraphic units of the Vazante Group suggesting that this particular source was, later in the evolution of the basin, somehow isolated or covered. Limited magmatism of the early Neoproterozoic is recognized in the São Francisco Craton (Silva et al., 2008), but other

possible sources for these zircon grains may be identified within the Congo Craton (Tack et al., 2001, Kokonyangi et al, 2004).

The correlation with Otavi Group suggested by Azmy et al (2006) was not confirmed by our data. In this correlation, the interpreted diamictite found in the top of the group should be interpreted as a Marinoan unit; in such case the sediment of the Lapa Formation should be deposited later than 650 Ma, but at ca. 650 Ma the Goiás Magmatic Arc (0.9-0.6 Ga) might have been in the vicinities of the Vazante sedimentary basin and would have likely provided detrital material. Also the Sr isotopic data for carbonatic rocks of Vazante Group reported in the literature (Azmy et al. 2001, Misi et al., 2005) are around 0.7068 (Lapa Formation), being comparable to that of the sea water at 780-700 Ma (Halverson et al. 2007).

ACKNOWLEDGEMENTS

This work benefited from financial support from the Companhia de Pesquisa de Recursos Minerais and CNPq. We are grateful to the Companhia Mineira de Metais for the great assistance during field work. We also thank the staff of the Laboratório de Geocronologia da Universidade de Brasília for their assistance.

3.7- ROCHAS ÍGNEAS ASSOCIADAS

A limitada associação de rochas ígneas a rochas do Grupo Vazante tem dificultado a determinação precisa de sua idade. Duas restritas associações foram identificadas e tornaram-se alvo deste trabalho, um dique máfico alojado em rochas da Formação Serra do Poço Verde e um pequeno corpo tonalítico em contato tectônico com metarritimitos da Formação Serra do Garrote (?).

3.7.1 – Dique Máfico

Estas rochas, compostas principalmente por plagioclásio e ortopiroxênio alterados hidrotermalmente, foram recentemente estudadas por Babinski *et al.* (2007) e representam um magmatismo máfico de reduzida escala. Os pequenos corpos apresentam-se de forma descontínua alojados na Zona de Cisalhamento de Vazante. Os melhores afloramentos são encontrados em subsuperfície na Mina da Votorantim Metais, em Vazante.

Visando datar o magmatismo pelo método U-Pb, duas amostras (~70 Kg) foram coletadas em superfície e a cerca de 100 metros de profundidade. Apenas 5 grãos de zircão foram encontrados, e destes um forneceu dados discordantes (Tab. 3.3) e o outro teve a análise abortada em função do alto conteúdo de urânio. Devido suas características morfológicas e idades $^{207}Pb/^{206}Pb$ dos grãos concordantes (1917, 2113 e 2963 Ma), os zircões foram interpretados como xenocristais.

		Razões								Idades				
Grão	f_{206} %	$^{206}Pb/^{204}Pb$	$^{207}Pb/^{206}Pb$	±	$^{207}Pb/^{235}U$	±	$^{206}Pb/^{238}U$	±	Rho	$^{207}Pb/^{206}Pb$	±	$^{206}Pb/^{238}U$	±	Disc. %
~~1~~	~~4.87~~	~~331~~	~~0.194100~~	~~1.25~~	~~7.077~~	~~3.99~~	~~0.264419~~	~~3.79~~	~~0.95~~	~~2777~~	~~20~~	~~1512~~	~~51~~	~~45.54~~
3	0.00	infinito	0.217536	1.23	15.380	1.89	0.512768	1.43	0.94	2963	20	2668	31	9.93
4	0.53	2841	0.131136	2.44	6.950	4.52	0.384390	3.80	0.83	2113	42	2097	68	0.78
5	1.38	1110	0.117376	3.73	5.476	7.74	0.338334	6.78	0.28	1917	65	1879	110	1.98

Tabela 3.3 – Dados U-Pb (LAM-ICP-MS) da amostra DM-1.

Alternativamente foi tentada a produção de uma isócrona Sm-Nd em rocha total, porém a rocha mostrou-se muito homogênea (Tab. 3.4) e não houve espalhamento suficiente da razão $^{147}Sm/^{144}Nd$ para a obtenção de um alinhamento razoável. As idades modelo das amostras analisadas são próximas a 1.1 Ga, valores idênticos aos encontrado por Babinski *et al* (2007) para a mesma unidade.

Amostra	Rocha	Dados de GPS		Sm	Nd	^{143}Nd	^{147}Sm	T_{DM}	$\varepsilon_{Nd}(0)$	$\varepsilon_{Nd}(800)$
		Latitude	Longitude	(ppm)	(ppm)	^{144}Nd	^{144}Nd	(Ga)		
DM-1	máfica	-17.950958	-46.843156	6.18	23.89	0.512634±06	0.156	1.08	-0.09	
DM-2	máfica	-17.953199	-46.847993	5.89	22.86	0.512625±08	0.156	1.09	1.04	
DM-3	máfica	-17,953929	-46,848071	6.14	23.25	0.512672±16	0.160	1.04	0.66	
UNAI-19	tonalito	-16.230626	-47.252393	4.18	25.1	0.511374±14	0.101	2.24	-24.65	-14.86

Tabela 3.4 – Dados Sm-Nd de amostras do dique máfico alojado na Fm Serra do Poço Verde e do tonalito da região de Unaí.

3.7.2 – Corpo Arrependido

A região centro-sudeste da Faixa Brasília é essencialmente representada por rochas sedimentares, assim a exposição isolada de uma rocha ígnea que ocorre no limite norte do Grupo Vazante passa a ter grande relevância. Esta rocha ocorre em um único afloramento com cerca de 450x250 metros. O contato com os sedimentos do Grupo Vazante ocorre por meio de falha, o que torna a sua relação temporal com o grupo indefinida. Exceto nas proximidades da falha, onde é folheada, a rocha apresenta-se bastante muito homogênea e maciça. A rocha foi alterada por processos hidrotermais que formaram considerável volume de epidoto e carbonato, no entanto é possível observar relictos de plagioclásio e hornblenda, além de poucos grãos de quartzo, o que permite sugerir que a composição original da rocha tenha sido semelhante à tonalítica.

Amostras foram coletadas para análises geocronológicas de U-Pb e Sm-Nd. Os grãos de zircão extraídos da amostra são prismas bipiramidais 2:1-3:1, com cerca de 60 μm de diâmetro, límpidos e incolores. Apesar de apresentar somente um tipo morfológico, as análises revelaram dois grupos de idades bem distintas (Tab. 3.5). Os dados do grupo Paleoproterozóico não permitiram calcular uma concórdia (Fig.3.8), porém suas idades $^{207}Pb/^{206}Pb$ apresentaram-se bastante uniformes, o que possibilitou calcular o valor médio de 2144±29 Ma. Esta idade é interpretada como herança. A população mais jovem apresentou razões isotópicas homogêneas e foi possível calcular a *Concordia Age* de 785±10 Ma a partir de 7 análises. Esta idade é interpretada como a idade de cristalização da rocha. A amostra analisada para Sm-Nd (Tab. 3.3) forneceu T_{DM} de 2.24 Ga e ε_{Nd} (800) de -14.86, o que denota a origem crustal do protolito.

Grão	f_{206} %	Razões $^{206}Pb/^{204}Pb$	$^{207}Pb/^{206}Pb$	±	$^{207}Pb/^{235}U$	±	$^{206}Pb/^{238}U$	±	Rho	Idades $^{207}Pb/^{206}Pb$	±	$^{206}Pb/^{238}U$	±	Disc. %
5	**0.97**	**1803**	**0.062996**	**4.01**	**1.117**	**4.02**	**0.128095**	**3.10**	**0.77**	**708**	**83**	**777**	**23**	**-9.73**
7	**0.02**	**80485**	**0.066154**	**6.30**	**1.140**	**6.21**	**0.123720**	**4.54**	**0.73**	**811**	**126**	**752**	**32**	**7.31**
9	**0.27**	**6532**	**0.064400**	**5.80**	**1.152**	**5.22**	**0.129842**	**4.29**	**0.82**	**755**	**118**	**787**	**32**	**-4.26**
15	**1.07**	**1624**	**0.064393**	**8.20**	**1.134**	**7.97**	**0.129233**	**5.73**	**0.72**	**755**	**164**	**783**	**42**	**-3.83**
16	**1.85**	**938**	**0.065219**	**5.75**	**1.187**	**6.20**	**0.134387**	**4.19**	**0.68**	**781**	**116**	**813**	**32**	**-4.02**
20	**0.22**	**7795**	**0.065891**	**4.83**	**1.220**	**4.01**	**0.134618**	**3.65**	**0.91**	**803**	**98**	**814**	**28**	**-1.40**
24	**0.44**	**3998**	**0.065698**	**9.81**	**1.208**	**8.00**	**0.133611**	**7.31**	**0.91**	**797**	**193**	**808**	**55**	**-1.46**
1	0.38	3938	0.132540	5.40	7.177	5.69	0.393976	4.05	0.71	2132	92	2141	73	-0.44
~~*2*~~	~~*0.87*~~	~~*1786*~~	~~*0.136257*~~	~~*4.57*~~	~~*6.218*~~	~~*5.44*~~	~~*0.332670*~~	~~*4.04*~~	~~*0.74*~~	~~*2180*~~	~~*77*~~	~~*1851*~~	~~*65*~~	~~*15.08*~~
6	0.40	3672	0.133219	3.92	7.385	3.99	0.404399	3.10	0.78	2141	67	2189	57	-2.26
8	0.00	infinito	0.134395	6.51	7.054	6.34	0.378413	4.75	0.75	2156	109	2069	84	4.05
10	0.29	5125	0.131443	4.11	7.198	3.74	0.395191	3.03	0.81	2117	70	2147	55	-1.39
11	0.00	infinito	0.135082	6.34	7.538	4.42	0.403817	4.62	0.98	2165	107	2187	85	-0.99
13	0.26	5609	0.131239	5.58	7.539	4.97	0.420122	4.06	0.82	2115	95	2261	77	-6.92
14	0.23	6356	0.131426	3.84	7.577	3.42	0.419947	2.79	0.81	2117	66	2260	53	-6.76
17	0.30	4859	0.131097	3.93	7.539	3.78	0.413750	3.04	0.80	2113	67	2232	57	-5.65
21	0.00	infinito	0.134691	3.06	7.956	2.74	0.428385	2.28	0.83	2160	52	2298	44	-6.41
22	0.00	infinito	0.133551	3.46	7.620	2.90	0.413750	2.55	0.88	2145	59	2232	48	-4.05
26	0.00	infinito	0.134517	4.74	7.847	4.16	0.422903	3.48	0.84	2158	80	2274	66	-5.37

Tabela 3.5 – Dados U-Pb (LAM-ICP-MS) da amostra UNAI-19. Os grãos em negrito são da população jovem. O grão 2 foi excluído do cálculo da idade. Os erros estão apresentados em 1 sigma. Correções de chumbo comum foram realizadas a partir da razão $^{206}Pb/^{204}Pb$.

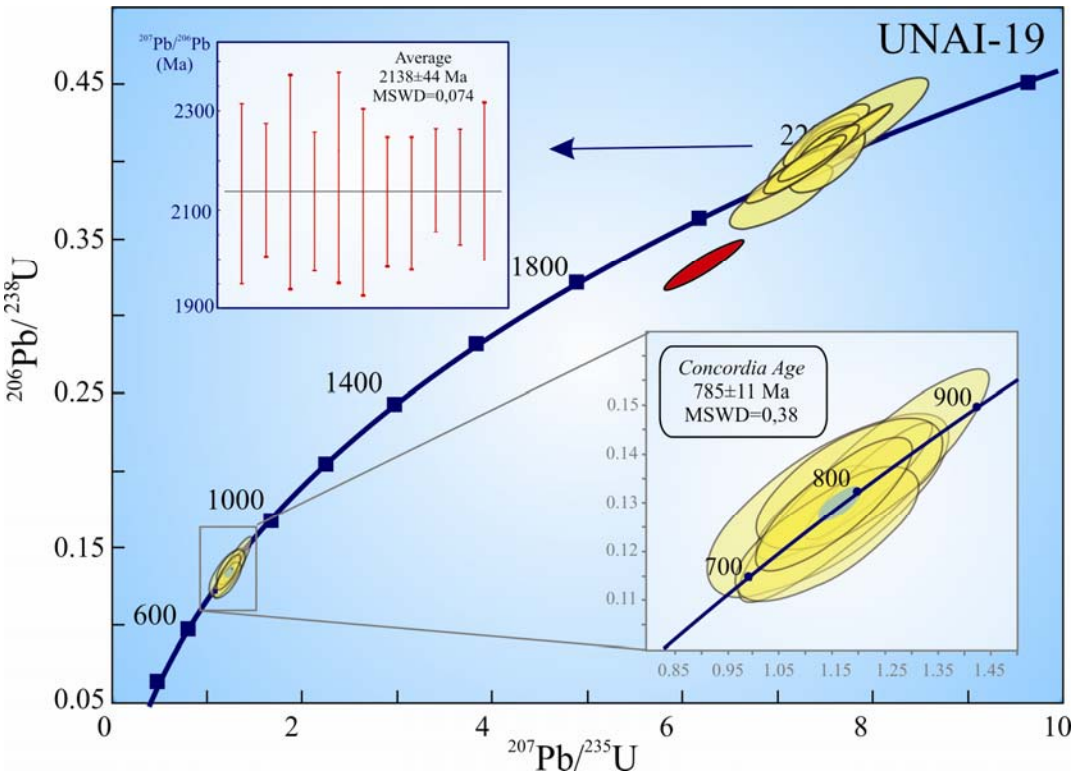

Figura 3.8 – Diagrama da Concórdia para análises das duas populações de zircão da amostra UNAI-19.

3.8 - APPENDIX A – U-Pb DATA OF THE VAZANTE GROUP

Notes: 1. Uncertainties given at the one σ level (%).
2. f^{206}% denotes the percentage of ^{206}Pb that is common Pb.
3. Correction for common Pb made using the measured $^{206}Pb/^{204}Pb$ ratio.
4. For %Disc., 0% denotes a concordant analysis.

Table 3.6 – U-Pb LAM-ICP-MS data of the sample STO-3.

Grain	f_{206} %	Ratios							Rho	Ages (Ma)				Disc. %
		$^{206}Pb/^{204}Pb$	$^{207}Pb/^{206}Pb$	±	$^{207}Pb/^{235}U$	±	$^{206}Pb/^{238}U$	±		$^{207}Pb/^{206}Pb$	±	$^{206}Pb/^{238}U$	±	
~~1~~	~~2.22~~	~~750~~	~~0.119143~~	~~1.49~~	~~3.469~~	~~3.13~~	~~0.211167~~	~~2.75~~	~~0.90~~	~~1943~~	~~26~~	~~1235~~	~~31~~	~~36.45~~
3	2.88	590	0.073190	6.98	1.743	7.61	0.172729	3.05	0.83	1019	135	1027	29	-0.78
~~4~~	~~3.71~~	~~450~~	~~0.103018~~	~~1.72~~	~~2.882~~	~~2.18~~	~~0.202883~~	~~1.34~~	~~0.23~~	~~1679~~	~~32~~	~~1191~~	~~15~~	~~29.09~~
5	0.00	infinite	0.073318	0.95	1.733	1.33	0.171452	0.94	0.85	1023	19	1020	9	0.26
7	0.22	6908	0.116735	2.74	5.492	3.56	0.341184	2.27	0.94	1907	48	1892	37	0.76
8	0.14	11852	0.094493	0.71	3.455	1.75	0.265154	1.60	0.90	1518	13	1516	22	0.12
~~10~~	~~9.86~~	~~169~~	~~0.134646~~	~~2.97~~	~~3.824~~	~~3.21~~	~~0.205955~~	~~1.23~~	~~0.88~~	~~2159~~	~~51~~	~~1207~~	~~14~~	~~44.09~~
11	0.00	infinite	0.078164	0.75	2.101	1.63	0.194990	1.45	0.95	1151	15	1148	15	0.23
12	0.10	16239	0.077957	0.66	2.093	2.08	0.194740	1.97	0.95	1146	13	1147	21	-0.11
~~13~~	~~0.00~~	~~infinite~~	~~0.089055~~	~~2.38~~	~~2.240~~	~~4.29~~	~~0.182455~~	~~3.57~~	~~0.97~~	~~1405~~	~~45~~	~~1080~~	~~35~~	~~23.12~~
14	0.00	infinite	0.104571	2.40	4.402	7.71	0.305292	7.33	0.90	1707	43	1717	110	-0.63
15	0.00	infinite	0.081166	0.62	2.344	1.61	0.209490	1.48	0.90	1225	12	1226	17	-0.05
~~16~~	~~0.71~~	~~2545~~	~~0.057508~~	~~1.61~~	~~0.449~~	~~1.84~~	~~0.056610~~	~~0.90~~	~~0.40~~	~~511~~	~~35~~	~~355~~	~~3~~	~~30.54~~
20	0.20	8707	0.072406	0.57	1.668	5.64	0.167127	5.61	0.94	997	12	996	52	0.11
~~21~~	~~2.26~~	~~695~~	~~0.120101~~	~~1.66~~	~~5.089~~	~~2.15~~	~~0.307344~~	~~1.36~~	~~0.79~~	~~1958~~	~~29~~	~~1728~~	~~21~~	~~11.75~~

Table 3.7 – U-Pb LAM-ICP-MS data of the sample ROC-1.

Grain	f_{206} %	Ratios							Rho	Ages (Ma)				Disc. %
		$^{206}Pb/^{204}Pb$	$^{207}Pb/^{206}Pb$	±	$^{207}Pb/^{235}U$	±	$^{206}Pb/^{238}U$	±		$^{207}Pb/^{206}Pb$	±	$^{206}Pb/^{238}U$	±	
1	0.00	infinite	0.070646	1.05	1.521	3.83	0.156190	3.69	0.65	947	21	936	32	1.23
2	0.05	32759	0.126924	2.39	6.771	3.28	0.386918	2.25	0.89	2056	42	2109	40	-2.56
3	0.22	6709	0.127409	1.69	6.738	2.08	0.383580	1.23	0.78	2063	29	2093	22	-1.48
4	0.00	infinite	0.069816	1.01	1.514	2.02	0.157297	1.75	0.46	923	21	942	15	-2.04
5	0.04	41771	0.132573	2.73	7.528	3.75	0.411833	2.57	0.84	2132	47	2223	48	-4.27
6	0.00	infinite	0.071770	0.97	1.686	1.99	0.170425	1.74	0.79	979	20	1014	16	-3.58
7	0.00	infinite	0.133654	0.95	7.298	2.23	0.396015	2.01	0.79	2147	17	2151	37	-0.19
8	0.00	infinite	0.079956	0.95	2.229	2.64	0.202211	2.47	0.79	1196	19	1187	27	0.73
9	0.05	37766	0.071582	1.81	1.653	2.36	0.167502	1.51	0.55	974	37	998	14	-2.49
10	0.00	infinite	0.202949	0.93	15.689	4.86	0.560657	4.77	0.88	2850	15	2869	110	-0.68
11	0.00	infinite	0.126930	0.95	6.621	3.07	0.378297	2.92	0.94	2056	17	2068	51	-0.60
12	0.00	infinite	0.124950	0.93	6.405	1.62	0.371797	1.32	0.83	2028	16	2038	23	-0.48
15	0.09	17629	0.081908	1.78	2.427	2.33	0.214939	1.50	0.82	1243	35	1255	17	-0.95
16	0.01	106707	0.110137	3.93	5.102	5.51	0.335991	3.86	0.93	1802	70	1867	62	-3.65
17	0.02	70269	0.165072	1.85	11.486	2.44	0.504642	1.58	0.89	2508	31	2634	34	-5.00
18	0.02	91552	0.096393	1.98	3.703	2.67	0.278647	1.79	0.92	1555	37	1585	25	-1.87
19	0.00	infinite	0.108285	0.95	4.811	3.35	0.322264	3.22	0.95	1771	17	1801	50	-1.70
21	0.57	2903	0.077469	5.25	2.222	6.46	0.208058	3.77	0.81	1133	101	1218	42	-7.52
22	0.14	12334	0.073016	3.81	1.784	4.73	0.177178	2.79	0.84	1014	75	1052	27	-3.66

Tabele 3.7 - ROC -1 (continued)

Grain	f_{206} %	Ratios							Rho	Ages (Ma)				Disc. %
		$^{206}Pb/^{204}Pb$	$^{207}Pb/^{206}Pb$	±	$^{207}Pb/^{235}U$	±	$^{206}Pb/^{238}U$	±		$^{207}Pb/^{206}Pb$	±	$^{206}Pb/^{238}U$	±	
23	0.00	infinite	0.112759	0.96	5.126	6.03	0.329736	5.96	0.92	1844	17	1837	95	0.39
24	0.00	infinite	0.178086	0.98	12.698	2.83	0.517152	2.66	0.89	2635	16	2687	58	-1.97
25	0.00	infinite	0.134784	0.95	7.518	2.59	0.404565	2.41	0.79	2161	17	2190	45	-1.33
26	0.00	infinite	0.077254	0.96	2.023	2.74	0.189900	2.56	0.78	1128	19	1121	26	0.61
27	0.00	infinite	0.091784	0.95	3.293	1.76	0.260210	1.48	0.88	1463	18	1491	20	-1.91
28	0.09	16626	0.105141	2.72	4.539	3.75	0.313121	2.58	0.80	1717	49	1756	40	-2.29
29	0.03	45747	0.130984	3.53	7.342	4.89	0.406533	3.39	0.84	2111	61	2199	63	-4.16
30	0.14	12235	0.079681	7.39	2.415	9.15	0.219795	5.39	0.92	1189	139	1281	62	-7.71
31	0.04	36906	0.135663	1.50	7.689	1.93	0.411066	1.20	0.66	2173	26	2220	23	-2.17
32	0.06	25162	0.153381	2.27	9.689	3.15	0.458169	2.19	0.74	2384	38	2431	44	-1.99
33	0.24	6357	0.109520	1.94	5.029	2.41	0.333025	1.42	0.71	1791	35	1853	23	-3.44
34	0.00	infinite	0.086558	0.96	2.856	2.33	0.239269	2.13	0.53	1351	18	1383	26	-2.39
35	0.00	infinite	0.133480	0.96	7.491	2.05	0.407046	1.80	0.87	2144	17	2201	34	-2.67
35	0.00	infinite	0.127402	0.96	6.596	5.81	0.375491	5.73	0.91	2062	17	2055	100	0.35
38	0.68	2521	0.073343	4.73	1.651	5.93	0.163310	3.58	0.62	1023	93	975	32	4.72
39	0.10	16937	0.068807	7.42	1.501	9.15	0.158215	5.35	0.90	893	146	947	47	-6.04
41	0.00	infinite	0.183940	0.94	13.194	2.13	0.520247	1.91	0.93	2689	15	2700	42	-0.43
43	0.38	3906	0.130736	1.78	7.028	2.20	0.389911	1.28	0.83	2108	31	2122	23	-0.69
~~44~~	~~0.03~~	~~44832~~	~~0.108175~~	~~7.69~~	~~4.880~~	~~10.90~~	~~0.327151~~	~~7.72~~	~~0.92~~	~~1769~~	~~134~~	~~1825~~	~~122~~	~~-3.15~~
45	0.20	8365	0.078931	6.18	2.300	7.62	0.211328	4.46	0.87	1170	118	1236	50	-5.60
46	0.19	7840	0.136082	2.47	7.747	3.08	0.412873	1.83	0.86	2178	42	2228	34	-2.30
47	0.10	16195	0.089886	2.97	3.213	4.13	0.259271	2.87	0.90	1423	56	1486	38	-4.43
48	0.11	15285	0.080834	3.45	2.435	4.25	0.218434	2.48	0.75	1217	66	1274	29	-4.62
49	0.00	infinite	0.118112	0.95	6.000	2.49	0.368404	2.30	0.85	1928	17	2022	40	-4.88
51	0.19	8342	0.106381	4.21	4.709	5.20	0.321028	3.05	0.88	1738	75	1795	48	-3.25
52	0.00	infinite	0.134427	0.94	7.499	1.94	0.404610	1.69	0.71	2157	16	2190	31	-1.56
53	0.00	infinite	0.070258	0.99	1.511	2.37	0.155983	2.16	0.58	936	20	934	19	0.16
55	0.00	infinite	0.133701	0.95	7.398	4.92	0.401323	4.83	0.84	2147	16	2175	89	-1.30
57	0.00	infinite	0.070403	1.02	1.563	1.76	0.160963	1.44	0.46	940	21	962	13	-2.34
59	0.11	14314	0.114104	4.52	5.550	5.55	0.352754	3.21	0.83	1866	79	1948	54	-4.39
60	0.14	11314	0.105963	5.27	4.712	6.47	0.322487	3.75	0.77	1731	94	1802	59	-4.09
61	0.00	infinite	0.123441	0.94	6.556	1.25	0.385173	0.82	0.76	2007	17	2100	15	-4.68
64	0.00	infinite	0.095358	0.94	3.666	2.40	0.278829	2.20	0.86	1535	18	1585	31	-3.28
65	0.00	infinite	0.128167	0.94	6.993	1.93	0.395737	1.68	0.77	2073	17	2149	31	-3.69
66	0.03	56631	0.070030	1.97	1.525	2.60	0.157890	1.70	0.43	929	40	945	15	-1.70
69	0.00	infinite	0.133041	0.98	7.479	2.21	0.407720	1.98	0.81	2138	17	2204	37	-3.09
70	0.00	infinite	0.167848	1.07	10.958	1.45	0.473503	0.98	0.92	2536	18	2499	20	1.47
71	0.28	5756	0.090023	2.62	3.130	3.23	0.252202	1.90	0.77	1426	49	1450	25	-1.67
74	0.04	39289	0.130643	2.38	7.206	3.21	0.400021	2.16	0.87	2107	41	2169	40	-2.97
75	0.03	52477	0.123084	3.15	6.369	4.38	0.375310	3.04	0.82	2001	55	2054	53	-2.64
76	0.27	5652	0.108962	6.98	5.042	8.57	0.335632	4.98	0.77	1782	122	1866	80	-4.68
78	0.18	9422	0.068867	2.11	1.548	2.59	0.163032	1.50	0.91	895	43	974	14	-8.81
80	0.09	17224	0.094700	1.69	3.734	2.16	0.286001	1.36	0.77	1522	31	1622	19	-6.53
81	0.10	15045	0.136634	3.86	7.987	5.38	0.423957	3.74	0.95	2185	66	2278	71	-4.28
82	0.02	91495	0.138046	1.49	7.997	1.91	0.420133	1.19	0.82	2203	26	2261	23	-2.64
83	0.00	infinite	0.079930	0.96	2.313	3.72	0.209858	3.59	0.64	1195	19	1228	40	-2.74
84	0.25	6384	0.105968	7.17	4.014	8.82	0.274694	5.14	0.94	1731	126	1565	71	9.62
85	0.29	5166	0.129939	3.45	7.280	4.27	0.406357	2.50	0.76	2097	59	2198	46	-4.82
86	0.00	infinite	0.127430	0.96	6.725	7.00	0.382751	6.94	0.95	2063	17	2089	123	-1.27
87	0.28	5770	0.082549	3.52	2.689	4.33	0.236215	2.53	0.82	1259	67	1367	31	-8.61
88	0.00	infinite	0.070410	0.96	1.498	2.42	0.154300	2.22	0.55	940	20	925	19	1.63
89	0.02	90967	0.090447	2.63	3.215	3.62	0.257827	2.48	0.73	1435	49	1479	33	-3.05
90	0.00	infinite	0.108890	0.95	4.787	2.35	0.318821	2.15	0.76	1781	17	1784	33	-0.17
94	0.00	infinite	0.080752	0.97	2.348	1.75	0.210923	1.46	0.77	1215	19	1234	16	-1.51
~~96~~	~~0.18~~	~~8954~~	~~0.088051~~	~~9.20~~	~~2.914~~	~~11.29~~	~~0.239998~~	~~6.55~~	~~0.93~~	~~1384~~	~~167~~	~~1387~~	~~81~~	~~-0.22~~

Tabele 3.7 - ROC -1 (continued)

Grain	f_{206} %	Ratios $^{206}Pb/^{204}Pb$	$^{207}Pb/^{206}Pb$	±	$^{207}Pb/^{235}U$	±	$^{206}Pb/^{238}U$	±	Rho	Ages (Ma) $^{207}Pb/^{206}Pb$	±	$^{206}Pb/^{238}U$	±	Disc. %
97	0.00	infinite	0.114037	0.94	5.487	3.20	0.348989	3.06	0.86	1865	17	1930	51	-3.49
98	0.00	infinite	0.078368	0.94	2.183	4.87	0.202065	4.78	0.91	1156	19	1186	52	-2.61
99	0.00	infinite	0.079869	0.98	2.252	3.14	0.204519	2.99	0.71	1194	19	1200	33	-0.48
100	0.00	364783	0.097996	0.96	3.865	3.38	0.286034	3.24	0.82	1586	18	1622	46	-2.23
101	0.00	infinite	0.095349	0.96	3.661	2.63	0.278500	2.45	0.91	1535	18	1584	34	-3.18
102	0.00	infinite	0.070322	1.00	1.534	2.34	0.158182	2.11	0.59	938	20	947	19	-0.95
103	0.00	infinite	0.095213	0.96	3.565	1.99	0.271572	1.75	0.82	1532	18	1549	24	-1.08
104	0.00	infinite	0.132797	0.95	7.459	2.23	0.407375	2.01	0.86	2135	17	2203	37	-3.17
105	0.18	9555	0.071572	5.03	1.647	6.20	0.166902	3.62	0.62	974	99	995	33	-2.18
106	0.00	infinite	0.074160	1.06	1.809	5.38	0.176946	5.27	0.55	1046	21	1050	51	-0.43
107	0.12	14116	0.080997	5.11	2.391	6.26	0.214108	3.60	0.54	1221	97	1251	41	-2.40
108	0.00	infinite	0.100827	0.96	4.132	4.64	0.297245	4.54	0.74	1639	18	1678	67	-2.33
109	0.13	10214	0.220170	4.83	17.889	5.92	0.589292	3.43	0.93	2982	76	2987	81	-0.15
110	0.48	3132	0.118285	7.19	5.921	8.85	0.363035	5.15	0.91	1930	123	1997	88	-3.42
115	0.08	21920	0.069192	1.76	1.543	2.34	0.161723	1.54	0.83	904	36	966	14	-6.84
116	0.00	infinite	0.109151	0.96	4.937	2.71	0.328076	2.53	0.79	1785	17	1829	40	-2.45
117	0.27	5482	0.132053	4.28	7.156	5.27	0.393048	3.08	0.87	2125	73	2137	56	-0.54
118	0.94	1801	0.076630	2.92	1.977	3.54	0.187104	2.00	0.14	1112	57	1106	20	0.53
119	0.42	3959	0.078393	5.99	2.265	7.40	0.209572	4.34	0.85	1157	114	1227	48	-6.02
120	0.04	41766	0.131417	3.05	7.208	4.23	0.397787	2.93	0.94	2117	53	2159	54	-1.98
121	0.02	69648	0.121075	1.62	6.094	2.11	0.365055	1.34	0.90	1972	29	2006	23	-1.72
122	0.09	15834	0.134049	4.05	7.405	5.70	0.400654	4.02	0.92	2152	69	2172	74	-0.95
125	0.01	169952	0.070263	2.68	1.516	3.76	0.156448	2.64	0.56	936	54	937	23	-0.10
126	0.21	8129	0.078973	4.91	2.161	6.02	0.198468	3.49	0.86	1171	94	1167	37	0.37
127	0.31	5370	0.072636	3.34	1.852	4.10	0.184888	2.38	0.53	1004	66	1094	24	-8.95
128	0.33	4486	0.131061	2.00	7.347	2.48	0.406560	1.46	0.83	2112	35	2199	27	-4.12
129	0.03	58101	0.076334	2.05	2.008	2.75	0.190757	1.83	0.50	1104	41	1125	19	-1.96

Table 3.8 – U-Pb LAM-ICP-MS data of the sample SG-1.

Grain	f_{206} %	Ratios $^{206}Pb/^{204}Pb$	$^{207}Pb/^{206}Pb$	±	$^{207}Pb/^{235}U$	±	$^{206}Pb/^{238}U$	±	Rho	Ages (Ma) $^{207}Pb/^{206}Pb$	±	$^{206}Pb/^{238}U$	±	Disc. %
1	0.00	infinite	0.171028	0.98	11.954	1.28	0.506943	0.81	0.80	2568	16	2644	18	-2.95
2	0.00	infinite	0.136866	0.98	7.961	1.18	0.421888	0.67	0.70	2188	17	2269	13	-3.71
3	0.00	infinite	0.095241	0.99	3.550	1.19	0.270314	0.67	0.67	1533	18	1542	9	-0.62
4	0.17	8148	0.174673	4.48	11.907	5.33	0.494385	2.89	0.93	2603	73	2590	61	0.51
5	0.00	infinite	0.106506	0.98	4.705	1.28	0.320394	0.82	0.80	1740	18	1792	13	-2.94
6	0.00	infinite	0.155235	0.99	9.864	1.29	0.460835	0.83	0.87	2404	17	2443	17	-1.62
7	0.00	infinite	0.122184	0.97	6.489	1.17	0.385194	0.64	0.78	1988	17	2101	12	-5.64
8	0.00	infinite	0.132534	0.98	7.439	1.16	0.407073	0.63	0.58	2132	17	2202	12	-3.27
9	0.00	infinite	0.094379	0.98	3.577	1.17	0.274857	0.65	0.71	1516	18	1565	9	-3.28
10	0.23	7258	0.084751	1.71	2.597	2.09	0.222264	1.20	0.55	1310	33	1294	14	1.22
11	0.42	3452	0.136159	2.64	7.766	3.24	0.413680	1.88	0.82	2179	45	2232	35	-2.42
12	0.06	21363	0.181966	2.05	13.317	2.17	0.530798	0.71	0.94	2671	34	2745	16	-2.77
13	0.08	20016	0.106952	1.88	4.777	1.99	0.323956	0.65	0.66	1748	34	1809	10	-3.48
14	0.19	7885	0.132095	2.54	7.412	3.11	0.406934	1.79	0.84	2126	44	2201	33	-3.52
15	0.03	50101	0.163714	6.20	10.791	6.24	0.478059	0.71	0.75	2494	101	2519	15	-0.98
16	0.00	infinite	0.083773	0.96	2.633	1.22	0.227935	0.76	0.77	1287	19	1324	9	-2.83
17	0.00	infinite	0.107595	0.95	4.768	1.22	0.321409	0.76	0.73	1759	17	1797	12	-2.13
18	0.00	infinite	0.083149	0.96	2.604	1.22	0.227174	0.75	0.74	1273	19	1320	9	-3.69

Tabele 3.8 - SG -1 (continued)

Grain	f_{206} %	Ratios $^{206}Pb/^{204}Pb$	$^{207}Pb/^{206}Pb$	±	$^{207}Pb/^{235}U$	±	$^{206}Pb/^{238}U$	±	Rho	Ages (Ma) $^{207}Pb/^{206}Pb$	±	$^{206}Pb/^{238}U$	±	Disc. %
20	0.00	infinite	0.095562	0.94	3.511	1.13	0.266504	0.63	0.69	1539	17	1523	9	1.05
~~21~~	~~0.00~~	~~infinite~~	~~0.129371~~	~~0.94~~	~~5.983~~	~~1.21~~	~~0.335413~~	~~0.76~~	~~0.87~~	~~2089~~	~~16~~	~~1865~~	~~12~~	~~10.76~~
22	0.15	9673	0.134481	3.16	7.794	3.88	0.420328	2.25	0.64	2157	54	2262	43	-4.85
23	0.11	13209	0.135388	3.07	8.036	3.76	0.430500	2.17	0.82	2169	53	2308	42	-6.41
24	0.00	infinite	0.121590	0.99	6.221	1.19	0.371061	0.66	0.64	1980	17	2034	11	-2.76
25	0.00	infinite	0.134133	0.97	7.463	1.24	0.403546	0.78	0.85	2153	17	2185	14	-1.51
26	0.00	infinite	0.128141	0.95	7.002	1.16	0.396299	0.66	0.76	2073	17	2152	12	-3.83
27	0.00	infinite	0.132624	0.95	7.292	1.18	0.398766	0.70	0.91	2133	17	2163	13	-1.42
~~28~~	~~2.58~~	~~657~~	~~0.084448~~	~~5.89~~	~~2.042~~	~~7.16~~	~~0.175402~~	~~4.07~~	~~0.75~~	~~1303~~	~~110~~	~~1042~~	~~39~~	~~20.04~~
29	0.00	infinite	0.135227	0.99	7.468	1.21	0.400521	0.69	0.84	2167	17	2171	13	-0.21
31	0.00	infinite	0.126376	1.29	6.704	1.72	0.384754	1.14	0.88	2048	23	2098	20	-2.46
33	0.02	75954	0.135017	2.57	7.657	2.65	0.411317	0.66	0.87	2164	44	2221	12	-2.62
34	0.01	105590	0.120576	1.28	6.084	1.75	0.365941	1.19	0.96	1965	23	2010	21	-2.32
36	0.14	10499	0.120989	2.09	6.208	2.61	0.372132	1.56	0.84	1971	37	2039	27	-3.48
38	0.11	13180	0.132810	5.34	7.535	6.54	0.411470	3.78	0.92	2135	91	2222	71	-4.04
39	0.00	infinite	0.129017	0.95	6.898	1.20	0.387755	0.73	0.93	2085	17	2112	13	-1.33
40	0.72	2285	0.081858	3.75	2.555	4.68	0.226361	2.80	0.29	1242	72	1315	33	-5.90
41	0.36	4155	0.135274	5.69	7.530	7.01	0.403736	4.09	0.93	2168	96	2186	75	-0.86
42	0.24	5996	0.136642	2.62	7.793	3.25	0.413617	1.91	0.87	2185	45	2231	36	-2.12
43	0.19	8372	0.107833	2.66	4.873	3.28	0.327784	1.92	0.88	1763	48	1828	30	-3.66
44	0.12	12829	0.127130	2.40	6.854	2.94	0.391033	1.69	0.77	2059	42	2128	31	-3.35
45	0.00	infinite	0.132774	0.97	7.068	1.22	0.386059	0.74	0.83	2135	17	2105	13	1.43
~~46~~	~~0.37~~	~~4147~~	~~0.130749~~	~~5.53~~	~~6.129~~	~~7.11~~	~~0.339979~~	~~4.47~~	~~0.97~~	~~2108~~	~~94~~	~~1887~~	~~73~~	~~10.51~~
47	0.10	14714	0.118534	3.30	6.059	4.04	0.370707	2.34	0.84	1934	58	2033	41	-5.09
48	0.00	infinite	0.288410	0.94	28.884	1.17	0.726362	0.69	0.91	3409	15	3520	19	-3.25
49	0.00	infinite	0.095626	0.99	3.686	1.22	0.279591	0.71	0.61	1540	19	1589	10	-3.17
54	0.00	infinite	0.127376	0.94	6.897	1.14	0.392684	0.63	0.72	2062	17	2135	11	-3.55
55	0.00	infinite	0.138271	0.98	7.939	1.21	0.416424	0.70	0.62	2206	17	2244	13	-1.75
57	0.00	infinite	0.119170	0.97	5.821	1.17	0.354254	0.66	0.70	1944	17	1955	11	-0.57
59	0.00	infinite	0.137063	0.94	7.976	1.13	0.422063	0.62	0.79	2190	16	2270	12	-3.63
64	0.00	infinite	0.135940	0.95	7.459	1.14	0.397930	0.64	0.79	2176	16	2160	12	0.76
65	0.00	infinite	0.093033	1.00	3.161	1.21	0.246445	0.68	0.81	1489	19	1420	9	4.60
70	0.00	infinite	0.133166	0.94	7.390	1.14	0.402480	0.64	0.88	2140	16	2180	12	-1.88
71	0.00	infinite	0.131599	0.94	7.252	1.14	0.399666	0.64	0.79	2119	16	2168	12	-2.27

Table 3.9 – U-Pb LAM-ICP-MS data of the sample UNAI-11.

Grain	f_{206} %	Ratios $^{206}Pb/^{204}Pb$	$^{207}Pb/^{206}Pb$	±	$^{207}Pb/^{235}U$	±	$^{206}Pb/^{238}U$	±	Rho	Ages (Ma) $^{207}Pb/^{206}Pb$	±	$^{206}Pb/^{238}U$	±	Disc. %
1	0.00	infinite	0.129797	0.95	6.972	1.20	0.389574	0.74	0.86	2095	17	2121	13	-1.22
2	0.00	infinite	0.137021	0.97	7.790	1.24	0.412312	0.77	0.84	2190	17	2225	14	-1.63
3	0.00	infinite	0.130612	0.96	7.024	1.22	0.390015	0.76	0.83	2106	17	2123	14	-0.79
4	0.57	2632	0.129366	4.09	6.942	5.06	0.389205	2.98	0.92	2089	70	2119	54	-1.42
5	0.97	1526	0.134879	3.15	7.460	3.93	0.401134	2.36	0.84	2162	54	2174	43	-0.55
6	0.00	infinite	0.129136	0.96	6.731	1.22	0.378058	0.76	0.81	2086	17	2067	13	0.91
7	0.00	infinite	0.129365	0.95	7.083	1.17	0.397087	0.69	0.89	2089	17	2156	13	-3.17
8	0.00	infinite	0.134238	0.94	7.484	1.13	0.404341	0.63	0.76	2154	16	2189	12	-1.62
9	0.00	infinite	0.129159	0.94	6.970	1.15	0.391377	0.65	0.86	2087	16	2129	12	-2.04
10	0.00	infinite	0.130675	0.95	7.109	1.15	0.394572	0.65	0.77	2107	17	2144	12	-1.75
11	0.00	infinite	0.130134	0.95	7.074	1.16	0.394242	0.66	0.88	2100	17	2142	12	-2.03

Tabele 3.9 - UNAI -11 (continued)

Grain	f_{206} %	Ratios							Rho	Ages (Ma)				Disc. %
		$^{206}Pb/^{204}Pb$	$^{207}Pb/^{206}Pb$	±	$^{207}Pb/^{235}U$	±	$^{206}Pb/^{238}U$	±		$^{207}Pb/^{206}Pb$	±	$^{206}Pb/^{238}U$	±	
12	0.00	infinite	0.130134	0.95	7.074	1.16	0.394242	0.66	0.88	2100	17	2142	12	-2.03
13	0.00	infinite	0.129978	0.95	7.139	1.25	0.398375	0.81	0.84	2098	17	2162	15	-3.05
14	0.00	infinite	0.129400	0.95	7.074	1.23	0.396495	0.78	0.86	2090	17	2153	14	-3.02
15	0.00	infinite	0.129957	0.95	7.086	1.21	0.395449	0.75	0.75	2097	17	2148	14	-2.42
16	0.00	infinite	0.128839	0.95	6.973	1.16	0.392553	0.68	0.82	2082	17	2135	12	-2.52
18	0.00	infinite	0.129185	0.95	7.103	1.16	0.398750	0.67	0.74	2087	17	2163	12	-3.66
19	0.00	infinite	0.129222	0.99	7.134	1.22	0.400402	0.72	0.76	2087	17	2171	13	-4.00
19	0.09	17493	0.127949	1.50	6.866	1.64	0.389212	0.64	0.84	2070	26	2119	12	-2.38
22	0.00	infinite	0.133065	0.96	7.370	1.17	0.401702	0.67	0.73	2139	17	2177	12	-1.78
24	0.43	3439	0.134144	5.98	7.221	7.34	0.390434	4.25	0.92	2153	101	2125	77	1.30
25	1.47	1023	0.129812	9.37	6.597	11.50	0.368562	6.67	0.75	2095	156	2023	115	3.47
26	0.00	infinite	0.132748	0.94	7.286	1.14	0.398055	0.63	0.82	2135	16	2160	12	-1.19
27	0.00	infinite	0.128991	0.94	7.027	1.13	0.395088	0.63	0.87	2084	16	2146	11	-2.98
28	0.03	47876	0.135252	3.86	7.510	3.92	0.402707	0.67	0.90	2167	66	2181	12	-0.66
29	0.13	11752	0.127443	1.77	6.874	2.17	0.391216	1.26	0.87	2063	31	2128	23	-3.17
31	0.00	infinite	0.129321	0.96	7.206	1.17	0.404132	0.67	0.81	2089	17	2188	12	-4.75
32	0.00	infinite	0.129777	0.95	7.204	1.17	0.402576	0.67	0.71	2095	17	2181	12	-4.10
33	0.00	infinite	0.129485	0.94	7.111	1.17	0.398321	0.69	0.93	2091	16	2161	13	-3.36
34	0.00	infinite	0.159388	0.95	10.597	1.18	0.482191	0.70	0.87	2449	16	2537	15	-3.58
35	0.00	infinite	0.129285	0.96	7.091	1.17	0.397775	0.67	0.81	2088	17	2159	12	-3.38
36	0.00	infinite	0.121162	0.95	6.200	1.17	0.371118	0.67	0.85	1973	17	2035	12	-3.10
37	0.00	infinite	0.129197	0.96	6.995	1.16	0.392660	0.66	0.69	2087	17	2135	12	-2.30
38	0.06	26385	0.123832	1.73	6.350	1.85	0.371886	0.66	0.86	2012	30	2038	12	-1.30
39	0.00	infinite	0.128277	0.95	6.889	1.15	0.389520	0.65	0.89	2074	17	2121	12	-2.22
40	0.02	63546	0.137516	2.84	7.934	2.91	0.418444	0.67	0.82	2196	48	2253	13	-2.61
41	0.00	infinite	0.134862	0.95	7.657	1.20	0.411789	0.72	0.90	2162	17	2223	14	-2.82
42	0.00	infinite	0.128444	0.95	7.210	1.16	0.407093	0.67	0.90	2077	17	2202	13	-6.01
43	0.05	28503	0.129781	1.45	7.106	1.61	0.397108	0.70	0.87	2095	25	2156	13	-2.90
44	0.00	infinite	0.134917	0.96	7.661	1.21	0.411805	0.74	0.80	2163	17	2223	14	-2.78
45	0.00	infinite	0.128824	0.95	7.129	1.17	0.401347	0.69	0.79	2082	17	2175	13	-4.48
46	0.03	50002	0.132453	1.56	7.370	1.70	0.403572	0.67	0.68	2131	27	2185	12	-2.57
47	0.00	infinite	0.128726	0.96	7.171	1.17	0.404021	0.68	0.83	2081	17	2188	13	-5.14
50	0.00	infinite	0.160518	0.96	10.689	1.18	0.482951	0.69	0.85	2461	16	2540	15	-3.21
51	0.12	11971	0.128038	5.39	7.198	6.59	0.407725	3.80	0.92	2071	92	2205	71	-6.44
52	0.16	9013	0.131345	3.42	7.363	4.21	0.406601	2.45	0.80	2116	59	2199	46	-3.94
53	0.06	25392	0.127503	1.54	6.952	1.69	0.395458	0.70	0.89	2064	27	2148	13	-4.08
54	0.06	25697	0.127760	1.53	6.952	1.67	0.394645	0.67	0.77	2067	27	2144	12	-3.72
55	0.04	39087	0.128189	3.10	7.068	3.22	0.399876	0.85	0.95	2073	54	2168	16	-4.59
57	0.00	infinite	0.128537	0.95	6.927	1.17	0.390872	0.69	0.89	2078	17	2127	12	-2.35
58	0.06	23618	0.128297	2.47	6.870	2.56	0.388386	0.67	0.87	2075	43	2115	12	-1.96
59	0.00	infinite	0.137306	0.96	7.752	1.18	0.409448	0.68	0.84	2193	17	2212	13	-0.86
60	0.06	27236	0.127882	2.43	6.718	2.54	0.381019	0.74	0.93	2069	42	2081	13	-0.58
61	0.08	17426	0.135872	2.23	7.804	2.34	0.416572	0.70	0.87	2175	38	2245	13	-3.20
62	0.13	11654	0.119615	4.31	5.912	5.30	0.358435	3.07	0.88	1950	75	1975	52	-1.24
63	0.08	17926	0.128276	1.87	6.798	2.00	0.384352	0.71	0.93	2074	33	2097	13	-1.07
64	0.00	infinite	0.146842	0.97	8.875	1.23	0.438348	0.76	0.87	2309	17	2343	15	-1.46
66	0.00	infinite	0.127876	0.96	6.882	1.18	0.390343	0.69	0.83	2069	17	2124	12	-2.68
67	0.00	infinite	0.128384	0.96	7.035	1.20	0.397404	0.72	0.89	2076	17	2157	13	-3.91
69	0.00	infinite	0.128601	0.95	6.871	1.21	0.387497	0.75	0.95	2079	17	2111	13	-1.55
70	0.00	infinite	0.128887	0.95	6.887	1.21	0.387555	0.74	0.93	2083	17	2111	13	-1.37
71	0.34	4342	0.128302	5.03	7.025	6.18	0.397132	3.59	0.91	2075	86	2156	66	-3.90
72	0.00	infinite	0.135912	0.95	7.673	1.20	0.409460	0.74	0.94	2176	16	2212	14	-1.69
73	0.20	7457	0.132627	4.28	7.465	5.28	0.408232	3.10	0.87	2133	73	2207	58	-3.46
74	0.00	infinite	0.129155	0.96	7.090	1.21	0.398129	0.74	0.88	2087	17	2160	14	-3.54
75	0.00	infinite	0.136214	0.95	7.874	1.37	0.419247	0.99	0.96	2180	16	2257	19	-3.55

Tabele 3.9 - UNAI -11 (continued)

Grain	f_{206} %	Ratios							Rho	Ages (Ma)				Disc. %
		$^{206}Pb/^{204}Pb$	$^{207}Pb/^{206}Pb$	±	$^{207}Pb/^{235}U$	±	$^{206}Pb/^{238}U$	±		$^{207}Pb/^{206}Pb$	±	$^{206}Pb/^{238}U$	±	
76	0.16	9421	0.127277	1.86	6.885	2.29	0.392326	1.33	0.88	2061	32	2134	24	-3.54
78	0.00	infinite	0.128673	0.94	7.157	1.16	0.403400	0.68	0.90	2080	17	2185	13	-5.04
80	0.58	2553	0.129297	2.63	6.926	3.24	0.388498	1.89	0.59	2088	45	2116	34	-1.31
81	0.00	infinite	0.131923	0.95	7.453	1.18	0.409718	0.71	0.82	2124	17	2214	13	-4.23
82	0.06	24587	0.121428	3.51	6.215	3.60	0.371195	0.76	0.92	1977	61	2035	13	-2.92
83	0.00	infinite	0.128582	0.94	6.965	1.23	0.392876	0.80	0.93	2079	16	2136	14	-2.77
84	0.29	5098	0.136041	7.40	7.393	9.23	0.394148	5.52	0.97	2177	123	2142	100	1.62
85	0.07	22208	0.134759	2.71	7.695	2.85	0.414148	0.88	0.89	2161	47	2234	17	-3.38
86	0.14	10487	0.134106	3.37	7.554	4.18	0.408522	2.47	0.88	2152	58	2208	46	-2.59
89	0.00	infinite	0.128708	0.93	7.019	1.20	0.395535	0.76	0.95	2080	16	2148	14	-3.27
90	0.06	23369	0.127674	2.81	6.883	2.90	0.391018	0.71	0.93	2066	49	2128	13	-2.97
92	0.00	infinite	0.138604	0.94	8.099	1.15	0.423771	0.66	0.81	2210	16	2278	13	-3.07
93	0.17	8675	0.128189	2.79	6.986	3.43	0.395259	1.99	0.93	2073	48	2147	36	-3.56
94	0.01	198851	0.134875	0.98	7.556	1.34	0.406318	0.92	0.89	2162	17	2198	17	-1.65
95	0.12	12375	0.136284	3.07	7.729	3.79	0.411315	2.21	0.87	2181	53	2221	41	-1.85
96	0.00	infinite	0.128239	0.96	6.924	1.22	0.391601	0.75	0.95	2074	17	2130	14	-2.71
97	0.00	infinite	0.130574	0.97	7.217	1.28	0.400880	0.84	0.95	2106	17	2173	16	-3.20
103	0.00	infinite	0.128464	0.97	6.922	1.21	0.390798	0.73	0.93	2077	17	2127	13	-2.38
104	0.35	4292	0.127779	2.71	6.839	3.34	0.388177	1.96	0.92	2068	47	2114	35	-2.26
105	0.09	16811	0.128668	3.89	7.112	3.96	0.400858	0.73	0.92	2080	67	2173	13	-4.48
106	0.40	3659	0.130668	3.12	7.183	3.84	0.398694	2.23	0.93	2107	54	2163	41	-2.66

Table 3.10 – U-Pb LAM-ICP-MS data of the sample UNAI-12.

Grain	f_{206} %	Ratios							Rho	Ages (Ma)				Disc. %
		$^{206}Pb/^{204}Pb$	$^{207}Pb/^{206}Pb$	±	$^{207}Pb/^{235}U$	±	$^{206}Pb/^{238}U$	±		$^{207}Pb/^{206}Pb$	±	$^{206}Pb/^{238}U$	±	
1	0.22	6818	0.125399	2.04	6.626	2.56	0.383244	1.55	0.94	2034	36	2091	28	-2.80
2	0.14	10655	0.125923	3.88	6.709	4.78	0.386408	2.80	0.93	2042	67	2106	50	-3.15
3	0.17	8688	0.126073	3.21	6.766	4.01	0.389221	2.40	0.96	2044	56	2119	43	-3.68
4	0.22	6636	0.125038	3.97	6.943	4.93	0.402722	2.92	0.95	2029	69	2182	54	-7.50
5	0.00	infinite	0.127760	0.94	7.011	1.60	0.397997	1.29	0.95	2067	17	2160	24	-4.47
6	0.05	27969	0.125684	1.16	6.740	1.33	0.388942	0.66	0.91	2038	20	2118	12	-3.90
7	0.05	28859	0.128453	2.19	6.837	2.97	0.386023	2.00	0.90	2077	38	2104	36	-1.32
8	0.14	10501	0.131275	2.97	7.012	3.64	0.387379	2.11	0.91	2115	51	2111	38	0.21
9	0.00	infinite	0.093856	0.95	3.520	1.60	0.272005	1.29	0.87	1505	18	1551	18	-3.04
10	0.00	infinite	0.127420	0.93	7.126	1.53	0.405618	1.21	0.88	2063	16	2195	23	-6.41
11	0.82	1774	0.132265	3.53	7.640	4.43	0.418939	2.68	0.93	2128	61	2256	51	-5.99
12	0.24	6227	0.131456	2.23	7.259	2.78	0.400479	1.66	0.92	2118	39	2171	30	-2.54
13	0.05	28766	0.126613	2.40	6.822	3.28	0.390781	2.24	0.93	2051	42	2126	40	-3.66
14	0.32	4613	0.124785	2.37	6.609	2.96	0.384118	1.78	0.92	2026	41	2095	32	-3.44
15	0.00	infinite	0.127819	0.96	6.789	1.45	0.385216	1.09	0.93	2068	17	2101	19	-1.57
16	0.16	9271	0.129474	5.25	7.033	6.48	0.393959	3.79	0.87	2091	90	2141	69	-2.41
17	0.00	infinite	0.127910	0.94	7.005	2.85	0.397185	2.69	0.89	2069	16	2156	49	-4.19
18	0.00	infinite	0.154421	0.94	9.873	2.50	0.463681	2.32	0.95	2395	16	2456	47	-2.52
19	0.18	8397	0.127524	3.05	6.982	3.78	0.397095	2.23	0.87	2064	53	2156	41	-4.43
20	0.24	6225	0.130852	3.64	7.519	4.47	0.416735	2.60	0.92	2109	62	2246	49	-6.46

Tabele 3.10 - UNAI -12 (continued)

Grain	f_{206} %	Ratios							Rho	Ages (Ma)				Disc. %
		$^{206}Pb/^{204}Pb$	$^{207}Pb/^{206}Pb$	±	$^{207}Pb/^{235}U$	±	$^{206}Pb/^{238}U$	±		$^{207}Pb/^{206}Pb$	±	$^{206}Pb/^{238}U$	±	
21	0.42	3528	0.129097	3.82	7.122	4.75	0.400113	2.82	0.92	2086	66	2170	52	-4.02
22	0.06	24690	0.129298	2.10	6.892	2.90	0.386576	1.99	0.49	2088	36	2107	36	-0.89
23	0.00	infinite	0.166359	0.93	11.246	1.29	0.490288	0.89	0.95	2521	16	2572	19	-2.01
24	0.24	6316	0.127045	5.54	6.805	6.85	0.388493	4.04	0.84	2057	95	2116	72	-2.84
25	0.09	16094	0.130734	1.41	7.256	1.76	0.402536	1.05	0.93	2108	25	2181	19	-3.46
26	0.10	14538	0.131459	3.54	7.174	4.35	0.395766	2.54	0.92	2118	61	2150	46	-1.51
27	1.38	1125	0.102857	2.01	4.622	3.26	0.325920	2.57	0.96	1676	37	1819	41	-8.49
28	0.06	23131	0.128296	5.13	6.800	7.25	0.384439	5.11	0.90	2075	88	2097	91	-1.07
29	0.07	21052	0.131212	2.02	7.121	2.73	0.393632	1.83	0.92	2114	35	2140	33	-1.20
~~30~~	~~0.20~~	~~7532~~	~~0.126486~~	~~8.81~~	~~6.761~~	~~10.78~~	~~0.387678~~	~~6.21~~	~~0.92~~	~~2050~~	~~148~~	~~2112~~	~~111~~	~~-3.04~~
31	0.17	8652	0.128253	1.71	6.734	2.12	0.380805	1.26	0.93	2074	30	2080	22	-0.28
32	0.49	3033	0.126035	2.44	6.701	2.98	0.385601	1.71	0.71	2043	42	2102	31	-2.89
33	0.19	8230	0.119192	8.16	5.785	10.00	0.351985	5.79	0.93	1944	139	1944	96	0.00
34	0.00	infinite	0.132667	0.97	7.403	2.99	0.404721	2.83	0.54	2134	17	2191	52	-2.68
35	0.00	infinite	0.135899	0.96	7.959	2.47	0.424775	2.28	0.94	2176	17	2282	44	-4.90
36	0.00	infinite	0.127405	0.95	7.001	2.24	0.398530	2.03	0.91	2062	17	2162	37	-4.84
37	0.11	12783	0.132252	5.82	7.496	7.21	0.411074	4.26	0.91	2128	98	2220	79	-4.31
38	0.00	infinite	0.129059	0.95	7.120	3.05	0.400095	2.90	0.87	2085	17	2169	53	-4.04
40	0.22	6494	0.128266	6.75	7.472	8.28	0.422495	4.80	0.95	2074	114	2272	91	-9.52
41	0.24	6052	0.128439	5.02	7.048	6.21	0.398014	3.65	0.93	2077	86	2160	67	-4.01
42	0.00	infinite	0.128246	0.95	6.931	3.61	0.391943	3.49	0.94	2074	17	2132	63	-2.79
43	0.00	infinite	0.129113	2.23	7.012	3.02	0.393883	2.03	0.92	2086	39	2141	37	-2.63
44	0.00	infinite	0.129015	0.97	6.834	3.56	0.384203	3.43	0.86	2085	17	2096	61	-0.54
45	0.00	infinite	0.129206	0.96	6.961	4.51	0.390744	4.41	0.90	2087	17	2126	79	-1.87
45	1.00	1489	0.138203	4.32	7.482	5.35	0.392617	3.14	0.38	2205	73	2135	57	3.17
47	0.36	4066	0.126723	2.44	6.955	3.06	0.398038	1.84	0.94	2053	42	2160	34	-5.21
48	0.00	infinite	0.130121	0.95	7.400	5.97	0.412463	5.90	0.94	2100	17	2226	110	-6.03
~~49~~	~~0.13~~	~~11535~~	~~0.136839~~	~~8.72~~	~~8.165~~	~~10.71~~	~~0.432752~~	~~6.22~~	~~0.92~~	~~2188~~	~~144~~	~~2318~~	~~120~~	~~-5.97~~
50	0.17	8649	0.127869	3.72	7.136	4.57	0.404778	2.65	0.90	2069	64	2191	49	-5.90
51	0.06	23778	0.132706	1.68	7.630	2.19	0.417008	1.41	0.90	2134	29	2247	27	-5.29
52	0.00	infinite	0.132913	1.06	7.997	1.81	0.436361	1.47	0.97	2137	18	2334	29	-9.24
53	0.09	15939	0.128116	2.68	6.986	3.66	0.395488	2.49	0.82	2072	46	2148	45	-3.67
54	0.11	13462	0.133813	1.91	7.695	2.37	0.417052	1.40	0.95	2149	33	2247	27	-4.58
55	0.19	7764	0.133045	3.12	7.534	3.82	0.410678	2.20	0.93	2139	54	2218	41	-3.72
56	0.00	infinite	0.134948	2.13	7.677	2.88	0.412580	1.93	0.93	2163	37	2227	36	-2.93
57	0.08	17866	0.129158	5.13	7.187	7.28	0.403595	5.17	0.84	2087	88	2186	95	-4.75
59	0.11	14289	0.121450	2.82	6.337	3.47	0.378406	2.02	0.88	1978	49	2069	36	-4.61
60	0.00	infinite	0.130043	3.56	7.336	4.94	0.409130	3.43	0.93	2099	61	2211	64	-5.36
61	0.49	3024	0.134172	4.14	7.321	5.13	0.395718	3.02	0.81	2153	71	2149	55	0.18
62	0.00	infinite	0.130070	0.96	7.025	3.81	0.391700	3.69	0.90	2099	17	2131	67	-1.52
63	0.08	17635	0.131838	2.39	7.132	3.27	0.392345	2.23	0.92	2123	41	2134	40	-0.52
64	0.00	infinite	0.130137	0.97	7.300	7.34	0.406847	7.27	0.94	2100	17	2200	134	-4.79
65	0.00	infinite	0.129685	0.97	7.244	3.27	0.405120	3.12	0.94	2094	17	2193	58	-4.72

Table 3.11 – U-Pb LAM-ICP-MS data of the sample MC-3.

Grain	f_{206} %	Ratios							Rho	Ages (Ma)				Disc. %
		$^{206}Pb/^{204}Pb$	$^{207}Pb/^{206}Pb$	±	$^{207}Pb/^{235}U$	±	$^{206}Pb/^{238}U$	±		$^{207}Pb/^{206}Pb$	±	$^{206}Pb/^{238}U$	±	
1	0.00	infinite	0.080454	0.96	2.372	1.22	0.213814	0.76	0.87	1208	19	1249	9	-3.39
2	0.00	infinite	0.080851	0.96	2.396	1.25	0.214952	0.80	0.87	1218	19	1255	9	-3.06
3	0.00	infinite	0.111751	0.95	5.434	1.20	0.352668	0.74	0.92	1828	17	1947	12	-6.52
4	0.00	infinite	0.078885	0.96	1.972	1.20	0.181333	0.71	0.80	1169	19	1074	7	8.13
5	0.00	infinite	0.077419	0.95	1.940	1.30	0.181743	0.89	0.94	1132	19	1076	9	4.90
6	0.00	infinite	0.080958	0.96	2.143	1.18	0.191948	0.69	0.82	1220	19	1132	7	7.25
7	0.00	infinite	0.111513	0.95	5.164	1.26	0.335849	0.83	0.89	1824	17	1867	13	-2.33
8	0.00	infinite	0.096398	0.95	3.702	1.27	0.278556	0.85	0.92	1556	18	1584	12	-1.83
9	0.00	infinite	0.110750	0.94	5.228	1.21	0.342349	0.76	0.92	1812	17	1898	13	-4.76
10	0.00	infinite	0.095597	0.94	3.656	1.19	0.277393	0.73	0.92	1540	18	1578	10	-2.49
11	0.00	infinite	0.116588	1.06	5.227	4.09	0.325133	3.95	0.93	1905	19	1815	62	4.72
12	0.00	infinite	0.121902	0.93	6.289	1.25	0.374173	0.83	0.96	1984	17	2049	15	-3.26
13	0.00	infinite	0.080496	0.97	2.306	4.02	0.207807	3.90	0.97	1209	19	1217	43	-0.66
14	0.00	infinite	0.133131	0.94	7.586	1.18	0.413247	0.72	0.91	2140	16	2230	13	-4.21
15	0.00	infinite	0.080589	0.95	2.311	1.16	0.207937	0.66	0.79	1211	19	1218	7	-0.53
16	0.00	infinite	0.080227	0.96	2.312	1.17	0.209040	0.67	0.77	1203	19	1224	7	-1.76
17	0.00	infinite	0.096151	0.96	3.805	1.19	0.286989	0.71	0.82	1551	18	1626	10	-4.88
17	0.00	infinite	0.080459	0.94	2.384	1.18	0.214923	0.71	0.91	1208	18	1255	8	-3.87
19	0.07	22822	0.123814	5.04	6.164	5.39	0.361051	1.90	0.97	2012	87	1987	32	1.23
20	0.04	45181	0.080200	1.94	2.305	2.03	0.208462	0.61	0.71	1202	38	1221	7	-1.56
21	0.01	160978	0.080536	0.93	2.374	1.12	0.213795	0.62	0.86	1210	18	1249	7	-3.21
22	0.01	116286	0.079689	4.81	2.268	4.86	0.206456	0.68	0.89	1189	92	1210	7	-1.73
~~23~~	~~1.05~~	~~1614~~	~~0.080758~~	~~6.08~~	~~2.045~~	~~7.48~~	~~0.183672~~	~~4.35~~	~~0.90~~	~~1216~~	~~115~~	~~1087~~	~~43~~	~~10.58~~
25	0.00	infinite	0.077763	0.94	2.101	1.31	0.195991	0.92	0.94	1141	19	1154	10	-1.13
26	0.00	infinite	0.096353	0.97	3.549	1.23	0.267128	0.76	0.84	1555	18	1526	10	1.83
27	0.00	infinite	0.111363	0.94	5.052	1.22	0.329025	0.78	0.94	1822	17	1834	12	-0.65
28	0.00	infinite	0.110457	0.94	4.822	1.15	0.316638	0.66	0.88	1807	17	1773	10	1.86
29	0.94	1593	0.128566	4.00	6.858	4.90	0.386898	2.83	0.70	2078	69	2108	51	-1.44
30	0.00	infinite	0.077488	0.94	2.061	1.20	0.192864	0.75	0.93	1134	19	1137	8	-0.27
31	0.00	infinite	0.096847	1.03	3.667	1.34	0.274600	0.86	0.89	1564	19	1564	12	0.01
32	0.00	infinite	0.111076	0.94	5.216	1.19	0.340593	0.72	0.82	1817	17	1890	12	-3.99
33	0.00	infinite	0.080273	0.94	2.321	1.15	0.209737	0.66	0.77	1204	18	1227	7	-1.97
34	0.00	infinite	0.111057	0.93	5.147	1.20	0.336147	0.75	0.91	1817	17	1868	12	-2.83
35	0.00	infinite	0.097952	1.15	3.869	1.34	0.286505	0.70	0.49	1586	21	1624	10	-2.43
36	0.00	infinite	0.081223	0.95	2.480	1.15	0.221421	0.65	0.71	1227	19	1289	8	-5.10
37	0.00	infinite	0.080944	0.96	2.470	1.20	0.221276	0.72	0.87	1220	19	1289	8	-5.62
38	0.00	infinite	0.081710	1.01	2.404	1.26	0.213339	0.76	0.54	1239	20	1247	9	-0.65
39	0.00	infinite	0.077051	0.96	2.079	1.19	0.195710	0.71	0.76	1122	19	1152	7	-2.65
40	0.00	infinite	0.080644	1.00	2.360	1.21	0.212214	0.69	0.20	1213	20	1241	8	-2.29
41	0.01	259837	0.080393	0.95	2.376	1.18	0.214309	0.70	0.82	1207	19	1252	8	-3.74
42	0.00	infinite	0.080499	0.95	2.392	1.17	0.215470	0.69	0.84	1209	19	1425	12	-4.02
43	0.00	infinite	0.095497	0.96	3.699	1.18	0.280902	0.68	0.71	1538	18	1422	12	-3.77
44	0.00	infinite	0.110566	0.96	5.085	1.17	0.333522	0.68	0.78	1809	17	1420	12	-2.58
45	0.03	60246	0.112290	6.59	5.135	6.72	0.331652	1.31	0.93	1837	115	1417	12	-0.52
46	0.00	infinite	0.109070	0.96	5.049	1.19	0.335760	0.71	0.87	1784	17	1414	11	-4.61
47	0.14	11857	0.094032	7.67	3.498	9.42	0.269828	5.47	0.77	1509	138	1412	11	-2.07
48	0.21	7363	0.110009	3.84	5.100	4.69	0.336212	2.69	0.88	1800	68	1409	11	-3.83
49	0.00	infinite	0.079901	0.96	2.335	1.16	0.211984	0.65	0.63	1195	19	1406	11	-3.75
50	0.02	96519	0.080465	2.70	2.331	2.78	0.210098	0.66	0.55	1208	52	1404	11	-1.73
51	0.00	infinite	0.131294	0.94	7.338	1.18	0.405326	0.71	0.93	2115	16	1401	11	-3.70
52	0.00	infinite	0.114929	0.94	5.692	1.15	0.359173	0.67	0.89	1879	17	1398	11	-5.29
53	0.00	infinite	0.079932	0.98	2.333	1.23	0.211705	0.75	0.71	1195	19	1238	8	-3.56
54	0.00	infinite	0.077269	0.95	2.128	1.27	0.199704	0.84	0.91	1128	19	1174	9	-4.04
55	0.37	4424	0.079248	2.50	2.370	3.09	0.216900	1.82	0.75	1178	49	1265	21	-7.39
56	0.00	infinite	0.077464	0.96	2.128	1.19	0.199223	0.71	0.79	1133	19	1171	8	-3.35

Tabele 3.11 – MC-3 (continued)

Grain	f_{206} %	Ratios							Rho	Ages (Ma)				Disc. %
		$^{206}Pb/^{204}Pb$	$^{207}Pb/^{206}Pb$	±	$^{207}Pb/^{235}U$	±	$^{206}Pb/^{238}U$	±		$^{207}Pb/^{206}Pb$	±	$^{206}Pb/^{238}U$	±	
57	0.00	infinite	0.079990	0.95	2.339	1.17	0.212081	0.68	0.76	1197	19	1240	8	-3.61
58	0.00	infinite	0.111098	0.96	5.225	1.21	0.341080	0.73	0.87	1817	17	1892	12	-4.09
59	0.01	119263	0.110304	0.96	4.995	1.17	0.328411	0.66	0.75	1804	17	1831	11	-1.45
60	0.77	2187	0.080505	3.95	2.229	4.92	0.200783	2.92	0.72	1209	76	1180	31	2.47
61	0.00	infinite	0.121339	0.95	6.046	1.16	0.361361	0.66	0.82	1976	17	1989	11	-0.64
62	0.00	infinite	0.080119	0.97	2.341	1.18	0.211925	0.67	0.70	1200	19	1239	8	-3.26
63	0.00	infinite	0.095513	0.96	3.754	1.15	0.285072	0.63	0.39	1538	18	1617	9	-5.11
64	0.05	28286	0.125824	1.80	6.803	1.92	0.392110	0.67	0.83	2040	32	2133	12	-4.52
65	0.00	infinite	0.122989	0.96	6.413	1.17	0.378155	0.66	0.72	2000	17	2068	12	-3.38
66	0.12	14097	0.079467	2.06	2.310	2.51	0.210837	1.45	0.26	1184	40	1233	16	-4.18
67	0.00	infinite	0.108237	1.01	4.786	1.27	0.320671	0.78	0.92	1770	18	1793	12	-1.30
68	0.19	8918	0.080337	4.12	2.379	5.03	0.214761	2.88	0.63	1205	79	1254	33	-4.05
69	0.13	12189	0.112905	3.74	5.249	4.62	0.337208	2.72	0.71	1847	66	1873	44	-1.44
70	0.20	8215	0.079206	3.19	2.317	3.91	0.212199	2.26	0.61	1177	62	1241	25	-5.37
72	0.15	11282	0.079425	2.29	2.333	2.82	0.213000	1.64	0.74	1183	45	1245	19	-5.25
73	0.00	infinite	0.160954	0.94	10.348	1.16	0.466297	0.68	0.78	2466	16	2467	14	-0.06
74	0.10	16006	0.110367	2.33	4.976	2.44	0.327000	0.74	0.77	1805	42	1824	12	-1.02
75	0.05	29498	0.094634	2.54	3.645	2.64	0.279374	0.71	0.80	1521	47	1588	10	-4.43
76	0.00	infinite	0.079688	0.94	2.379	1.18	0.216477	0.72	0.88	1189	18	1263	8	-6.22
77	0.04	42011	0.110583	1.88	5.179	1.99	0.339650	0.64	0.76	1809	34	1885	10	-4.20
78	0.00	infinite	0.079749	0.95	2.335	1.16	0.212314	0.66	0.71	1191	19	1241	7	-4.23
79	0.00	infinite	0.132806	0.95	7.403	1.15	0.404276	0.65	0.72	2135	16	2189	12	-2.50
80	0.00	infinite	0.080102	0.96	2.344	1.18	0.212231	0.68	0.72	1199	19	1241	8	-3.43
81	0.00	infinite	0.080039	0.97	2.261	1.18	0.204900	0.68	0.52	1198	19	1202	7	-0.30
82	0.02	103423	0.079542	2.67	2.282	2.76	0.208067	0.69	0.77	1186	52	1219	8	-2.77
~~83~~	~~3.16~~	~~526~~	~~0.077985~~	~~8.03~~	~~2.247~~	~~9.34~~	~~0.209014~~	~~4.77~~	~~0.88~~	~~1146~~	~~152~~	~~1224~~	~~53~~	~~-6.72~~
84	0.35	4424	0.112719	3.63	5.252	4.39	0.337938	2.46	0.50	1844	64	1877	40	-1.79
85	0.00	infinite	0.080244	0.95	2.310	1.16	0.208823	0.67	0.84	1203	19	1223	7	-1.62
86	0.27	6151	0.080487	2.65	2.363	3.20	0.212947	1.79	0.65	1209	51	1245	20	-2.94
87	0.00	infinite	0.077791	0.95	2.158	1.14	0.201177	0.64	0.62	1142	19	1182	7	-3.51
88	0.00	infinite	0.080681	0.96	2.356	1.18	0.211810	0.69	0.81	1214	19	1238	8	-2.04
89	0.16	9948	0.089379	3.90	3.165	4.71	0.256854	2.65	0.81	1412	73	1474	35	-4.35
90	0.00	infinite	0.103244	1.03	4.320	1.29	0.303456	0.76	0.90	1683	19	1708	11	-1.50
91	0.02	70515	0.081138	1.65	2.286	1.96	0.204357	1.06	0.87	1225	32	1199	12	2.13
92	0.00	infinite	0.080486	0.94	2.328	1.14	0.209807	0.64	0.78	1209	18	1228	7	-1.56
93	0.00	infinite	0.081561	1.02	2.410	1.23	0.214289	0.68	0.66	1235	20	1252	8	-1.35
94	0.00	infinite	0.110003	0.94	5.202	1.17	0.342952	0.71	0.86	1799	17	1901	12	-5.64
95	0.00	infinite	0.080181	0.99	2.363	1.21	0.213721	0.69	0.28	1201	19	1249	8	-3.93
96	0.00	infinite	0.076540	0.94	2.052	1.16	0.194488	0.68	0.75	1109	19	1146	7	-3.28
97	0.00	infinite	0.129474	0.94	7.181	1.23	0.402267	0.79	0.93	2091	17	2179	15	-4.24
98	0.00	infinite	0.080935	0.99	2.388	1.28	0.213961	0.80	0.71	1220	19	1250	9	-2.46
99	0.00	infinite	0.080125	0.95	2.366	1.21	0.214124	0.75	0.83	1200	19	1251	9	-4.22
100	0.00	infinite	0.079779	0.99	2.336	1.19	0.212340	0.66	0.71	1192	19	1241	7	-4.18
101	0.00	infinite	0.080419	0.99	2.318	1.22	0.209054	0.71	0.59	1207	19	1224	8	-1.37
102	0.00	infinite	0.110864	0.97	5.249	1.21	0.343410	0.72	0.77	1814	18	1903	12	-4.93

Table 3.12 – U-Pb LAM-ICP-MS data of the sample SL-1. Sample without correction for common Pb.

Grain	f_{206} %	Ratios							Rho	Ages (Ma)				Disc. %
		$^{206}Pb/^{204}Pb$	$^{207}Pb/^{206}Pb$	±	$^{207}Pb/^{235}U$	±	$^{206}Pb/^{238}U$	±		$^{207}Pb/^{206}Pb$	±	$^{206}Pb/^{238}U$	±	
1			0.079759	0.97	2.215	1.18	0.201413	0.67	0.74	1191	19	1183	7	0.68
2			0.080351	0.99	2.224	1.20	0.200748	0.68	0.57	1206	19	1179	7	2.18
3			0.080193	0.98	2.220	1.19	0.200773	0.67	0.74	1202	19	1179	7	1.85
4			0.080022	0.94	2.272	1.18	0.205960	0.70	0.88	1198	19	1207	8	-0.81
5			0.079792	0.95	2.234	1.17	0.203049	0.69	0.78	1192	19	1192	7	0.01
6			0.080937	0.96	2.296	1.20	0.205750	0.72	0.85	1220	19	1206	8	1.13
7			0.134148	0.96	6.961	1.25	0.376358	0.80	0.88	2153	17	2059	14	4.35
8			0.082070	1.07	2.314	1.26	0.204537	0.66	0.57	1247	21	1200	7	3.81
9			0.080202	0.96	2.204	1.18	0.199284	0.69	0.80	1202	19	1171	7	2.54
10			0.080657	0.97	2.225	1.18	0.200074	0.68	0.71	1213	19	1176	7	3.08
11			0.079328	0.95	2.237	1.17	0.204486	0.68	0.88	1180	19	1199	7	-1.61
12			0.079557	0.95	2.245	1.16	0.204625	0.66	0.82	1186	19	1200	7	-1.19
13			0.122206	0.96	5.980	1.17	0.354894	0.66	0.80	1989	17	1958	11	1.55
14			0.109580	0.95	4.924	1.20	0.325907	0.73	0.90	1792	17	1819	11	-1.45
~~15~~			~~0.292121~~	~~0.99~~	~~3.431~~	~~1.40~~	~~0.085189~~	~~0.99~~	~~0.87~~	~~3429~~	~~15~~	~~527~~	~~5~~	~~84.63~~
16			0.080747	0.95	2.334	1.15	0.209651	0.65	0.65	1215	19	1227	7	-0.96
~~17~~			~~0.180759~~	~~1.48~~	~~4.688~~	~~2.11~~	~~0.188097~~	~~1.51~~	~~0.57~~	~~2660~~	~~24~~	~~1111~~	~~15~~	~~58.23~~
18			0.077328	1.00	2.189	1.22	0.205338	0.69	0.38	1130	20	1204	8	-6.57
19			0.116953	1.00	5.737	1.23	0.355746	0.73	0.86	1910	18	1962	12	-2.71
20			0.080091	0.97	2.234	1.18	0.202322	0.68	0.74	1199	19	1188	7	0.95
21			0.109701	0.97	4.879	1.21	0.322594	0.72	0.90	1794	17	1802	11	-0.44
22			0.080530	0.96	2.303	1.16	0.207428	0.65	0.71	1210	19	1215	7	-0.42
23			0.121891	1.52	5.710	1.76	0.339735	0.88	0.66	1984	27	1885	14	4.97
24			0.115281	0.95	5.375	1.17	0.338179	0.67	0.76	1884	17	1878	11	0.34
25			0.111621	0.97	4.971	1.21	0.323020	0.72	0.73	1826	18	1804	11	1.18
26			0.110587	0.96	5.111	1.17	0.335189	0.67	0.87	1809	17	1863	11	-3.01
27			0.079818	0.96	2.296	1.20	0.208656	0.72	0.82	1192	19	1222	8	-2.45
28			0.080341	0.97	2.263	1.20	0.204317	0.71	0.68	1205	19	1198	8	0.57
29			0.136120	0.96	7.484	1.23	0.398737	0.76	0.87	2178	17	2163	14	0.70
30			0.080452	0.98	2.286	1.22	0.206124	0.72	0.72	1208	19	1208	8	0.00
31			0.079874	0.98	2.239	1.21	0.203284	0.71	0.59	1194	19	1193	8	0.08
32			0.079719	0.96	2.240	1.19	0.203822	0.70	0.73	1190	19	1196	8	-0.49
33			0.079381	0.95	2.268	1.25	0.207187	0.81	0.89	1182	19	1214	9	-2.72
34			0.120689	0.94	6.077	1.15	0.365187	0.65	0.69	1966	17	2007	11	-2.05
35			0.132673	0.95	7.113	1.18	0.388834	0.69	0.78	2134	17	2117	13	0.76
36			0.122553	0.96	6.171	1.18	0.365171	0.68	0.84	1994	17	2007	12	-0.65
37			0.079966	0.99	2.268	1.19	0.205678	0.67	0.63	1196	19	1206	7	-0.80
38			0.092487	0.96	3.450	1.16	0.270519	0.66	0.84	1477	18	1543	9	-4.47
40			0.097707	0.97	3.735	1.19	0.277228	0.69	0.75	1581	18	1577	10	0.22
41			0.120500	0.96	5.942	1.19	0.357609	0.71	0.85	1964	17	1971	12	-0.37
42	0.38	4397	0.080050	0.93	2.198	1.14	0.199165	0.66	0.86	1198	18	1171	7	2.29
43	1.26	1339	0.079892	0.94	2.113	1.15	0.191820	0.66	0.78	1194	18	1131	7	5.28
44	1.22	1379	0.079947	0.93	2.066	1.15	0.187384	0.67	0.89	1196	18	1107	7	7.40
45	0.19	8477	0.095575	0.94	3.434	1.20	0.260621	0.75	0.72	1539	18	1493	10	3.02
46	0.21	7386	0.120833	0.94	5.436	1.20	0.326284	0.74	0.74	1969	17	1820	12	7.53
47	0.13	12330	0.111957	0.93	4.714	1.20	0.305378	0.75	0.87	1831	17	1718	11	6.20
49	0.20	7521	0.131951	0.93	6.996	1.15	0.384522	0.68	0.90	2124	16	2097	12	1.26
50	0.24	6554	0.110426	0.94	4.716	1.15	0.309756	0.67	0.82	1806	17	1740	10	3.70
51	0.35	4402	0.116502	0.95	5.227	1.15	0.325428	0.65	0.82	1903	17	1816	10	4.57
52	0.00	infinite	0.080673	0.95	2.245	1.16	0.201855	0.66	0.81	1213	19	1185	7	2.33
~~55~~	~~0.08~~	~~20024~~	~~0.084256~~	~~0.94~~	~~2.267~~	~~1.32~~	~~0.195180~~	~~0.92~~	~~0.93~~	~~1298~~	~~18~~	~~1149~~	~~10~~	~~11.48~~
56	0.08	19889	0.079523	1.31	2.214	1.46	0.201955	0.65	0.91	1185	26	1186	7	-0.05
57	0.09	17065	0.114368	2.25	5.261	2.34	0.333628	0.66	0.93	1870	40	1856	11	0.75
59	0.28	5912	0.079249	1.46	2.162	1.78	0.197903	1.02	0.86	1178	29	1164	11	1.21
61	0.16	9631	0.123036	0.93	6.173	1.16	0.363903	0.68	0.91	2001	16	2001	12	0.00
62	0.21	8030	0.080638	1.01	2.314	1.29	0.208108	0.80	0.55	1213	20	1219	9	-0.50

Table 3.12 – SL-1 (continued)

Grain	f_{206} %	Ratios							Rho	Ages (Ma)				Disc. %
		$^{206}Pb/^{204}Pb$	$^{207}Pb/^{206}Pb$	±	$^{207}Pb/^{235}U$	±	$^{206}Pb/^{238}U$	±		$^{207}Pb/^{206}Pb$	±	$^{206}Pb/^{238}U$	±	
63	0.08	21130	0.077958	1.75	2.033	1.90	0.189104	0.72	0.91	1146	34	1117	7	2.56
65	0.10	15905	0.110725	0.93	5.012	1.13	0.328280	0.65	0.82	1811	17	1830	10	-1.03
66	0.21	8072	0.081001	0.94	2.392	1.33	0.214202	0.94	0.94	1221	18	1251	11	-2.43
67	0.38	4031	0.122692	5.72	5.954	7.04	0.351944	4.10	0.91	1996	98	1944	68	2.60
~~68~~	~~15.36~~	~~114~~	~~0.193581~~	~~0.99~~	~~3.293~~	~~1.22~~	~~0.123388~~	~~0.70~~	~~0.40~~	~~2773~~	~~16~~	~~750~~	~~5~~	~~72.95~~
69	0.03	52802	0.127874	0.93	6.472	1.17	0.367094	0.71	0.94	2069	16	2016	12	2.57
70	0.14	10660	0.117185	2.70	5.492	3.32	0.339898	1.94	0.92	1914	48	1886	32	1.44
71	0.03	52060	0.132922	0.94	7.266	1.15	0.396485	0.66	0.90	2137	16	2153	12	-0.74
73	0.28	6048	0.081243	0.94	2.261	1.15	0.201828	0.67	0.92	1227	18	1185	7	3.44
74	0.13	12547	0.080557	0.93	2.307	1.13	0.207684	0.64	0.75	1211	18	1216	7	-0.48
76	0.29	5811	0.081359	2.55	2.218	3.14	0.197760	1.83	0.83	1230	49	1163	19	5.43
78	0.18	9405	0.080505	0.93	2.321	1.18	0.209106	0.72	0.91	1209	18	1224	8	-1.21
79	0.22	7550	0.080297	0.93	2.268	1.16	0.204811	0.69	0.84	1204	18	1201	8	0.26
81	0.19	7755	0.124924	2.44	6.364	3.00	0.369453	1.74	0.88	2028	43	2027	30	0.04
82	0.22	7114	0.110200	0.93	4.980	1.15	0.327746	0.67	0.90	1803	17	1827	11	-1.37
83	0.42	3997	0.080343	0.94	2.264	1.16	0.204333	0.69	0.87	1205	18	1199	7	0.57
84	0.60	2788	0.080401	0.93	2.261	1.16	0.203929	0.68	0.88	1207	18	1196	7	0.87
85	0.01	128726	0.120032	0.93	5.937	1.17	0.358724	0.71	0.94	1957	16	1976	12	-0.99
86	0.18	8387	0.135492	0.93	7.602	1.14	0.406904	0.66	0.88	2170	16	2201	12	-1.40
87	0.07	20669	0.118932	3.44	5.704	3.52	0.347840	0.73	0.95	1940	60	1924	12	0.82
88	0.17	9650	0.079445	3.11	2.179	3.84	0.198963	2.24	0.33	1183	60	1170	24	1.14
~~90~~	~~16.77~~	~~103~~	~~0.233449~~	~~1.12~~	~~4.972~~	~~1.59~~	~~0.154481~~	~~1.13~~	~~0.75~~	~~3076~~	~~18~~	~~926~~	~~10~~	~~69.89~~
91	0.19	8080	0.127527	4.51	6.088	5.57	0.346213	3.27	0.89	2064	77	1916	54	7.15
92	0.05	32099	0.115205	0.94	5.646	1.19	0.355455	0.72	0.92	1883	17	1961	12	-4.12
93	0.14	10844	0.110426	1.01	5.090	1.24	0.334339	0.71	0.42	1806	18	1859	11	-2.93
94	0.14	10278	0.132794	0.94	7.363	1.23	0.402137	0.80	0.96	2135	16	2179	15	-2.04
95	0.44	3439	0.115475	1.00	5.718	1.21	0.359151	0.69	0.60	1887	18	1978	12	-4.81
96	0.60	2793	0.080725	1.00	2.355	1.22	0.211575	0.70	0.77	1215	20	1237	8	-1.85
97	0.78	2127	0.081452	1.04	2.412	1.25	0.214800	0.70	0.66	1232	20	1254	8	-1.78
98	0.38	3940	0.134520	0.97	7.459	1.28	0.402177	0.84	0.88	2158	17	2179	15	-0.99
99	0.00	infinite	0.081582	0.97	2.314	1.80	0.205715	1.52	0.97	1236	19	1206	17	2.39
100	0.37	4510	0.084540	1.22	2.426	1.92	0.208101	1.48	0.85	1305	23	1219	16	6.61

Table 3.13 – U-Pb LAM-ICP-MS data of the sample SL-3.

Grain	f_{206} %	Ratios							Rho	Ages (Ma)				Disc. %
		$^{206}Pb/^{204}Pb$	$^{207}Pb/^{206}Pb$	±	$^{207}Pb/^{235}U$	±	$^{206}Pb/^{238}U$	±		$^{207}Pb/^{206}Pb$	±	$^{206}Pb/^{238}U$	±	
1	0.02	102721	0.079480	4.48	2.238	6.41	0.204210	4.58	0.96	1184	86	1198	50	-1.16
2	0.04	37042	0.108291	1.64	4.867	2.34	0.325976	1.68	0.82	1771	30	1819	27	-2.71
3	0.06	28283	0.078019	2.07	2.238	2.93	0.208058	2.08	0.58	1147	41	1218	23	-6.20
4	0.03	52820	0.134544	2.84	7.627	4.03	0.411124	2.87	0.88	2158	49	2220	54	-2.87
5	0.31	4944	0.107695	1.33	4.913	1.90	0.330847	1.36	0.78	1761	24	1842	22	-4.64
6	0.09	17744	0.115191	2.28	5.676	3.26	0.357406	2.34	0.94	1883	40	1970	40	-4.62
7	0.03	46853	0.106841	1.98	4.739	2.80	0.321711	1.99	0.62	1746	36	1798	31	-2.97
~~8~~	~~1.59~~	~~1051~~	~~0.065204~~	~~2.16~~	~~1.839~~	~~3.06~~	~~0.204573~~	~~2.18~~	~~0.51~~	~~781~~	~~45~~	~~1200~~	~~24~~	~~-53.64~~
9	0.80	1922	0.103294	1.11	4.723	1.60	0.331649	1.16	0.79	1684	20	1846	19	-9.63
10	0.53	2538	0.188581	1.65	14.128	2.35	0.543369	1.68	0.83	2730	27	2798	38	-2.48
11	0.06	27186	0.078684	3.63	2.286	5.14	0.210704	3.65	0.50	1164	70	1233	41	-5.87
~~12~~	~~0.48~~	~~3475~~	~~0.077187~~	~~2.22~~	~~2.284~~	~~3.17~~	~~0.214617~~	~~2.27~~	~~0.89~~	~~1126~~	~~44~~	~~1253~~	~~26~~	~~-11.31~~
13	0.16	9727	0.103559	1.91	4.419	2.72	0.309471	1.93	0.19	1689	35	1738	29	-2.92

Table 3.13 – SL-3 (continued)

Grain	f_{206} %	Ratios							Rho	Ages (Ma)				Disc. %
		$^{206}Pb/^{204}Pb$	$^{207}Pb/^{206}Pb$	±	$^{207}Pb/^{235}U$	±	$^{206}Pb/^{238}U$	±		$^{207}Pb/^{206}Pb$	±	$^{206}Pb/^{238}U$	±	
14	0.03	58794	0.110147	3.60	5.072	5.10	0.333990	3.61	0.88	1802	64	1858	58	-3.10
15	0.02	87785	0.120665	2.62	6.184	3.71	0.371677	2.63	0.85	1966	46	2037	46	-3.62
16	0.14	9749	0.184087	1.07	13.419	1.54	0.528683	1.11	0.79	2690	18	2736	25	-1.70
17	0.20	8267	0.079798	1.55	2.278	2.21	0.207039	1.58	0.47	1192	30	1213	17	-1.76
18	0.62	2506	0.105355	1.72	4.762	2.45	0.327802	1.75	0.83	1721	31	1828	28	-6.23
19	0.18	9283	0.081200	0.95	2.341	1.32	0.209127	0.93	0.94	1226	18	1224	10	0.17
~~20~~	~~0.66~~	~~2525~~	~~0.073255~~	~~2.79~~	~~2.091~~	~~3.96~~	~~0.207019~~	~~2.82~~	~~0.63~~	~~1021~~	~~55~~	~~1213~~	~~31~~	~~-18.80~~
21	0.35	4339	0.123384	3.16	6.150	3.96	0.361525	2.38	0.88	2006	55	1989	41	0.81
22	0.31	5366	0.077226	2.46	2.182	3.50	0.204928	2.48	0.59	1127	48	1202	27	-6.63
23	0.73	2075	0.116179	2.02	5.956	2.88	0.371783	2.05	0.77	1898	36	2038	36	-7.35
24	0.05	34906	0.080560	4.46	2.272	6.32	0.204529	4.47	0.73	1211	85	1200	49	0.92
25	0.31	5367	0.077150	2.14	2.218	3.03	0.208466	2.15	0.64	1125	42	1221	24	-8.49
26	0.40	4136	0.076578	2.14	2.137	3.05	0.202370	2.18	0.29	1110	42	1188	24	-7.01
27	0.03	53997	0.080398	3.67	2.273	5.20	0.205036	3.68	0.69	1207	71	1202	40	0.37
28	0.16	9500	0.109537	4.08	4.884	5.78	0.323351	4.10	0.93	1792	72	1806	64	-0.80
~~29~~	~~1.64~~	~~945~~	~~0.094080~~	~~3.39~~	~~4.206~~	~~4.84~~	~~0.324261~~	~~3.45~~	~~0.84~~	~~1510~~	~~63~~	~~1811~~	~~54~~	~~-19.92~~
30	0.02	94544	0.078149	3.61	2.067	5.11	0.191803	3.62	0.87	1151	70	1131	37	1.70
31	0.02	84692	0.129300	4.17	6.705	5.93	0.376123	4.22	0.95	2088	72	2058	74	1.45
32	0.02	79397	0.079765	1.92	2.190	2.72	0.199087	1.93	0.47	1191	37	1170	21	1.74
~~33~~	~~2.18~~	~~768~~	~~0.059018~~	~~2.04~~	~~1.632~~	~~2.93~~	~~0.200598~~	~~2.10~~	~~0.69~~	~~568~~	~~44~~	~~1179~~	~~23~~	~~-107.57~~
34	0.19	7462	0.158574	1.51	10.142	2.16	0.463875	1.54	0.87	2441	25	2457	31	-0.66
35	0.06	29142	0.080102	1.61	2.229	2.31	0.201832	1.65	0.19	1199	32	1185	18	1.20
36	0.25	6581	0.076505	1.44	2.162	2.05	0.204921	1.46	0.71	1108	28	1202	16	-8.43
~~37~~	~~0.00~~	~~infinite~~	~~0.085861~~	~~1.59~~	~~2.408~~	~~1.88~~	~~0.203366~~	~~0.99~~	~~0.16~~	~~1335~~	~~30~~	~~1193~~	~~11~~	~~10.61~~
38	1.25	1348	0.076257	1.74	1.922	2.22	0.182796	1.38	0.86	1102	34	1082	14	1.78
~~39~~	~~0.33~~	~~5112~~	~~0.086945~~	~~2.77~~	~~2.366~~	~~4.01~~	~~0.197356~~	~~2.89~~	~~0.63~~	~~1359~~	~~53~~	~~1161~~	~~31~~	~~14.58~~
40	0.21	8028	0.078312	1.24	2.244	1.76	0.207867	1.25	0.75	1155	24	1217	14	-5.42
41	0.14	11879	0.078535	1.41	2.277	2.00	0.210246	1.42	0.53	1160	28	1230	16	-6.01
42	0.08	20748	0.079571	2.06	2.311	2.93	0.210599	2.09	0.88	1186	40	1232	23	-3.85
43	0.25	6696	0.080084	3.11	2.338	4.41	0.211726	3.13	0.83	1199	60	1238	35	-3.25
44	0.34	4478	0.109236	1.95	5.056	2.77	0.335682	1.97	0.78	1787	35	1866	32	-4.43
45	0.07	24264	0.079817	1.95	2.329	2.77	0.211586	1.96	0.67	1192	38	1237	22	-3.76
46	0.01	107012	0.094855	2.24	3.563	3.17	0.272400	2.25	0.82	1525	42	1553	31	-1.82
47	0.05	31851	0.123635	1.76	6.464	2.50	0.379195	1.78	0.87	2009	31	2073	31	-3.14
48	0.09	18521	0.079858	1.38	2.398	1.99	0.217787	1.44	0.91	1193	27	1270	17	-6.43
49	0.55	3013	0.077263	1.95	2.208	2.77	0.207261	1.97	0.59	1128	38	1214	22	-7.64
50	0.36	4668	0.078339	3.16	2.312	4.48	0.214046	3.17	0.53	1155	62	1250	36	-8.21
51	0.20	7968	0.094973	1.44	3.640	2.05	0.277945	1.46	0.80	1528	27	1581	20	-3.50
52	0.24	6973	0.078179	2.27	2.263	3.21	0.209969	2.28	0.29	1151	44	1229	25	-6.71
53	0.18	9034	0.079848	5.04	2.301	7.13	0.209000	5.04	0.50	1193	96	1223	56	-2.54
54	0.38	4373	0.078791	3.16	2.265	4.47	0.208448	3.17	0.57	1167	61	1221	35	-4.60
55	0.20	8477	0.078718	1.37	2.247	1.96	0.207029	1.40	0.88	1165	27	1213	16	-4.11
56	0.68	2448	0.076665	1.85	2.156	2.63	0.203948	1.87	0.49	1112	37	1196	20	-7.55
57	0.39	4227	0.077069	1.57	2.195	2.24	0.206550	1.59	0.79	1123	31	1210	18	-7.79
58	0.05	33181	0.121358	1.99	6.089	2.82	0.363898	2.00	0.83	1976	35	2001	34	-1.23
59	0.35	4444	0.109414	1.33	5.049	1.88	0.334706	1.34	0.38	1790	24	1861	22	-3.99

Table 3.14 – U-Pb SHRIMP data of the sample ARREP.

Grain. spot	U (ppm)	Th (ppm)	Th/U	Pb* (ppm)	$^{206}Pb/^{204}Pb$	f_{206} %	Ratios						Rho	Ages (Ma)						Disc. %
							$^{206}Pb/^{238}U$	±	$^{207}Pb/^{235}U$	±	$^{207}Pb/^{206}Pb$	±		$^{206}Pb/^{238}U$	±	$^{207}Pb/^{235}U$	±	$^{207}Pb/^{206}Pb$	±	
~~1.1~~	~~126~~	~~110~~	~~0.90~~	~~36.5~~	~~3902~~	~~0.38~~	~~0.3352~~	~~1.9~~	~~6.16~~	~~2.7~~	~~0.1332~~	~~1.9~~	0.91	~~1864~~	~~31~~	1999	23	2141	~~33~~	~~13~~
2.1	173	86	0.52	55.6	48111	0.03	0.3745	1.8	6.61	1.9	0.1279	0.80	0.93	2051	31	2061	17	2070	14	1
~~3.1~~	~~449~~	~~638~~	~~1.47~~	~~75.0~~	~~1527~~	~~1.00~~	~~0.1926~~	~~1.7~~	~~3.186~~	~~2.7~~	~~0.1200~~	~~2.1~~	0.88	~~1136~~	~~17~~	1454	21	1956	~~38~~	~~42~~
4.1	109	42	0.40	33.0	5007	0.31	0.3523	1.9	5.54	2.6	0.1142	1.7	0.88	1946	33	1907	22	1867	31	-4
5.1	185	67	0.37	60.9	infinite	--	0.3828	1.8	6.87	2.0	0.1302	0.96	0.88	2089	32	2095	18	2101	17	1
6.1	194	89	0.48	64.2	101788	0.01	0.3843	1.7	6.78	1.9	0.1279	0.71	0.94	2096	31	2083	17	2069	13	-1
~~7.1~~	~~269~~	~~143~~	~~0.55~~	~~87.2~~	~~3511~~	~~0.42~~	~~0.3758~~	~~1.7~~	~~7.00~~	~~1.9~~	~~0.1351~~	~~0.81~~	~~1.00~~	~~2057~~	~~30~~	~~2111~~	~~17~~	~~2165~~	~~14~~	~~5~~
8.1	79	45	0.59	25.7	7245	0.20	0.3804	2.1	7.10	2.3	0.1353	1.1	0.91	2078	37	2124	20	2168	20	4
9.1	87	26	0.31	28.7	infinite	--	0.3854	1.9	7.18	2.1	0.1350	0.94	0.91	2101	34	2134	19	2165	16	3
10.1	220	74	0.35	79.2	infinite	--	0.4190	1.8	7.46	2.0	0.1292	0.85	0.91	2256	34	2168	18	2087	15	-8
11.1	151	65	0.45	49.6	8072	0.19	0.3819	1.8	6.72	2.1	0.1276	1.1	0.91	2085	32	2075	18	2066	19	-1
12.1	165	73	0.46	54.7	12235	0.12	0.3854	1.8	6.85	2.0	0.1290	0.95	0.93	2102	32	2092	18	2084	17	-1
13.1	157	58	0.38	53.0	infinite	--	0.3928	1.8	6.96	2.1	0.1285	1.0	0.88	2136	33	2106	18	2078	18	-3
14.1	225	143	0.66	73.2	infinite	--	0.3798	1.7	6.98	1.8	0.1332	0.59	0.95	2075	30	2109	16	2141	10	3
15.1	201	151	0.78	71.1	20011	0.07	0.4119	1.7	7.72	1.8	0.1359	0.64	0.94	2224	32	2199	16	2176	11	-2
16.1	114	74	0.67	37.7	9692	0.16	0.3835	1.8	6.68	2.2	0.1264	1.2	0.91	2093	33	2070	19	2048	21	-2
17.1	172	83	0.50	55.5	9981	0.15	0.3755	1.8	6.89	2.1	0.1331	1.1	0.92	2055	32	2097	18	2139	19	4
18.1	182	74	0.42	55.4	12356	0.13	0.3528	1.8	5.47	4.2	0.1125	3.8	0.44	1948	30	1896	35	1840	68	-6
19.1	170	71	0.43	50.1	7779	0.20	0.3415	1.8	5.77	2.2	0.1224	1.3	0.82	1894	29	1942	19	1992	23	5
20.1	152	80	0.54	52.2	152041	0.01	0.3996	1.8	7.28	2.4	0.1322	1.6	0.75	2167	33	2146	21	2127	29	-2
21.1	198	98	0.51	65.3	12115	0.12	0.3831	1.8	6.77	2.1	0.1282	0.97	0.91	2091	33	2082	18	2073	17	-1
22.1	237	120	0.52	76.4	78680	0.02	0.3747	1.7	6.76	1.8	0.1308	0.65	0.94	2051	30	2081	16	2109	11	3
23.1	113	55	0.50	37.6	4044	0.37	0.3868	1.9	6.59	2.5	0.1235	1.6	0.90	2108	34	2058	22	2007	28	-5
~~24.1~~	~~286~~	~~581~~	~~2.10~~	~~41.2~~	~~437~~	~~3.45~~	~~0.1619~~	~~1.7~~	~~2.81~~	~~4.1~~	~~0.1259~~	~~3.7~~	0.87	~~967~~	~~16~~	1358	30	2042	~~65~~	~~53~~
25.1	95	68	0.74	32.1	infinite	--	0.3934	1.9	7.07	2.2	0.1303	1.1	0.89	2138	35	2120	19	2102	19	-2
26.1	170	126	0.77	52.8	9668	0.16	0.3602	1.8	5.85	2.0	0.1178	0.86	0.91	1983	30	1954	17	1923	15	-3
26.2	219	75	0.35	67.7	infinite	--	0.3601	1.7	6.03	1.9	0.1215	0.68	0.93	1983	29	1980	16	1978	12	0
27.1	129	48	0.38	44.0	7918	0.19	0.3949	1.8	7.20	2.2	0.1322	1.3	0.91	2145	33	2137	19	2128	22	-1
28.1	102	42	0.43	34.8	4084	0.37	0.3946	2.0	6.88	2.7	0.1265	1.8	0.88	2144	36	2096	24	2050	32	-5
29.1	117	45	0.40	39.1	35716	0.04	0.3900	1.9	7.04	2.1	0.1309	0.95	0.91	2123	34	2116	19	2110	17	-1
30.1	145	103	0.73	50.7	44873	0.03	0.4062	1.9	7.33	2.2	0.1309	1.1	0.88	2198	36	2152	19	2110	19	-4

Table 3.15 – U-Pb SHRIMP data of the sample RETIRO.

Grain. spot	U (ppm)	Th (ppm)	Th/U	Pb* (ppm)	$^{206}Pb/^{204}Pb$	f_{206} %	Ratios						Ages (Ma)						Disc. %
							$^{206}Pb/^{238}U$	±	$^{207}Pb/^{235}U$	±	$^{207}Pb/^{206}Pb$	±	$^{206}Pb/^{238}U$	±	$^{207}Pb/^{235}U$	±	$^{207}Pb/^{206}Pb$	±	
1.1	126.07	45.71	0.3626	54	8139	0.18	0.406260	2.13	7.258	2.42	0.129570	0.91	2198	40	2144	22	2092	16	-5.0
2.1	138.34	41.75	0.30183	57	15492	0.10	0.390540	2.05	7.047	2.20	0.130870	0.58	2125	37	2117	20	2110	10	-0.7
2.2	466.41	225.38	0.48322	112	846	1.76	0.225630	1.85	3.405	2.46	0.109440	1.41	1312	22	1506	19	1790	26	26.7
3.1	205.12	2184.2	10.648	20	390	3.83	0.090030	2.07	1.620	2.65	0.130520	1.42	556	11	978	17	2105	25	73.6
4.1	52.57	896.05	17.044	1	2441	0.61	0.015500	2.26	0.276	2.63	0.129310	1.05	99	2	248	6	2089	19	95.3
3.2	6194.7	1787.5	0.28855	105	26	58.26	0.011470	19.70	0.252	85.32	0.159450	80.59	74	14	228	191	2450	3514	97.0
4.1	95.86	30.25	0.31562	36	2424	0.62	0.359950	1.96	6.448	2.28	0.129920	0.94	1982	34	2039	20	2097	17	5.5
5.1	115.64	30.32	0.26217	46	5680	0.26	0.383320	1.98	6.817	2.24	0.128990	0.82	2092	35	2088	20	2084	15	-0.4
6.1	326.13	73.87	0.22651	115	1357	1.10	0.342200	2.69	6.056	2.92	0.128340	0.84	1897	44	1984	26	2075	15	8.6
7.1	132.66	42.55	0.32073	55	6068	0.25	0.393430	2.03	7.039	2.24	0.129760	0.74	2139	37	2116	20	2095	13	-2.1
8.1	120.2	34.97	0.2909	48	13607	0.11	0.381440	2.30	6.753	2.54	0.128410	0.83	2083	41	2080	23	2076	15	-0.3
9.1	104.36	33.63	0.32223	41	3699	0.40	0.372770	2.51	6.628	2.86	0.128950	1.11	2042	44	2063	26	2084	20	2.0
10.1	96.66	26.38	0.27295	40	5015	0.30	0.403660	2.36	7.175	2.63	0.128910	0.91	2186	44	2133	24	2083	16	-4.9

Capítulo 4 – GRUPOS CANASTRA & IBIÁ

Age, provenance and tectonic setting of the Canastra and the Ibiá Groups (Brasília Belt, Brazil)

Rodrigues, J.B. [a,b,*], Pimentel, M.M.[b] , Dardenne, M.A.[b], Armstrong,R.A.[c]

a - Companhia de Pesquisa de Recursos Minerais, b - Universidade de Brasília, c - Australian National University
** corresponding author*

ABSTRACT

The Brasília Belt is one of the best preserved Neoproterozoic orogens in Brazil. It comprises a thick Meso-Neoproterozoic sedimentary/metasedimentary pile including the Canastra and Ibiá groups, which are the object of this study. The Canastra Group constitutes a regressive sedimentary sequence made mainly of greenschist-facies metapelitic and metapsammitic rocks, including phyllite, metarhythmite, quartzite, with minor intercalations of limestone as well as carbonaceous and carbonatic phyllite. The Ibiá Group is formed by a basal diamictite (Cubatão Formation) followed upwards by metapelitic rocks (phyllites and calc-schists). It rests on an erosional unconformity on top of the Canastra Group. The depositional age of the original sediments is unknown.

The present provenance study based on U-Pb zircon geochronology has been performed on a selection of seven samples in order to identify the various source areas of the original sediments as well as to establish maximum depositional ages for the original sediments. In addition, seven new Sm-Nd analyses are presented and discussed together with previously published data. The tectonic setting and possible source areas of the Canastra and Ibiá metasediments are also discussed.

LAM-ICPMS U-Pb dating of detrital zircon grains suggests that the maximum depositional age of the Canastra and Ibiá groups are ca. 1030 and 640 Ma, respectively. The provenance signature of the Canastra Group comprises a wide range of detrital zircon ages with a significant Paleoproterozoic component (~1.8 and ~2.1 Ga) and an important Mesoproterozoic source (1.1- 1.2 Ga) especially for the Paracatu Formation. This is consistent with a passive margin setting for the deposition of the Canastra sediments.

Zircon grains from the diamictite of the Ibiá Group present ages raging from 936 to 2500 Ma. In contrast, the overlying calciphyllite of the Rio Verde Formation reveals a dominant Neoproterozoic provenance pattern with important peaks at 665, 740 and 850 Ma. The São Francisco-Congo and Goiás Magmatic Arc are, most probably, the two main source regions for the Ibiá Group which may represent, therefore, a former fore-arc sedimentary sequence.

4.1 - INTRODUCTION

The Brasília Belt is a N-S trending Neoproterozoic Belt that extends along the western side of the São Francisco-Congo Craton (Fig. 4.1). This complex fold-and-thrust belt resulted from the collision between the Amazonian and São Francisco-Congo cratons, and displays tectonic vergence towards the east. In the northern segment of the belt, most of the sedimentary units is preserved, which allows the reconstruction of the paleogeography and depositional systems. On the other hand, in the southern segment the intense deformation and metamorphism obliterated the original stratigraphic relationships (Dardenne, 2000).

The Brasília Belt can be organized into four main constituents (Dardenne, 2000, Pimentel et al., 2001):

- An exotic continental block made of Archaean rock units (the Crixás-Goiás region) (Fig.4.1);
- Reworked sialic basement of Paleoproterozoic age, exposed mainly in the Almas-Cavalcante region (Cruz et al., 2000);
- The Goiás Magmatic Arc in the west, formed by volcano-sedimentary rocks and tonalite/granodiorite gneisses with ages ranging from ca. 930 to 640 Ma (Pimentel et al 1991, 1997 and Pimentel & Fuck 1992);
- Thick sedimentary and metasedimentary sequences, organized in the following units: (i) Araí Group: represents a 1,77 Ga old continental rift (Pimentel et al., 2001), comprising coarse grained clastic and pelitic rocks, associated with alkali rich volcanic layers; (ii) Serra da Mesa Group: a meso/paleoproterozoic sequence mainly composed by quartzite and micaschist; (iii) Paranoá Group: formed by sandy, pelitic and carbonate rocks which underlie extense areas in the northern segment of Brasília Belt; (iv) Canastra Group: it represents an association of psammitic and pelitic metasediments frequently containing carbonate and consisting essentially of phyllite and quartzite, metamorphosed at greenschist facies.; (v) Vazante Group: thick marine pelitic-dolomitic sequence; (vi) Araxá Group: mainly comprises micaschist and micaceous quartzites, but encloses various others rock types, such as metavolcanic and granitoids rocks, besides a typical ophiolitic melange; (vii) Ibiá Group: constituted by phyllite, calciferous phyllite, chlorite schist, sericite schist, metadiamictite and minor quartzite, and; (viii) Bambuí: it is represented mainly by pelitic and carbonatic sediments that overlie other sediments of the Brasilia Belts and vast areas of the São Francisco Craton.

The contacts between the different metasedimentary units are mostly tectonic, particularly in the southern part of the belt. This, associated with the scarcity of interlayered igneous rocks and with the limited amount of geochronological data, has hampered the comprehensive understanding of their tectonic significance.

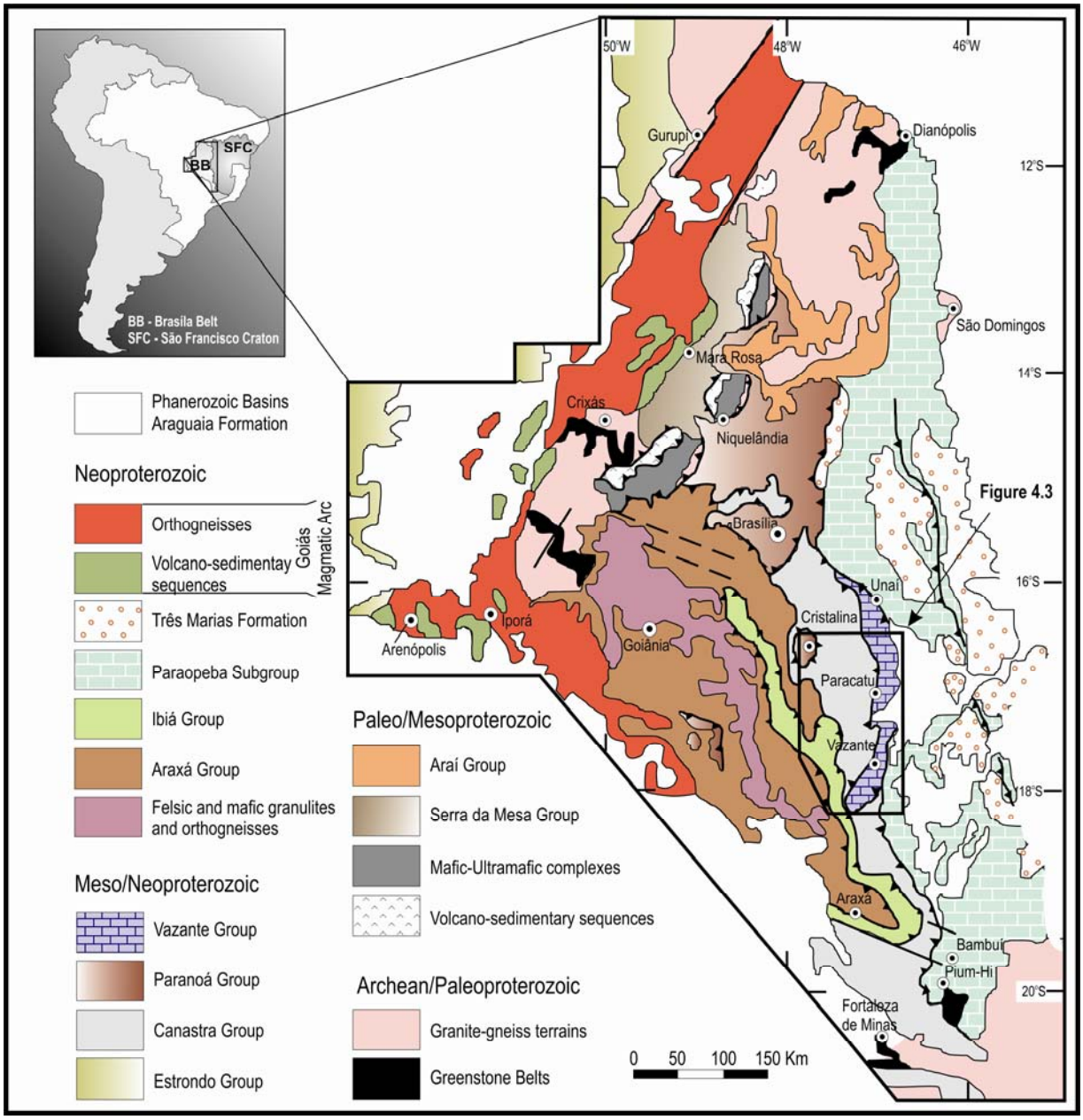

Figure 4.1 - Simplified geological map of Brasília Belt (based on Dardenne, 2000).

4.2– GEOLOGIC SETTING

4.2.1 - Canastra Group

The Canastra Group (Barbosa, 1955) is exposed in the central-southern area of the Brasília Belt (Fig. 4.1), and is composed of psammitic and pelitic sediments. Due to intense deformation, the stratigraphic organization of the Canastra Group is not fully understood. In previous studies, the Canastra Group has been correlated with the Araxá Group, exposed to the west, and these two groups were considered to be part of the same stratigraphic unit (Barbosa, 1963, Braun, 1970, Braun & Batista, 1976). In the most recent studies, however,

they have been mapped as separate units despite the similar lithological contents (Seer, 1999; Valeriano *et al.*, 2004a, b; Dardenne, 2000). The Canastra Group is metamorphosed under greenschist facies conditions, although locally amphibolite facies assemblages have been reported (Silva, 2003).

Detailed field studies in the Paracatu-Coromandel area (Campos Neto, 1984; Freitas Silva, 1991; Pereira et al., 1994) resulted in the proposition of the stratigraphic column (Freitas Silva & Dardenne 1994) for the Canastra Group shown in Figure 4.2, which is used in this work. According to this, the Canastra Group is formed by the following lithostratigraphic units, which are separated from each other by faults:

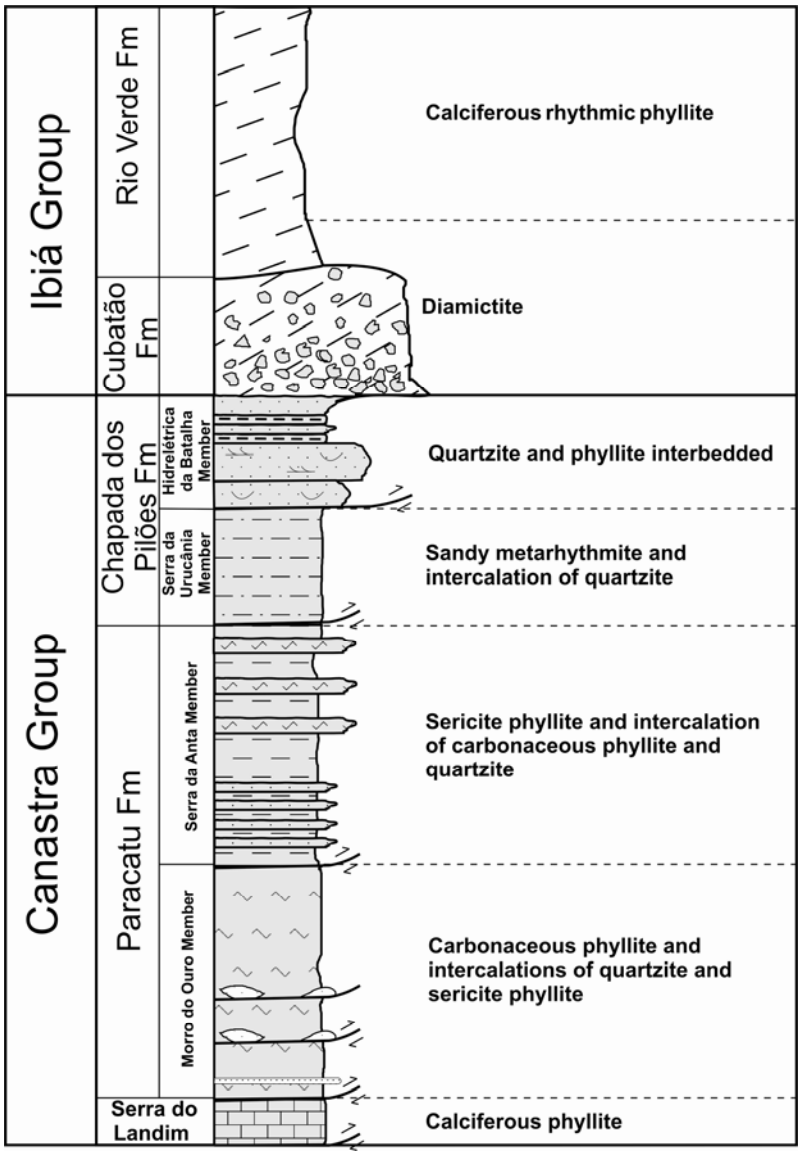

Figure 4.2 - Lithostratigraphic column of the Canastra and Ibiá groups (modified from Dardenne, 2000).

- **Serra do Landim Formation:** This unit was initially considered part of the Vazante Group (Madalloso & Valle, 1978) due to lithological similarities, and was later incorporated into the Canastra Group by Freitas-Silva and Dardenne (1994); it is made mainly of calcishale/calcischists with marble and limestone lenses.

- **Paracatu Formation**: This is made of the basal 100 m-thick Morro do Ouro Member, which includes dark carbonaceous phyllite and intercalations of fine quartzite; the Serra da Anta Member, at the top, is composed of a layer of sericite phyllite with intercalation of fine-grained quartzite;

- **Chapada dos Pilões Formation**: This is divided into two members. The basal member, Serra da Urucânia, comprises a rhythmic succession of quartzite and phyllite, and the upper sequence, the Hidroelétrica Batalha Member, consists of fine-grained quartzite and thin layers of phyllite.

In nortwestern Minas Gerais, the Canastra Group represents a regressive megacycle (Dardenne, 2000). The lower part, made of sedimentary rocks rich in organic matter and pyrite, represents deep water deposits, being overlain by turbiditic rocks, with gravitational flow structures. This is covered by platformal sediments, characterized by storm structures. The uppermost part is formed by shallow platform deposits, with tidal structures indicating sediment transport to the west.

Few isotopic studies were carried out on rocks of the Canastra Group. Paleoproterozoic sources are indicated by Sm-Nd model ages which show values of ca. 2.2 Ga (Pimentel et al., 2001b). U-Pb zircon ages for samples collected in its southern limit are in the range between 1226 to 2875 Ma (Valeriano et al., 2004a). The youngest grain, with the age of 1226 Ma, has been considered to represent the maximum depositional age of the original sediment.

4.2.2 - Ibiá Group

Similarly to the Canastra Group, the Ibiá Group is also exposed only in the southern Brasília Belt. It is made mainly of calcischist metamorphosed at greenschist facies. Pereira et al. (1994) have divided the Ibiá Group into the Cubatão and Rio Verde formations. The Cubatão Formation comprises the basal diamictite which tipically displays a calcischist matrix and is exposed mainly in the Coromandel-Guarda Mor region (Fig. 4.3). The diamictite is covered by a thick layer of homogenous calcischist, calciphyllite and rare fine-grained

quartzite comprising the Rio Verde Formation. Locally the Cubatão Formation rests directly on the Canastra Group metasediments (Pereira et al., 1994).

The tectonic-stratigraphic situation of the Ibiá Group is still controversial. Correlation between the Cubatão diamictite and the Neoproterozoic Jequitaí Formation at the base of the Bambuí Group has been suggested by Pereira (1992). $^{207}Pb/^{206}Pb$ ages of 2133 and 2101 Ma have been reported for zircon grains extracted from granitic a pebble of the Cubatão Formation (Dardenne et al., 2003) suggesting a Paleoproterozoic granitic source. However, the available Sm-Nd model ages between 1.1 to 1.33 Ga for the metapelitic rocks (Seer, 1999, Pimentel et al., 2001, Klein, 2008), are similar to those observed in the Araxá Group, what led Pimentel et al. (2001) to suggest similar young sources for both units.

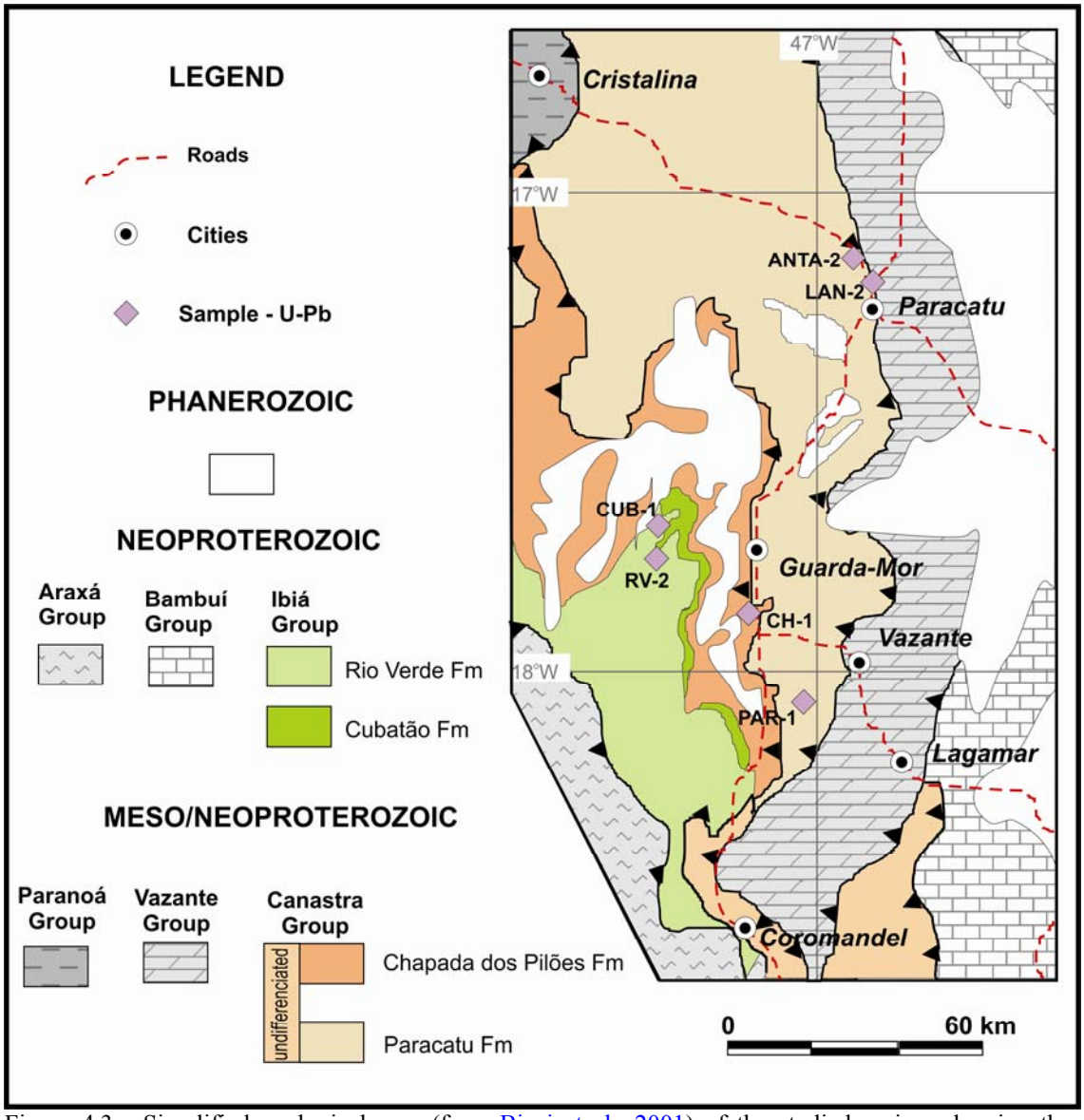

Figure 4.3 - Simplified geological map (from Bizzi et al., 2001) of the studied region, showing the sample locations.

4.3 - ANALYTICAL PROCEDURES

For LAM-MC-ICP-MS and SHRIMP samples were crushed with a jaw crusher and powdered to approximately 500 μm. Heavy mineral concentrates were obtained by panning and were subsequently purified using a Frantz isodynamic separator. Zircon grains were selected from the least magnetic fraction. The grains were set in epoxy resin mounts, without selection and their surface were then polished to expose the grains interiors.

The U-Pb analyses by LAM-ICP-MS were carried out using the Finnigan Neptune coupled to a Nd-YAG laser (λ=213nm) ablation system (New Wave Research, USA) at the Geochronology Laboratory of the Universidade de Brasília. The analytical procedures follow those outlined in Buhn et al. (in press), where the mounts were cleaned in a HNO_3 solution (3%) and ultraclean water bath. The ablation was done with spot size of 25-30μm in raster mode, at frequency of 9-13 Hz and intensity of 0.19-1.02 J/cm^2. The ablated material was carried by Ar (~0.90 L/min) and He (~0.40 L/min) in analyses of 40 cycles of 1 second. Unknown were bracketed by measurements of the international standard GJ-1 following the sequence 1 blank, 1 standard, 3 unknown, 1 blank and 1 standard. The accuracy was controlled using the standard TEMORA-2. Raw data were reduced using a home made spreadsheet and corrections were done for background, instrumental mass-bias drift and common Pb. The ages were calculated using ISOPLOT 3.0 (Ludwig, 2003).

The SHRIMP samples were mounted with standard zircon crystals SL13+FC1, and the mount was photographed at 150× magnification in reflected and transmitted light. Cathodoluminescence (CL) images were obtained in order to reveal internal structures of the zircon grains. Ion microprobe analyses were carried out using SHRIMP I and II at the Research School of Earth Sciences, Australian National University, Canberra, Australia. SHRIMP analytical methods and data treatment follow those described by Williams (1998) and Williams and Meyer (1998). The ion microprobe primary beam in both equipments typically produce spots with diameter between 20–30 μm. Uncertainties reported in tables and figures are given at 1σ level, and final ages are quoted at the 95% confidence level. The data have been processed using SQUID and ISOPLOT 3.0 (Ludwig, 2003).

Sm-Nd isotopic measurements were carried out on a multi-collector Finnigan MAT 262 mass spectrometer in static mode and followed the method described by Gioia and Pimentel (2000). Whole-rock powders (ca. 50 mg) were mixed with a ^{149}Sm–^{150}Nd spike solution and disolved in HF, HNO_3 and HCl in Savillex capsules. Sm and Nd extraction of

whole-rock samples was done by cation exchange techniques, using Teflon columns containing LN-Spec resin (HDEHP—di-ethylhexil phosphoric acid supported on PTFE powder). Sm and Nd samples were loaded onto Re evaporation filaments of a double filament assembly. Uncertainties for Sm/Nd and $^{143}Nd/^{144}Nd$ ratios are better than ±0.5% (2σ) and ±0.005% (2σ), respectively, based on repeated analyses of international rock standards BHVO-1 and BCR-1. $^{143}Nd/^{144}Nd$ ratios were normalised to $^{146}Nd/^{144}Nd$ of 0.7219. T_{DM} values were calculated using De Paolo's (1981) model.

4.4 - RESULTS

4.4.1 – U-Pb Zircon Ages

Four samples of the Canastra Group and two of the Ibiá Group have been selected for LAM-MC-ICP-MS analyses. The frequency diagrams do not include analyses with high common lead content and more than 10% discordant. In addition, zircon grains from one pebble of the Cubatão Formation was analysed by SHRIMP. Sample locations are shown in Figure 4.3 and analytical results are in Tables 4.1 (Canastra), 4.2 (Ibiá-SHRIMP) and 4.3 (Ibiá-LAM-ICP-MS).

4.4.1.1 – Serra do Landim Formation, Canastra Group

Outcrop LAN-2 is a folded calci-shale of the Serra do Landin Formation (Fig. 4.3). The sample (about 20Kg) provided only 44 zircon grains. They are small (~60 μm), rounded to prismatic, colourless or yellowish crystals. All of them were analysed and 41 yielded concordant data. The relative probability

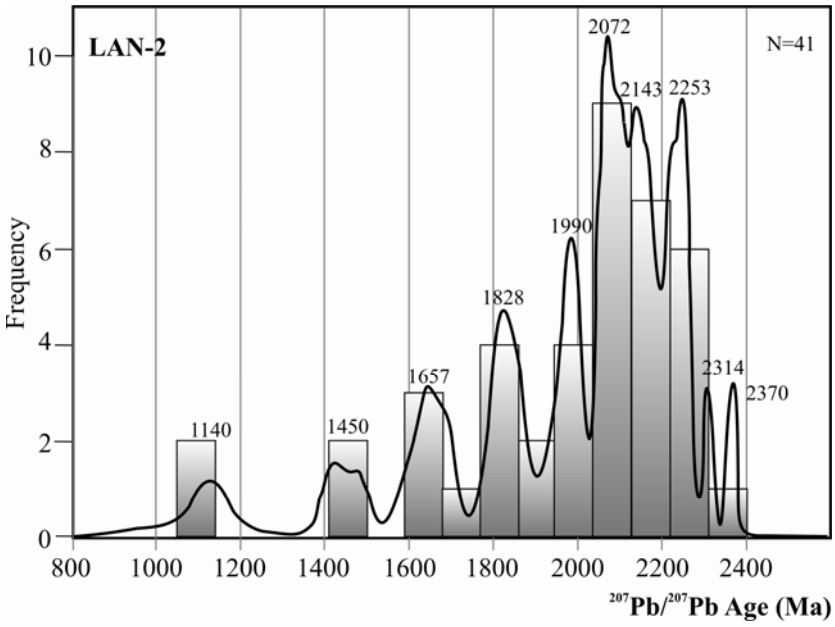

Figure 4.4 - Relative probability distribution diagram of $^{207}Pb/^{206}Pb$ zircon ages of sample LAN-2.

distribution of the $^{207}Pb/^{206}Pb$ ages (Fig. 4.4) shows a main concentration between 2072 and 2253 Ma. The youngest concordant grain has the age of 1079±45 Ma (grain 18).

4.4.1.2 – Paracatu Formation, Canastra Group

Both samples of the Paracatu Formation present zircon grains with high common lead content, resulting in a large nurmber of analyses discarded. Sample PAR-1 is from a thick (more than 40 meters) sequence of medium-fine quartzite (Fig. 4.3). The zircon grains are rounded to prismatic, pink and small (100 μm). Out of 81 grains analysed, 57 results are considered to be useful. The probably density plot (Fig. 4.5) shows a broad distribution, with various peaks, but with a main concentration of age values between 1040 and 1400 Ma. The youngest peak is represented by the 1040 Ma population.

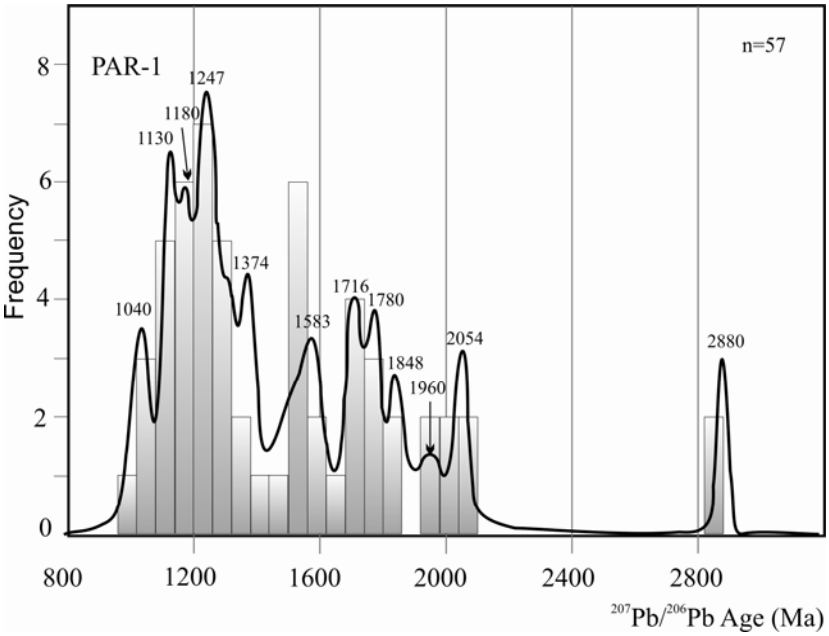

Figure 4.5 - Relative probability distribution diagram of $^{207}Pb/^{206}Pb$ zircon ages of sample PAR-1.

Sample ANTA-2 is a medium quartzite collected ca. 100 km to the north of sample PAR-1 (Fig. 4.3). The zircon grains are prismatic with only a few showing obvious transport features. They are small (~ 80 μm), colourless and clear. Out of the 77 analyses carried out, 47 produced concordant data. The data distribution is presented in Figure 4.6 and it shows three o main peaks, at 1244, 1555 and 1760-1810 Ma. The youngest concordant grain yielded the age of 1063±30 Ma (grain 37).

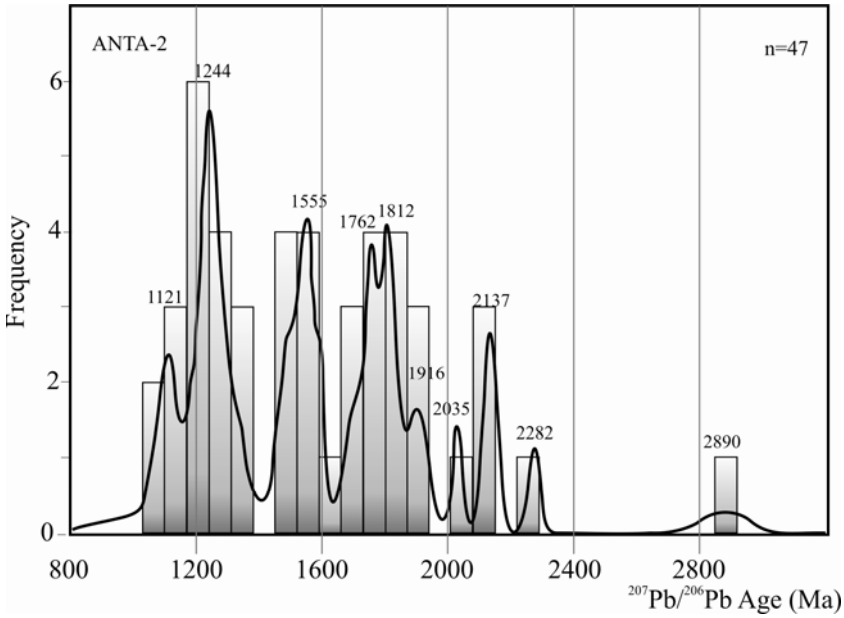

Figure 4.6 - Relative probability distribution diagram of $^{207}Pb/^{206}Pb$ zircon ages of the sample ANTA-2.

4.4.1.3 – Chapada dos Pilões Formation, Canastra Group

Zircon grains from a fine-grained quartzite of the Chapada dos Pilões Formation (sample CH-2) constitute two morphologically distinct groups. The predominant zircon type is approximately 100 μm long prismatic (3:1) crystals, pink to colourless, presenting typical transport features. A less abundant population is composed of large (> 300 μm) pink to colourless rounded zircon grains. In despite of the morphological differences no difference in provenance is shown by the analytical data. Two main peaks are found, at approximately 2.13 and 1.77 Ga. The youngest population is ca 1070 Ma old. (Fig. 4.7)

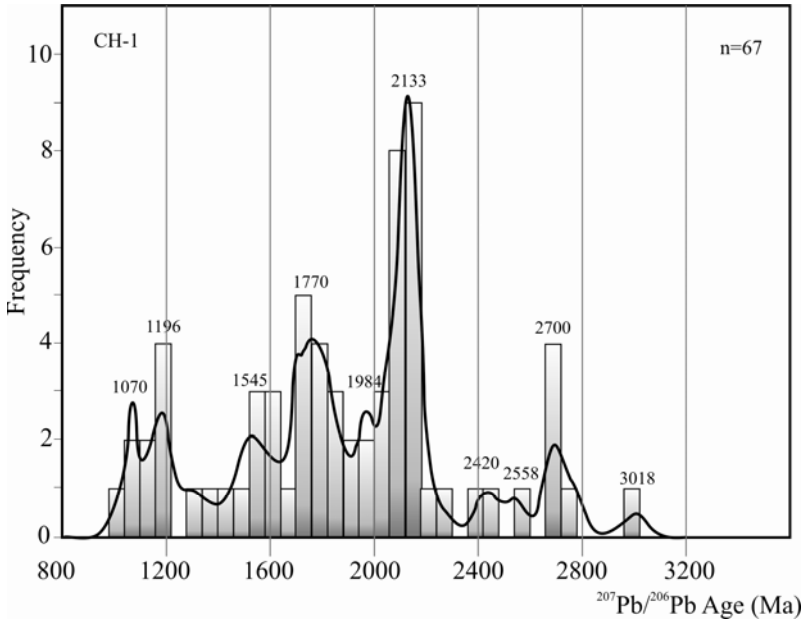

Figure 4.7 - Relative probability distribution diagram of $^{207}Pb/^{206}Pb$ zircon ages of the sample CH-1.

Table 4.1 – U-Pb LAM-ICP-MS data of the Canastra Group.

Sample LAN-2, Serra do Landim Formation

			Radiogenic Ratios						Ages					
Grain	$^{206}Pb/^{204}Pb$	f_{206} %	$^{206}Pb/^{238}U$	±	$^{207}Pb/^{235}U$	±	$^{207}Pb/^{206}Pb$	±	$^{206}Pb/^{238}U$	±	$^{207}Pb/^{206}Pb$	±	Rho	Disc. %
1	infinite	0.00	0.244264	7.61	3.018	7.73	0.089607	1.34	1409	96	1417	25	0.49	0.59
2	1385	1.07	0.394848	3.63	7.385	3.73	0.135641	0.83	2145	66	2172	14	0.95	1.24
~~3~~	~~234~~	~~7.16~~	~~0.197289~~	~~1.06~~	~~3.683~~	~~1.53~~	~~0.135389~~	~~1.11~~	~~1161~~	~~11~~	~~2169~~	~~19~~	~~0.90~~	~~46.49~~
4	infinite	0.00	0.356423	7.60	5.830	7.70	0.118635	1.23	1965	128	1936	22	0.95	-1.52
5	4295	0.36	0.326601	11.09	5.010	11.14	0.111257	1.07	1822	174	1820	19	0.89	-0.10
6	1345	1.15	0.330313	4.34	5.060	4.50	0.111105	1.18	1840	69	1818	21	0.97	-1.23
7	40052	0.04	0.392237	2.24	7.155	2.38	0.132291	0.81	2133	41	2129	14	0.96	-0.22
8	237052	0.01	0.402780	1.89	7.632	2.03	0.137419	0.73	2182	35	2195	13	0.94	0.60
9	4929	0.30	0.409996	3.91	8.000	3.98	0.141518	0.72	2215	73	2246	12	0.77	1.38
10	7135	0.21	0.393253	2.82	7.216	2.93	0.133075	0.81	2138	51	2139	14	0.87	0.05
11	2565	0.62	0.293254	6.91	4.095	7.02	0.101281	1.26	1658	100	1648	23	0.87	-0.61
12	3099	0.47	0.413454	3.87	8.123	3.94	0.142499	0.70	2231	73	2258	12	0.95	1.20
13	11388	0.13	0.406649	4.24	7.817	4.30	0.139423	0.71	2200	78	2220	12	0.95	0.92
~~14~~	~~351~~	~~4.39~~	~~0.336127~~	~~1.84~~	~~6.947~~	~~2.18~~	~~0.149908~~	~~1.18~~	~~1868~~	~~30~~	~~2345~~	~~20~~	~~0.90~~	~~20.34~~
15	20922	0.07	0.424529	3.32	8.597	3.38	0.146865	0.65	2281	63	2310	11	0.97	1.24
16	infinite	0.00	0.406600	4.64	7.803	4.70	0.139184	0.72	2199	86	2217	12	0.90	0.80
17	22408	0.07	0.410047	2.08	7.949	2.19	0.140597	0.70	2215	39	2235	12	0.92	0.87
18	962	1.76	0.182190	4.55	1.899	8.40	0.075602	7.06	1079	45	1085	135	0.77	0.52
19	1247	1.26	0.300983	7.24	4.208	7.44	0.101406	1.68	1696	107	1650	31	0.97	-2.80
20	19822	0.07	0.413730	3.82	8.129	3.88	0.142506	0.68	2232	72	2258	12	0.97	1.15
21	3832	0.40	0.335307	4.17	5.233	4.31	0.113185	1.06	1864	67	1851	19	0.96	-0.70
22	3767	0.38	0.433596	2.49	9.069	2.57	0.151688	0.64	2322	48	2365	11	0.96	1.82
23	9114	0.16	0.392745	3.22	7.209	3.32	0.133132	0.80	2136	58	2140	14	0.93	0.19
24	1004	1.51	0.357191	4.12	5.948	4.36	0.120766	1.44	1969	70	1968	25	0.97	-0.06
25	infinite	0.00	0.381861	23.20	6.764	23.22	0.128464	0.96	2085	401	2077	17	0.90	-0.38
26	infinite	0.00	0.374406	3.16	6.550	3.27	0.126876	0.82	2050	55	2055	14	0.97	0.24
27	infinite	0.00	0.397711	7.44	7.435	7.48	0.135578	0.74	2158	135	2171	13	0.94	0.60
28	infinite	0.00	0.381137	23.21	6.736	23.23	0.128174	0.96	2082	400	2073	17	0.90	-0.41
29	10307	0.14	0.395047	4.73	7.319	4.79	0.134366	0.76	2146	86	2156	13	0.96	0.45
30	1075	1.51	0.255656	1.51	3.263	2.11	0.092561	1.47	1468	20	1479	28	0.20	0.77
31	2803	0.54	0.375776	4.33	6.595	4.41	0.127282	0.87	2057	76	2061	15	0.96	0.21
32	1844	0.83	0.341307	5.22	5.390	5.35	0.114532	1.18	1893	85	1873	21	0.93	-1.09
33	4042	0.38	0.362600	2.70	6.102	2.86	0.122047	0.95	1994	46	1986	17	0.96	-0.41
34	48951	0.03	0.363247	2.85	6.091	3.02	0.121618	0.98	1998	49	1980	17	0.95	-0.88
35	2043	0.82	0.190960	2.48	2.035	3.16	0.077307	1.96	1127	26	1129	38	0.77	0.22
36	50660	0.03	0.301261	2.49	4.316	2.73	0.103901	1.12	1698	37	1695	20	0.92	-0.15
37	135518	0.01	0.384611	2.30	6.893	2.45	0.129983	0.84	2098	41	2098	15	0.96	0.00
38	infinite	0.00	0.385524	3.78	6.950	3.87	0.130746	0.82	2102	67	2108	14	0.88	0.28
39	937	1.70	0.281907	5.30	3.836	5.54	0.098684	1.62	1601	75	1599	30	0.25	-0.10
40	10155	0.15	0.379668	1.14	6.697	1.45	0.127931	0.89	2075	20	2070	16	0.91	-0.24
41	752	2.06	0.323653	2.82	4.880	3.19	0.109359	1.49	1808	44	1789	27	0.91	-1.05
42	infinite	0.00	0.385290	4.69	6.927	4.77	0.130394	0.88	2101	83	2103	15	0.90	0.11
43	infinite	0.00	0.367629	5.04	6.258	5.13	0.123459	0.98	2018	87	2007	17	0.91	-0.57
~~44~~	~~564~~	~~3.00~~	~~0.179820~~	~~1.37~~	~~2.240~~	~~1.89~~	~~0.090357~~	~~1.29~~	~~1066~~	~~13~~	~~1433~~	~~24~~	~~0.67~~	~~25.62~~

Sample PAR-1, Paracatu Formation

Grain	$^{206}Pb/^{204}Pb$	f_{206} %	Ratios $^{206}Pb/^{238}U$	±	$^{207}Pb/^{235}U$	±	$^{207}Pb/^{206}Pb$	±	Ages (Ma) $^{206}Pb/^{238}U$	±	$^{207}Pb/^{206}Pb$	±	Rho	Disc. %
2	10670	0.15	0.251945	4.34	3.271	7.22	0.094166	5.77	1449	56	1511	105	0.92	4.17
3	3429	0.49	0.192366	5.69	2.132	9.69	0.080391	7.85	1134	59	1207	147	0.91	6.00
4	2612	0.64	0.204649	3.06	2.255	5.10	0.079907	4.07	1200	33	1195	78	0.83	-0.46
5	infinite	0.00	0.234766	1.57	2.848	1.84	0.087978	0.96	1359	19	1382	18	0.92	1.63
6	infinite	0.00	0.177201	1.83	1.894	2.16	0.077521	1.15	1052	18	1135	23	0.91	7.31
8	522	3.21	0.201221	1.79	2.343	2.09	0.084437	1.07	1182	19	1303	21	0.89	9.27
~~9~~	~~82~~	~~20.36~~	~~0.159478~~	~~9.85~~	~~1.648~~	~~18.91~~	~~0.074960~~	~~16.14~~	~~954~~	~~87~~	~~1067~~	~~294~~	~~0.63~~	~~10.64~~
~~10~~	~~130~~	~~13.16~~	~~0.147801~~	~~15.66~~	~~1.569~~	~~27.53~~	~~0.077015~~	~~22.64~~	~~889~~	~~129~~	~~1122~~	~~396~~	~~0.65~~	~~20.77~~
12	1579	1.06	0.198296	2.07	2.164	2.33	0.079142	1.06	1166	22	1176	21	0.90	0.81
13	2402	0.70	0.192903	1.91	2.047	2.14	0.076966	0.97	1137	20	1120	19	0.95	-1.50
15	4378	0.36	0.293089	6.00	4.212	10.11	0.104219	8.13	1657	87	1701	143	0.95	2.57
17	2730	0.61	0.216764	1.52	2.475	1.80	0.082800	0.97	1265	17	1264	19	0.91	-0.02
~~18~~	~~224~~	~~7.03~~	~~0.280810~~	~~5.02~~	~~4.487~~	~~8.82~~	~~0.115893~~	~~7.26~~	~~1595~~	~~71~~	~~1894~~	~~125~~	~~0.45~~	~~15.75~~
19	2215	0.70	0.326859	1.65	4.909	1.92	0.108930	0.97	1823	26	1782	18	0.94	-2.33
20	15680	0.11	0.209366	1.24	2.273	1.57	0.078754	0.96	1225	14	1166	19	0.87	-5.10
25	6294	0.25	0.282428	1.54	3.805	1.95	0.097712	1.20	1604	22	1581	22	0.84	-1.43
~~28~~	~~165~~	~~10.14~~	~~0.178182~~	~~12.08~~	~~2.163~~	~~20.35~~	~~0.088058~~	~~16.38~~	~~1057~~	~~117~~	~~1384~~	~~286~~	~~0.50~~	~~23.61~~
29	1153	1.30	0.385332	1.02	6.755	1.40	0.127149	0.96	2101	18	2059	17	0.85	-2.05
30	541	3.07	0.215832	2.07	2.526	2.29	0.084894	0.97	1260	24	1313	19	0.94	4.06
~~32~~	~~288~~	~~5.70~~	~~0.221230~~	~~4.95~~	~~4.076~~	~~8.59~~	~~0.133631~~	~~7.02~~	~~1288~~	~~58~~	~~2146~~	~~118~~	~~0.86~~	~~39.97~~
~~34~~	~~232~~	~~6.75~~	~~0.289084~~	~~3.56~~	~~4.926~~	~~5.18~~	~~0.123587~~	~~3.76~~	~~1637~~	~~51~~	~~2009~~	~~65~~	~~0.90~~	~~18.50~~
36	infinite	0.00	0.221862	1.21	2.482	1.54	0.081136	0.94	1292	14	1225	18	0.95	-5.47
37	718	2.24	0.262693	8.75	3.496	13.60	0.096526	10.41	1504	116	1558	184	0.89	3.49
38	7919	0.19	0.354319	5.12	5.898	8.72	0.120730	7.05	1955	86	1967	121	0.89	0.60
~~39~~	~~187~~	~~8.99~~	~~0.176046~~	~~3.01~~	~~2.131~~	~~4.87~~	~~0.087797~~	~~3.83~~	~~1045~~	~~29~~	~~1378~~	~~72~~	~~0.01~~	~~24.14~~
40	1107	1.51	0.196045	5.03	2.100	8.77	0.077672	7.19	1154	53	1138	137	0.77	-1.37
~~41~~	~~314~~	~~5.33~~	~~0.189455~~	~~6.31~~	~~2.217~~	~~10.72~~	~~0.084875~~	~~8.66~~	~~1118~~	~~64~~	~~1313~~	~~159~~	~~0.82~~	~~14.80~~
~~42~~	~~20~~	~~86.43~~	~~0.122559~~	~~3.10~~	~~5.350~~	~~3.55~~	~~0.316625~~	~~1.72~~	~~745~~	~~22~~	~~3554~~	~~26~~	~~0.83~~	~~79.03~~
43	2048	0.65	0.555543	1.55	15.780	1.90	0.206013	1.09	2848	36	2874	18	0.93	0.91
44	524	2.91	0.344828	8.36	5.853	14.15	0.123095	11.42	1910	137	2002	190	0.93	4.58
45	866	1.92	0.211420	1.32	2.406	1.73	0.082553	1.12	1236	15	1259	22	0.78	1.77
47	infinite	0.00	0.304284	1.79	4.486	2.03	0.106934	0.97	1713	27	1748	18	0.91	2.02
~~50~~	~~291~~	~~5.90~~	~~0.155439~~	~~2.12~~	~~2.980~~	~~3.75~~	~~0.139025~~	~~3.10~~	~~931~~	~~18~~	~~2215~~	~~53~~	~~0.58~~	~~57.95~~
~~51~~	~~infinite~~	~~0.00~~	~~0.200809~~	~~1.67~~	~~2.388~~	~~2.62~~	~~0.086244~~	~~2.02~~	~~1180~~	~~18~~	~~1344~~	~~39~~	~~0.51~~	~~12.20~~
54	infinite	0.00	0.323391	1.49	4.840	1.77	0.108536	0.96	1806	23	1775	17	0.95	-1.76
55	infinite	0.00	0.197033	1.00	2.232	1.39	0.082174	0.97	1159	11	1250	19	0.89	7.23
56	infinite	0.00	0.173811	1.38	1.840	1.68	0.076799	0.97	1033	13	1116	19	0.94	7.43
57	infinite	0.00	0.200962	1.47	2.251	1.75	0.081227	0.95	1180	16	1227	19	0.95	3.79
~~58~~	~~463~~	~~3.62~~	~~0.190945~~	~~9.94~~	~~2.146~~	~~16.00~~	~~0.081517~~	~~12.54~~	~~1126~~	~~102~~	~~1234~~	~~228~~	~~0.88~~	~~8.71~~
60	infinite	0.00	0.294998	1.52	4.280	1.80	0.105217	0.96	1666	22	1718	18	0.92	3.01
~~62~~	~~494~~	~~3.34~~	~~0.217693~~	~~8.01~~	~~2.561~~	~~24.57~~	~~0.085318~~	~~23.23~~	~~1270~~	~~92~~	~~1323~~	~~394~~	~~0.92~~	~~4.02~~
63	infinite	0.00	0.177259	1.80	1.798	2.07	0.073581	1.02	1052	17	1030	20	0.92	-2.13
65	infinite	0.00	0.202800	1.86	2.224	2.09	0.079531	0.95	1190	20	1185	19	0.95	-0.42
68	5835	0.28	0.251121	5.07	3.335	8.71	0.096319	7.09	1444	65	1554	127	0.86	7.06
69	77304	0.02	0.370419	1.18	6.260	5.31	0.122569	5.18	2031	20	1994	89	0.96	-1.88
70	301961	0.01	0.312393	1.30	4.458	1.60	0.103495	0.94	1752	20	1688	17	0.96	-3.84
~~71~~	~~202~~	~~8.23~~	~~0.194021~~	~~5.26~~	~~2.430~~	~~9.40~~	~~0.090828~~	~~7.79~~	~~1143~~	~~55~~	~~1443~~	~~142~~	~~0.44~~	~~20.78~~
~~72~~	~~180~~	~~9.14~~	~~0.210613~~	~~5.09~~	~~2.145~~	~~10.86~~	~~0.073854~~	~~9.59~~	~~1232~~	~~57~~	~~1037~~	~~182~~	~~0.30~~	~~-18.76~~
73	3041	0.53	0.270837	1.18	3.626	2.22	0.097093	1.88	1545	16	1569	35	0.19	1.53
74	3102	0.50	0.339001	1.83	5.273	2.58	0.112822	1.81	1882	30	1845	32	0.44	-1.98
75	1219	1.36	0.213222	2.90	2.449	4.90	0.083288	3.95	1246	33	1276	75	0.68	2.35
76	5207	0.29	0.345412	1.41	5.357	1.72	0.112474	0.97	1913	23	1840	18	0.91	-3.96
78	1244	1.30	0.250888	3.08	3.247	5.41	0.093865	4.44	1443	40	1505	82	0.87	4.14
79	1263	1.34	0.179241	1.40	1.795	1.82	0.072645	1.17	1063	14	1004	24	0.77	-5.85
82	infinite	0.00	0.305872	0.97	4.416	1.41	0.104721	1.02	1720	15	1709	19	0.43	-0.64

PAR-1 (continued)

Grain	$^{206}Pb/^{204}Pb$	f_{206} %	Ratios $^{206}Pb/^{238}U$	±	$^{207}Pb/^{235}U$	±	$^{207}Pb/^{206}Pb$	±	Ages (Ma) $^{206}Pb/^{238}U$	±	$^{207}Pb/^{206}Pb$	±	Rho	Disc. %
83	infinite	0.00	0.192397	1.40	2.046	1.71	0.077125	0.98	1134	15	1124	19	0.92	-0.88
84	1587	0.99	0.307727	6.51	4.352	11.49	0.102566	9.47	1730	98	1671	165	0.20	-3.50
85	5120	0.26	0.559918	2.39	15.918	2.58	0.206183	0.95	2866	55	2876	15	0.91	0.33
87	1257	1.34	0.183964	3.33	1.909	5.65	0.075273	4.56	1089	33	1076	89	0.92	-1.19
88	3233	0.52	0.194481	2.57	2.104	3.80	0.078456	2.81	1146	27	1158	55	0.81	1.11
~~89~~	~~107~~	~~16.07~~	~~0.130690~~	~~4.60~~	~~1.297~~	~~7.56~~	~~0.071962~~	~~6.00~~	~~792~~	~~34~~	~~985~~	~~118~~	~~0.56~~	~~19.60~~
90	75321	0.02	0.208555	1.02	2.355	6.03	0.081896	5.95	1221	11	1243	112	0.85	1.76
~~91~~	~~1654~~	~~0.95~~	~~0.307870~~	~~5.66~~	~~5.235~~	~~9.54~~	~~0.123313~~	~~7.68~~	~~1730~~	~~85~~	~~2005~~	~~130~~	~~0.64~~	~~13.69~~
~~92~~	~~580~~	~~2.66~~	~~0.328119~~	~~6.88~~	~~7.193~~	~~11.62~~	~~0.158991~~	~~9.36~~	~~1829~~	~~109~~	~~2445~~	~~150~~	~~0.94~~	~~25.18~~
94	1906	0.80	0.360294	1.52	5.934	2.58	0.119453	2.08	1984	26	1948	37	0.32	-1.82
95	401	4.20	0.185279	5.01	1.987	8.34	0.077782	6.67	1096	50	1141	127	0.93	3.99
96	infinite	0.00	0.372053	1.65	6.456	1.90	0.125854	0.95	2039	29	2041	17	0.96	0.09
97	1428	1.15	0.234003	2.83	2.673	4.70	0.082854	3.75	1355	34	1266	72	0.76	-7.08
98	2333	0.70	0.233935	4.37	3.025	6.61	0.093794	4.97	1355	53	1504	91	0.91	9.90
100	infinite	0.00	0.224132	1.35	2.675	1.67	0.086546	0.99	1304	16	1350	19	0.82	3.46
101	10287	0.16	0.234108	4.36	2.942	7.27	0.091146	5.82	1356	53	1450	107	0.95	6.46
~~102~~	~~infinite~~	~~0.00~~	~~0.187330~~	~~1.19~~	~~2.118~~	~~1.59~~	~~0.081997~~	~~1.06~~	~~1107~~	~~12~~	~~1245~~	~~21~~	~~0.88~~	~~11.13~~
103	infinite	0.00	0.236739	1.59	3.085	2.47	0.094517	1.89	1370	20	1518	35	0.60	9.80
104	infinite	0.00	0.190483	1.27	2.142	1.72	0.081542	1.17	1124	13	1235	23	0.88	8.96
~~106~~	~~364~~	~~4.63~~	~~0.178414~~	~~1.88~~	~~2.007~~	~~3.13~~	~~0.081579~~	~~2.50~~	~~1058~~	~~18~~	~~1235~~	~~48~~	~~0.66~~	~~14.34~~
108	infinite	0.00	0.240689	1.25	2.907	1.58	0.087584	0.97	1390	16	1373	19	0.94	-1.23
109	infinite	0.00	0.175293	0.98	1.792	1.38	0.074138	0.97	1041	9	1045	19	0.86	0.38

Sample ANTA-2, Paracatu Formation

Grain	$^{206}Pb/^{204}Pb$	f_{206} %	Ratios $^{206}Pb/^{238}U$	±	$^{207}Pb/^{235}U$	±	$^{207}Pb/^{206}Pb$	±	Ages (Ma) $^{206}Pb/^{238}U$	±	$^{207}Pb/^{206}Pb$	±	Rho	Disc. %
~~1~~	infinite	~~0.00~~	~~0.491330~~	~~9.32~~	~~11.255~~	~~18.90~~	~~0.166133~~	~~16.44~~	~~2576~~	~~195~~	~~2519~~	~~253~~	~~0.88~~	~~-2.28~~
~~2~~	~~infinite~~	~~0.00~~	~~0.158776~~	~~0.90~~	~~1.799~~	~~1.48~~	~~0.082157~~	~~1.17~~	~~950~~	~~8~~	~~1249~~	~~23~~	~~0.39~~	~~23.96~~
~~3~~	~~1575~~	~~1.06~~	~~0.211967~~	~~1.88~~	~~3.710~~	~~2.23~~	~~0.126935~~	~~1.19~~	~~1239~~	~~21~~	~~2056~~	~~21~~	~~0.89~~	~~39.72~~
4	2080	0.73	0.348605	2.97	5.629	6.45	0.117113	5.72	1928	49	1913	99	0.21	-0.80
~~5~~	~~1487~~	~~1.14~~	~~0.175636~~	~~0.97~~	~~2.225~~	~~1.62~~	~~0.091890~~	~~1.29~~	~~1043~~	~~9~~	~~1465~~	~~24~~	~~0.26~~	~~28.81~~
~~6~~	~~236~~	~~7.37~~	~~0.134793~~	~~1.19~~	~~3.024~~	~~2.04~~	~~0.162735~~	~~1.66~~	~~815~~	~~9~~	~~2484~~	~~28~~	~~0.74~~	~~67.19~~
7	infinite	0.00	0.264187	3.33	3.428	3.53	0.094106	1.16	1511	45	1510	22	0.88	-0.07
~~8~~	~~178~~	~~8.81~~	~~0.307441~~	~~1.46~~	~~8.473~~	~~5.22~~	~~0.199880~~	~~5.01~~	~~1728~~	~~22~~	~~2825~~	~~79~~	~~0.72~~	~~38.83~~
~~9~~	~~402~~	~~4.37~~	~~0.118202~~	~~1.32~~	~~2.055~~	~~1.89~~	~~0.126071~~	~~1.35~~	~~720~~	~~9~~	~~2044~~	~~24~~	~~0.59~~	~~64.76~~
11	infinite	0.00	0.326814	1.96	4.987	2.24	0.110667	1.08	1823	31	1810	20	0.90	-0.69
~~12~~	~~1608~~	~~0.98~~	~~0.295638~~	~~1.27~~	~~5.492~~	~~1.69~~	~~0.134740~~	~~1.11~~	~~1670~~	~~19~~	~~2161~~	~~19~~	~~0.84~~	~~22.73~~
13	infinite	0.00	0.215053	4.19	2.424	4.32	0.081751	1.06	1256	48	1240	21	0.70	-1.30
14	infinite	0.00	0.190139	3.79	2.018	3.93	0.076960	1.04	1122	39	1120	21	0.90	-0.18
15	infinite	0.00	0.311789	2.48	4.609	2.69	0.107212	1.03	1750	38	1753	19	0.89	0.17
~~16~~	~~620~~	~~2.68~~	~~0.208320~~	~~4.34~~	~~2.302~~	~~16.18~~	~~0.080142~~	~~15.59~~	~~1220~~	~~48~~	~~1200~~	~~280~~	~~0.62~~	~~-1.61~~
17	infinite	0.00	0.261539	3.01	3.326	3.22	0.092230	1.16	1498	40	1472	22	0.88	-1.74
~~17~~	~~447~~	~~3.69~~	~~0.227618~~	~~0.73~~	~~4.127~~	~~1.37~~	~~0.131498~~	~~1.15~~	~~1322~~	~~9~~	~~2118~~	~~20~~	~~0.25~~	~~37.58~~
~~18~~	~~169~~	~~9.71~~	~~0.213130~~	~~6.72~~	~~2.366~~	~~48.74~~	~~0.080512~~	~~48.28~~	~~1245~~	~~76~~	~~1210~~	~~737~~	~~0.54~~	~~-2.97~~
~~18~~	~~311~~	~~5.54~~	~~0.151001~~	~~3.29~~	~~2.418~~	~~3.92~~	~~0.116129~~	~~2.13~~	~~907~~	~~28~~	~~1897~~	~~38~~	~~0.78~~	~~52.22~~
~~19~~	~~279~~	~~6.17~~	~~0.150738~~	~~1.45~~	~~3.174~~	~~1.85~~	~~0.152694~~	~~1.15~~	~~905~~	~~12~~	~~2376~~	~~20~~	~~0.84~~	~~61.91~~
19	2753	0.59	0.263858	4.63	3.419	5.35	0.093978	2.68	1510	62	1508	50	0.63	-0.12
20	2551	0.64	0.232925	2.46	2.775	3.92	0.086420	3.05	1350	30	1348	58	0.79	-0.16
21	4125	0.38	0.312386	3.14	4.620	3.52	0.107272	1.60	1752	48	1754	29	0.92	0.07
~~22~~	~~1389~~	~~1.16~~	~~0.256107~~	~~5.52~~	~~3.209~~	~~12.26~~	~~0.090871~~	~~10.95~~	~~1470~~	~~72~~	~~1444~~	~~195~~	~~0.91~~	~~-1.80~~
23	133073	0.01	0.419247	2.58	8.320	2.77	0.143932	1.02	2257	49	2275	17	0.91	0.79
24	8478	0.20	0.213632	3.17	2.424	3.36	0.082296	1.14	1248	36	1253	22	0.78	0.35
25	13516	0.12	0.210439	2.64	2.365	2.81	0.081502	0.94	1231	30	1234	18	0.70	0.20

ANTA-2 (continued)

Grain	$^{206}Pb/^{204}Pb$	f_{206} %	Ratios $^{206}Pb/^{238}U$	±	$^{207}Pb/^{235}U$	±	$^{207}Pb/^{206}Pb$	±	Ages (Ma) $^{206}Pb/^{238}U$	±	$^{207}Pb/^{206}Pb$	±	Rho	Disc. %
26	infinite	0.00	0.216029	1.72	2.461	2.02	0.082615	1.04	1261	20	1260	20	0.77	-0.06
27	3871	0.41	0.271271	2.03	3.602	2.26	0.096290	1.01	1547	28	1553	19	0.15	0.40
28	40784	0.04	0.201469	2.53	2.207	2.72	0.079438	1.01	1183	27	1183	20	0.73	-0.01
29	10177	0.15	0.300237	2.65	4.238	6.80	0.102379	6.27	1692	39	1668	112	0.81	-1.49
30	infinite	0.00	0.189681	2.04	2.003	2.40	0.076588	1.26	1120	21	1110	25	0.12	-0.82
32	infinite	0.00	0.230473	5.38	2.726	5.50	0.085793	1.15	1337	65	1334	22	0.85	-0.26
~~32~~	~~4456~~	~~0.38~~	~~0.203131~~	~~2.79~~	~~2.199~~	~~12.09~~	~~0.078511~~	~~11.77~~	~~1192~~	~~30~~	~~1160~~	~~217~~	~~0.48~~	~~-2.78~~
33	infinite	0.00	0.181344	1.63	1.882	1.97	0.075255	1.12	1074	16	1075	22	0.59	0.09
~~34~~	~~1129~~	~~1.49~~	~~0.187523~~	~~7.56~~	~~1.962~~	~~13.28~~	~~0.075878~~	~~10.91~~	~~1108~~	~~77~~	~~1092~~	~~204~~	~~0.67~~	~~-1.47~~
35	19977	0.07	0.388293	3.94	7.079	4.08	0.132231	1.05	2115	71	2128	18	0.95	0.61
36	3059	0.43	0.567224	3.37	16.184	5.67	0.206929	4.57	2896	78	2882	72	0.95	-0.51
37	1506	1.12	0.179255	3.06	1.839	8.44	0.074390	7.87	1063	30	1052	151	0.57	-1.03
~~38~~	~~3498~~	~~0.46~~	~~0.250316~~	~~4.21~~	~~3.082~~	~~10.40~~	~~0.089309~~	~~9.51~~	~~1440~~	~~54~~	~~1411~~	~~172~~	~~0.93~~	~~-2.08~~
39	7843	0.20	0.304450	2.38	4.403	2.72	0.104887	1.31	1713	36	1712	24	0.67	-0.06
~~40~~	~~1105~~	~~1.49~~	~~0.223491~~	~~3.57~~	~~2.566~~	~~13.12~~	~~0.083259~~	~~12.62~~	~~1300~~	~~42~~	~~1275~~	~~228~~	~~0.03~~	~~-1.96~~
41	1751	0.96	0.191569	1.97	2.032	7.33	0.076917	7.06	1130	20	1119	135	0.21	-0.97
~~42~~	~~890~~	~~1.76~~	~~0.306057~~	~~4.06~~	~~4.350~~	~~15.94~~	~~0.103088~~	~~15.42~~	~~1721~~	~~61~~	~~1680~~	~~261~~	~~0.64~~	~~-2.43~~
43	6049	0.28	0.202398	3.13	2.216	4.31	0.079408	2.96	1188	34	1182	57	0.54	-0.50
44	infinite	0.00	0.318359	1.83	4.793	2.10	0.109198	1.05	1782	28	1786	19	0.87	0.24
45	infinite	0.00	0.330183	2.91	5.138	3.11	0.112855	1.07	1839	46	1846	19	0.75	0.36
46	infinite	0.00	0.389755	4.58	7.180	4.74	0.133613	1.21	2122	82	2146	21	0.95	1.13
47	infinite	0.00	0.217968	2.60	2.497	2.91	0.083094	1.29	1271	30	1271	25	0.57	0.02
~~48~~	~~216~~	~~8.03~~	~~0.142352~~	~~1.22~~	~~3.440~~	~~1.74~~	~~0.175279~~	~~1.24~~	~~858~~	~~10~~	~~2609~~	~~20~~	~~0.91~~	~~67.11~~
~~49~~	~~814~~	~~2.05~~	~~0.205659~~	~~7.73~~	~~2.265~~	~~13.58~~	~~0.079878~~	~~11.16~~	~~1206~~	~~84~~	~~1194~~	~~206~~	~~0.15~~	~~-0.98~~
50	infinite	0.00	0.303472	5.52	4.331	5.72	0.103514	1.53	1709	82	1688	28	0.54	-1.21
~~51~~	~~207~~	~~8.46~~	~~0.119219~~	~~1.56~~	~~2.910~~	~~2.59~~	~~0.177057~~	~~2.07~~	~~726~~	~~11~~	~~2625~~	~~34~~	~~0.13~~	~~72.35~~
~~52~~	~~298~~	~~5.70~~	~~0.174899~~	~~1.11~~	~~3.586~~	~~1.94~~	~~0.148689~~	~~1.59~~	~~1039~~	~~11~~	~~2331~~	~~27~~	~~0.19~~	~~55.42~~
~~53~~	~~1042~~	~~1.48~~	~~0.329004~~	~~7.26~~	~~4.988~~	~~14.63~~	~~0.109951~~	~~12.70~~	~~1834~~	~~115~~	~~1799~~	~~215~~	~~0.45~~	~~-1.94~~
54	infinite	0.00	0.211238	5.61	2.362	5.84	0.081113	1.60	1235	63	1224	31	0.51	-0.92
~~55~~	~~1568~~	~~0.97~~	~~0.354428~~	~~1.30~~	~~9.168~~	~~1.68~~	~~0.187598~~	~~1.06~~	~~1956~~	~~22~~	~~2721~~	~~17~~	~~0.90~~	~~28.13~~
56	9504	0.17	0.262854	1.84	3.394	2.46	0.093649	1.63	1504	25	1501	31	0.21	-0.23
57	infinite	0.00	0.340803	5.74	5.433	5.83	0.115615	1.03	1891	93	1889	18	0.72	-0.05
58	1238	1.33	0.230247	4.69	2.709	9.53	0.085333	8.29	1336	56	1323	153	0.08	-0.96
59	infinite	0.00	0.323405	2.57	4.931	2.76	0.110585	0.98	1806	40	1809	18	0.91	0.15
~~60~~	~~503~~	~~3.33~~	~~0.201183~~	~~1.17~~	~~3.584~~	~~1.72~~	~~0.129193~~	~~1.26~~	~~1182~~	~~13~~	~~2087~~	~~22~~	~~0.54~~	~~43.38~~
~~61~~	~~210~~	~~8.33~~	~~0.127177~~	~~1.01~~	~~3.021~~	~~2.38~~	~~0.172269~~	~~2.15~~	~~772~~	~~7~~	~~2580~~	~~35~~	~~0.14~~	~~70.09~~
62	infinite	0.00	0.222173	2.10	2.574	2.33	0.084014	0.99	1293	25	1293	19	0.78	-0.04
~~63~~	~~729~~	~~2.27~~	~~0.220180~~	~~0.89~~	~~3.950~~	~~1.36~~	~~0.130099~~	~~1.02~~	~~1283~~	~~10~~	~~2099~~	~~18~~	~~0.77~~	~~38.89~~
106	8232	0.19	0.296665	0.77	4.534	1.31	0.110832	1.06	1675	11	1813	19	0.71	7.63
107	14439	0.12	0.210009	2.44	2.351	2.62	0.081178	0.97	1229	27	1226	19	0.80	-0.25
108	infinite	0.00	0.313802	4.01	4.652	4.08	0.107528	0.77	1759	61	1758	14	0.80	-0.08
109	infinite	0.00	0.281097	4.01	3.819	4.07	0.098523	0.68	1597	56	1596	13	0.77	-0.03
110	infinite	0.00	0.344484	4.74	5.597	4.86	0.117832	1.06	1908	78	1924	19	0.88	0.80
~~111~~	~~199~~	~~8.72~~	~~0.137021~~	~~1.20~~	~~2.854~~	~~1.96~~	~~0.151081~~	~~1.55~~	~~828~~	~~9~~	~~2358~~	~~26~~	~~0.02~~	~~64.90~~
112	3985	0.38	0.368545	5.00	6.360	5.07	0.125165	0.83	2023	86	2031	15	0.44	0.42
~~113~~	~~406~~	~~4.03~~	~~0.241802~~	~~1.04~~	~~4.847~~	~~1.60~~	~~0.145383~~	~~1.22~~	~~1396~~	~~13~~	~~2292~~	~~21~~	~~0.64~~	~~39.10~~
115	3504	0.46	0.271718	2.42	3.597	3.16	0.096010	2.04	1550	33	1548	38	0.31	-0.10
116	infinite	0.00	0.271343	1.68	3.592	1.97	0.096019	1.02	1548	23	1548	19	0.61	0.03
117	infinite	0.00	0.273815	2.66	3.653	2.85	0.096760	1.02	1560	37	1563	19	0.89	0.16
118	5709	0.26	0.389138	6.70	7.099	6.83	0.132309	1.33	2119	120	2129	23	0.75	0.47

Sample CH-2, Chapada dos Pilões Formation

Grain	$^{206}Pb/^{204}Pb$	f_{206} %	Ratios						Ages				Rho	Disc. %
			$^{206}Pb/^{238}U$	±	$^{207}Pb/^{235}U$	±	$^{207}Pb/^{206}Pb$	±	$^{206}Pb/^{238}U$	±	$^{207}Pb/^{206}Pb$	±		
1	5147	0.25	0.591584	2.18	18.232	3.57	0.223518	2.83	2996	52	3006	45	0.89	0.34
2	1597	0.93	0.395764	2.22	7.395	2.69	0.135514	1.52	2150	41	2171	26	0.84	0.97
~~3~~	~~467~~	~~3.25~~	~~0.348699~~	~~2.05~~	~~4.938~~	~~3.33~~	~~0.102713~~	~~2.63~~	~~1928~~	~~34~~	~~1674~~	~~48~~	~~0.86~~	~~-15.22~~
4	1318	1.07	0.470085	3.51	10.424	4.22	0.160829	2.34	2484	72	2464	39	0.97	-0.79
5	417	3.68	0.334105	3.93	5.281	6.42	0.114634	5.08	1858	63	1874	89	0.87	0.85
6	3405	0.44	0.392595	5.02	7.153	5.43	0.132136	2.06	2135	91	2127	36	0.97	-0.39
7	2382	0.58	0.498643	7.44	13.338	7.69	0.193999	1.97	2608	158	2776	32	0.97	6.07
8	3027	0.49	0.387788	2.52	7.004	3.30	0.130994	2.12	2113	45	2111	37	0.97	-0.06
9	1603	0.97	0.322455	2.32	4.908	3.31	0.110392	2.37	1802	36	1806	42	0.96	0.23
10	2014	0.75	0.370123	2.83	6.367	4.52	0.124755	3.52	2030	49	2025	61	0.95	-0.23
11	2197	0.68	0.383350	2.67	6.845	4.17	0.129511	3.20	2092	48	2091	55	0.97	-0.03
12	1206	1.22	0.409592	5.03	7.983	6.41	0.141362	3.98	2213	94	2244	67	0.95	1.38
13	22643	0.07	0.400751	1.47	7.456	2.16	0.134935	1.58	2172	27	2163	27	0.92	-0.43
14	4795	0.32	0.360868	1.37	6.010	2.27	0.120786	1.82	1986	23	1968	32	0.91	-0.94
15	9956	0.15	0.390505	2.07	6.960	3.11	0.129262	2.33	2125	37	2088	40	0.96	-1.78
16	1008	1.49	0.375848	2.47	6.685	4.02	0.128991	3.16	2057	43	2084	55	0.83	1.31
~~17~~	~~3137~~	~~0.49~~	~~0.330240~~	~~2.84~~	~~5.059~~	~~7.30~~	~~0.111095~~	~~6.72~~	~~1840~~	~~45~~	~~1817~~	~~117~~	~~0.87~~	~~-1.22~~
18	1270	1.23	0.306974	2.08	4.504	2.81	0.106404	1.89	1726	31	1739	34	0.96	0.74
19	infinite	0.00	0.175335	1.78	1.787	2.55	0.073936	1.82	1041	17	1040	36	0.78	-0.16
20	infinite	0.00	0.359175	2.13	5.990	2.61	0.120946	1.50	1978	36	1970	27	0.96	-0.41
21	1876	0.71	0.546531	4.96	13.842	7.93	0.183683	6.18	2811	112	2686	99	0.97	-4.63
~~22~~	~~infinite~~	~~0.00~~	~~0.310382~~	~~13.62~~	~~4.547~~	~~19.27~~	~~0.106255~~	~~13.64~~	~~1743~~	~~205~~	~~1736~~	~~231~~	~~0.46~~	~~-0.37~~
23	3200	0.48	0.338921	1.69	5.202	2.73	0.111313	2.14	1881	28	1821	38	0.80	-3.32
24	613	2.57	0.294743	3.30	4.022	5.31	0.098980	4.16	1665	48	1605	76	0.95	-3.75
~~25~~	~~405~~	~~3.86~~	~~0.302095~~	~~7.95~~	~~3.943~~	~~9.61~~	~~0.094657~~	~~5.40~~	~~1702~~	~~118~~	~~1521~~	~~99~~	~~0.96~~	~~-11.86~~
26	608	2.76	0.194584	3.64	2.098	6.26	0.078210	5.09	1146	38	1152	98	0.92	0.52
27	1130	1.43	0.255703	3.55	3.201	5.05	0.090784	3.59	1468	46	1442	67	0.97	-1.79
28	infinite	0.00	0.347990	3.63	5.609	5.19	0.116902	3.71	1925	60	1909	65	0.80	-0.82
~~29~~	~~2247~~	~~0.71~~	~~0.287963~~	~~7.11~~	~~3.888~~	~~11.70~~	~~0.097915~~	~~9.29~~	~~1631~~	~~102~~	~~1585~~	~~164~~	~~0.97~~	~~-2.94~~
30	infinite	0.00	0.332172	2.58	5.131	3.80	0.112027	2.79	1849	41	1833	50	0.67	-0.89
31	infinite	0.00	0.267938	2.83	3.514	4.03	0.095110	2.87	1530	38	1530	53	0.77	-0.01
32	3924	0.43	0.205319	3.21	2.277	5.54	0.080446	4.51	1204	35	1208	86	0.76	0.34
33	1377	1.16	0.283586	3.25	3.781	4.88	0.096698	3.64	1609	46	1561	67	0.97	-3.08
34	infinite	0.01	0.494940	2.11	11.514	2.92	0.168719	2.02	2592	45	2545	34	0.95	-1.85
~~35~~	~~93~~	~~18.88~~	~~0.090480~~	~~13.68~~	~~0.748~~	~~16.85~~	~~0.059995~~	~~9.85~~	~~558~~	~~73~~	~~603~~	~~200~~	~~0.97~~	~~7.46~~
36	4293	0.37	0.292387	2.13	4.037	3.67	0.100137	2.99	1653	31	1627	55	0.82	-1.65
37	1496	1.02	0.346311	2.04	5.543	3.11	0.116092	2.34	1917	34	1897	42	0.96	-1.06
38	1819	0.92	0.198446	2.50	2.160	4.23	0.078959	3.41	1167	27	1171	66	0.70	0.35
39	873	1.89	0.220483	2.23	2.550	3.63	0.083867	2.86	1284	26	1289	55	0.91	0.39
40	1067	1.46	0.316288	2.29	4.586	4.81	0.105161	4.23	1772	35	1717	76	0.93	-3.17
~~41~~	~~146~~	~~10.46~~	~~0.315410~~	~~7.72~~	~~4.654~~	~~10.70~~	~~0.107016~~	~~7.41~~	~~1767~~	~~118~~	~~1749~~	~~130~~	~~0.97~~	~~-1.03~~
42	infinite	0.00	0.204853	1.33	2.258	1.91	0.079941	1.37	1201	15	1196	27	0.62	-0.48
~~43~~	~~268~~	~~6.39~~	~~0.152717~~	~~8.18~~	~~1.447~~	~~9.22~~	~~0.068743~~	~~4.26~~	~~916~~	~~69~~	~~891~~	~~86~~	~~0.97~~	~~-2.82~~
44	1730	0.77	0.544885	1.92	13.967	3.17	0.185908	2.52	2804	44	2706	41	0.56	-3.61
45	10797	0.14	0.396900	2.35	7.269	3.92	0.132832	3.13	2155	43	2136	54	0.90	-0.89
46	infinite	0.00	0.261879	1.89	3.374	2.73	0.093441	1.97	1499	25	1497	37	0.78	-0.17
47	infinite	0.00	0.386406	2.03	6.976	2.97	0.130943	2.16	2106	36	2111	37	0.67	0.21
48	infinite	0.00	0.308498	2.17	4.516	3.09	0.106173	2.20	1733	33	1735	40	0.79	0.08
49	6204	0.24	0.396633	1.51	7.334	2.48	0.134115	1.96	2154	28	2153	34	0.87	-0.05
50	1224	1.38	0.178159	5.62	1.844	5.67	0.075081	0.73	1057	55	1071	15	0.87	1.28
51	1170	1.22	0.447848	2.06	8.536	4.26	0.138232	3.72	2386	41	2205	63	0.97	-8.19
52	517	3.05	0.293117	2.30	4.044	4.33	0.100068	3.67	1657	33	1625	67	0.95	-1.95
53	2072	0.75	0.325599	1.47	4.950	2.40	0.110250	1.90	1817	23	1804	34	0.93	-0.75

CH-2 (continued)

Grain	$^{206}Pb/^{204}Pb$	f_{206} %	Ratios $^{206}Pb/^{238}U$	±	$^{207}Pb/^{235}U$	±	$^{207}Pb/^{206}Pb$	±	Ages $^{206}Pb/^{238}U$	±	$^{207}Pb/^{206}Pb$	±	Rho	Disc. %
54	659	2.35	0.320572	1.00	4.774	3.65	0.108000	3.51	1793	16	1766	63	0.94	-1.50
~~55~~	~~435~~	~~3.85~~	~~0.196057~~	~~3.57~~	~~2.072~~	~~5.59~~	~~0.076655~~	~~4.30~~	~~1154~~	~~38~~	~~1112~~	~~84~~	~~0.97~~	~~-3.76~~
56	1594	0.89	0.464034	1.90	9.983	2.94	0.156026	2.24	2457	39	2413	38	0.96	-1.84
57	infinite	0.00	0.199671	1.52	2.174	2.16	0.078965	1.54	1174	16	1171	30	0.70	-0.20
58	4093	0.38	0.316890	2.76	4.654	3.59	0.106525	2.29	1775	43	1741	41	0.97	-1.94
59	infinite	0.00	0.314017	1.75	4.629	2.43	0.106911	1.68	1760	27	1747	30	0.96	-0.75
~~60~~	~~19034~~	~~0.08~~	~~0.304725~~	~~9.15~~	~~4.381~~	~~13.10~~	~~0.104275~~	~~9.37~~	~~1715~~	~~136~~	~~1702~~	~~163~~	~~0.87~~	~~-0.77~~
61	infinite	0.00	0.382847	5.26	6.783	7.39	0.128502	5.19	2090	93	2078	89	0.91	-0.58
62	infinite	0.00	0.273324	3.07	3.596	4.02	0.095429	2.60	1558	42	1537	48	0.91	-1.37
63	infinite	0.00	0.190634	2.52	2.026	3.66	0.077074	2.65	1125	26	1123	52	0.37	-0.15
64	infinite	0.00	0.382540	3.71	6.824	5.18	0.129375	3.62	2088	66	2089	62	0.67	0.07
65	infinite	0.00	0.232504	3.32	2.771	4.68	0.086436	3.30	1348	40	1348	62	0.82	0.03
66	infinite	0.00	0.523126	2.09	13.139	2.89	0.182159	2.00	2712	46	2673	33	0.91	-1.49
67	infinite	0.00	0.376928	3.60	6.610	5.15	0.127185	3.69	2062	63	2059	64	0.71	-0.12
68	1100	1.54	0.182581	2.12	1.906	3.61	0.075721	2.93	1081	21	1088	58	0.87	0.61
69	infinite	0.00	0.379189	1.27	6.643	1.89	0.127051	1.41	2072	22	2058	25	0.66	-0.73
70	3382	0.46	0.332660	1.98	5.057	3.41	0.110253	2.78	1851	32	1804	50	0.87	-2.64
80	infinite	0.00	0.391264	1.08	7.270	1.54	0.134760	1.10	2129	19	2161	19	0.91	1.49
81	infinite	0.00	0.387943	2.70	7.014	3.02	0.131128	1.35	2113	49	2113	23	0.80	-0.01
83	infinite	0.00	0.301423	1.83	4.327	2.05	0.104109	0.92	1698	27	1699	17	0.70	0.02
86	2553	0.58	0.388078	6.55	7.062	6.67	0.131975	1.25	2114	117	2124	22	0.96	0.49
90	3529	0.39	0.517419	2.79	13.224	3.49	0.185355	2.09	2688	61	2701	34	0.82	0.49
91	infinite	0.00	0.392866	1.37	7.202	1.77	0.132954	1.12	2136	25	2137	19	0.81	0.06
93	infinite	0.00	0.389417	2.31	7.069	2.54	0.131665	1.04	2120	42	2120	18	0.76	0.01

Notes: Uncertainties given at the one σ level (%).

f^{206}% denotes the percentage of ^{206}Pb that is common Pb.

Correction for common Pb made using the measured $^{206}Pb/^{204}Pb$ ratio.

For % Disc., 0% denotes a concordant analysis.

4.4.1.4 – Cubatão Formation, Ibiá Group

Zircon grains from ca. 3 cm pebbles of the Cubatão Formation were investigated by SHRIMP. The age obtained was 2133 ± 24 Ma, with MSWD of 2.3 (Fig. 4.8).

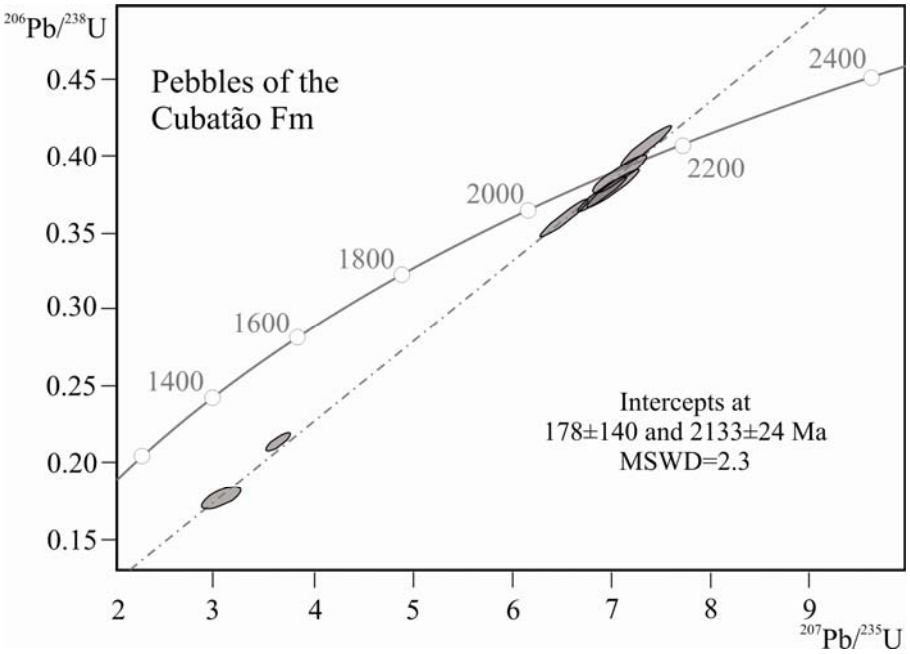

Figure 4.8 - Concordia diagram for zircon of pebbles from Cubatão Formation.

Sample CUB-1 is a diamictite with pebbles of granitic and mafic rocks, siltstone and phyllite set in a fine grained carbonatic matrix. Most zircon grains present transport features; they are rounded and/or spherical, yellowish, pink and vary from 50 to 300 μm in diameter. All analysed zircons produced concordant analyses indicating three main age peak at 936, 1190 and 1840 Ma (Fig. 4.9). The youngest grain presented 935±11 Ma.

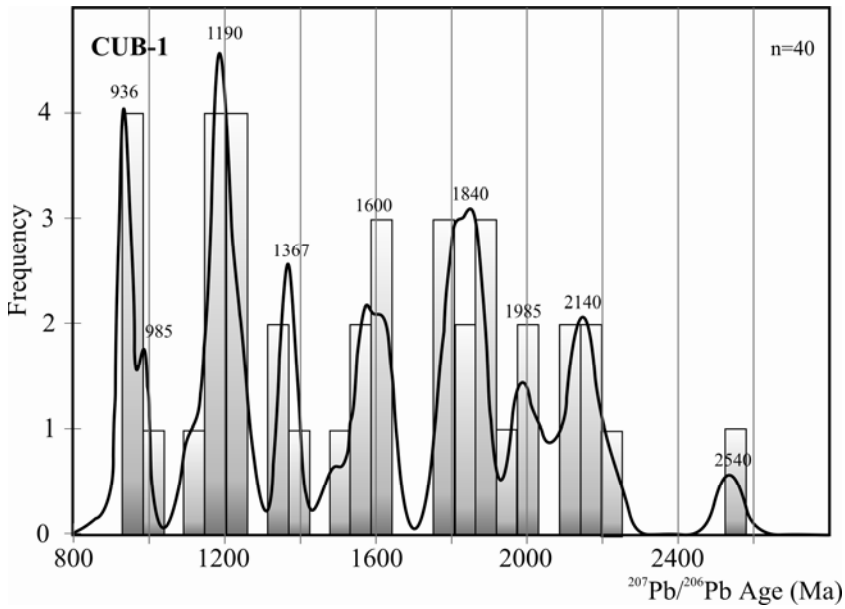

Figure 4.9 - Relative probability distribution diagram of $^{207}Pb/^{206}Pb$ zircon ages of sample CUB-1.

Table 4.2. Summary of SHRIMP U-Th-Pb zircon results for sample Cubatão.

Grain. spot	U (ppm)	Th (ppm)	Th/U	Pb* (ppm)	$^{206}Pb/^{204}Pb$	f_{206} %	Ratios						Ages (Ma)						Disc. %
							$^{206}Pb/^{238}U$	±	$^{207}Pb/^{235}U$	±	$^{207}Pb/^{206}Pb$	±	$^{206}Pb/^{238}U$	±	$^{207}Pb/^{235}U$	±	$^{207}Pb/^{206}Pb$	±	
1.1	120	57	0.47	53	6407	0.23	0.40640	0.00850	7.351	0.167	0.13119	0.00088	2198	39	2155	21	2114	12	-4
2.1	298	168	0.56	69	653	2.28	0.21137	0.00384	3.631	0.084	0.12460	0.00154	1236	20	1556	19	2023	22	39
3.1	141	66	0.47	55	8780	0.17	0.35871	0.00824	6.511	0.160	0.13165	0.00085	1976	39	2047	22	2120	11	7
4.1	110	40	0.37	45	4110	0.36	0.38751	0.00834	7.080	0.173	0.13251	0.00123	2111	39	2122	22	2132	16	1
5.1	77	81	1.05	15	1349	1.11	0.17409	0.00464	3.046	0.125	0.12690	0.00356	1035	26	1419	32	2055	50	50
6.1	160	88	0.55	67	5839	0.26	0.37588	0.00823	6.888	0.163	0.13290	0.00088	2057	39	2097	21	2137	12	4
7.1	153	66	0.43	62	5161	0.29	0.37806	0.00869	7.009	0.172	0.13446	0.00084	2067	41	2113	22	2157	11	4
~~8.1~~	~~53~~	~~1~~	~~0.01~~	~~9~~	~~3934~~	~~0.38~~	~~0.17332~~	~~0.00394~~	~~1.896~~	~~0.104~~	~~0.07934~~	~~0.00375~~	~~1030~~	~~22~~	~~1080~~	~~37~~	~~1181~~	~~96~~	~~13~~

Notes: 1. Uncertainties given at the one σ level (%)
2. f^{206}% denotes the percentage of ^{206}Pb that is common Pb.
3. Correction for common Pb made using the measured $^{206}Pb/^{204}Pb$ ratio.
4. For % Disc., 0% denotes a concordant analysis.

4.4.1.5 – Rio Verde Formation, Ibiá Group

Sample RV-1 is a folded calciferous phyllite from the northern segment of the Ibiá Group (Fig. 4.3). The zircon grains are clear, prismatic (3:1 to 5:1), colourless with few transport features. Most of the analyses resulted in concordant data. Out of the 76 concordant analyses, 65 indicate neoproterozoic ages, with main-peaks at 665, 740 and 850 Ma and minor peaks at 640, 960 and 1070 Ma (Fig. 4.10). The youngest peak age of 640 Ma is interpreted as the maximum depositional age for Rio Verde Formation.

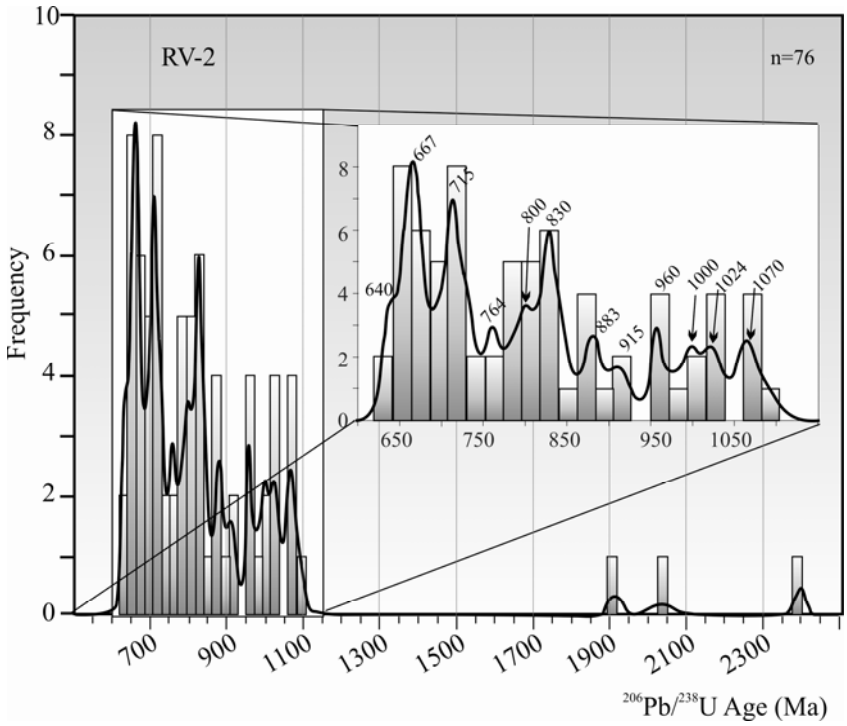

Figure 4.10 - Relative probability distribution diagram of $^{206}Pb/^{238}U$ zircon ages of sample RV-1.

Table 4.3. Summary of LAM-ICP-MS zircon results for samples of the Ibiá Group.

Cubatão Formation – Sample CUB-1

Grain	$^{206}Pb/^{204}Pb$	f_{206} %	Ratios $^{206}Pb/^{238}U$	±	$^{207}Pb/^{235}U$	±	$^{207}Pb/^{206}Pb$	±	Ages $^{206}Pb/^{238}U$	±	$^{207}Pb/^{206}Pb$	±	Rho	Disc. %
1	13287	0.13	0.201879	3.36	2.214	3.71	0.079557	1.58	1185	40	1186	19	0.90	0.05
2	3261	0.51	0.207819	4.09	2.310	4.98	0.080604	2.84	1217	50	1212	34	0.82	-0.44
3	75619	0.02	0.322052	1.79	4.891	2.24	0.110141	1.35	1800	32	1802	24	0.80	0.11
4	74363	0.02	0.290112	2.34	3.996	2.72	0.099910	1.40	1642	38	1622	23	0.86	-1.21
5	17174	0.09	0.276279	2.21	3.694	2.72	0.096973	1.58	1573	35	1567	25	0.81	-0.38
6	12703	0.13	0.207217	2.36	2.306	3.09	0.080716	2.00	1214	29	1215	24	0.76	0.05

Grain	$^{206}Pb/^{204}Pb$	f_{206} %	Ratios						Ages				Rho	Disc. %
			$^{206}Pb/^{238}U$	±	$^{207}Pb/^{235}U$	±	$^{207}Pb/^{206}Pb$	±	$^{206}Pb/^{238}U$	±	$^{207}Pb/^{206}Pb$	±		
7	36177	0.04	0.410120	1.54	7.901	2.10	0.139720	1.43	2215	34	2224	32	0.73	0.37
8	70199	0.02	0.200639	1.48	2.195	2.04	0.079343	1.41	1179	17	1181	17	0.72	0.17
9	22794	0.07	0.397605	1.67	7.385	2.21	0.134710	1.44	2158	36	2160	31	0.76	0.10
10	19131	0.08	0.325112	1.57	4.982	2.18	0.111148	1.51	1815	29	1818	27	0.72	0.20
11	7415	0.22	0.281313	1.58	3.820	2.22	0.098496	1.56	1598	25	1596	25	0.71	-0.13
12	2584	0.60	0.334771	1.32	5.281	1.89	0.114408	1.35	1861	25	1871	25	0.70	0.49
13	4454	0.37	0.234337	1.61	2.814	2.21	0.087102	1.50	1357	22	1363	20	0.73	0.41
14	9642	0.18	0.155443	1.76	1.503	2.43	0.070139	1.67	931	16	932	16	0.73	0.11
15	1399	1.06	0.392479	1.58	7.279	2.17	0.134504	1.49	2134	34	2158	32	0.73	1.08
16	16850	0.10	0.202929	1.42	2.235	2.02	0.079863	1.44	1191	17	1194	17	0.70	0.22
17	52681	0.03	0.314632	1.73	4.686	2.21	0.108022	1.37	1763	31	1766	24	0.78	0.16
18	12519	0.12	0.366663	2.36	6.267	3.31	0.123960	2.31	2014	48	2014	47	0.71	0.02
19	1723	0.98	0.186450	2.17	1.966	2.94	0.076463	1.98	1102	24	1107	22	0.74	0.46
20	4872	0.29	0.478594	1.64	11.078	2.12	0.167872	1.34	2521	41	2537	34	0.77	0.61
21	42745	0.04	0.155688	2.75	1.505	6.70	0.070093	6.11	933	26	931	57	0.41	-0.18
22	765	2.18	0.206452	5.10	2.318	6.16	0.081426	3.45	1210	62	1232	42	0.83	1.77
23	48775	0.04	0.165321	1.59	1.643	2.10	0.072066	1.37	986	16	988	14	0.76	0.15
24	7285	0.24	0.157881	1.73	1.538	2.62	0.070639	1.97	945	16	947	19	0.66	0.21
25	3130	0.52	0.258629	3.82	3.321	4.36	0.093138	2.11	1483	57	1491	31	0.88	0.53
26	17861	0.09	0.335920	2.12	5.315	2.64	0.114761	1.57	1867	40	1876	29	0.80	0.49
27	1913	0.78	0.381674	3.74	6.847	4.15	0.130106	1.80	2084	78	2099	38	0.90	0.73
28	16843	0.09	0.390389	1.40	7.148	1.97	0.132800	1.38	2125	30	2135	29	0.71	0.50
29	10733	0.14	0.335923	2.59	5.292	2.94	0.114253	1.39	1867	48	1868	26	0.88	0.06
30	8907	0.17	0.366573	2.94	6.276	3.50	0.124173	1.91	2013	59	2017	39	0.84	0.19
31	2398	0.67	0.276040	2.85	3.684	3.24	0.096792	1.56	1571	45	1563	24	0.88	-0.52
32	47382	0.03	0.288244	2.05	4.011	2.49	0.100921	1.42	1633	33	1641	23	0.82	0.51
33	19579	0.08	0.213455	1.86	2.416	2.80	0.082074	2.10	1247	23	1247	26	0.66	0.01
34	124896	0.01	0.323293	1.36	4.930	1.90	0.110588	1.33	1806	24	1809	24	0.71	0.18
35	71755	0.02	0.195476	4.85	2.107	5.08	0.078166	1.52	1151	56	1151	17	0.95	0.01
36	2226	0.74	0.238593	2.17	2.891	2.87	0.087874	1.88	1379	30	1380	26	0.76	0.03
37	132340	0.01	0.330414	1.26	5.139	1.83	0.112792	1.33	1840	23	1845	24	0.69	0.24
38	110153	0.02	0.156144	1.32	1.513	1.88	0.070262	1.34	935	12	936	13	0.70	0.08
39	1277	1.28	0.243623	3.23	2.932	3.56	0.087294	1.50	1406	45	1367	21	0.91	-2.82
40	193327	0.01	0.356985	1.36	5.969	1.89	0.121270	1.31	1968	27	1975	26	0.72	0.36

Rio Verde Formation – Sample RV-1

Grain	$^{206}Pb/^{204}Pb$	f_{206} %	Ratios						Ages				Rho	Disc. %
			$^{206}Pb/^{238}U$	±	$^{207}Pb/^{235}U$	±	$^{207}Pb/^{206}Pb$	±	$^{206}Pb/^{238}U$	±	$^{207}Pb/^{206}Pb$	±		
~~1~~	~~473~~	~~3.76~~	~~0.093475~~	~~0.98~~	~~1.036~~	~~1.88~~	~~0.080374~~	~~1.60~~	~~576~~	~~5~~	~~1206~~	~~31~~	~~0.38~~	~~52.24~~
2	infinite	0.00	0.151991	5.73	1.452	5.90	0.069288	1.38	912	49	907	28	0.40	-0.53
3	infinite	0.00	0.172177	3.60	1.742	3.75	0.073396	1.04	1024	34	1025	21	0.68	0.08
4	infinite	0.00	0.152428	2.31	1.456	2.61	0.069301	1.21	915	20	908	25	0.70	-0.75
5	infinite	0.00	0.112752	3.53	0.971	3.67	0.062433	1.02	689	23	689	22	0.69	0.04
6	1850	0.94	0.129059	2.67	1.164	2.91	0.065389	1.18	782	20	787	24	0.43	0.56
7	infinite	0.00	0.184609	2.68	1.931	2.88	0.075872	1.06	1092	27	1092	21	0.41	-0.04
8	infinite	0.00	0.124330	2.29	1.103	2.61	0.064326	1.24	755	16	752	26	0.55	-0.41
9	6233	0.28	0.134749	3.18	1.233	3.34	0.066366	1.02	815	24	818	21	0.72	0.37
10	12528	0.14	0.129795	7.27	1.171	7.34	0.065437	1.02	787	54	788	21	0.86	0.22
11	4154	0.41	0.162694	6.43	1.606	6.51	0.071596	1.02	972	58	974	21	0.79	0.28
12	15863	0.11	0.116944	2.72	1.019	2.90	0.063182	1.00	713	18	714	21	0.85	0.20

Rio Verde Formation – Sample RV-1 (continued)

Grain	$^{206}Pb/^{204}Pb$	f_{206} %	Ratios						Ages				Rho	Disc. %
			$^{206}Pb/^{238}U$	±	$^{207}Pb/^{235}U$	±	$^{207}Pb/^{206}Pb$	±	$^{206}Pb/^{238}U$	±	$^{207}Pb/^{206}Pb$	±		
13	infinite	0.00	0.165625	5.34	1.646	5.43	0.072074	0.99	988	49	988	20	0.88	0.01
14	infinite	0.00	0.120535	2.12	1.060	2.34	0.063762	1.00	734	15	734	21	0.84	0.01
15	infinite	0.00	0.125519	1.81	1.119	2.07	0.064635	1.00	762	13	762	21	0.63	0.03
16	infinite	0.00	0.172998	2.86	1.754	3.03	0.073535	0.99	1029	27	1029	20	0.80	0.01
17	infinite	0.00	0.162331	4.51	1.599	4.61	0.071435	0.98	970	40	970	20	0.75	0.02
18	3548	0.49	0.135217	3.51	1.239	3.65	0.066461	0.98	818	27	821	20	0.79	0.41
20	infinite	0.00	0.137331	3.51	1.264	3.65	0.066736	0.98	830	27	830	20	0.79	0.00
21	infinite	0.00	0.103699	2.14	0.871	2.36	0.060903	0.98	636	13	636	21	0.84	-0.04
22	infinite	0.00	0.345921	2.41	5.612	2.60	0.117670	0.97	1915	40	1921	17	0.83	0.31
23	3751	0.47	0.107257	5.51	0.909	5.60	0.061476	0.98	657	34	656	21	0.91	-0.13
24	infinite	0.00	0.116887	4.27	1.017	4.39	0.063098	1.03	713	29	712	22	0.06	-0.15
25	infinite	0.00	0.108038	2.14	0.918	2.35	0.061642	0.98	661	13	662	21	0.84	0.05
~~26~~	~~infinite~~	~~0.00~~	~~0.146491~~	~~3.24~~	~~1.453~~	~~3.91~~	~~0.071957~~	~~2.20~~	~~881~~	~~27~~	~~985~~	~~44~~	~~0.84~~	~~10.51~~
27	6014	0.29	0.150136	3.93	1.428	4.06	0.068994	1.03	902	33	899	21	0.89	-0.35
29	infinite	0.00	0.117763	2.54	1.027	2.73	0.063271	0.99	718	17	717	21	0.89	-0.04
30	infinite	0.00	0.450835	19.34	9.141	19.37	0.147053	0.99	2399	##	2312	17	0.94	-3.76
31	13951	0.12	0.160966	2.58	1.579	2.76	0.071137	0.97	962	23	961	20	0.82	-0.08
32	infinite	0.00	0.108795	2.06	0.926	2.30	0.061715	1.03	666	13	664	22	0.73	-0.22
33	1328	1.33	0.106922	2.19	0.906	2.58	0.061456	1.37	655	14	655	29	0.63	0.06
34	17311	0.10	0.138149	6.64	1.275	6.71	0.066914	1.00	834	52	835	21	0.49	0.11
35	24517	0.07	0.179614	3.15	1.855	3.30	0.074903	0.98	1065	31	1066	20	0.86	0.10
36	3873	0.45	0.131843	1.88	1.197	2.13	0.065862	1.00	798	14	802	21	0.87	0.45
37	5231	0.34	0.104742	6.81	0.882	6.89	0.061059	1.07	642	41	641	23	0.58	-0.13
38	29442	0.06	0.130811	8.48	1.182	8.55	0.065530	1.05	792	63	791	22	0.80	-0.14
40	2068	0.85	0.107943	4.75	0.919	4.92	0.061755	1.29	661	30	666	27	0.67	0.73
41	infinite	0.00	0.145679	6.91	1.372	6.99	0.068282	1.06	877	56	877	22	0.82	0.05
42	infinite	0.00	0.144836	4.48	1.360	5.88	0.068123	3.81	872	36	872	77	0.90	0.04
43	infinite	0.00	0.132560	3.41	1.204	3.57	0.065873	1.05	802	26	802	22	0.78	-0.01
44	42611	0.04	0.137166	3.15	1.261	3.33	0.066700	1.10	829	24	828	23	0.70	-0.03
45	662740	0.00	0.109008	3.51	0.929	3.64	0.061805	0.96	667	22	667	21	0.91	0.06
46	4106	0.43	0.119310	3.94	1.046	4.09	0.063574	1.12	727	27	727	24	0.05	0.12
47	infinite	0.00	0.146397	1.67	1.381	1.93	0.068413	0.97	881	14	881	20	0.73	0.04
48	infinite	0.00	0.137043	1.19	1.260	1.53	0.066680	0.96	828	9	828	20	0.82	-0.02
49	2982	0.59	0.109818	2.08	0.937	2.31	0.061888	1.00	672	13	670	21	0.52	-0.22
51	7005	0.25	0.109363	3.36	0.933	3.51	0.061897	1.02	669	21	671	22	0.82	0.23
52	1593	1.10	0.114878	3.51	0.995	3.86	0.062823	1.59	701	23	702	34	0.35	0.17
53	infinite	0.00	0.138186	2.02	1.273	2.32	0.066836	1.15	834	16	833	24	0.58	-0.21
54	3783	0.47	0.109756	2.61	0.938	2.82	0.062012	1.05	671	17	675	22	0.47	0.47
55	21108	0.08	0.113548	3.19	0.979	3.34	0.062552	1.00	693	21	693	21	0.84	-0.04
56	22113	0.08	0.128519	3.36	1.154	3.54	0.065145	1.12	779	25	779	23	0.37	-0.05
57	2434	0.70	0.173226	7.21	1.759	7.29	0.073667	1.09	1030	68	1032	22	0.29	0.24
58	1753	1.00	0.113505	5.72	0.980	5.91	0.062615	1.47	693	37	695	31	0.10	0.30
59	infinite	0.00	0.135241	3.83	1.237	3.96	0.066324	1.01	818	29	817	21	0.91	-0.13
61	infinite	0.00	0.180481	4.24	1.866	4.37	0.074982	1.09	1070	42	1068	22	0.69	-0.15
62	infinite	0.00	0.117049	1.28	1.026	1.66	0.063578	1.05	714	9	728	22	0.86	1.94
62	infinite	0.00	0.450483	1.42	10.483	1.74	0.168767	1.01	2397	28	2545	17	0.96	5.82
63	3896	0.45	0.104102	2.59	0.875	2.80	0.060974	1.07	638	16	638	23	0.64	-0.01
64	13461	0.13	0.121527	4.00	1.072	4.16	0.063975	1.14	739	28	741	24	0.72	0.19
65	infinite	0.00	0.179742	2.09	1.857	2.38	0.074927	1.13	1066	21	1067	23	0.92	0.09
66	3691	0.41	0.371656	4.34	6.482	4.48	0.126493	1.13	2037	75	2050	20	0.75	0.62
67	infinite	0.00	0.119063	2.11	1.043	2.42	0.063518	1.20	725	14	726	25	0.90	0.06
68	infinite	0.00	0.139140	3.33	1.288	3.48	0.067114	1.04	840	26	841	21	0.26	0.18
69	171449	0.01	0.116284	2.59	1.010	2.80	0.063022	1.05	709	17	709	22	0.64	-0.03
70	3050	0.58	0.115686	3.11	1.005	3.28	0.063024	1.05	706	21	709	22	0.55	0.47

Rio Verde Formation – Sample RV-1 (continued)

Grain	$^{206}Pb/^{204}Pb$	f_{206} %	Ratios						Ages				Rho	Disc. %
			$^{206}Pb/^{238}U$	±	$^{207}Pb/^{235}U$	±	$^{207}Pb/^{206}Pb$	±	$^{206}Pb/^{238}U$	±	$^{207}Pb/^{206}Pb$	±		
73	infinite	0.00	0.179721	2.07	1.854	2.31	0.074837	1.02	1065	20	1064	20	0.92	-0.12
74	infinite	0.00	0.139635	3.17	1.290	3.35	0.067027	1.06	843	25	839	22	0.63	-0.47
75	infinite	0.00	0.166907	3.37	1.664	3.51	0.072326	0.99	995	31	995	20	0.72	0.01
76	3272	0.54	0.108371	3.28	0.923	3.43	0.061770	1.01	663	21	666	21	0.28	0.43
77	2219	0.79	0.110798	3.77	0.950	3.90	0.062169	1.03	677	24	680	22	0.17	0.38
79	76500	0.02	0.119798	4.28	1.051	4.48	0.063625	1.33	729	29	729	28	0.97	-0.03
80	infinite	0.00	0.171716	1.97	1.735	2.24	0.073271	1.06	1022	19	1021	21	0.53	-0.01
81	infinite	0.00	0.167588	1.79	1.673	2.05	0.072392	1.00	999	17	997	20	0.16	-0.18
82	2149	0.80	0.159993	1.07	1.570	1.47	0.071173	1.02	957	9	962	21	0.36	0.59
83	1114	1.57	0.128283	6.50	1.152	6.61	0.065115	1.17	778	47	778	24	0.58	0.00

Notes: 1. Uncertainties given at the one σ level (%)
2. f^{206}% denotes the percentage of ^{206}Pb that is common Pb.
3. Correction for common Pb made using the measured $^{206}Pb/^{204}Pb$ ratio.
4. For % Disc., 0% denotes a concordant analysis.

4.4.2 – Sm-Nd Results

The Sm-Nd data for rocks of the Canastra and Ibiá groups are presented in Table 4.4. Samples of the Canastra Group show low REE contents, with Sm value, ranging from 1.61 to 7.85 ppm, and Nd contents between 10.7 and 50.1 ppm. Most T_{DM} model ages fall in the interval between ca. 1.8 and 2.4 Ga suggesting provenance dominantly from a source with Paleoproterozoic model ages (Fig. 4.11). One sample indicated the younger T_{DM} model age of ca. 1.5 Ga and might indicate some participation of younger sources.

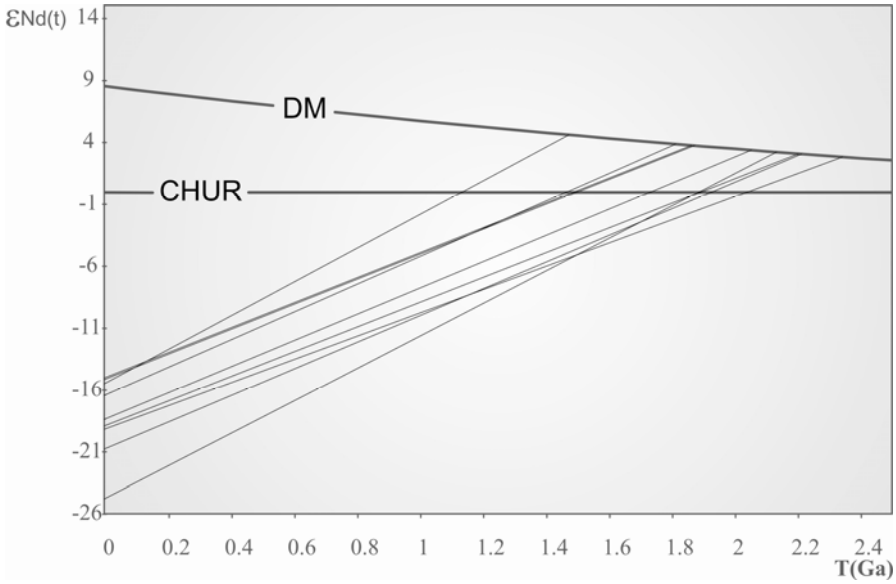

Figure 4.11 - Nd isotopic composition of the sediments of the Canastra Group.

T_{DM} data for the Ibiá Group, on the other hand, show a much more important contribution from younger sources. The results for the metapelitic rocks show a bimodal pattern (Fig. 4.12) with one group presenting younger T_{DM} values between 1.16 and 1.46 and another with model ages between 1.58 and 2.01. The group with intermediate age values in diagram of Fig. 12 includes diamictite samples and rocks from the Rio Verde Formation. It seems that the matrix has recorded some contribution of younger material, as suggested by the values of 1.77 Ga (CUB-1) obtained in samples with matrix predominance. The youngest group show T_{DM} ages of ~1.3 Ga and is composed by rocks of the Rio Verde Formation.

Sample	Rock	Sm (ppm)	Nd (ppm)	$^{143}Nd/^{144}Nd$	$^{147}Sm/^{144}Nd$	T_{DM} (Ga)
Canastra Group						
[1]PSL6-9		3.81	17.85	0.511962(04)	0.129	1.9
[1]UNAÍ-1		4.88	26.11	0.511577(06)	0.113	2.21
[1]UNAÍ-2		5.47	26.69	0.511659(09)	0.124	2.34
[1]PALM-1		2.56	13.53	0.511699(10)	0.114	2.05
[1]PALM-2		7.85	50.08	0.511372(05)	0.095	2.13
[2]At-12a	quartizite	0.36	1.82	0.511672(25)	0.1210	2.20
LAN-2	calciphylite	8.07	41.20	0.511866(20)	0.1185	1.87
PAR-1	quartzite			0.511873	0.1185	1.86
ANTA-2	quartzite	1.61	10.67	0.511850(05)	0.0912	1.47
CH-1	quartzite	5.96	32.77	0.511799(07)	0.1099	1.81
Ibiá Group						
HS-133[1]		4.35	20.04	0.512319(05)	0.131	1.33
94-II-79[1]		5.94	30.42	0.511771(05)	0.118	2.01
94-1-145[1]		6.71	31.42	0.512320(05)	0.129	1.29
94-I-134B[1]		10.79	57.39	0.511770(06)	0.114	1.93
HS-370B[1]		5.66	26.33	0.512322(07)	0.13	1.3
HS523A[1]		12.04	62.00	0.512305(04)	0.117	1.16
IPC61[3]	Schist	5.63	33.56	0.511872(06)	0.1015	1.58
IPC60[3]	Schist	3.68	12.48	0.512424(07)	0.1783	2.69
37-10-CUB4[1]	pebble	1.36	7.08	0.511620(05)	0.116	2.20
36-10-CUB2F[1]	pebble	2.58	13.14	0.511601(08)	0.119	2.25
35-10-CUB[1]	pebble	4.29	20.55	0.511617(09)	0.126	2.47
133[2]	calciphylite	4.53	20.07	0.512319	0.131	1.33
RV-1	calciphylite	5.52	23.11	0.512380(08)	0.1444	1.46
CUB-2	diamictite	5.98	33.10	0.511735(07)	0.1091	1.89
CUB-1	diamictite	14.06	80.43	0.511776(10)	0.1057	1.77

Table 4.4 - Sm-Nd data for samples of Canastra and Ibiá Groups. Data from [1] Pimentel et al. (2001), [2]Seer et al (2001) and [3] (Klein, 2008).

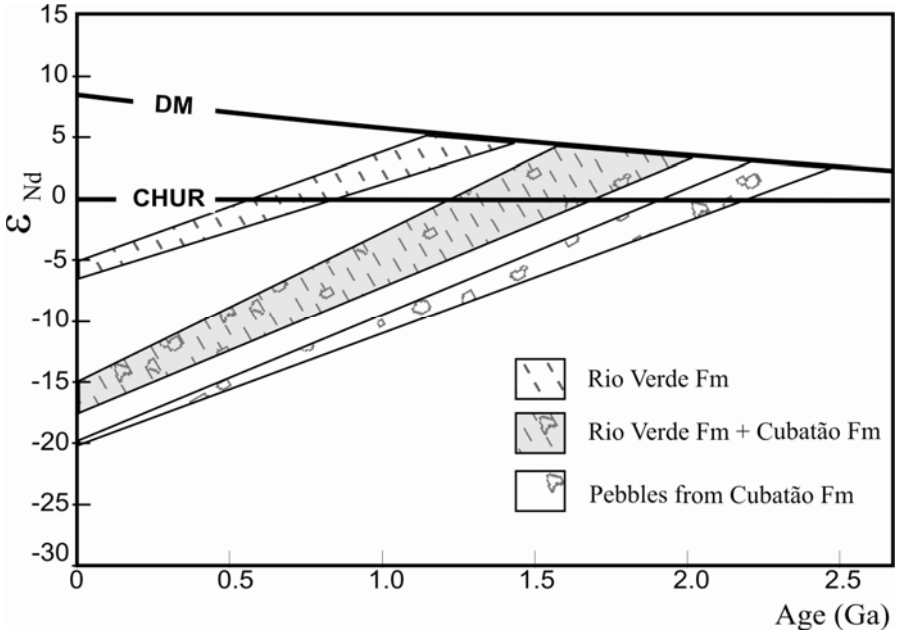

Figure 4.12 - Nd isotopic diagram of samples from Ibiá Group.

4.5- DISCUSSION

4.5.1 Depositional Age

4.5.1.1 – Canastra Group

Although the analysed samples present some differences in the provenance age patterns, the values of ~1.03 Ga for the youngest zircon is common to all samples, and is interpreted as the maximum depositional age for the Canastra Group.

4.5.1.2 – Ibiá Group

The provenance age patterns for the Cubatão and Rio Verde formations are very different from each other. The youngest age peak of the Cubatão Formation is ca. 936 Ma. On the other hand, in the Rio Verde Formation most of the detrital zircon ages are younger than 750 Ma with the youngest peak at ca. 640 Ma. The contact between the two formations has been described to be transitional (Pereira, 1992, Pereira et al., 1994), therefore, the maximum depositional age of the Ibiá Group is given by the data of the Rio Verde Formation. Considering the age of ca. 630 Ma for the main metamorphic event in the Brasília Belt (Pimentel et al., 1999) and the maximum depositional age of ca. 640 Ma for the Ibiá Group, it appears that the deposition and subsequent deformation of the Rio Verde Formation took place in a time interval of approximately 10 My.

4.5.2 Source Region and Tectonic Implications

The U-Pb data show that the ages of detrital zircons of the Canastra Group vary significantly between formations, both in values and relative abundances. For the Serra do Landim and Chapada dos Pilões formations, the data indicate that terrains of ~2.1 Ga are the main sources, with secondary contributions of ~1.8 Ga rocks. Various likely sources with this age interval are recognized within the São Francisco-Congo Craton, such as the Paleoproterozoic granitoids of the Quadrilátero Ferrífero (Noce et al., 2007b), the Mantiqueira and Juiz de Fora Complex (Noce et al., 2007a, Silva et al., 2002b, 2005) and the magmatism associated to ~1.8 Ga rift opening in the Espinhaço and Araí groups (Cordani et al., 1992, Schobbenhaus et al., 1994, Pimentel et al.,1994, 1991b).

Both samples of the Paracatu Formation show a strong contribution from mesoproterozoic sources, with a main peak at ca. 1.2 Ga. There is little evidence of a significant volume of 1.2 Ga old continental crust within the São Francisco-Congo Craton. However, such mesoproterozoic ages have been described in terrains of the Brasília Belt, such as the large mafic-ultramafic layered complexes of Barro Alto, Niquelândia and Canabrava and associated volcano-sedimentary sequences (Moraes et al., 2006, Pimentel et al., 2004, Correia et al., 1999) and a recently identified magmatic arc located immediately westward of the study area (Klein, 2008). Mesoproterozoic rock units within the São Francisco-Congo Craton have also been described in Africa and may not be discarded as sediment sources for the Brasília Belt metasediments (Hanson et al., 1988, Tack et al., 1994, Ring et al., 1999).

The combined U-Pb and Sm-Nd data reinforce the suggestion that the Canastra sedimentary rocks represent part of a passive margin setting developed along the western margin of the São Francisco-Congo continent (Pimentel et al., 2001).

The detrital zircon age pattern obtained for the Rio Verde Formation is similar to those presented by Piuzana et al (2003a) for rocks of the Araxá Group (Fig. 4.13), suggesting similar source areas and possibly similar tectonic settings for both units, which is endorsed by the Sm-Nd data. The bimodal pattern of the T_{DM} of Ibiá Group is interpreted as the result of mixed contribution from Paleo-Mesoproterozoic areas with a juvenile Neoproterozoic component.

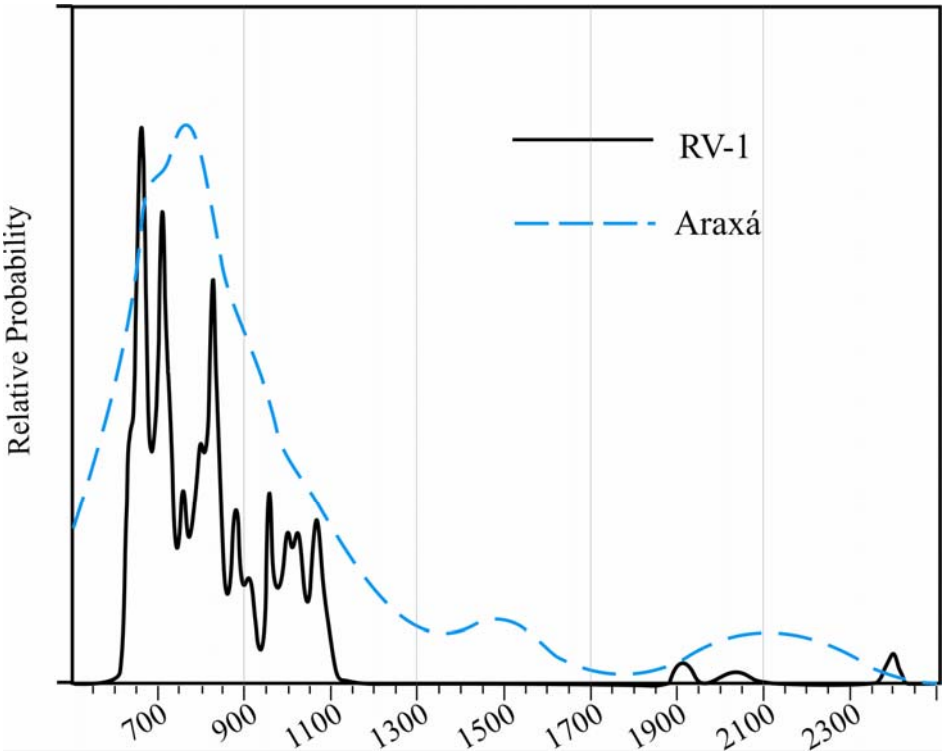

Figure 4.13. Relative probability distribution diagrams for detrital zircons of the Araxá (data from Piuzana et al., 2003a) and the Ibiá groups, showing the similarity in the age patterns.

4.6- CONCLUSIONS

(i) The U-Pb and Sm-Nd data suggest that the Canastra Group is younger than ca. 1.0 Ga and comprised a passive margin sequence deposited along the southwestern margin of the São Francisco-Congo continent.

(ii) The lithostratigraphic units of the Canastra Group show differences in the detrital zircon age distributions indicating varied provenance of the original sediments. The source of Paleoproterozoic zircon grains may be attributed to the Sao Francisco-Congo Craton, however the origin of the Mesoproterozoic (1.2-1.0 Ga) population remain uncertain.

(iii) The Sm-Nd data of the Ibiá Group suggest proximity of a relatively juvenile Neoproterozoic terrain, which is confirmed by the U-Pb data. The upper formation presents an age spectrum dominated by Neoproterozoic detrital zircon suggesting that the Goiás Magmatic Arc represented the main source of the original sediments.

(iv) The maximum depositional age of the Ibiá Group is given by the youngest U-Pb age peak at ca. 640 Ma. This upper limit, combined with the age of the metamorphic/deformational peak of the Brasilia Belt at 630 Ma, suggests a short time interval for the sedimentation of

the Ibiá Group. The provenance patterns of the Ibiá and Araxá groups, as indicated by both the U-Pb and Sm-Nd systems, are very similar, suggesting similar sources and tectonic settings for both. They are here interpreted as comprising fore or back-arc sequences.

ACKNOWLEDGEMENTS

This work benefited from financial support from the Companhia de Pesquisa de Recursos Minerais and CNPq. We also thank the staff of the Laboratório de Geocronologia da Universidade de Brasília for their technical assistance.

Capítulo 5 – GRUPO BAMBUÍ E FORMAÇÃO JEQUITAÍ

Provenance of the Jequitaí Formation and Bambuí Group, Brasília Belt, central Brazil: Combined in situ U-Pb age data and Nd-Sr isotopes

Rodrigues, J.B.[a,b,*], Pimentel, M.M.[b]; Matteini, M.[b], Buhn, B.[b], Alvarenga, C.J.S.[b], Dardenne, M. A.[b], Armstrong, R.A.[c]

a - Companhia de Pesquisa de Recursos Minerais, b- Universidade de Brasília, c – Australian National University

* corresponding author

ABSTRACT

The age and tectonic significance of the glacial deposits of the Jequitaí Formation and the overlying carbonatic-siliciclastic sequence of the Bambuí Group, in central Brazil, are discussed in this study on the basis of U–Pb detrital zircon ages combined with, Nd and Sr isotope data. The Jequitaí Formation is a glacial unit covering large areas of the São Francisco Craton and is also exposed within the Brasília Belt. It is overlain by the carbonatic Sete Lagoas Formation, the basal unit of the Bambuí Group which represents a carbonate-siliciclastic sequence with upward increase of the siliciclastic component. The data presented in this study define the maximum depositional ages of 880 and 610 Ma for the Jequitaí Formation and Bambuí Group, respectively. The age distribution of the detrital zircon grains of the Jequitaí rocks indicates a dominant Paleoproterozoic source (2.0-2.2 Ga) as well as minor Mesoproterozoic and early Neoproterozoic (~900 Ma) components. These are all, probably derived from the São Francisco Craton.

The Sm-Nd and detrital zircon for the Bambuí Group demonstrate longitudinal and temporal variation of the source areas. Rocks exposed in the northern area show main contribution from Paleoproterozoic sources, as well as an important component from Neoproterozoic ages, and a small Archean population. Samples from the southern part of the group show a simple age pattern, with the dominant presence of Neoproterozoic zircons (mainly ca. 650 Ma old). The Sm-Nd data show an increasing contribution derived from younger materials upward in the stratigraphic sequence, with T_{DM} ages varying from ca. 2.5 Ga in the bottom to values around 1.5 Ga at the top. The data reinforce the interpretation that the Bambuí Group represents a foreland basin with the original sediments being derived mainly from the Brasília Belt, to the west, although some contribution from the São Francisco Craton is not discarded.

5.1 – INTRODUCTION

The late stages of the Neoproteorozoic Era are characterized by glacial events which were apparently worldwide spread. Currently, at least two events are usually recognized, the Sturtian (~713 Ma) and Marinoan (~640 Ma) (Hoffman et al., 1998, Hyde et al., 2000, Hoffman and Schrag, 2002, Stern et al., 2006, Halverson et al., 2007, among others). Cap

carbonate layers occur directly above glacial deposits in several parts of the globe, indicating a sudden climatic change from very cold to warm environments (Hoffman and Schrag, 2002).

In Brazil, one of the main examples of this cryogenic period are the Jequitaí Formation diamictites and the overlying carbonates of the Sete Lagoas Formation of the Bambuí Group (Fig. 5.1).

The Bambuí Group is part of the Neoproterozoic São Francisco Basin, which comprises the glaciogenic Macaúbas Group at the base and the Bambui Group at the top (Dardenne, 1978). The Bambuí Group is represented mainly by pelitic and carbonatic sediments, which cover large areas of the São Francisco Craton (Fig. 5.1). In some areas, the Bambuí Group overlies the Jequitaí Formation, which is interpreted as a Sturtian glacial deposit. Previous studies (Pimentel et al. 2001) indicate that, at least the upper formations of the Bambuí Group may represent a foreland basin in relation to the Brasília Belt, however the timing of tectonic inversion of the belt remained unknown.

The new U-Pb zircon analyses, Sm-Nd model ages and Sr data for carbonatic rocks presented in this paper, combined with previous published studies are instrumental to establish important constraints on the age, provenance and tectonic nature and evolution of the Bambuí Group and Jequitaí Formation.

5.2 - GEOLOGIC SETTINGS

The Jequitaí Formation is a glacial unit which covers large areas of the São Francisco Craton and is also exposed within the Brasília Belt (Fig. 5.1). This formation is mainly composed by diamictites, conglomerates and minor sandstones deposited in a glaciomarine setting (Dardenne, 2000, Martins Neto & Alkmin, 2001). The pebbles (dolomite, quartzite, gneiss and granite) show striations and facets. The matrix is pelitic, or rarely psamitic, with the common presence of carbonate.

The Jequitaí Formation and Bambuí Group represent one of the main representatives of the glacial-carbonate deposits which characterize the Neoproterozoic stratigraphic record worldwide. They have been studied in detail for almost a century. In this work we partially adopt the stratigraphic scheme proposed by Dardenne (2000) for the Bambuí Group, which comprises five stratigraphic units: - Sete Lagoas, Serra de Santa Helena, Lagoa do Jacaré, Serra da Saudade and Três Marias formations:

- Sete Lagoas Fomation: This dominantly made of carbonatic rocks, including dolomite, thin layers of mudstone and siltstone, laminated and stromatolitic dolomite,

intraformational breccias, dolarenite and oolitic limestone. Its basal contact rests unconformably mostly on granite-gneiss basement or on the Jequitaí Formation. Nearby Sete Lagoas, Vieira et al (2007) identified two depositional sequences, the lower is represented by lime mudstone, calcite crystal-fans and crystalline limestone. The upper sequence comprises pelitic and carbonatic layers, overlain by thick bed of black crystalline limestone. The contact between the two sequences is marked by first order unconformity which has been recognized in seismic profiles, what led Zálan & Romeiro-Silva (2007) to suggest that only the upper sequence belongs to Sete Lagoas Formation and the first may be related to the Macaúbas Group.

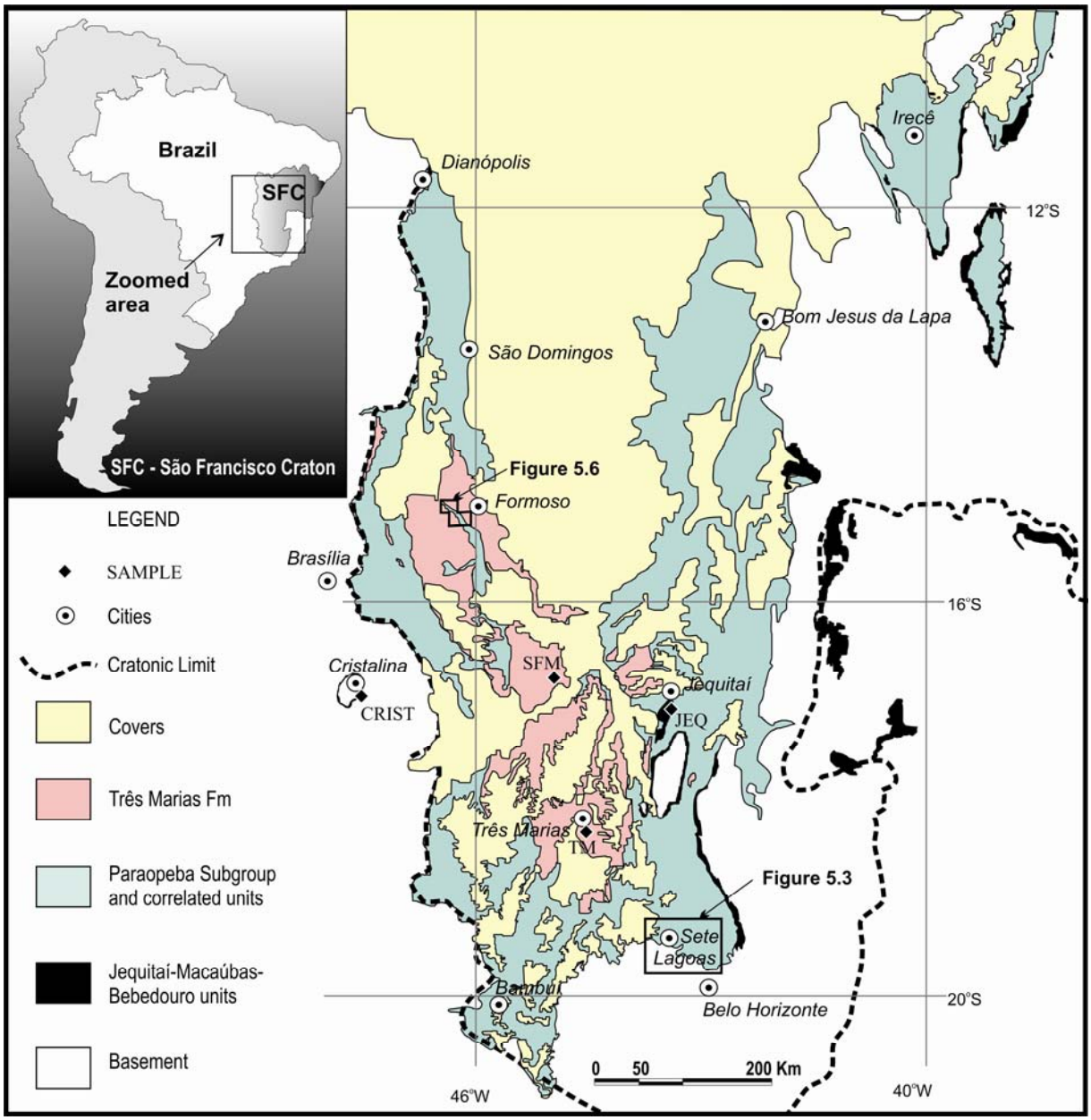

Figure 5.1 – Geographic distribution of Bambuí Group and Jequitaí Formation (modified from Bizzi et al., 2001) showing samples locations.

- Serra de Santa Helena Formation: It rests on top of the Sete Lagoas Formation or unconformably on the basement cristaline rocks; this unit is mainly constituted by shale and laminated siltstone. Locally there are very fine sandstone layers with cross and parallel stratification. The contact with Lagoa do Jacaré Formation is gradational.
- Lagoa do Jacaré Formation: Comprises oolitic and pisolitic limestones, greenish carbonatic siltistones with thin limestone intercalations and thin layers of mudstone;
- Serra da Saudade Fomation: This is represented by shale, mudstone, greenish siltstone and lenses of gray limestone;
- Três Marias Formation: This is a siliciclastic unit constituted by arkoses and green siltstone presenting common crossbedding and wave marks, interpreted as an alluvial and shallow marine deposit (Chiavegatto, 1992).

The Samburá Unit is an informal stratigraphic unit which is exposed in small areas in the western part of the Bambuí Group, it comprises mainly siltstone, sandstone and polymictic conglomerates. Its precise stratigraphic position and sedimentary setting remain under discussion. Castro & Dardenne (1996) classified it as a fan delta deposit directly overlying the limestones of Sete Lagoas Formation. On the other hand, Gonzaga (2001) described the presence of faceting pebbles and dropstones, suggestive of a glacial origin. Lima and Uhlein (2005) interpreted the Samburá Unit as a lateral variation of the Sete Lagoas Formation.

The Bambuí sediments were deposited on an epicontinental platform, initially in shallow water, evolving to costal reef and finally to alluvial environment (Marini et al, 1984a; Dardenne, 2000; D'Agrella-Filho et al, 2000). The shallowing upward sequence took place in three regressive megacycles (Dardenne, 2000). The first is represented by the Sete Lagoas Formation, followed by the second, which includes the Serra de Santa Helena and Lagoa do Jacaré formations and, finally, the last cycle composed by Serra de Santa Helena and Três Marias formations. The composition of clays from Três Marias Formation is suggestive of an active continental margin for the tectonic setting of deposition (Guimarães, 1997).

Despite the relatively large number of isotopic data for rocks of the Bambuí Group, its depositional age remains unknown. Rb-Sr analyses of clay minerals (Bonhomme et al., 1982; Parenti Couto et al., 1981; Thomaz Filho et al., 1998, Chang, 1997) indicated ages in the range between 560 and 900 Ma. Several attempts to date the carbonatic rocks by the whole-rock Pb-Pb method have been carried out without much success (Babinski et al, 1993,

Iyer et al, 1995, Babinski et al, 1995, Babinski et al 1999, D'Agrella-Filho et al, 2000). Recently, Babinski et al (2007) present a good-quality Pb-Pb isochron indicating the age of 740±20 Ma which has been interpreted as the best estimate for the depositional age of the basal sequence of the Sete Lagoas Formation.

Sm-Nd model ages between ca. 1.3 and 2,0 Ga for pelitic and psammitic rocks of this group (Pimentel et al., 2001 and Silva et al., 2006) indicate Proterozoic sources of the original sediments. Coelho et al (2007) reported SHRIMP age data for detrital zircon grains of the Paraopeba Subgroup (that includes Sete Lagoas, Serra de Santa Helena, Lagoa do Jacaré and Serra da Saudade formations), ranging between 1.44 and 2.66 Ga, with a main age peak at ca. 2.1 Ga.

Carbon isotope data for carbonates of the Sete Lagoas Formation (Chang et al, 1993, Martins, 1999, Santos et al, 2000 and 2004, Misi et al., 2005, Babinski et al., 2007) consistently reveal negative excursions of $\delta^{13}C‰$(PDB) at the base of the unit (~-5). $\delta^{13}C‰$(PDB) values become gradually positive towards the top (~+15), similar to post-glacial sequences, as described in deposits associated to the Sturtian Glaciation. The Sr isotopic composition of carbonates vary within the interval between 0.70734 to 0.7081 (Kawashita et al., 1987, Chang et al, 1993, Misi et al, 2007, Babinski et al, 2007), which is comparable to ocean water values in the interval between ca. 650 and 610 Ma, according to Halverson et al (2007).

5.3 - ANALYTICAL PROCEDURES

Except for the SHRIMP analyses, all other isotopic analyses were carried out at the Geochronology Laboratory of the Universidade de Brasília. The LAM-ICP-MS analyses were performed using a Finnigan Neptune LA-MC-ICP-MS coupled to a Nd-YAG laser (λ=213nm) ablation system (New Wave Research, USA). Sm-Nd and Sr isotopic measurements were carried out on a multi-collector Finnigan MAT 262 mass spectrometer in static mode.

For LA-MC-ICP-MS and SHRIMP samples were crushed with a jaw crusher and powdered to approximately 500 μm. Heavy mineral concentrates were obtained by panning and were subsequently purified using a Frantz isodynamic separator. The grains were set in epoxy resin mounts, without selection and their surface was polished to expose the interior of the grains.

The U-Pb analyses by LAM-ICP-MS follow the analytical procedures outlined in Buhn et al. (in press), where the mounts were cleaned in a HNO_3 solution (3%) and ultraclean water bath. The ablation was done with spot size of 25-30μm in raster mode, at frequency of 9-13 Hz and intensity of 0.19-1.02 J/cm^2. The ablated material was carried by Ar (~0.90 L/min) and He (~0.40 L/min) in analyses of 40 cycles of 1 second. Unknown were bracketed by measurements of the international standard GJ-1 following the sequence 1 blank, 1 standard, 3 unknown, 1 blank and 1 standard. The accuracy was controlled using the standard TEMORA-2. Raw data were reduced using a home made spreadsheet and corrections were done for background, instrumental mass-bias drift and common Pb. The ages were calculated using ISOPLOT 3.0 (Ludwig, 2003).

The SHRIMP samples were mounted with standard zircon crystals SL13+FC1, and the mount was photographed at 150× magnification in reflected and transmitted light. Cathodoluminescence (CL) images were obtained in order to reveal internal structures of the zircon grains. Ion microprobe analyses were carried out using SHRIMP I and II at the Research School of Earth Sciences, Australian National University, Canberra, Australia. SHRIMP analytical methods and data treatment follow those described by Williams (1998) and Williams and Meyer (1998). The ion microprobe primary beam in both equipments typically produce spots with diameter between 20–30 μm. Uncertainties reported in tables and figures are given at 1σ level, and final ages are quoted at the 95% confidence level. The data have been processed using SQUID and ISOPLOT 3.0 (Ludwig, 2003).

For $^{87}Sr/^{86}Sr$ determination in carbonate, it was used the international standard 987 (carbonate) and the technique presented by Gioia et al. (1999), where about 50 mg whole-rock powders were dissolved in 1 ml of acetic acid (0.5 N). The overflow was evaporated and taken in 1 mL of 6N HCl. For the Sr extraction, the solution was passed through a cation exchange column containing the Sr-spec resin (Dt Bu CH18-C-6 in 1-octanol). Sm–Nd isotopic analysis followed the method described by Gioia and Pimentel (2000). Whole-rock powders (ca. 50 mg) were mixed with a ^{149}Sm–^{150}Nd spike solution and dissolved in HF, HNO_3 and HCl in Savillex capsules. Sm and Nd extraction of whole-rock samples was done by cation exchange techniques, using Teflon columns containing LN-Spec resin (HDEHP—di-ethylhexil phosphoric acid supported on PTFE powder). Uncertainties for Sm/Nd and $^{143}Nd/^{144}Nd$ ratios are better than ±0.5% (2σ) and ±0.005% (2σ), respectively, based on repeated analyses of international rock standards BHVO-1 and BCR-1. $^{143}Nd/^{144}Nd$ ratios were normalised to $^{146}Nd/^{144}Nd$ of 0.7219. T_{DM} values were calculated using De Paolo's

(1981) model. Sm, Nd and Sr samples were loaded onto Re evaporation filaments of a double filament assembly.

5.4- RESULTS

For the U-Pb investigation nine samples were selected; four were analysed by SHRIMP and five by LAM-ICP-MS. The probability density plots used $^{206}Pb/^{238}U$ and $^{207}Pb/^{206}Pb$ ages of concordant data (better than 90% of concordance) with low common lead contents. The complete analytical data set is the APPENDIX B. New Sm-Nd and Sr-Sr determinations are also presented.

5.4.1 – U-Pb Data

5.4.1.1. Jequitaí Formation

Two samples from the Jequitaí Formation had their detrital zircons analysed by SHRIMP, they are from the Jequitaí (JEQ) and Cristalina (CRIST) areas (Fig. 5.1). The sample JEQ presented ages from 880 to 3104 Ma, whereas in sample CRIST ages ranged from ~1200 to 3007 Ma. Both samples show a main age peak age at ca. 2.1 Ga and various minor age populations (Fig. 5.2). The youngest age peak was found only in Jequitaí sample (~0.88 Ga).

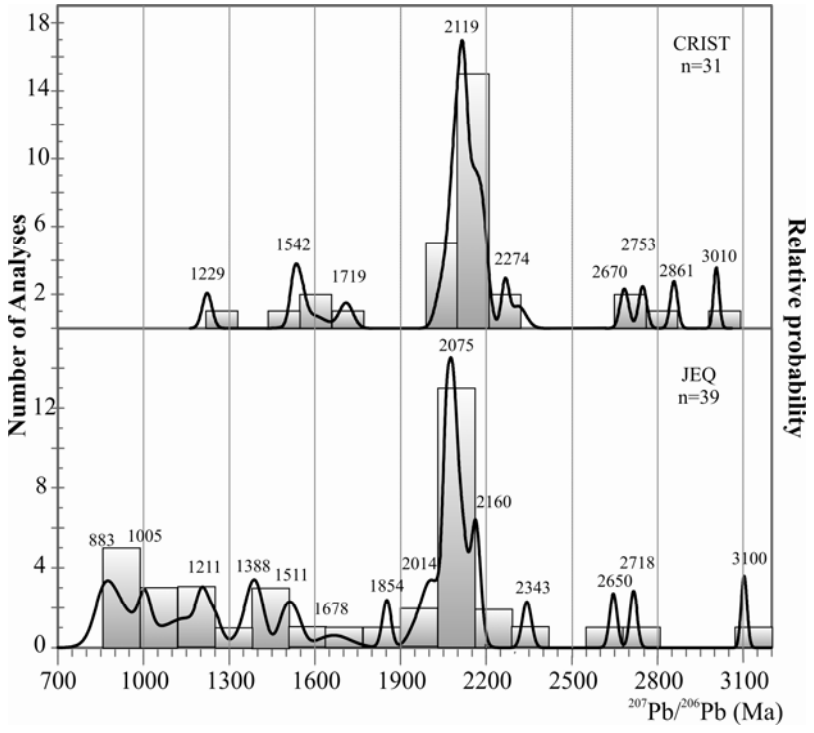

Figure 5.2 – Age pattern for samples of the Jequitaí diamictite of the Jequitaí (JEQ) and Cristalina (CRIST) region.

5.4.1.2 –- Sample CAR-1 (19° 41'35.5" S, 43° 58'49.1" W)- Carrancas Conglomerate

This sample belongs to a special sedimentary facies at the lower part of the Sete Lagoas Formation, named the Carrancas conglomerate, exposed in a very limited area in the surroundings of Belo Horizonte (Fig. 5.3). It was deposited in paleochannels and contains pebbles of granitic rocks, carbonate and quartz in a carbonatic matrix.

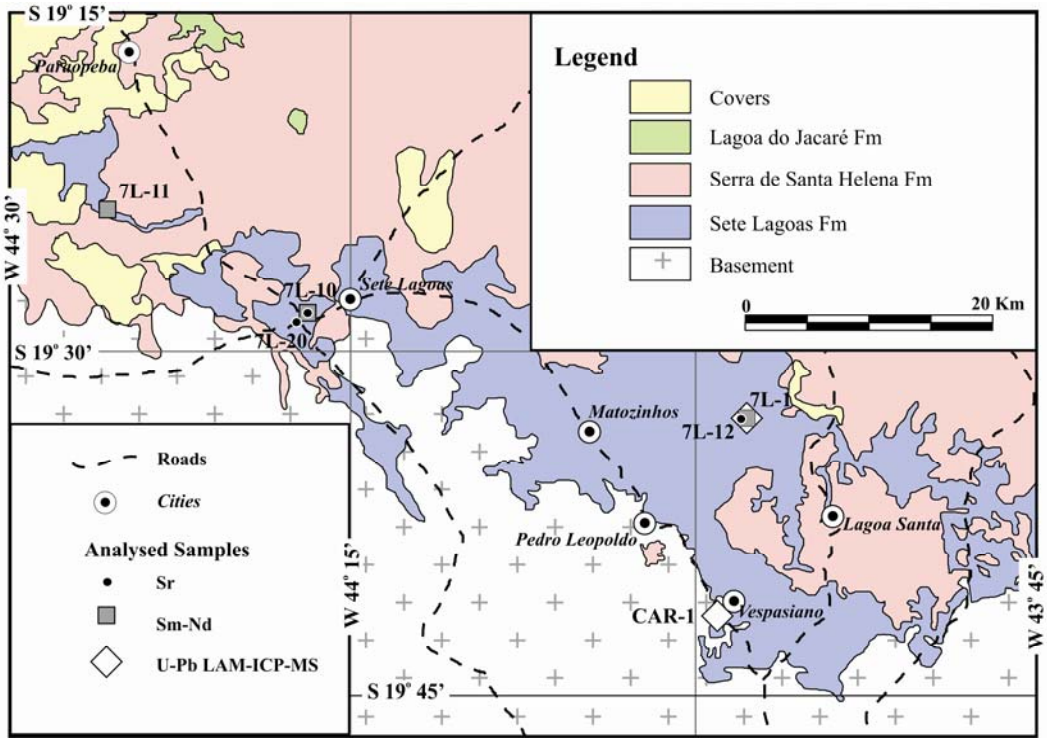

Figure 5.3 – Simplified geological map of the Sete Lagoas Region (modified from Heineck et al., 2004) with sample location (see Figure 5.1 for localization).

Sixty one zircon grains from this sample were analysed, but twenty were discarded due to high common lead contents or discordance greater than 10%. Two distinct populations are recognized: (i) large (>400 μm), idiomorphic, brown zircon crystals, and (ii) smaller grains, of different shapes, colours and sizes (100-200 μm). Fragments of cloudy yellow monazite were also found and analysed (6 analyses). The zircon age distribution presents a range of 1.4 to 3.1 Ga, with a main peak at 2.80-2.85 Ga and the monazite at 2.05 Ga (Fig. 5.4). The youngest grain has the age of 1309±23 Ma (-9.33% of discordance).

5.4.1.3 –Sete Lagoas Formation

Two samples of the Sete Lagoas Formation were studied. The sample 7L-1 (19° 32'54.4" S, 43° 57'45.2" W) is a foliated argillaceous siltstone that belongs to the base of the

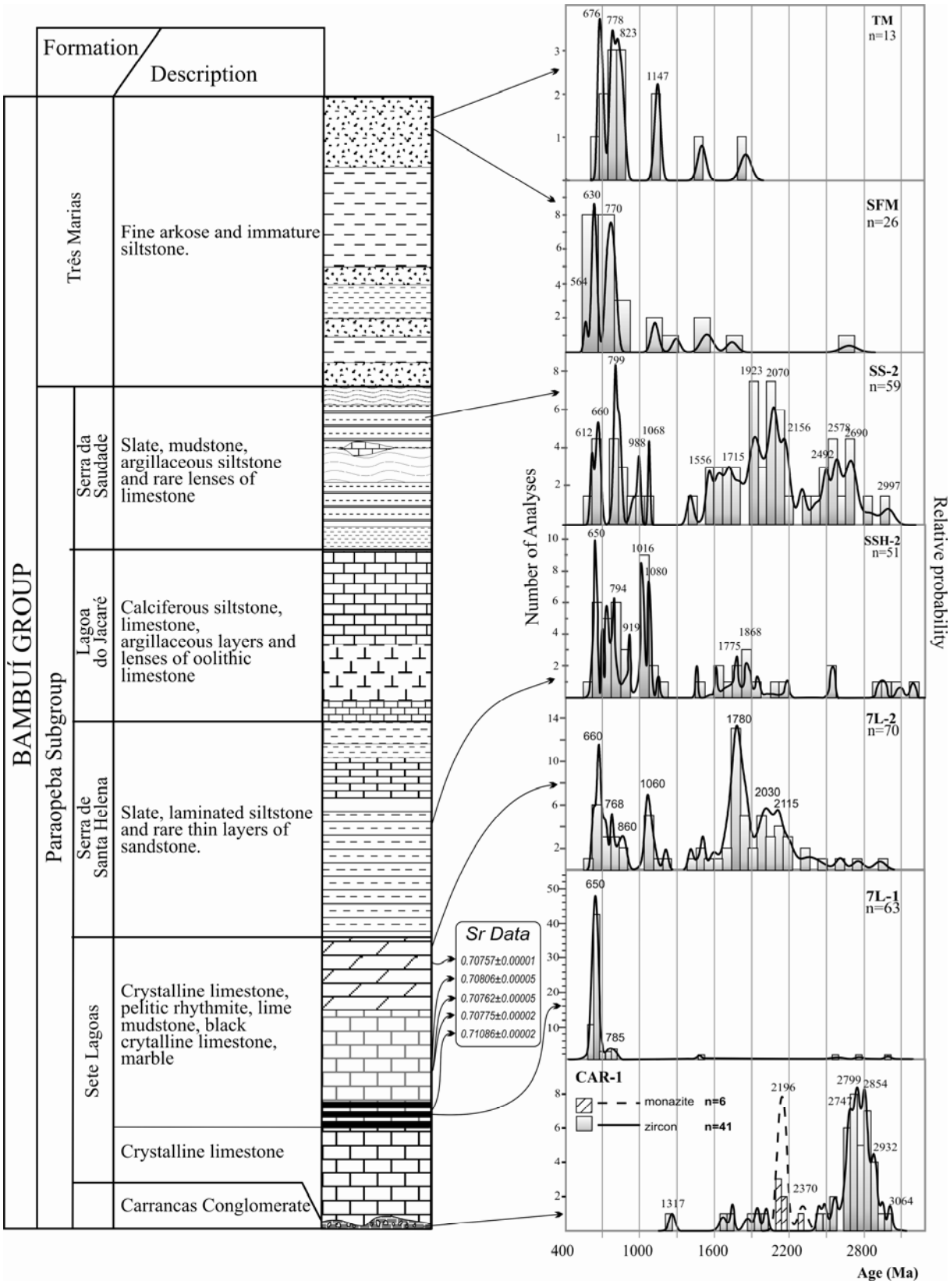

Figure 5.4 – Stratigraphic column of Bambuí Group (modified from Dardenne, 2000) and relative probability distribution diagram of the preferred age ($^{207}Pb/^{206}Pb$ for CAR-1 and $^{206}Pb/^{238}U$ for all others samples). In the box are shown the $^{87}Sr/^{86}Sr$ results of carbonatic rocks.

second sequence of the Sete Lagoas Formation (Vieira et al. 2007) and is from the southern region of the Bambuí Group (Fig. 5.3). The zircon grains are ~ 80 μm in size, prismatic, clear, transparent, colourless, pink or yellowish, without obvious transport features.

A total of 80 zircons were analysed. Seventeen produced discordant data and were discarded. Almost all zircons presented ages between 610-850 Ma, the probability density plot (Fig. 5.4) using the $^{206}Pb/^{238}U$ age, shows a simple provenance pattern with the main peak at 650 Ma. The youngest population comprising five grains dated at ca. 610 Ma (Fig. 5.5) establish the maximum age of the deposition of the original sediments.

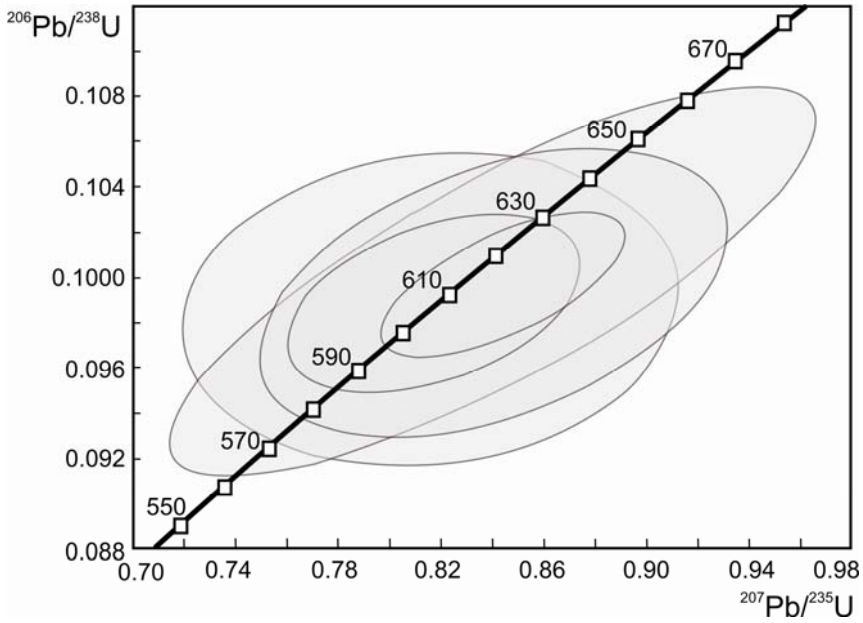

Figure 5.5 – Concordia diagram of the youngest population of the sample 7L-1

The second analysed sample, 7L-2 (15° 04'54.77" S, 46° 32'04.6" W), is a marble from the upper section of the Sete Lagoas Formation, exposed in the Serra de São Domingos area (Fig 5.6). The zircon grains are about 100 microns, rounded, prismatic, clear, colourless or yellowish.

Seventy seven zircon grains were analyzed and 7 analyses were discarded due to high common lead content or discordance. The probability density plot of $^{206}Pb/^{238}U$ ages (Fig. 5.4) show a main age peak at ca. 1780 Ma and minor peaks at 660, 1060 and ~2100 Ma. The youngest zircon (z-61) presents the age of 609 Ma (5% of discordance).

Five $^{87}Sr/^{86}Sr$ analyses in carbonatic rocks of the upper sequence were carried out and the data set (Fig. 5.4) is compatible with deposition between 640 and 600 Ma, according the curve of Halverson et al. (2007).

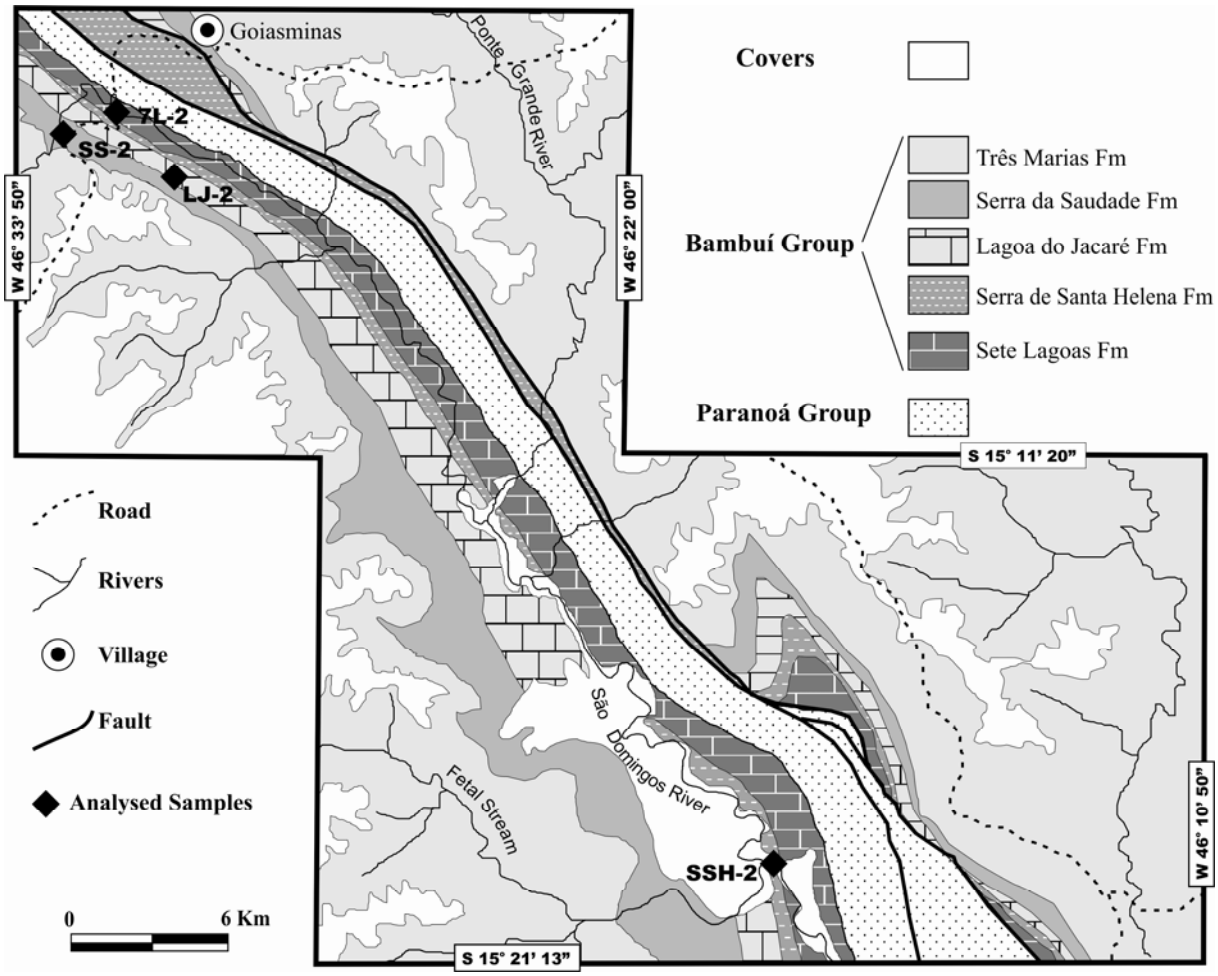

Figure 5.6 – Simplified geological map of the Serra de São Domingos Region (see Figure 1 for localization) with sample locations (from Alvarenga, 1978).

5.4.1.4 – Sample SSH-2 (15°19'15.2"S, 46°19'17.1"W) – Serra de Santa Helena Formation

This sample is an argillaceous siltstone from the middle portion of Serra de Santa Helena Formation in the Serra de São Domingos area (Fig. 5.6). The zircon grains present varied shapes and sizes. Colourless, brownish, yellowish, clear, with inclusions, prismatic and rounded grains are observed. A total of 63 zircons were analysed, and 12 discordant grains were discarded. The probability density plot (Fig. 5.4) shows main peaks at 650, 794, 1016 and 1090 Ma, a secondary group is represented by small peak between 1400-2200 Ma.

5.4.1.5 – Sample SS-2 (15°05'20.8"S, 46°33'06.3" W) – Serra da Saudade Formation

This is a black argillaceous siltstone sample from the Serra da Saudade Formation (Fig. 5.6). From the total of 68 analyses carried out, 56 were considered valid. The results

present broader age distribution (Fig. 5.4), with main peaks at 660, 799, 1923 and 2070. The youngest population is represented by the peak of 612 Ma.

5.4.1.6 – Três Marias Formation

The zircon grains from the arkose samples collected in the Três Marias (TM) and Santa Fé de Minas (SFM) (Fig. 5.1) are prismatic and well preserved, with little evidence of sedimentary transport. The data produced by SHRIMP is presented in Figure 5.4 and it shows dominant Neoproterozoic contributions with two main peaks at 676 and ~800 Ma for the sample TM and 630 and 770 Ma for SFM. The youngest grain was found in SFM sample and furnished the concordant age of 616 Ma.

5.4.2 – Sm-Nd Model Ages

Sm-Nd analyses are listed in Table 5.1 and are plotted in the Fig. 5.7. The seven analysed samples showed a range in Sm and Nd concentrations of 2.4-8.2 ppm and 9.9-41.3 ppm, respectively. The $^{147}Sm/^{144}Nd$ ratios vary from 0.105 to 0.143.

The results show T_{DM} values within the same age interval obtained by Pimentel et al (2001) for the Bambuí Group. Sample 7L-10 was discarded due to the probable fractionation indicated by the high value of the $^{147}Sm/^{144}Nd$ ratio.

The Sete Lagoas Formation data show a bimodal distribution of T_{DM} values (Fig. 5.7). The oldest interval (2.16-2.47 Ga) is not present in the others formations. The younger group, however, shows T_{DM} values in the interval between 1.58 and 1.87 Ga, similar to the pattern presented by the Serra da Saudade and Três Marias formations. The Serra de Santa Helena and Lagoa do Jacaré formations present a broader range of ages, showing heterogeneous influence of young and old terrains.

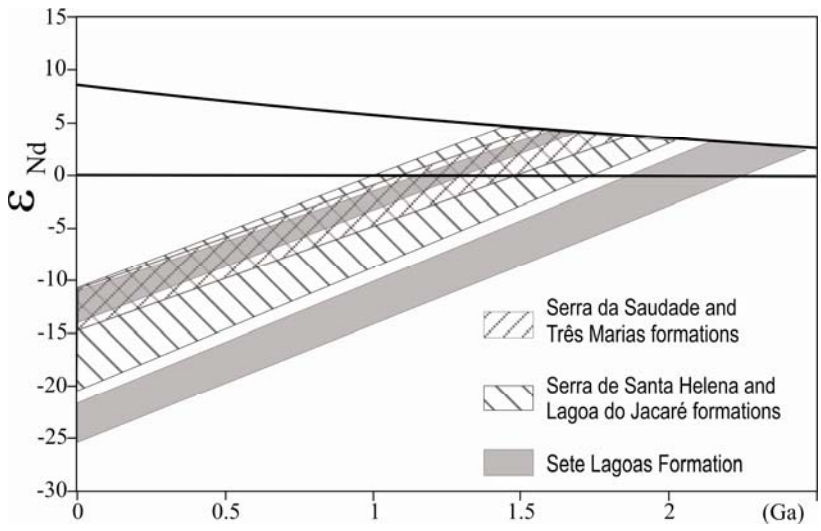

Figure 5.7 – Nd Evolution diagram for the Bambuí Group samples.

Sample	Rock	Sm (ppm)	Nd (ppm)	$^{143}Nd/^{144}Nd$	$^{147}Sm/^{144}Nd$	T_{DM} (Ga)
TRÊS MARIAS FORMATION						
MGV-11*		8.76	42.81	0.511967(04)	0.124	1.81
SLA*		7.53	37.88	0.511891(04)	0.114	1.75
MGV-27*		6.08	33.52	0.511961(06)	0.110	1.58
EGB-81*		7.03	35.56	0.511958(08)	0.119	1.73
BX*		7.5	40.26	0.512028(09)	0.113	1.53
SERRA DA SAUDADE FORMATION						
EGC-148*		7.71	39.39	0.511950(05)	0.118	1.73
MGV-13*		14.86	70.57	0.512083(05)	0.127	1.81
EGC-145*		10.46	50.83	0.511983(06)	0.124	1.79
EGC-151*		7.67	39.08	0.511948(05)	0.119	1.74
EGC-143*		7.64	38.85	0.511951(04)	0.119	1.74
SS-2	siltstone	8.17	41.33	0.511877(16)	0.120	1.87
LAGOA DO JACARÉ FORMATION						
MF538*		1.24	3.68	0.512260(05)	0.204	-
MF-12*		0.139	1.51	0.511792(06)	0.080	1.42
LJ-2	mudstone	6.43	35.90	0.511938(08)	0.118	1.87
SERRA DE SANTA HELENA FORMATION						
EGC-15II*		10.82	61.35	0.512022(05)	0.107	1.44
MGV-26*		6.25	32.49	0.511979(04)	0.116	1.65
EGC-132*		5.21	26.81	0.512059(04)	0.117	1.55
EGC-103		6.09	32.56	0.511978(03)	0.114	1.6
MGV-15*		7.53	36.52	0.511947(05)	0.125	1.86
MGV-23*		5.82	29.02	0.512087(03)	0.121	1.56
SSH-2	siltstone	7.4	40.5	0.511594(11)	0.105	2.02
SETE LAGOAS FORMATION						
MF-10B*		0.47	2.00	0.512037(05)	0.142	-
MF-19*		1.24	3.68	0.512260(05)	0.204	-
PADF-3*		7.29	36.91	0.512004(04)	0.119	1.67
PADF-11*		7.47	36.11	0.512070(04)	0.126	1.67
BARRO-2F*		4.41	24.82	0.511520(05)	0.107	2.16
BARRO-3F*		3.83	21.03	0.511507(06)	0.110	2.25
BARRO-3G*		17.4	106.9	0.511338(08)	0.098	2.47
7L-11	siltstone	4.71	25.35	0.511922(09)	0.112	1.67
7L-10	mudstone	2.35	9.90	0.512028(16)	0.143	2.19
7L-2	marble	3.49	17.33	0.512068(24)	0.122	1.6
7L-1	siltstone	5.329	28.236	0.511925(09)	0.114	1.70

Table 5.1 - Sm-Nd data for samples of Bambuí Group. (*) samples from Pimentel et al (2001)

5.5- DISCUSSION

5.5.1 Depositional Age

The Jequitaí Formation has been correlated with the worldwide Sturtian Glaciation and the detrital zircon age spectra presented in this work is coherent with this interpretation. The youngest zircon grain presents the age of 880 Ma which is considered to represent the

upper limit for the deposition of the original glacial sediments. However, the youngest zircon group found in the upper sequence of the overlying Sete Lagoas Formation present concondant ages of approximately 610 Ma, which represents our best estimate for the maximum depositional age of these rocks and consequently for the rest of the Bambuí Group.

The Pb-Pb whole-rock isochronic age of ca. 740 Ma obtained for carbonate from the lower sequence of the Sete Lagoas Formation (Babinski et al, 2007) is, however, incompatible with the youngest detrital zircon of 610 Ma. This incompatibility reinforces the previous sedimentological-geophysical interpretation (Zálan & Romeiro-Silva, 2007) that the lower sequence is a distinct unit, probably related to the Jequitaí basin.

5.5.2 Source Areas and Tectonic Implications

The age distribution pattern presented by the Jequitaí Formation indicates Paleoproterozoic terrains of the São Francisco-Congo Craton (Noce et al., 2007a,b, Oliveira et al, 2002, Carvalho & Oliveira, 2003, D'el Rey Silva et al., 2007, Rios et al., 2007) as the most likely source region. Early Neoproterozoic (~0.9 Ga) magmatic rocks are also exposed in the cratonic area (Machado et al., 1989, Tack et al., 2001, Kokonyangi et al., 2004, Silva et al., 2008).

The pattern obtained for the Carrancas conglomerate suggests that the Belo Horizonte Complex, an Archaean/Paleoproterozoic block which represents the sialic basement on which the conglomerate rests, is the major source of the unit. The unit probably is a deposit formed in small river basins receiving sediments derived from the nearby basement. The ages show identical behaviour when compared to the data presented by Teixeira et al (1996) for the Belo Horizonte Complex, in which the metaigneous rocks crystallization ages between 2860 and 2712 Ma, and the titanites and monazites from granitoids indicated U-Pb ages from 2320 to 2030 Ma.

The age spectra for the samples of the Bambuí Group are quite different, suggesting that the source areas change significantly along the basin. In any case, the most striking feature of the detrital age patterns of the Bambuí Group (Fig. 5.4) is the strong influence of Neoproterozoic sources.

The Neoproterozoic ages suggest that the most likely sources for these zircon grains are the magmatic rocks of the Brasília Belt including the Goiás Magmatic Arc (Pimentel et al.,1991a, 1997, Ebert et al., 1996, Rodrigues et al., 1998, Campos Neto and Caby, 1999,

Piuzana et al., 2003a,b, Laux et al., 2004, 2005, Oliveira et al., 2004, among others), exposed to the west of the Bambuí Group.

All samples from the Serra de São Domingos region reveal, additionally to the abundant neoproterozoic population, an important amount of Meso-Paleoproterozoic and Archean zircon grains (samples 7L-2, SSH-2 and SS-2 in the Fig. 5.4). This suggests that the São Francisco Craton was also an important supplier for the Bambuí sediments, at least for that particular area.

The samples from the southern segment of the Bambuí Group present the prevalent input of Neoproterozoic zircons (Brasília Belt), with a single main peak around 640 Ma (except for sample CAR-1). These rocks were deposited in a different paleogeographic configuration, in which the sediments derived apparently from one single source.

Sample 7L-1, at the base of the upper sequence of the Sete Lagoas Formation was collected from a layer of lime mudstone-pelite rhytmite, which was probabily deposited in deep and anoxic waters (Vieira et al., 2007). It seems that during its deposition the high sea level caused almost complete flooding of the cratonic source areas. On the other hand, the region to the west, corresponding to the axis of crustal thickening of the Brasília Belt, were uplifted and exposed to fast erosion. The euedral and prismatic shape of the majority of the zircons suggest magmatic origin and short distance transport.

Combined with previous geological knowledge of the Três Marias Formation, the new geochronological data endorse an active continental margin setting for its deposition.

Except for the Sete Lagoas Formation, that presents a clear bimodal behaviour, the Sm-Nd T_{DM} ages indicate an increasing contribution from young terrains in the Bambuí Basin, culminating in the young and narrow interval of 1.53-1.87 Ga model ages for samples from the Serra da Saudade and Três Marias formations.

Noteworthy is the youngest zircon age gap between the Jequitaí and the overlying Sete Lagoas Formation. The absence of zircon grains younger than 800 Ma in the Jequitaí sediments and the massive presence of ~640 Ma in the Sete Lagoas Formation indicate a significant change in the source region.

The maximum depositional age of 610 Ma indicates that the deformational event affecting the Bambuí Group must be younger than the metamorphic peak of the Brasília Belt.

5.6- CONCLUSION

The U-Pb provenance data, combined with Nd and Sr isotopic composition of detrital and carbonatic rocks of the Jequitaí Formation and Bambuí Group shed new light on the age of sedimentation, glacial event and tectonic significance of these units in the Brasília Belt. The main conclusions are:

i. Analyses of the detrital zircons indicate the maximum depositional age of ca. 900 Ma for the Jequitaí Formation.

ii. The zircon age pattern of the Jequitaí diamictite is dominated by a Paleoproterozoic zircon population (2.0-2.2 Ga) but also indicates contribution from Mesoproterozoic (various small peaks) and early Neoproterozoic (~900 Ma) source areas, what lead to suggesting that the São Francisco Craton represents the main source.

iii. The presence of ca. 610 Ma-old detrital zircons in the upper sequence of the Sete Lagoas Formation indicates the maximum depositional age for the Bambuí Group.

iv. U-Pb and Sm-Nd data endorse the interpretation that Bambuí Group was deposited in a foreland basin, and was mostly the product of erosion of the Brasília Belt. The data also demonstrate that the source region change significantly along the basin and along the stratigraphy.

v. The provenance of the Carrancas conglomerate is very different from the Jequitaí diamictite and reflects derivation from the Belo Horizonte Complex and deposition in a local basin.

vi. The U-Pb pattern age of the upper sequence associated with previously published Pb-Pb isochronic age of ca. 740 Ma of the lower of the Sete Lagoas Formation and geophysical data suggest that the lower sequence does not belong to the Bambuí Group and most likely represents the cap carbonate of the Jequitaí glacial deposits, whereas the rest of the Bambuí Group is considerably younger (<610 Ma).

vii. The tectonic process that involved the rocks of the Bambuí Group was not coeval with the metamorphic peak of the Brasília Belt of 630 Ma and represents a younger event.

ACKNOWLEDGEMENTS

This work benefited from financial support from the Companhia de Pesquisa de Recursos Minerais and CNPq. We also thank the staff of the Laboratório de Geocronologia da Universidade de Brasília for their technical assistance.

5.7 - APPENDIX B – U-PB DATA OF THE BAMBUÍ GROUP AND JEQUITÁI FORMATION

Notes: 1. Uncertainties given at the two σ level (%).
2. f^{206}% denotes the percentage of ^{206}Pb that is common Pb.
3. Correction for common Pb made using the measured $^{206}Pb/^{204}Pb$ ratio.
4. For %Disc., 0% denotes a concordant analysis.

Table 5.2 – U-Pb SHRIMP data of the sample JEQ – Jequitaí Formation.

						Ratios								Ages						
Grain. spot	**U (ppm)**	**Th (ppm)**	**Th/U**	**Pb* (ppm)**	**f_{206} %**	**$^{206}Pb/^{204}Pb$**	**$^{207}Pb/^{206}Pb$**	**±**	**$^{207}Pb/^{235}U$**	**±**	**$^{206}Pb/^{238}U$**	**±**	**Rho**	**$^{207}Pb/^{206}Pb$**	**±**	**$^{207}Pb/^{235}U$**	**±**	**$^{206}Pb/^{238}U$**	**±**	**Disc. %**
1.1			0.83		0.24	7752	0.128744	1.64	6.641	3.38	0.374113	2.95	0.87	2081	29	2065	29	2049	52	1.57
~~2.1~~			~~0.48~~		~~0.00~~	~~infinite~~	~~0.074122~~	~~1.71~~	~~1.612~~	~~3.33~~	~~0.157709~~	~~2.85~~	~~0.86~~	~~1045~~	~~35~~	~~975~~	~~21~~	~~944~~	~~25~~	~~10.67~~
3.1			0.20		0.03	53494	0.082014	1.28	2.266	3.02	0.200382	2.74	0.91	1246	25	1202	21	1177	29	5.82
4.1			1.01		0.36	5129	0.068554	1.98	1.388	3.35	0.146865	2.71	0.81	885	41	884	20	883	22	0.22
5.1			1.29		0.03	58880	0.128700	0.79	6.674	2.87	0.376103	2.76	0.96	2080	14	2069	25	2058	49	1.08
5.2	124	76	0.63	41.5	0.14	12955	0.128219	0.98	6.879	3.74	0.389115	3.61	0.97	2074	17	2096	33	2119	65	-2.13
~~6.1~~	~~111~~	~~81~~	~~0.76~~	~~14.9~~	~~1.27~~	~~1477~~	~~0.062991~~	~~7.23~~	~~1.339~~	~~8.14~~	~~0.154161~~	~~3.75~~	~~0.46~~	~~708~~	~~154~~	~~863~~	~~46~~	~~924~~	~~32~~	~~23.40~~
7.1	48	25	0.53	8.3	2.00	937	0.076850	7.28	2.092	8.37	0.197461	4.12	0.49	1117	145	1146	56	1162	44	-3.82
8.1	180	65	0.37	41.0	0.22	8537	0.095249	1.28	3.482	3.80	0.265160	3.57	0.94	1533	24	1523	30	1516	48	1.11
9.1	211	73	0.36	68.0	0.08	24022	0.127138	0.57	6.566	3.60	0.374586	3.55	0.99	2059	10	2055	31	2051	62	0.38
10.1	63	62	1.01	21.6	0.06	33105	0.131358	0.95	7.173	3.75	0.396021	3.63	0.97	2116	17	2133	33	2151	66	-1.60
~~11.1~~	~~909~~	~~605~~	~~0.69~~	~~122.3~~	~~0.63~~	~~2973~~	~~0.102479~~	~~1.26~~	~~2.199~~	~~3.74~~	~~0.155594~~	~~3.52~~	~~0.94~~	~~1669~~	~~23~~	~~1181~~	~~26~~	~~932~~	~~31~~	~~79.08~~
12.1	132	103	0.80	17.9	0.35	5385	0.068023	2.21	1.480	4.23	0.157828	3.60	0.85	869	46	922	25	945	32	-7.99
13.1	194	29	0.16	68.1	0.16	11867	0.149689	0.93	8.438	3.67	0.408816	3.55	0.97	2342	16	2279	33	2210	66	6.01
13.2	71	102	1.49	38.4	0.16	11834	0.237532	0.64	20.717	3.69	0.632555	3.64	0.99	3104	10	3125	35	3160	91	-1.78
~~14.1~~	~~39~~	~~7~~	~~0.19~~	~~7.3~~	~~0.92~~	~~2038~~	~~0.077532~~	~~5.26~~	~~2.298~~	~~6.47~~	~~0.214933~~	~~3.78~~	~~0.58~~	~~1135~~	~~105~~	~~1212~~	~~45~~	~~1255~~	~~43~~	~~9.57~~
14.2	217	79	0.38	37.2	0.04	51660	0.080309	1.00	2.207	3.69	0.199310	3.55	0.96	1205	20	1183	25	1172	38	2.82
15.1	156	92	0.61	36.1	0.27	6905	0.093377	1.22	3.461	3.77	0.268828	3.57	0.95	1496	23	1518	29	1535	49	-2.56
16.1	35	85	2.49	11.9	1.19	1567	0.126187	2.92	6.713	4.81	0.385833	3.82	0.79	2046	52	2074	42	2103	69	-2.76
17.1	160	98	0.63	29.5	0.45	4130	0.078528	2.24	2.313	4.23	0.213618	3.59	0.85	1160	44	1216	30	1248	41	-7.03
18.1	61	33	0.56	21.2	0.28	6611	0.131728	1.54	7.304	4.00	0.402117	3.69	0.92	2121	27	2149	35	2179	68	-2.65
~~19.1~~	~~66~~	~~60~~	~~0.93~~	~~8.7~~	~~0.00~~	~~infinite~~	~~0.074510~~	~~1.75~~	~~1.569~~	~~4.06~~	~~0.152720~~	~~3.66~~	~~0.90~~	~~1055~~	~~35~~	~~958~~	~~25~~	~~916~~	~~31~~	~~15.18~~

Grain. spot	U (ppm)	Th (ppm)	Th/U	Pb* (ppm)	f_{206} %	Ratios $^{206}Pb/^{204}Pb$	$^{207}Pb/^{206}Pb$	±	$^{207}Pb/^{235}U$	±	$^{206}Pb/^{238}U$	±	Rho	Ages $^{207}Pb/^{206}Pb$	±	$^{207}Pb/^{235}U$	±	$^{206}Pb/^{238}U$	±	Disc. %
20.1	136	12	0.09	45.7	0.36	5129	0.129147	0.99	6.948	3.72	0.390168	3.58	0.96	2086	17	2105	32	2124	65	-1.75
20.2	51	45	0.91	17.8	0.28	6640	0.128725	1.64	7.112	4.06	0.400704	3.71	0.92	2081	29	2126	36	2172	68	-4.22
21.2	112	45	0.41	16.6	0.00	infinite	0.075937	2.93	1.816	4.66	0.173457	3.62	0.78	1093	59	1051	30	1031	35	6.04
22.1	63	59	0.96	17.2	1.06	1763	0.102344	3.20	4.441	5.02	0.314697	3.87	0.77	1667	59	1720	41	1764	60	-5.48
~~23.1~~	~~56~~	~~36~~	~~0.66~~	~~8.1~~	~~0.79~~	~~2375~~	~~0.063358~~	~~5.57~~	~~1.450~~	~~6.69~~	~~0.166004~~	~~3.70~~	~~0.55~~	~~720~~	~~118~~	~~910~~	~~39~~	~~990~~	~~34~~	~~-27.25~~
24.1	196	91	0.48	25.8	0.14	13313	0.067730	1.51	1.428	3.87	0.152952	3.56	0.92	860	31	901	23	917	30	-6.23
24.2	137	80	0.60	18.9	0.06	30152	0.070332	2.53	1.552	4.42	0.160077	3.63	0.82	938	52	951	27	957	32	-2.00
25.1	96	97	1.04	33.6	0.06	30464	0.123020	1.27	6.895	3.88	0.406486	3.67	0.95	2000	23	2098	34	2199	68	-9.02
26.1	270	319	1.22	86.4	0.00	infinite	0.113228	0.85	5.825	3.75	0.373082	3.65	0.97	1852	15	1950	32	2044	64	-9.40
27.1	114	97	0.89	38.5	0.00	infinite	0.135020	0.80	7.350	3.74	0.394790	3.66	0.98	2164	14	2155	33	2145	67	0.90
27.2	74	42	0.59	25.9	0.06	29564	0.135243	0.98	7.586	3.80	0.406833	3.68	0.97	2167	17	2183	34	2200	69	-1.51
28.1	221	204	0.95	34.6	0.08	23463	0.072668	1.01	1.822	3.70	0.181808	3.56	0.96	1005	20	1053	24	1077	35	-6.70
28.2	94	35	0.38	14.1	0.47	3975	0.070983	3.58	1.703	5.15	0.173958	3.70	0.72	957	73	1009	32	1034	35	-7.44
~~29.1~~	~~72~~	~~43~~	~~0.62~~	~~9.7~~	~~0.00~~	~~infinite~~	~~0.080522~~	~~7.95~~	~~1.760~~	~~8.42~~	~~0.158498~~	~~2.80~~	~~0.33~~	~~1210~~	~~156~~	~~1031~~	~~53~~	~~948~~	~~25~~	~~21.60~~
~~30.1~~	~~85~~	~~56~~	~~0.68~~	~~11.3~~	~~0.75~~	~~2311~~	~~0.065350~~	~~12.32~~	~~1.382~~	~~12.65~~	~~0.153377~~	~~2.88~~	~~0.23~~	~~786~~	~~259~~	~~881~~	~~72~~	~~920~~	~~25~~	~~-17.09~~
31.1	226	146	0.67	44.5	0.18	9196	0.087294	1.76	2.751	2.91	0.228539	2.31	0.80	1367	34	1342	21	1327	28	2.94
32.1	414	475	1.18	184.7	0.03	54093	0.179203	0.81	12.815	2.36	0.518633	2.21	0.94	2646	13	2666	22	2693	49	-1.81
33.1	142	135	0.98	47.6	0.07	20697	0.128203	1.32	6.900	2.82	0.390345	2.50	0.88	2073	23	2099	25	2124	45	-2.46
~~33.2~~	~~2047~~	~~3654~~	~~1.84~~	~~284.2~~	~~1.31~~	~~1226~~	~~0.095331~~	~~1.12~~	~~2.096~~	~~2.42~~	~~0.159439~~	~~2.15~~	~~0.89~~	~~1535~~	~~21~~	~~1147~~	~~17~~	~~954~~	~~19~~	~~37.86~~
~~34.1~~	~~79~~	~~54~~	~~0.71~~	~~10.6~~	~~0.60~~	~~2913~~	~~0.064201~~	~~9.39~~	~~1.362~~	~~10.13~~	~~0.153833~~	~~3.79~~	~~0.37~~	~~748~~	~~198~~	~~873~~	~~58~~	~~922~~	~~33~~	~~-23.28~~
~~35.1~~	~~92~~	~~72~~	~~0.81~~	~~35.1~~	~~0.73~~	~~2025~~	~~0.133197~~	~~2.56~~	~~8.091~~	~~3.94~~	~~0.440554~~	~~2.99~~	~~0.76~~	~~2141~~	~~45~~	~~2241~~	~~35~~	~~2353~~	~~59~~	~~-9.93~~
36.1	64	40	0.65	21.2	0.04	34994	0.133830	1.55	7.169	3.12	0.388526	2.71	0.87	2149	27	2133	27	2116	49	1.53
37.1	169	130	0.79	33.5	0.00	infinite	0.088573	1.71	2.820	2.98	0.230938	2.44	0.82	1395	33	1361	22	1339	29	3.98
38.1	113	74	0.67	32.8	0.15	10117	0.120329	1.67	5.580	3.01	0.336316	2.50	0.83	1961	30	1913	26	1869	41	4.70
39.1	283	156	0.57	60.9	0.00	infinite	0.088446	1.35	3.053	2.85	0.250377	2.51	0.88	1392	26	1421	22	1440	32	-3.46
~~40.1~~	~~156~~	~~103~~	~~0.68~~	~~31.7~~	~~0.31~~	~~5368~~	~~0.080748~~	~~2.96~~	~~2.620~~	~~3.93~~	~~0.235353~~	~~2.59~~	~~0.66~~	~~1215~~	~~58~~	~~1306~~	~~29~~	~~1362~~	~~32~~	~~-12.11~~
41.1	158	219	1.44	53.9	0.21	7290	0.125299	1.83	6.861	3.10	0.397154	2.50	0.81	2033	32	2094	27	2156	46	-6.04
42.1	156	146	0.97	67.0	0.00	infinite	0.186997	0.78	12.901	2.59	0.500382	2.47	0.95	2716	13	2672	24	2615	53	3.70
~~43.1~~	~~119~~	~~27~~	~~0.24~~	~~49.2~~	~~0.47~~	~~2908~~	~~0.186021~~	~~3.08~~	~~12.264~~	~~5.43~~	~~0.478140~~	~~4.47~~	~~0.82~~	~~2707~~	~~51~~	~~2625~~	~~50~~	~~2519~~	~~93~~	~~6.95~~
44.1	190	434	2.37	64.1	0.00	infinite	0.128789	1.12	6.994	2.56	0.393859	2.30	0.90	2082	20	2111	23	2141	42	-2.84

Table 5.3 – U-Pb SHRIMP data of the sample CRIST – Jequitaí Formation.

Grain. spot	U (ppm)	Th (ppm)	Th/U	Pb* (ppm)	f_{206} %	Ratios							Rho	Ages						Disc. %
						$^{206}Pb/^{204}Pb$	$^{207}Pb/^{206}Pb$	±	$^{207}Pb/^{235}U$	±	$^{206}Pb/^{238}U$	±		$^{207}Pb/^{206}Pb$	±	$^{207}Pb/^{235}U$	±	$^{206}Pb/^{238}U$	±	
1.1B	115	186	1.67	34.1	4911	0.38	0.127787	1.27	6.054	3.57	0.343584	3.34	0.93	2068	22	1984	31	1904	55	8.61
2.1B	43	20	0.49	15.5	8481	0.22	0.129886	1.13	7.523	3.58	0.420069	3.40	0.95	2096	20	2176	32	2261	65	-7.27
~~2.2B~~	~~239~~	~~208~~	~~0.90~~	~~65.1~~	~~7325~~	~~0.26~~	~~0.128941~~	~~0.64~~	~~5.614~~	~~3.29~~	~~0.315768~~	~~3.22~~	~~0.98~~	~~2084~~	~~11~~	~~1918~~	~~28~~	~~1769~~	~~50~~	~~17.78~~
3.1B	98	168	1.77	43.9	104516	0.02	0.183473	0.91	13.191	3.41	0.521453	3.29	0.96	2685	15	2693	32	2705	73	-0.77
~~3.2B~~	~~279~~	~~457~~	~~1.69~~	~~84.0~~	~~3673~~	~~0.51~~	~~0.171583~~	~~0.67~~	~~8.260~~	~~3.29~~	~~0.349137~~	~~3.22~~	~~0.98~~	~~2573~~	~~11~~	~~2260~~	~~29~~	~~1930~~	~~54~~	~~33.29~~
~~4.1B~~	~~201~~	~~80~~	~~0.41~~	~~53.4~~	~~3103~~	~~0.60~~	~~0.148737~~	~~1.18~~	~~6.301~~	~~3.46~~	~~0.307234~~	~~3.26~~	~~0.94~~	~~2331~~	~~20~~	~~2019~~	~~30~~	~~1727~~	~~49~~	~~34.99~~
5.1B	75	50	0.69	17.3	6848	0.27	0.098273	2.48	3.614	4.20	0.266704	3.39	0.81	1592	46	1553	33	1524	46	4.43
6.1B	94	80	0.88	28.9	5155	0.36	0.130398	1.27	6.429	3.55	0.357604	3.31	0.93	2103	22	2036	31	1971	56	6.72
6.2B	186	94	0.52	62.8	13298	0.14	0.128757	1.07	6.972	3.46	0.392734	3.29	0.95	2081	19	2108	30	2135	60	-2.55
7.1B	153	107	0.72	46.7	infinite	-	0.130089	1.56	6.383	3.62	0.355872	3.27	0.90	2099	27	2030	31	1963	55	6.96
8.1B	239	101	0.44	54.9	34141	0.05	0.094960	0.79	3.500	3.32	0.267334	3.23	0.97	1527	15	1527	26	1527	44	0.00
9.1B	133	67	0.52	45.1	13877	0.13	0.136932	0.93	7.440	3.40	0.394082	3.27	0.96	2189	16	2166	30	2142	60	2.20
10.1	126	86	0.71	34.8	4958	0.38	0.104798	1.29	4.615	3.51	0.319418	3.27	0.93	1711	24	1752	29	1787	51	-4.26
11.1	118	140	1.23	57.4	6416	0.29	0.203952	0.78	15.919	3.35	0.566092	3.26	0.97	2858	13	2872	32	2892	76	-1.16
11.2	151	79	0.54	65.2	3625	0.52	0.190756	0.86	13.137	3.37	0.499481	3.26	0.97	2749	14	2690	31	2612	70	5.25
12.1	121	96	0.81	43.0	50323	0.04	0.131573	0.71	7.470	3.34	0.411795	3.26	0.98	2119	12	2169	29	2223	61	-4.68
12.2	252	131	0.54	85.8	35085	0.05	0.131398	1.45	7.173	3.53	0.395916	3.21	0.91	2117	25	2133	31	2150	59	-1.56
13.1	249	197	0.82	84.8	10359	0.18	0.125815	1.18	6.870	3.43	0.396041	3.22	0.94	2040	21	2095	30	2151	59	-5.14
20.1	94	54	0.60	32.5	7164	0.26	0.131208	1.16	7.238	3.50	0.400077	3.30	0.94	2114	20	2141	31	2169	61	-2.54
20.2	83	44	0.55	28.6	infinite	-	0.132632	0.79	7.314	3.40	0.399945	3.31	0.97	2133	14	2151	30	2169	61	-1.65
21.1	83	75	0.93	29.4	infinite	-	0.131726	0.91	7.501	3.48	0.412978	3.36	0.96	2121	16	2173	31	2229	63	-4.82
22.1	96	28	0.31	34.1	24230	0.08	0.135548	1.17	7.764	3.50	0.415442	3.30	0.94	2171	20	2204	31	2240	62	-3.07
23.1	102	93	0.94	31.7	6638	0.28	0.134472	1.28	6.696	3.54	0.361132	3.30	0.93	2157	22	2072	31	1988	56	8.54
24.1	101	58	0.59	36.2	infinite	-	0.136077	0.95	7.844	3.44	0.418075	3.30	0.96	2178	17	2213	30	2252	63	-3.28
25.1	95	46	0.50	50.1	18367	0.10	0.223580	0.61	18.915	3.37	0.613594	3.31	0.98	3007	10	3038	32	3084	81	-2.52
26.1	79	74	0.97	27.5	7187	0.26	0.130438	1.18	7.235	3.54	0.402262	3.34	0.94	2104	21	2141	31	2179	62	-3.47
14.1	231	149	0.67	54.1	infinite	-	0.096126	0.91	3.612	3.36	0.272543	3.24	0.96	1550	17	1552	26	1554	45	-0.22
~~15.1~~	~~1184~~	~~1246~~	~~1.09~~	~~139.5~~	~~187~~	~~10.02~~	~~0.149268~~	~~10.01~~	~~2.541~~	~~10.60~~	~~0.123443~~	~~3.48~~	~~0.33~~	~~2338~~	~~171~~	~~1284~~	~~74~~	~~750~~	~~25~~	~~211.53~~
15.2	323	306	0.98	92.3	1613	1.16	0.132960	1.68	6.036	3.63	0.329241	3.22	0.89	2137	29	1981	31	1835	51	16.50
16.1	166	174	1.08	51.2	2143	0.87	0.130183	1.21	6.384	3.46	0.355641	3.24	0.94	2100	21	2030	30	1961	55	7.08
~~17.1~~	~~623~~	~~511~~	~~0.85~~	~~87.9~~	~~158~~	~~11.86~~	~~0.149444~~	~~10.79~~	~~2.985~~	~~11.32~~	~~0.144878~~	~~3.40~~	~~0.30~~	~~2340~~	~~185~~	~~1404~~	~~83~~	~~872~~	~~28~~	~~168.24~~
18.1	172	95	0.57	56.4	6696	0.28	0.134457	0.78	7.075	3.34	0.381638	3.25	0.97	2157	14	2121	29	2084	58	3.51

CRIST (continued)

Grain. spot	U (ppm)	Th (ppm)	Th/U	Pb* (ppm)	f_{206} %	Ratios $^{206}Pb/^{204}Pb$	$^{207}Pb/^{206}Pb$	±	$^{207}Pb/^{235}U$	±	$^{206}Pb/^{238}U$	±	Rho	Ages $^{207}Pb/^{206}Pb$	±	$^{207}Pb/^{235}U$	±	$^{206}Pb/^{238}U$	±	Disc. %
19.1	361	59	0.17	67.6	36733	0.05	0.081099	0.86	2.436	3.32	0.217814	3.21	0.97	1224	17	1253	24	1270	37	-3.66
27.1	37	10	0.29	13.6	14189	0.13	0.147132	1.57	8.745	3.89	0.431098	3.56	0.91	2313	27	2312	35	2311	69	0.09
27.2	136	38	0.29	48.8	infinite	-	0.143277	0.77	8.249	3.36	0.417541	3.27	0.97	2267	13	2259	30	2249	62	0.80
28.1	141	115	0.84	45.9	32467	0.06	0.137882	1.03	7.197	3.53	0.378566	3.37	0.96	2201	18	2136	31	2070	60	6.34
~~29.1~~	~~76~~	~~124~~	~~1.69~~	~~21.4~~	~~1247~~	~~1.50~~	~~0.128993~~	~~2.54~~	~~5.753~~	~~4.25~~	~~0.323491~~	~~3.41~~	~~0.80~~	~~2084~~	~~45~~	~~1939~~	~~36~~	~~1807~~	~~54~~	~~15.36~~

Table 5.4 – U-Pb SHRIMP data of the sample TM – Três Marias Formation.

Grain. spot	U (ppm)	Th (ppm)	Th/U	Pb* (ppm)	f_{206} %	Ratios $^{206}Pb/^{204}Pb$	$^{207}Pb/^{206}Pb$	±	$^{207}Pb/^{235}U$	±	$^{206}Pb/^{238}U$	±	Rho	Ages $^{207}Pb/^{206}Pb$	±	$^{207}Pb/^{235}U$	±	$^{206}Pb/^{238}U$	±	Disc. %
1.1	307	194	0.65	33.5	0.05	35262	0.064672	1.49	1.130	3.09	0.126704	2.70	0.88	764	31	768	16	769	20	-0.70
2.1	518	239	0.48	46.7	0.79	2368	0.059783	3.16	0.858	4.14	0.104119	2.67	0.64	596	68	629	19	639	16	-6.70
~~3.1~~	~~406~~	~~448~~	~~1.14~~	~~66.9~~	~~0.37~~	~~5014~~	~~0.082515~~	~~1.87~~	~~2.176~~	~~3.30~~	~~0.191234~~	~~2.72~~	~~0.82~~	~~1258~~	~~36~~	~~1173~~	~~23~~	~~1128~~	~~28~~	~~11.50~~
4.1	197	174	0.91	18.0	0.14	13265	0.062133	2.60	0.910	3.82	0.106245	2.80	0.73	679	56	657	18	651	17	4.27
5.1	581	312	0.56	59.5	0.29	6427	0.063979	1.88	1.049	3.26	0.118870	2.67	0.82	741	40	728	17	724	18	2.33
~~6.1~~	~~119~~	~~111~~	~~0.96~~	~~10.8~~	~~0.60~~	~~3126~~	~~0.057574~~	~~6.17~~	~~0.831~~	~~6.85~~	~~0.104642~~	~~2.99~~	~~0.44~~	~~514~~	~~136~~	~~614~~	~~31~~	~~642~~	~~18~~	~~-19.95~~
~~7.1~~	~~131~~	~~152~~	~~1.19~~	~~11.0~~	~~1.66~~	~~1125~~	~~0.051537~~	~~10.13~~	~~0.679~~	~~10.56~~	~~0.095619~~	~~3.00~~	~~0.28~~	~~265~~	~~232~~	~~526~~	~~42~~	~~589~~	~~17~~	~~-55.00~~
8.1	547	475	0.90	43.0	1.24	1503	0.059952	4.67	0.747	5.39	0.090375	2.70	0.50	602	101	567	23	558	14	7.90
9.1	110	93	0.87	18.2	0.58	3236	0.076746	3.75	2.020	4.78	0.190882	2.97	0.62	1115	75	1122	32	1126	31	-1.02
~~10.1~~	~~669~~	~~479~~	~~0.74~~	~~54.1~~	~~0.00~~	~~infinite~~	~~0.063080~~	~~1.11~~	~~0.818~~	~~2.89~~	~~0.094040~~	~~2.67~~	~~0.92~~	~~711~~	~~24~~	~~607~~	~~13~~	~~579~~	~~15~~	~~22.70~~
11.1	251	143	0.59	25.5	0.00	infinite	0.064635	2.29	1.056	3.60	0.118506	2.77	0.77	762	48	732	19	722	19	5.61
12.1	101	93	0.94	23.3	0.74	2513	0.089963	3.17	3.289	4.33	0.265159	2.95	0.68	1425	61	1478	33	1516	40	-6.03
13.1	467	328	0.73	40.3	0.13	14658	0.059644	1.80	0.824	3.23	0.100257	2.69	0.83	591	39	611	15	616	16	-4.09
14.1	315	67	0.22	60.2	0.16	11861	0.082401	1.51	2.524	3.11	0.222122	2.72	0.87	1255	29	1279	22	1293	32	-2.94
15.1	227	127	0.58	24.9	0.08	23271	0.066288	2.35	1.164	3.64	0.127346	2.78	0.76	815	49	784	20	773	20	5.54
~~16.1~~	~~97~~	~~70~~	~~0.74~~	~~10.7~~	~~2.07~~	~~901~~	~~0.056010~~	~~9.63~~	~~0.966~~	~~10.11~~	~~0.125051~~	~~3.06~~	~~0.30~~	~~453~~	~~214~~	~~686~~	~~49~~	~~760~~	~~22~~	~~-40.39~~
17.1	379	128	0.35	40.4	0.20	9285	0.063755	1.81	1.088	3.31	0.123770	2.78	0.84	734	38	748	17	752	20	-2.49

TM (continued)

Grain. spot	U (ppm)	Th (ppm)	Th/U	Pb* (ppm)	f_{206} %	Ratios							Rho	Ages						Disc. %
						$^{206}Pb/^{204}Pb$	$^{207}Pb/^{206}Pb$	±	$^{207}Pb/^{235}U$	±	$^{206}Pb/^{238}U$	±		$^{207}Pb/^{206}Pb$	±	$^{207}Pb/^{235}U$	±	$^{206}Pb/^{238}U$	±	
18.1	207	144	0.72	17.9	0.03	63568	0.062058	2.41	0.864	3.71	0.100924	2.82	0.76	676	52	632	17	620	17	9.08
~~19.1~~	~~190~~	~~154~~	~~0.84~~	~~25.8~~	~~0.00~~	~~infinite~~	~~0.075464~~	~~1.52~~	~~1.645~~	~~3.29~~	~~0.158081~~	~~2.92~~	~~0.89~~	~~1081~~	~~30~~	~~988~~	~~21~~	~~946~~	~~26~~	~~14.25~~
20.1	223	134	0.62	23.7	0.19	9802	0.065441	2.70	1.117	3.89	0.123817	2.80	0.72	789	57	762	21	752	20	4.79
~~21.1~~	~~154~~	~~123~~	~~0.83~~	~~19.6~~	~~0.77~~	~~2432~~	~~0.065560~~	~~4.60~~	~~1.329~~	~~5.42~~	~~0.147062~~	~~2.88~~	~~0.53~~	~~792~~	~~97~~	~~859~~	~~31~~	~~884~~	~~24~~	~~-10.41~~
22.1	357	116	0.34	40.2	0.01	156172	0.065684	1.37	1.186	3.04	0.130917	2.71	0.89	796	29	794	17	793	20	0.41
23.1	177	143	0.84	15.4	0.45	4187	0.059996	5.09	0.837	5.84	0.101178	2.88	0.49	603	110	617	27	621	17	-2.87
24.1	520	360	0.72	46.3	0.08	23610	0.061934	1.65	0.884	3.15	0.103541	2.68	0.85	672	35	643	15	635	16	5.78
~~25.1~~	~~484~~	~~641~~	~~1.37~~	~~35.6~~	~~1.19~~	~~1567~~	~~0.059880~~	~~4.85~~	~~0.698~~	~~5.55~~	~~0.084554~~	~~2.71~~	~~0.49~~	~~599~~	~~105~~	~~538~~	~~23~~	~~523~~	~~14~~	~~14.52~~
~~26.1~~	~~417~~	~~479~~	~~1.19~~	~~35.1~~	~~5.10~~	~~367~~	~~0.068640~~	~~10.65~~	~~0.880~~	~~11.00~~	~~0.092986~~	~~2.77~~	~~0.25~~	~~888~~	~~220~~	~~641~~	~~51~~	~~573~~	~~15~~	~~54.92~~
~~27.1~~	~~561~~	~~196~~	~~0.36~~	~~50.3~~	~~0.19~~	~~10016~~	~~0.059062~~	~~1.69~~	~~0.849~~	~~3.16~~	~~0.104310~~	~~2.67~~	~~0.84~~	~~569~~	~~37~~	~~624~~	~~15~~	~~640~~	~~16~~	~~-10.98~~
~~28.1~~	~~150~~	~~32~~	~~0.22~~	~~24.2~~	~~0.25~~	~~7488~~	~~0.083281~~	~~2.28~~	~~2.150~~	~~3.66~~	~~0.187270~~	~~2.86~~	~~0.78~~	~~1276~~	~~45~~	~~1165~~	~~25~~	~~1107~~	~~29~~	~~15.29~~
29.1	211	89	0.44	34.2	0.00	infinite	0.080782	1.20	2.104	3.01	0.188875	2.76	0.92	1216	24	1150	20	1115	28	9.04
~~30.1~~	~~195~~	~~127~~	~~0.67~~	~~16.5~~	~~0.82~~	~~2278~~	~~0.055960~~	~~5.42~~	~~0.753~~	~~6.13~~	~~0.097639~~	~~2.85~~	~~0.47~~	~~451~~	~~120~~	~~570~~	~~26~~	~~601~~	~~16~~	~~-24.94~~
~~31.1~~	~~276~~	~~119~~	~~0.45~~	~~29.1~~	~~0.00~~	~~infinite~~	~~0.069131~~	~~2.00~~	~~1.172~~	~~3.39~~	~~0.122945~~	~~2.74~~	~~0.81~~	~~903~~	~~41~~	~~788~~	~~18~~	~~747~~	~~19~~	~~20.76~~
32.1	243	174	0.74	26.5	0.55	3419	0.062913	3.53	1.095	4.49	0.126227	2.77	0.62	705	75	751	24	766	20	-7.96
~~33.1~~	~~94~~	~~62~~	~~0.68~~	~~9.8~~	~~0.29~~	~~6421~~	~~0.066857~~	~~2.66~~	~~1.115~~	~~4.06~~	~~0.120999~~	~~3.07~~	~~0.76~~	~~833~~	~~55~~	~~761~~	~~21~~	~~736~~	~~21~~	~~13.17~~
~~34.1~~	~~97~~	~~152~~	~~1.62~~	~~8.4~~	~~1.48~~	~~1268~~	~~0.055941~~	~~9.16~~	~~0.764~~	~~9.67~~	~~0.098996~~	~~3.10~~	~~0.32~~	~~450~~	~~203~~	~~576~~	~~42~~	~~609~~	~~18~~	~~-26.05~~
~~35.1~~	~~629~~	~~256~~	~~0.42~~	~~62.9~~	~~0.53~~	~~3498~~	~~0.065808~~	~~2.05~~	~~1.050~~	~~3.39~~	~~0.115693~~	~~2.70~~	~~0.80~~	~~800~~	~~43~~	~~729~~	~~17~~	~~706~~	~~18~~	~~13.40~~
36.1	163	72	0.45	38.6	0.27	6987	0.093376	1.59	3.543	3.25	0.275171	2.83	0.87	1496	30	1537	25	1567	39	-4.56
~~37.1~~	~~371~~	~~86~~	~~0.24~~	~~36.4~~	~~0.00~~	~~infinite~~	~~0.068030~~	~~3.50~~	~~1.075~~	~~4.45~~	~~0.114588~~	~~2.75~~	~~0.62~~	~~869~~	~~72~~	~~741~~	~~23~~	~~699~~	~~18~~	~~24.33~~
~~38.1~~	~~298~~	~~112~~	~~0.39~~	~~30.1~~	~~0.55~~	~~3426~~	~~0.065338~~	~~3.34~~	~~1.053~~	~~4.39~~	~~0.116848~~	~~2.84~~	~~0.65~~	~~785~~	~~70~~	~~730~~	~~23~~	~~712~~	~~19~~	~~10.22~~
~~39.1~~	~~62~~	~~34~~	~~0.57~~	~~5.4~~	~~1.98~~	~~946~~	~~0.049738~~	~~19.67~~	~~0.687~~	~~19.99~~	~~0.100236~~	~~3.55~~	~~0.18~~	~~183~~	~~458~~	~~531~~	~~79~~	~~616~~	~~21~~	~~-70.32~~
40.1	322	42	0.13	36.3	0.00	infinite	0.067925	1.34	1.231	3.04	0.131438	2.73	0.90	866	28	815	17	796	20	8.82
~~41.1~~	~~122~~	~~97~~	~~0.82~~	~~10.6~~	~~1.06~~	~~1766~~	~~0.053137~~	~~6.99~~	~~0.734~~	~~7.61~~	~~0.100174~~	~~3.02~~	~~0.40~~	~~335~~	~~158~~	~~559~~	~~32~~	~~615~~	~~18~~	~~-45.62~~
42.1	85	52	0.63	38.1	0.07	28189	0.190160	0.91	13.614	3.11	0.519251	2.97	0.96	2744	15	2723	29	2696	65	1.76
43.1	164	11	0.07	18.8	0.18	10513	0.067129	2.72	1.235	3.95	0.133422	2.86	0.73	842	57	817	22	807	22	4.26
44.1	255	101	0.41	26.6	0.23	8131	0.062953	2.86	1.050	3.99	0.121014	2.78	0.70	707	61	729	21	736	19	-4.04
~~45.1~~	~~672~~	~~143~~	~~0.22~~	~~54.3~~	~~1.30~~	~~1444~~	~~0.065944~~	~~4.47~~	~~0.844~~	~~5.21~~	~~0.092855~~	~~2.68~~	~~0.52~~	~~805~~	~~94~~	~~621~~	~~24~~	~~572~~	~~15~~	~~40.57~~
~~46.1~~	~~123~~	~~82~~	~~0.69~~	~~10.9~~	~~0.86~~	~~2174~~	~~0.058394~~	~~7.68~~	~~0.824~~	~~8.27~~	~~0.102376~~	~~3.07~~	~~0.37~~	~~545~~	~~168~~	~~610~~	~~37~~	~~628~~	~~18~~	~~-13.33~~
47.1	120	119	1.02	10.5	0.30	6286	0.059907	4.85	0.836	5.73	0.101250	3.05	0.53	600	105	617	26	622	18	-3.46
48.1	195	223	1.18	52.4	0.35	5295	0.107870	1.32	4.627	3.06	0.311084	2.76	0.90	1764	24	1754	25	1746	42	1.01

Table 5.5 – U-Pb SHRIMP data of the sample SFM – Três Marias Formation.

Grain. spot	U (ppm)	Th (ppm)	Th/U	Pb* (ppm)	f_{206} %	Ratios							Rho	Ages						Disc. %
						$^{206}Pb/^{204}Pb$	$^{207}Pb/^{206}Pb$	±	$^{207}Pb/^{235}U$	±	$^{206}Pb/^{238}U$	±		$^{207}Pb/^{206}Pb$	±	$^{207}Pb/^{235}U$	±	$^{206}Pb/^{238}U$	±	
1.1	307	194	0.65	33.5	0.05	35262	0.064672	1.49	1.130	3.09	0.126704	2.70	0.88	764	31	768	16	769	20	-0.70
2.1	518	239	0.48	46.7	0.79	2368	0.059783	3.16	0.858	4.14	0.104119	2.67	0.64	596	68	629	19	639	16	-6.70
~~3.1~~	~~406~~	~~448~~	~~1.14~~	~~66.9~~	~~0.37~~	~~5014~~	~~0.082515~~	~~1.87~~	~~2.176~~	~~3.30~~	~~0.191234~~	~~2.72~~	~~0.82~~	~~1258~~	~~36~~	~~1173~~	~~23~~	~~1128~~	~~28~~	~~11.50~~
4.1	197	174	0.91	18.0	0.14	13265	0.062133	2.60	0.910	3.82	0.106245	2.80	0.73	679	56	657	18	651	17	4.27
5.1	581	312	0.56	59.5	0.29	6427	0.063979	1.88	1.049	3.26	0.118870	2.67	0.82	741	40	728	17	724	18	2.33
~~6.1~~	~~119~~	~~111~~	~~0.96~~	~~10.8~~	~~0.60~~	~~3126~~	~~0.057574~~	~~6.17~~	~~0.831~~	~~6.85~~	~~0.104642~~	~~2.99~~	~~0.44~~	~~514~~	~~136~~	~~614~~	~~31~~	~~642~~	~~18~~	~~-19.95~~
~~7.1~~	~~131~~	~~152~~	~~1.19~~	~~11.0~~	~~1.66~~	~~1125~~	~~0.051537~~	~~10.13~~	~~0.679~~	~~10.56~~	~~0.095619~~	~~3.00~~	~~0.28~~	~~265~~	~~232~~	~~526~~	~~42~~	~~589~~	~~17~~	~~-55.00~~
8.1	547	475	0.90	43.0	1.24	1503	0.059952	4.67	0.747	5.39	0.090375	2.70	0.50	602	101	567	23	558	14	7.90
9.1	110	93	0.87	18.2	0.58	3236	0.076746	3.75	2.020	4.78	0.190882	2.97	0.62	1115	75	1122	32	1126	31	-1.02
~~10.1~~	~~669~~	~~479~~	~~0.74~~	~~54.1~~	~~0.00~~	~~infinite~~	~~0.063080~~	~~1.11~~	~~0.818~~	~~2.89~~	~~0.094040~~	~~2.67~~	~~0.92~~	~~711~~	~~24~~	~~607~~	~~13~~	~~579~~	~~15~~	~~22.70~~
11.1	251	143	0.59	25.5	0.00	infinite	0.064635	2.29	1.056	3.60	0.118506	2.77	0.77	762	48	732	19	722	19	5.61
12.1	101	93	0.94	23.3	0.74	2513	0.089963	3.17	3.289	4.33	0.265159	2.95	0.68	1425	61	1478	33	1516	40	-6.03
13.1	467	328	0.73	40.3	0.13	14658	0.059644	1.80	0.824	3.23	0.100257	2.69	0.83	591	39	611	15	616	16	-4.09
14.1	315	67	0.22	60.2	0.16	11861	0.082401	1.51	2.524	3.11	0.222122	2.72	0.87	1255	29	1279	22	1293	32	-2.94
15.1	227	127	0.58	24.9	0.08	23271	0.066288	2.35	1.164	3.64	0.127346	2.78	0.76	815	49	784	20	773	20	5.54
~~16.1~~	~~97~~	~~70~~	~~0.74~~	~~10.7~~	~~2.07~~	~~901~~	~~0.056010~~	~~9.63~~	~~0.966~~	~~10.11~~	~~0.125051~~	~~3.06~~	~~0.30~~	~~453~~	~~214~~	~~686~~	~~49~~	~~760~~	~~22~~	~~-40.39~~
17.1	379	128	0.35	40.4	0.20	9285	0.063755	1.81	1.088	3.31	0.123770	2.78	0.84	734	38	748	17	752	20	-2.49
18.1	207	144	0.72	17.9	0.03	63568	0.062058	2.41	0.864	3.71	0.100924	2.82	0.76	676	52	632	17	620	17	9.08
~~19.1~~	~~190~~	~~154~~	~~0.84~~	~~25.8~~	~~0.00~~	~~infinite~~	~~0.075464~~	~~1.52~~	~~1.645~~	~~3.29~~	~~0.158081~~	~~2.92~~	~~0.89~~	~~1081~~	~~30~~	~~988~~	~~21~~	~~946~~	~~26~~	~~14.25~~
20.1	223	134	0.62	23.7	0.19	9802	0.065441	2.70	1.117	3.89	0.123817	2.80	0.72	789	57	762	21	752	20	4.79
~~21.1~~	~~154~~	~~123~~	~~0.83~~	~~19.6~~	~~0.77~~	~~2432~~	~~0.065560~~	~~4.60~~	~~1.329~~	~~5.42~~	~~0.147062~~	~~2.88~~	~~0.53~~	~~792~~	~~97~~	~~859~~	~~31~~	~~884~~	~~24~~	~~-10.41~~
22.1	357	116	0.34	40.2	0.01	156172	0.065684	1.37	1.186	3.04	0.130917	2.71	0.89	796	29	794	17	793	20	0.41
23.1	177	143	0.84	15.4	0.45	4187	0.059996	5.09	0.837	5.84	0.101178	2.88	0.49	603	110	617	27	621	17	-2.87
24.1	520	360	0.72	46.3	0.08	23610	0.061934	1.65	0.884	3.15	0.103541	2.68	0.85	672	35	643	15	635	16	5.78
~~25.1~~	~~484~~	~~641~~	~~1.37~~	~~35.6~~	~~1.19~~	~~1567~~	~~0.059880~~	~~4.85~~	~~0.698~~	~~5.55~~	~~0.084554~~	~~2.71~~	~~0.49~~	~~599~~	~~105~~	~~538~~	~~23~~	~~523~~	~~14~~	~~14.52~~
~~26.1~~	~~417~~	~~479~~	~~1.19~~	~~35.1~~	~~5.10~~	~~367~~	~~0.068640~~	~~10.65~~	~~0.880~~	~~11.00~~	~~0.092986~~	~~2.77~~	~~0.25~~	~~888~~	~~220~~	~~641~~	~~51~~	~~573~~	~~15~~	~~54.92~~
~~27.1~~	~~561~~	~~196~~	~~0.36~~	~~50.3~~	~~0.19~~	~~10016~~	~~0.059062~~	~~1.69~~	~~0.849~~	~~3.16~~	~~0.104310~~	~~2.67~~	~~0.84~~	~~569~~	~~37~~	~~624~~	~~15~~	~~640~~	~~16~~	~~-10.98~~
~~28.1~~	~~150~~	~~32~~	~~0.22~~	~~24.2~~	~~0.25~~	~~7488~~	~~0.083281~~	~~2.28~~	~~2.150~~	~~3.66~~	~~0.187270~~	~~2.86~~	~~0.78~~	~~1276~~	~~45~~	~~1165~~	~~25~~	~~1107~~	~~29~~	~~15.29~~
29.1	211	89	0.44	34.2	0.00	infinite	0.080782	1.20	2.104	3.01	0.188875	2.76	0.92	1216	24	1150	20	1115	28	9.04
~~30.1~~	~~195~~	~~127~~	~~0.67~~	~~16.5~~	~~0.82~~	~~2278~~	~~0.055960~~	~~5.42~~	~~0.753~~	~~6.13~~	~~0.097639~~	~~2.85~~	~~0.47~~	~~451~~	~~120~~	~~570~~	~~26~~	~~601~~	~~16~~	~~-24.94~~
~~31.1~~	~~276~~	~~119~~	~~0.45~~	~~29.1~~	~~0.00~~	~~infinite~~	~~0.069131~~	~~2.00~~	~~1.172~~	~~3.39~~	~~0.122945~~	~~2.74~~	~~0.81~~	~~903~~	~~41~~	~~788~~	~~18~~	~~747~~	~~19~~	~~20.76~~
32.1	243	174	0.74	26.5	0.55	3419	0.062913	3.53	1.095	4.49	0.126227	2.77	0.62	705	75	751	24	766	20	-7.96

SFM (continued)

Grain. spot	U (ppm)	Th (ppm)	Th/U	Pb* (ppm)	f_{206} %	Ratios							Rho	Ages						Disc. %
						$^{206}Pb/^{204}Pb$	$^{207}Pb/^{206}Pb$	±	$^{207}Pb/^{235}U$	±	$^{206}Pb/^{238}U$	±		$^{207}Pb/^{206}Pb$	±	$^{207}Pb/^{235}U$	±	$^{206}Pb/^{238}U$	±	
~~33.1~~	~~94~~	~~62~~	~~0.68~~	~~9.8~~	~~0.29~~	~~6421~~	~~0.066857~~	~~2.66~~	~~1.115~~	~~4.06~~	~~0.120999~~	~~3.07~~	~~0.76~~	~~833~~	~~55~~	~~761~~	~~21~~	~~736~~	~~21~~	~~13.17~~
~~34.1~~	~~97~~	~~152~~	~~1.62~~	~~8.4~~	~~1.48~~	~~1268~~	~~0.055941~~	~~9.16~~	~~0.764~~	~~9.67~~	~~0.098996~~	~~3.10~~	~~0.32~~	~~450~~	~~203~~	~~576~~	~~42~~	~~609~~	~~18~~	~~-26.05~~
~~35.1~~	~~629~~	~~256~~	~~0.42~~	~~62.9~~	~~0.53~~	~~3498~~	~~0.065808~~	~~2.05~~	~~1.050~~	~~3.39~~	~~0.115693~~	~~2.70~~	~~0.80~~	~~800~~	~~43~~	~~729~~	~~17~~	~~706~~	~~18~~	~~13.40~~
36.1	163	72	0.45	38.6	0.27	6987	0.093376	1.59	3.543	3.25	0.275171	2.83	0.87	1496	30	1537	25	1567	39	-4.56
~~37.1~~	~~371~~	~~86~~	~~0.24~~	~~36.4~~	~~0.00~~	~~infinite~~	~~0.068030~~	~~3.50~~	~~1.075~~	~~4.45~~	~~0.114588~~	~~2.75~~	~~0.62~~	~~869~~	~~72~~	~~741~~	~~23~~	~~699~~	~~18~~	~~24.33~~
~~38.1~~	~~298~~	~~112~~	~~0.39~~	~~30.1~~	~~0.55~~	~~3426~~	~~0.065338~~	~~3.34~~	~~1.053~~	~~4.39~~	~~0.116848~~	~~2.84~~	~~0.65~~	~~785~~	~~70~~	~~730~~	~~23~~	~~712~~	~~19~~	~~10.22~~
~~39.1~~	~~62~~	~~34~~	~~0.57~~	~~5.4~~	~~1.98~~	~~946~~	~~0.049738~~	~~19.67~~	~~0.687~~	~~19.99~~	~~0.100236~~	~~3.55~~	~~0.18~~	~~183~~	~~458~~	~~531~~	~~79~~	~~616~~	~~21~~	~~-70.32~~
40.1	322	42	0.13	36.3	0.00	infinite	0.067925	1.34	1.231	3.04	0.131438	2.73	0.90	866	28	815	17	796	20	8.82
~~41.1~~	~~122~~	~~97~~	~~0.82~~	~~10.6~~	~~1.06~~	~~1766~~	~~0.053137~~	~~6.99~~	~~0.734~~	~~7.61~~	~~0.100174~~	~~3.02~~	~~0.40~~	~~335~~	~~158~~	~~559~~	~~32~~	~~615~~	~~18~~	~~-45.62~~
42.1	85	52	0.63	38.1	0.07	28189	0.190160	0.91	13.614	3.11	0.519251	2.97	0.96	2744	15	2723	29	2696	65	1.76
43.1	164	11	0.07	18.8	0.18	10513	0.067129	2.72	1.235	3.95	0.133422	2.86	0.73	842	57	817	22	807	22	4.26
44.1	255	101	0.41	26.6	0.23	8131	0.062953	2.86	1.050	3.99	0.121014	2.78	0.70	707	61	729	21	736	19	-4.04
~~45.1~~	~~672~~	~~143~~	~~0.22~~	~~54.3~~	~~1.30~~	~~1444~~	~~0.065944~~	~~4.47~~	~~0.844~~	~~5.21~~	~~0.092855~~	~~2.68~~	~~0.52~~	~~805~~	~~94~~	~~621~~	~~24~~	~~572~~	~~15~~	~~40.57~~
~~46.1~~	~~123~~	~~82~~	~~0.69~~	~~10.9~~	~~0.86~~	~~2174~~	~~0.058394~~	~~7.68~~	~~0.824~~	~~8.27~~	~~0.102376~~	~~3.07~~	~~0.37~~	~~545~~	~~168~~	~~610~~	~~37~~	~~628~~	~~18~~	~~-13.33~~
47.1	120	119	1.02	10.5	0.30	6286	0.059907	4.85	0.836	5.73	0.101250	3.05	0.53	600	105	617	26	622	18	-3.46
48.1	195	223	1.18	52.4	0.35	5295	0.107870	1.32	4.627	3.06	0.311084	2.76	0.90	1764	24	1754	25	1746	42	1.01

Table 5.6 – U-Pb LAM-ICP-MS data of the sample CAR-1 – Carrancas Conglomerate. In the column 'Grains', 'z' means zircon ,'m' monazite, 'c' core and 'r' rim.

Grain	$^{206}Pb/^{204}Pb$	f_{206} %	Ratios							Ages				
			$^{207}Pb/^{206}Pb$	±	$^{207}Pb/^{235}U$	±	$^{206}Pb/^{238}U$	±	Rho	$^{207}Pb/^{206}Pb$	±	$^{206}Pb/^{238}U$	±	Disc. %
z01	12572	0.11	0.210307	10.41	16.296	10.66	0.561996	2.28	0.77	2908	159	2875	53	1.14
~~z04~~	~~1799~~	~~0.85~~	~~0.143799~~	~~9.08~~	~~7.046~~	~~14.08~~	~~0.355387~~	~~10.76~~	~~0.97~~	~~2273~~	~~149~~	~~1960~~	~~179~~	~~13.78~~
z05	infinite	0.00	0.196000	0.99	14.587	4.77	0.539783	4.66	0.95	2793	16	2783	105	0.38
z06	7460	0.18	0.197160	1.90	14.839	5.74	0.545872	5.42	0.89	2803	31	2808	122	-0.18
~~z07~~	~~infinite~~	~~0.00~~	~~0.193382~~	~~0.99~~	~~14.483~~	~~13.18~~	~~0.543172~~	~~13.14~~	~~0.80~~	~~2771~~	~~16~~	~~2797~~	~~291~~	~~-0.92~~
z08	infinite	0.00	0.212961	0.99	16.690	2.89	0.568413	2.72	0.94	2928	16	2901	63	0.92
~~z09~~	~~3265~~	~~0.49~~	~~0.091647~~	~~32.65~~	~~3.510~~	~~32.81~~	~~0.277747~~	~~3.31~~	~~0.80~~	~~1460~~	~~519~~	~~1580~~	~~46~~	~~-8.21~~
z11	infinite	0.00	0.204202	1.00	15.750	1.89	0.559398	1.61	0.90	2860	16	2864	37	-0.14
~~z12r~~	~~842~~	~~1.98~~	~~0.134010~~	~~1.68~~	~~3.861~~	~~3.23~~	~~0.208985~~	~~2.75~~	~~0.89~~	~~2151~~	~~29~~	~~1223~~	~~31~~	~~43.13~~
z12c	infinite	0.00	0.201683	1.09	15.317	3.24	0.550795	3.06	0.96	2840	18	2828	70	0.40
~~z13~~	~~2280~~	~~0.69~~	~~0.193242~~	~~1.03~~	~~8.425~~	~~2.30~~	~~0.316187~~	~~2.06~~	~~0.96~~	~~2770~~	~~17~~	~~1771~~	~~32~~	~~36.06~~
~~z14~~	~~infinite~~	~~0.00~~	~~0.193652~~	~~1.03~~	~~14.421~~	~~12.21~~	~~0.540103~~	~~12.17~~	~~0.85~~	~~2773~~	~~17~~	~~2784~~	~~269~~	~~-0.38~~
z15	infinite	0.00	0.187698	1.02	13.778	2.87	0.532373	2.68	0.96	2722	17	2751	60	-1.08
~~z17~~	~~infinite~~	~~0.00~~	~~0.157868~~	~~1.11~~	~~10.488~~	~~17.17~~	~~0.481831~~	~~17.14~~	~~0.90~~	~~2433~~	~~19~~	~~2535~~	~~350~~	~~-4.20~~
~~z18~~	~~1460~~	~~1.06~~	~~0.179315~~	~~1.09~~	~~8.237~~	~~2.61~~	~~0.333159~~	~~2.37~~	~~0.92~~	~~2647~~	~~18~~	~~1854~~	~~38~~	~~29.96~~
z19	infinite	0.00	0.206591	1.01	15.951	3.25	0.559977	3.09	0.93	2879	16	2867	71	0.43
z21	infinite	0.00	0.230854	1.06	19.459	1.31	0.611353	0.76	0.90	3058	17	3075	19	-0.57
z22	99166	0.01	0.189281	1.06	14.009	3.70	0.536783	3.55	0.95	2736	17	2770	79	-1.24
z23	infinite	0.00	0.167286	1.06	11.541	1.79	0.500356	1.44	0.94	2531	18	2615	31	-3.35
z24	35864	0.04	0.201589	1.06	15.334	2.08	0.551690	1.78	0.81	2839	17	2832	41	0.24
~~z25~~	~~145~~	~~10.62~~	~~0.252970~~	~~1.69~~	~~11.771~~	~~2.08~~	~~0.337477~~	~~1.21~~	~~0.88~~	~~3203~~	~~26~~	~~1875~~	~~20~~	~~41.48~~
z26	infinite	0.00	0.203962	1.19	15.649	4.33	0.556462	4.16	0.90	2858	19	2852	95	0.22
~~z27~~	~~192~~	~~9.24~~	~~0.206565~~	~~1.20~~	~~2.922~~	~~1.92~~	~~0.102581~~	~~1.49~~	~~0.93~~	~~2879~~	~~19~~	~~630~~	~~9~~	~~78.13~~
~~z28~~	~~407~~	~~4.23~~	~~0.200738~~	~~1.18~~	~~4.227~~	~~3.04~~	~~0.152736~~	~~2.81~~	~~0.96~~	~~2832~~	~~19~~	~~916~~	~~24~~	~~67.65~~
z29	57048	0.02	0.162856	1.02	10.913	4.31	0.486022	4.18	0.94	2486	17	2553	88	-2.73
~~z30~~	~~483~~	~~3.53~~	~~0.160575~~	~~1.56~~	~~3.779~~	~~2.11~~	~~0.170684~~	~~1.42~~	~~0.73~~	~~2462~~	~~26~~	~~1016~~	~~13~~	~~58.73~~
z31	118749	0.01	0.192778	1.01	14.231	3.43	0.535406	3.27	0.92	2766	17	2764	73	0.07
z33	infinite	0.00	0.122416	1.01	6.102	4.98	0.361516	4.87	0.96	1992	18	1989	83	0.12
~~z34~~	~~672~~	~~2.56~~	~~0.173822~~	~~1.10~~	~~3.622~~	~~1.60~~	~~0.151147~~	~~1.16~~	~~0.84~~	~~2595~~	~~18~~	~~907~~	~~10~~	~~65.03~~
z35	2132	0.76	0.087686	35.14	3.154	35.42	0.260892	4.44	0.90	1376	558	1494	59	-8.63
z36	infinite	0.00	0.198066	1.03	15.014	3.07	0.549783	2.89	0.94	2810	17	2824	66	-0.50
~~z37~~	~~620~~	~~2.71~~	~~0.195724~~	~~1.03~~	~~5.332~~	~~1.91~~	~~0.197578~~	~~1.61~~	~~0.93~~	~~2791~~	~~17~~	~~1162~~	~~17~~	~~58.35~~
~~z39~~	~~571~~	~~2.98~~	~~0.070721~~	~~37.29~~	~~1.664~~	~~37.48~~	~~0.170617~~	~~3.73~~	~~0.97~~	~~949~~	~~620~~	~~1016~~	~~35~~	~~-6.97~~
z40	8164	0.19	0.109645	0.85	4.844	2.85	0.320437	2.72	0.93	1794	15	1792	42	0.09
z41	606107	0.00	0.127441	1.01	6.617	3.18	0.376556	3.02	0.89	2063	18	2060	53	0.14
z42	infinite	0.00	0.209464	1.01	16.311	4.02	0.564761	3.89	0.92	2901	16	2886	90	0.52
z43	infinite	0.00	0.175982	1.08	12.223	3.81	0.503747	3.65	0.87	2615	18	2630	78	-0.56
~~z45~~	~~2058~~	~~0.82~~	~~0.185445~~	~~1.13~~	~~4.851~~	~~2.31~~	~~0.189708~~	~~2.02~~	~~0.91~~	~~2702~~	~~18~~	~~1120~~	~~21~~	~~58.56~~
~~z46~~	~~320~~	~~5.35~~	~~0.066343~~	~~61.51~~	~~1.378~~	~~61.64~~	~~0.150650~~	~~4.01~~	~~0.85~~	~~817~~	~~934~~	~~905~~	~~34~~	~~-10.69~~
~~z47~~	~~2221~~	~~0.72~~	~~0.092115~~	~~42.10~~	~~3.639~~	~~42.31~~	~~0.286541~~	~~4.13~~	~~0.90~~	~~1470~~	~~640~~	~~1624~~	~~59~~	~~-10.51~~
z48	27619	0.05	0.203755	1.01	15.626	1.39	0.556228	0.95	0.96	2857	16	2851	22	0.19
z49	63518	0.02	0.196338	1.08	14.617	3.62	0.539962	3.46	0.93	2796	18	2783	78	0.45
z50	infinite	0.00	0.222229	1.00	17.927	2.00	0.585075	1.74	0.95	2997	16	2969	41	0.92
z51	infinite	0.00	0.212993	1.00	16.731	2.89	0.569716	2.71	0.90	2928	16	2907	63	0.74
z52	infinite	0.00	0.216160	1.03	16.996	3.05	0.570268	2.87	0.88	2952	17	2909	67	1.47
z53	122058	0.01	0.188543	1.72	13.806	3.96	0.531068	3.57	0.90	2729	47	2746	98	-0.60
z54	59580	0.02	0.187061	1.73	13.556	4.07	0.525604	3.68	0.91	2716	47	2723	100	-0.24
z55	43065	0.03	0.193104	1.72	14.229	3.94	0.534424	3.55	0.90	2769	48	2760	98	0.31
z56	1822	0.74	0.190690	1.73	13.864	3.94	0.527312	3.54	0.90	2748	47	2730	97	0.66
z57	1049	1.29	0.187317	1.73	13.580	3.95	0.525809	3.55	0.90	2719	47	2724	97	-0.18
z58	2458	0.54	0.207566	1.74	16.000	3.98	0.559076	3.58	0.90	2887	50	2863	103	0.83
z59	17138	0.08	0.191410	1.72	14.094	3.93	0.534021	3.54	0.90	2754	47	2758	98	-0.15
z60	17667	0.08	0.188806	1.72	13.767	4.10	0.528832	3.73	0.91	2732	47	2737	102	-0.17

CAR-1 (continued)

Grain	$^{206}Pb/^{204}Pb$	f_{206} %	Ratios $^{207}Pb/^{206}Pb$	±	$^{207}Pb/^{235}U$	±	$^{206}Pb/^{238}U$	±	Rho	Ages $^{207}Pb/^{206}Pb$	±	$^{206}Pb/^{238}U$	±	Disc. %
z61c	13624	0.11	0.084698	1.79	2.902	5.09	0.248490	4.77	0.94	1309	23	1431	68	-9.33
z61r	2583	0.63	0.117277	1.74	5.614	3.93	0.347158	3.53	0.90	1915	33	1921	68	-0.31
z62	103317	0.01	0.173562	1.71	12.101	4.02	0.505672	3.64	0.91	2592	44	2638	96	-1.77
z63	12326	0.11	0.203965	1.78	15.846	4.08	0.563464	3.67	0.90	2858	51	2881	106	-0.80
z64	137789	0.01	0.194655	1.73	14.428	3.93	0.537579	3.52	0.90	2782	48	2773	98	0.31
z65	83857	0.02	0.105210	1.73	4.422	3.95	0.304837	3.55	0.90	1718	30	1715	61	0.16
z66	178838	0.01	0.192851	1.72	14.370	4.07	0.540434	3.69	0.91	2767	48	2785	103	-0.67
z67	39627	0.03	0.195368	1.73	14.599	3.95	0.541969	3.54	0.90	2788	48	2792	99	-0.14
m1	514	2.89	0.131687	1.83	7.105	5.26	0.391300	4.93	0.94	2121	39	2129	105	-0.39
m2	51090	0.03	0.153775	3.70	9.781	5.95	0.461295	4.67	0.78	2388	88	2445	114	-2.38
m3	139266	0.01	0.141470	1.81	8.348	5.20	0.427952	4.88	0.94	2245	41	2296	112	-2.28
m4	24973	0.06	0.118050	2.47	5.985	10.39	0.367679	10.09	0.97	1927	48	2018	204	-4.75
m5	1366	1.07	0.137811	2.59	7.981	6.55	0.420030	6.02	0.92	2200	57	2261	136	-2.76
m6	196409	0.01	0.099649	1.98	4.417	7.06	0.321510	6.78	0.96	1618	32	1797	122	-11.10
m7	20293	0.07	0.130809	2.26	7.306	7.38	0.405070	7.02	0.95	2109	48	2192	154	-3.96

Table 5.7 – U-Pb LAM-ICP-MS data of the sample 7L-1

Grain	$^{206}Pb/^{204}Pb$	f_{206} %	Ratios $^{207}Pb/^{206}Pb$	±	$^{207}Pb/^{235}U$	±	$^{206}Pb/^{238}U$	±	Rho	Ages $^{207}Pb/^{206}Pb$	±	$^{206}Pb/^{238}U$	±	Disc. %
~~1~~	~~5763~~	~~0.31~~	~~0.065287~~	~~3.20~~	~~0.927~~	~~3.91~~	~~0.102955~~	~~2.24~~	~~0.17~~	~~784~~	~~66~~	~~632~~	~~13~~	~~19.38~~
~~2~~	infinite	0.00	~~0.064656~~	~~1.26~~	~~0.903~~	~~4.01~~	~~0.101259~~	~~3.81~~	~~0.21~~	~~763~~	~~26~~	~~622~~	~~23~~	~~18.52~~
~~3~~	~~1364~~	~~1.30~~	~~0.064426~~	~~2.10~~	~~0.888~~	~~2.49~~	~~0.099930~~	~~1.34~~	~~0.26~~	~~756~~	~~44~~	~~614~~	~~8~~	~~18.74~~
4	23343	0.07	0.065650	2.14	1.154	2.92	0.127467	1.98	0.85	795	44	773	14	2.75
5	infinite	0.00	0.061510	1.00	0.895	1.96	0.105583	1.68	0.58	657	21	647	10	1.53
6	1910	0.92	0.064145	3.49	0.990	4.19	0.111892	2.33	0.77	746	72	684	15	8.40
7	infinite	0.00	0.062045	1.11	0.945	3.25	0.110412	3.05	0.83	676	23	675	20	0.08
~~8~~	~~2689~~	~~0.65~~	~~0.063277~~	~~8.59~~	~~1.161~~	~~10.65~~	~~0.133020~~	~~6.29~~	~~0.80~~	~~718~~	~~173~~	~~805~~	~~47~~	~~-12.20~~
9	10019	0.18	0.061462	7.32	0.885	9.07	0.104436	5.36	0.91	655	150	640	33	2.30
~~10~~	~~2039~~	~~0.87~~	~~0.054850~~	~~2.53~~	~~0.799~~	~~3.10~~	~~0.105604~~	~~1.80~~	~~0.56~~	~~406~~	~~56~~	~~647~~	~~11~~	~~-59.36~~
~~12~~	~~826~~	~~2.14~~	~~0.056159~~	~~4.27~~	~~0.772~~	~~5.36~~	~~0.099751~~	~~3.24~~	~~0.57~~	~~459~~	~~92~~	~~613~~	~~19~~	~~-33.64~~
13	5162	0.34	0.060583	3.94	0.900	4.80	0.107739	2.75	0.14	624	83	660	17	-5.63
14	43987	0.04	0.060966	3.73	0.890	5.28	0.105912	3.73	0.39	638	78	649	23	-1.71
15	infinite	0.00	0.065090	1.03	1.181	2.38	0.131647	2.14	0.91	777	22	797	16	-2.57
16	infinite	0.00	0.061014	0.98	0.919	2.90	0.109234	2.73	0.89	640	21	668	17	-4.47
~~17~~	~~infinite~~	~~0.00~~	~~0.067543~~	~~1.26~~	~~0.969~~	~~2.99~~	~~0.104017~~	~~2.71~~	~~0.18~~	~~855~~	~~26~~	~~638~~	~~16~~	~~25.35~~
~~18~~	infinite	0.00	~~0.063237~~	~~1.00~~	~~0.872~~	~~2.43~~	~~0.100065~~	~~2.21~~	~~0.79~~	~~716~~	~~21~~	~~615~~	~~13~~	~~14.16~~
19	1278	1.37	0.066443	4.10	1.128	4.91	0.123159	2.70	0.73	820	83	749	19	8.73
21	2925	0.61	0.061375	1.88	0.843	2.30	0.099659	1.32	0.67	652	40	612	8	6.13
22	infinite	0.00	0.061501	1.04	0.916	2.70	0.108020	2.49	0.84	657	22	661	16	-0.67
23	6440	0.27	0.061504	2.38	0.878	2.88	0.103549	1.62	0.39	657	50	635	10	3.31
24	infinite	0.00	0.061156	1.07	0.907	1.94	0.107596	1.62	0.24	645	23	659	10	-2.18
25	22375	0.08	0.061531	2.36	0.893	3.18	0.105231	2.13	0.83	658	50	645	13	1.95
27	30853	0.06	0.062085	2.02	0.921	2.61	0.107539	1.65	0.82	677	43	658	10	2.75
28	30375	0.06	0.060827	3.31	0.872	4.60	0.104017	3.20	0.69	633	70	638	19	-0.76
29	4525	0.39	0.062010	3.36	0.892	4.17	0.104314	2.46	0.79	674	70	640	15	5.16
~~31~~	~~37239~~	~~0.05~~	~~0.064946~~	~~4.61~~	~~0.925~~	~~6.36~~	~~0.103296~~	~~4.38~~	~~0.54~~	~~773~~	~~94~~	~~634~~	~~26~~	~~17.98~~
32	5224	0.34	0.061345	3.92	0.872	4.77	0.103111	2.72	0.85	651	82	633	16	2.87
34	4456	0.40	0.059563	4.55	0.856	5.59	0.104238	3.25	0.81	588	96	639	20	-8.76
35	3544	0.50	0.060596	2.82	0.874	3.35	0.104617	1.81	0.71	625	60	641	11	-2.64
36	5180	0.31	0.093136	4.28	3.323	5.29	0.258750	3.11	0.91	1491	79	1483	41	0.48

7L-1 (continued)

Grain	$^{206}Pb/^{204}Pb$	f_{206} %	Ratios						Rho	Ages				Disc. %
			$^{207}Pb/^{206}Pb$	±	$^{207}Pb/^{235}U$	±	$^{206}Pb/^{238}U$	±		$^{207}Pb/^{206}Pb$	±	$^{206}Pb/^{238}U$	±	
37	1037	1.71	0.061034	5.02	0.840	6.14	0.099849	3.53	0.82	640	104	614	21	4.20
38	infinite	0.00	0.062394	1.02	0.917	3.47	0.106594	3.32	0.90	688	22	653	21	5.05
39	5875	0.30	0.062459	3.66	0.902	4.44	0.104771	2.52	0.48	690	76	642	15	6.89
40	4405	0.40	0.061856	2.70	0.903	3.19	0.105889	1.69	0.26	669	57	649	10	3.04
41	3685	0.48	0.062598	7.37	0.896	8.98	0.103868	5.14	0.17	695	150	637	31	8.29
~~42~~	~~6760~~	~~0.26~~	~~0.064613~~	~~4.98~~	~~0.927~~	~~6.14~~	~~0.104055~~	~~3.59~~	~~0.61~~	~~762~~	~~102~~	~~638~~	~~22~~	~~16.23~~
43	13107	0.13	0.060542	4.86	0.885	6.02	0.106011	3.55	0.93	623	102	650	22	-4.26
44	7012	0.25	0.061913	4.30	0.909	5.30	0.106447	3.10	0.86	671	89	652	19	2.84
45	4012	0.44	0.059507	5.08	0.854	6.24	0.104047	3.62	0.43	586	107	638	22	-8.94
47	infinite	0.00	0.065920	1.07	1.214	2.64	0.133579	2.42	0.64	804	22	808	18	-0.55
48	infinite	0.00	0.062184	1.03	0.907	3.36	0.105746	3.20	0.66	680	22	648	20	4.77
49	infinite	0.00	0.061227	1.04	0.907	2.79	0.107398	2.59	0.51	647	22	658	16	-1.61
50	7281	0.24	0.063037	5.09	0.925	6.28	0.106396	3.67	0.33	709	105	652	23	8.13
~~51~~	~~529~~	~~3.14~~	~~0.139128~~	~~4.22~~	~~3.934~~	~~5.24~~	~~0.205075~~	~~3.10~~	~~0.90~~	~~2216~~	~~71~~	~~1203~~	~~34~~	~~45.74~~
52	8924	0.16	0.177426	6.15	12.030	7.58	0.491745	4.43	0.86	2629	99	2578	93	1.93
53	4586	0.39	0.061214	3.38	0.872	4.07	0.103358	2.26	0.62	647	71	634	14	1.96
~~54~~	~~2165~~	~~0.68~~	~~0.176147~~	~~3.23~~	~~9.943~~	~~3.98~~	~~0.409384~~	~~2.32~~	~~0.87~~	~~2617~~	~~53~~	~~2212~~	~~43~~	~~15.47~~
55	34854	0.05	0.060423	3.70	0.869	5.23	0.104346	3.70	0.62	619	78	640	22	-3.41
56	1888	0.94	0.060306	3.30	0.857	4.00	0.103069	2.26	0.09	615	70	632	14	-2.90
58	3504	0.50	0.060391	5.92	0.875	7.23	0.105122	4.14	0.29	618	123	644	25	-4.33
59	infinite	0.00	0.062182	1.09	0.944	1.73	0.110106	1.34	0.57	680	23	673	9	1.03
60	5376	0.33	0.061064	6.83	0.888	8.39	0.105445	4.88	0.59	641	140	646	30	-0.74
61	3124	0.57	0.059977	3.89	0.815	4.83	0.098593	2.87	0.12	603	82	606	17	-0.57
62	infinite	0.00	0.062282	1.14	0.945	5.97	0.110048	5.86	0.74	684	24	673	37	1.58
63	11284	0.16	0.060718	3.58	0.893	4.26	0.106631	2.31	0.58	629	75	653	14	-3.80
64	2999	0.58	0.064343	3.57	1.092	4.32	0.123092	2.44	0.69	753	74	748	17	0.61
65	552	3.21	0.061330	3.57	0.840	4.43	0.099294	2.62	0.43	651	75	610	15	6.23
66	1372	1.29	0.060232	4.79	0.853	5.95	0.102677	3.53	0.10	612	100	630	21	-2.97
67	infinite	0.00	0.061180	1.11	0.900	2.32	0.106689	2.03	0.23	646	24	653	13	-1.22
68	18408	0.10	0.059905	4.21	0.868	5.93	0.105131	4.17	0.69	600	89	644	26	-7.38
~~69~~	~~3708~~	~~0.48~~	~~0.058644~~	~~3.41~~	~~0.845~~	~~4.11~~	~~0.104522~~	~~2.30~~	~~0.47~~	~~554~~	~~73~~	~~641~~	~~14~~	~~-15.70~~
70	infinite	0.00	0.196089	1.03	14.480	3.05	0.535561	2.88	0.83	2794	17	2765	64	1.04
~~71~~	~~48096~~	~~0.03~~	~~0.178280~~	~~3.13~~	~~10.818~~	~~4.29~~	~~0.440110~~	~~2.93~~	~~0.92~~	~~2637~~	~~51~~	~~2351~~	~~58~~	~~10.84~~
72	infinite	0.00	0.063162	1.15	0.920	3.83	0.105586	3.65	0.37	714	24	647	22	9.34
73	infinite	0.00	0.061711	1.05	0.913	3.45	0.107358	3.28	0.57	664	22	657	20	1.01
74	16982	0.10	0.060821	2.19	0.875	2.72	0.104321	1.62	0.62	633	46	640	10	-1.07
75	56544	0.03	0.061439	3.11	0.897	4.33	0.105869	3.01	0.88	655	65	649	19	0.91
77	1223	1.45	0.062611	5.31	0.887	6.32	0.102728	3.42	0.26	695	109	630	21	9.30
~~78~~	~~2020~~	~~0.88~~	~~0.063661~~	~~4.67~~	~~0.885~~	~~5.50~~	~~0.100875~~	~~2.91~~	~~0.01~~	~~730~~	~~96~~	~~620~~	~~17~~	~~15.18~~
80	2608	0.68	0.060745	6.68	0.861	8.10	0.102769	4.58	0.32	630	138	631	27	-0.06
81	infinite	0.00	0.060861	1.01	0.899	4.91	0.107140	4.81	0.77	634	22	656	30	-3.44
84	3371	0.52	0.061397	7.41	0.875	8.95	0.103330	5.02	0.60	653	152	634	30	2.95
85	4643	0.38	0.061972	4.30	0.903	5.34	0.105630	3.16	0.78	673	89	647	19	3.84
88	621	2.85	0.059919	2.34	0.817	2.85	0.098841	1.63	0.42	601	50	608	9	-1.16
89	16198	0.11	0.060638	4.10	0.887	5.02	0.106092	2.90	0.60	626	86	650	18	-3.77
90	infinite	0.00	0.061322	0.98	0.950	3.24	0.112399	3.09	0.84	651	21	687	20	-5.55
91	infinite	0.00	0.209421	0.97	17.082	2.20	0.591571	1.98	0.73	2901	16	2996	47	-3.26
~~92~~	~~991~~	~~1.58~~	~~0.175069~~	~~4.20~~	~~7.425~~	~~5.05~~	~~0.307618~~	~~2.82~~	~~0.86~~	~~2607~~	~~68~~	~~1729~~	~~43~~	~~33.67~~
~~93~~	~~1034~~	~~1.71~~	~~0.063327~~	~~3.68~~	~~0.874~~	~~4.52~~	~~0.100052~~	~~2.61~~	~~0.38~~	~~719~~	~~76~~	~~615~~	~~15~~	~~14.53~~

Table 5.8 – U-Pb LAM-ICP-MS data of the sample 7L-2

Grain	$^{206}Pb/^{204}Pb$	f_{206} %	Ratios						Rho	Ages				
			$^{207}Pb/^{206}Pb$	±	$^{207}Pb/^{235}U$	±	$^{206}Pb/^{238}U$	±		$^{207}Pb/^{206}Pb$	±	$^{206}Pb/^{238}U$	±	Disc. %
1	infinito	0.00	0.119577	0.82	5.803	2.08	0.351998	1.91	0.92	1950	16	1944	37	0.3
2	28079	0.06	0.075296	2.52	1.950	3.47	0.187828	2.39	0.70	1076	50	1110	24	-3.1
3	8242	0.19	0.105945	4.61	4.545	5.66	0.311146	3.28	0.68	1731	82	1746	50	-0.9
4	infinito	0.00	0.115750	0.82	5.383	2.21	0.337290	2.05	0.93	1892	15	1874	38	0.9
5	infinito	0.00	0.103702	0.82	4.294	2.35	0.300333	2.20	0.94	1691	14	1693	37	-0.1
7	infinito	0.00	0.107529	0.95	4.776	3.69	0.322101	3.57	0.94	1758	17	1800	56	-2.4
8	infinito	0.00	0.139274	0.83	7.836	2.11	0.408065	1.94	0.92	2218	18	2206	43	0.5
9	infinito	0.00	0.063305	0.81	1.029	2.13	0.117907	1.97	0.92	719	6	719	14	0.0
10	4402	0.34	0.131101	0.89	6.992	2.18	0.386834	1.99	0.91	2113	19	2108	42	0.2
~~11~~	~~358~~	~~5.03~~	~~0.098198~~	~~1.36~~	~~1.006~~	~~2.46~~	~~0.074324~~	~~2.05~~	~~0.83~~	~~1590~~	~~25~~	~~462~~	~~9~~	~~29.1~~
12	9175	0.19	0.068130	4.96	1.269	6.04	0.135077	3.46	0.94	873	99	817	26	6.7
13	infinito	0.00	0.075489	0.89	1.893	2.14	0.181912	1.95	0.91	1082	10	1077	21	0.4
14	20512	0.09	0.064467	2.72	1.134	3.74	0.127544	2.58	0.57	757	56	774	19	-2.2
15	infinito	0.00	0.126834	0.94	7.060	2.50	0.403717	2.32	0.91	2055	17	2186	43	-6.4
16	11301	0.15	0.074923	1.01	1.854	2.19	0.179443	1.94	0.89	1066	11	1064	21	0.2
17	16435	0.11	0.060523	0.97	0.845	2.17	0.101208	1.94	0.90	622	6	621	12	0.1
18	infinito	0.00	0.067936	0.90	1.352	2.82	0.144324	2.68	0.95	867	8	869	23	-0.3
19	infinito	0.00	0.061287	0.93	0.895	2.21	0.105939	2.00	0.91	649	6	649	13	0.0
20	31289	0.05	0.126342	0.80	6.482	2.11	0.372097	1.95	0.93	2048	16	2039	40	0.4
21	infinito	0.00	0.110502	0.89	4.910	2.16	0.322257	1.96	0.91	1808	16	1801	35	0.4
22	22840	0.07	0.135745	0.83	7.437	2.14	0.397364	1.97	0.92	2174	18	2157	43	0.8
23	infinito	0.00	0.108389	0.88	4.717	2.16	0.315605	1.98	0.91	1773	16	1768	35	0.2
24	3804	0.43	0.091429	2.10	3.058	2.63	0.242586	1.58	0.81	1456	39	1400	20	3.8
27	12232	0.12	0.130487	0.82	6.911	2.17	0.384123	2.01	0.93	2105	17	2096	42	0.4
28	52541	0.03	0.123220	1.01	6.185	2.29	0.364026	2.06	0.90	2003	20	2001	41	0.1
29	infinito	0.00	0.091025	1.09	3.219	2.48	0.256470	2.23	0.90	1447	16	1472	33	-1.7
30	infinito	0.00	0.110306	0.87	4.888	2.18	0.321409	2.00	0.92	1804	16	1797	36	0.4
31	17144	0.10	0.062720	5.71	0.999	7.01	0.115542	4.05	0.38	699	117	705	27	-0.9
32	5547	0.32	0.061512	0.91	0.910	2.17	0.107325	1.97	0.91	657	6	657	13	0.0
34	infinito	0.00	0.062294	1.14	0.903	3.98	0.105122	3.81	0.12	684	24	644	23	5.6
35	infinito	0.00	0.094349	0.96	3.410	1.57	0.262148	1.24	0.91	1515	18	1501	17	0.9
36	infinito	0.00	0.147356	0.97	8.849	3.72	0.435511	3.59	0.77	2315	17	2331	70	-0.6
37	infinito	0.00	0.075379	1.04	1.830	2.55	0.176054	2.33	0.72	1079	21	1045	22	3.1
38	infinito	0.00	0.108422	1.00	4.827	2.28	0.322918	2.05	0.65	1773	18	1804	32	-1.7
39	infinito	0.00	0.127368	0.96	6.810	1.69	0.387796	1.39	0.89	2062	17	2113	25	-2.5
~~40~~	~~5575~~	~~0.31~~	~~0.061509~~	~~2.24~~	~~1.011~~	~~2.85~~	~~0.119220~~	~~1.77~~	~~0.96~~	~~657~~	~~47~~	~~726~~	~~12~~	~~-10.5~~
41	infinito	0.00	0.062867	1.02	0.941	2.11	0.108503	1.85	0.97	704	21	664	12	5.7
42	infinito	0.00	0.106533	0.95	4.650	1.76	0.316575	1.47	0.85	1741	17	1773	23	-1.8
43	19314	0.08	0.110252	4.75	4.378	6.79	0.288022	4.86	0.96	1804	84	1632	70	9.5
44	infinito	0.00	0.064059	0.98	1.109	1.87	0.125515	1.59	0.73	744	21	762	11	-2.5
45	infinito	0.00	0.073451	0.96	1.783	1.92	0.176091	1.66	0.70	1026	19	1046	16	-1.9
46	infinito	0.00	0.106857	0.95	4.638	2.44	0.314766	2.25	0.87	1746	17	1764	35	-1.0
47	infinito	0.00	0.107121	0.95	4.637	1.79	0.313920	1.52	0.90	1751	17	1760	23	-0.5
48	infinito	0.00	0.107535	0.96	4.671	3.61	0.315066	3.48	0.83	1758	18	1766	54	-0.4
49	6548	0.20	0.242939	2.59	19.278	3.26	0.575534	1.98	0.91	3139	41	2931	46	6.7
50	10043	0.15	0.119602	4.41	5.969	5.42	0.361959	3.16	0.77	1950	77	1991	54	-2.1
52	6500	0.27	0.062585	3.25	0.976	3.98	0.113068	2.30	0.29	694	68	691	15	0.5
53	13994	0.11	0.097406	2.54	3.745	3.35	0.278857	2.18	0.92	1575	47	1586	31	-0.7
55	7445	0.21	0.105127	2.29	4.465	2.83	0.308037	1.65	0.87	1717	42	1731	25	-0.8
~~56~~	~~2562~~	~~0.63~~	~~0.115664~~	~~8.85~~	~~4.056~~	~~10.89~~	~~0.254347~~	~~6.35~~	~~0.94~~	~~1890~~	~~151~~	~~1461~~	~~82~~	~~32.8~~
57	1881	0.83	0.116579	4.43	5.200	5.53	0.323478	3.31	0.93	1904	77	1807	52	5.1
~~58~~	~~5843~~	~~0.31~~	~~0.056704~~	~~3.60~~	~~0.704~~	~~4.41~~	~~0.090010~~	~~2.54~~	~~0.75~~	~~480~~	~~78~~	~~556~~	~~14~~	~~-15.7~~
59	4615	0.34	0.109606	4.54	4.859	5.59	0.321552	3.26	0.95	1793	81	1797	51	-0.2
60	165576	0.01	0.184282	0.95	13.535	2.20	0.532684	1.98	0.88	2692	16	2753	44	-2.3
61	102174	0.02	0.060830	2.55	0.827	3.48	0.098545	2.38	0.66	633	54	606	14	4.3

7L-2 (continued)

Grain	$^{206}Pb/^{204}Pb$	f_{206} %	Ratios $^{207}Pb/^{206}Pb$	±	$^{207}Pb/^{235}U$	±	$^{206}Pb/^{238}U$	±	Rho	Ages $^{207}Pb/^{206}Pb$	±	$^{206}Pb/^{238}U$	±	Disc. %
~~62~~	~~206~~	~~8.60~~	~~0.065808~~	~~8.35~~	~~0.861~~	~~10.31~~	~~0.094852~~	~~6.04~~	~~0.23~~	~~800~~	~~166~~	~~584~~	~~34~~	~~27.0~~
63	7566	0.22	0.071414	6.09	1.731	7.48	0.175829	4.34	0.79	969	120	1044	42	-7.7
64	2967	0.50	0.130567	4.64	6.985	5.74	0.387980	3.38	0.17	2106	79	2113	61	-0.4
65	11540	0.13	0.121430	2.70	6.070	3.30	0.362564	1.91	0.78	1977	47	1994	33	-0.9
66	infinito	0.00	0.079283	0.98	2.236	2.00	0.204567	1.75	0.53	1179	19	1200	19	-1.7
67	111920	0.02	0.067066	3.36	1.296	4.72	0.140203	3.31	0.26	840	68	846	26	-0.7
69	infinito	0.00	0.107335	0.97	4.693	2.82	0.317100	2.65	0.92	1755	18	1776	41	-1.2
70	5609	0.27	0.119715	4.54	6.080	5.57	0.368329	3.23	0.83	1952	79	2022	56	-3.6
~~71~~	~~495~~	~~3.36~~	~~0.148299~~	~~2.49~~	~~4.256~~	~~3.04~~	~~0.208130~~	~~1.75~~	~~0.76~~	~~2326~~	~~42~~	~~1219~~	~~19~~	~~47.6~~
72	14416	0.10	0.126074	3.37	6.553	4.15	0.376975	2.41	0.70	2044	58	2062	42	-0.9
73	infinito	0.00	0.121983	0.97	6.153	3.40	0.365807	3.26	0.92	1985	17	2010	56	-1.2
~~74~~	~~2267~~	~~0.68~~	~~0.131348~~	~~4.20~~	~~5.914~~	~~5.35~~	~~0.326534~~	~~3.32~~	~~0.97~~	~~2116~~	~~72~~	~~1822~~	~~53~~	~~13.9~~
75	infinito	0.00	0.108489	0.98	4.921	2.45	0.328958	2.25	0.83	1774	18	1833	36	-3.3
76	infinito	0.00	0.107424	0.95	4.765	4.52	0.321734	4.42	0.92	1756	17	1798	69	-2.4
77	27232	0.06	0.113313	1.69	5.213	2.20	0.333671	1.41	0.88	1853	30	1856	23	-0.2
78	45421	0.04	0.061370	3.13	0.915	4.32	0.108175	2.98	0.72	652	66	662	19	-1.5
79	infinito	0.00	0.176953	0.95	12.178	1.88	0.499143	1.62	0.96	2625	16	2610	35	0.5
80	infinito	0.00	0.147306	0.95	8.921	4.57	0.439233	4.47	0.89	2315	16	2347	87	-1.4
81	204928	0.01	0.114823	0.97	5.032	3.53	0.317833	3.40	0.90	1877	17	1779	53	5.2
82	infinito	0.00	0.128577	1.06	6.220	3.75	0.350852	3.60	0.61	2079	19	1939	60	6.7
83	infinito	0.00	0.109093	1.02	4.516	2.33	0.300211	2.10	0.68	1784	18	1692	31	5.2
84	infinito	0.00	0.178832	0.95	11.303	4.06	0.458411	3.95	0.92	2642	16	2433	79	7.9

Table 5.9 – U-Pb LAM-ICP-MS data of the sample SSH-2

Grain	$^{206}Pb/^{204}Pb$	f_{206} %	Ratios $^{207}Pb/^{206}Pb$	±	$^{207}Pb/^{235}U$	±	$^{206}Pb/^{238}U$	±	Rho	Ages $^{207}Pb/^{206}Pb$	±	$^{206}Pb/^{238}U$	±	Disc. %
1	infinite	0.00	0.063600	1.19	1.047	1.56	0.119425	1.00	0.87	728	25	727	7	0.15
~~2~~	~~infinite~~	~~0.00~~	~~0.064658~~	~~1.17~~	~~1.367~~	~~1.44~~	~~0.153306~~	~~0.84~~	~~0.59~~	~~763~~	~~25~~	~~919~~	~~7~~	~~-20.47~~
~~3~~	~~279~~	~~5.98~~	~~0.095697~~	~~10.91~~	~~2.545~~	~~13.37~~	~~0.192888~~	~~7.72~~	~~0.86~~	~~1542~~	~~192~~	~~1137~~	~~80~~	~~26.26~~
4	10656	0.15	0.106501	4.78	4.614	5.91	0.314234	3.47	0.95	1740	85	1762	53	-1.22
5	infinite	0.00	0.107146	0.94	4.678	1.17	0.316626	0.70	0.90	1751	17	1773	11	-1.24
~~9~~	~~infinite~~	~~0.00~~	~~0.063390~~	~~0.99~~	~~0.864~~	~~1.24~~	~~0.098799~~	~~0.75~~	~~0.75~~	~~721~~	~~21~~	~~607~~	~~4~~	~~15.80~~
~~10~~	~~2194~~	~~0.75~~	~~0.143523~~	~~8.52~~	~~4.643~~	~~11.35~~	~~0.234603~~	~~7.51~~	~~0.97~~	~~2270~~	~~140~~	~~1359~~	~~91~~	~~40.15~~
11	infinite	0.00	0.061871	1.00	0.911	1.25	0.106743	0.74	0.60	670	21	654	5	2.37
12	infinite	0.00	0.074027	0.94	1.741	1.14	0.170532	0.65	0.80	1042	19	1015	6	2.61
~~14~~	~~8573~~	~~0.21~~	~~0.062974~~	~~6.36~~	~~0.851~~	~~7.88~~	~~0.098061~~	~~4.66~~	~~0.04~~	~~707~~	~~130~~	~~603~~	~~27~~	~~14.75~~
16	74856	0.02	0.137486	1.54	7.650	1.82	0.403569	0.96	0.94	2196	27	2185	18	0.47
17	infinite	0.00	0.060257	1.23	0.862	1.79	0.103767	1.30	0.83	613	26	636	8	-3.86
~~18~~	~~1552~~	~~0.95~~	~~0.181426~~	~~3.74~~	~~10.158~~	~~4.90~~	~~0.406096~~	~~3.16~~	~~0.97~~	~~2666~~	~~61~~	~~2197~~	~~59~~	~~17.59~~
19	infinite	0.00	0.099621	1.02	3.904	1.28	0.284246	0.77	0.77	1617	19	1613	11	0.27
20	6723	0.26	0.065894	5.30	1.175	6.38	0.129276	3.56	0.02	803	107	784	26	2.40
25	3075	0.57	0.061335	2.94	0.884	3.67	0.104517	2.20	0.75	651	62	641	13	1.56
26	infinite	0.00	0.060831	0.97	0.887	1.19	0.105765	0.69	0.82	633	21	648	4	-2.34
29	2380	0.74	0.060500	3.32	0.850	4.01	0.101869	2.24	0.35	621	70	625	13	-0.62
31	40151	0.03	0.224711	2.88	19.083	3.10	0.615918	1.16	0.97	3015	45	3094	28	-2.62
32	infinite	0.00	0.166805	0.98	11.115	1.43	0.483303	1.03	0.95	2526	16	2542	22	-0.63
33	17616	0.09	0.119739	2.04	5.625	2.24	0.340703	0.92	0.90	1952	36	1890	15	3.19
34	infinite	0.00	0.066363	1.05	1.201	1.30	0.131202	0.76	0.80	818	22	795	6	2.83
~~35~~	~~174~~	~~10.07~~	~~0.077932~~	~~9.26~~	~~1.201~~	~~10.81~~	~~0.111779~~	~~5.58~~	~~0.15~~	~~1145~~	~~174~~	~~683~~	~~36~~	~~40.35~~
36	infinite	0.00	0.069982	1.03	1.476	1.26	0.152970	0.72	0.74	928	21	918	6	1.10

SSH-2 (continued)

Grain	$^{206}Pb/^{204}Pb$	f_{206} %	Ratios							Ages				
			$^{207}Pb/^{206}Pb$	±	$^{207}Pb/^{235}U$	±	$^{206}Pb/^{238}U$	±	Rho	$^{207}Pb/^{206}Pb$	±	$^{206}Pb/^{238}U$	±	Disc. %
37	2789	0.63	0.063293	3.03	1.056	3.60	0.120966	1.94	0.23	718	63	736	13	-2.51
38	16430	0.10	0.071876	2.76	1.689	3.35	0.170436	1.90	0.74	982	55	1015	18	-3.27
39	4584	0.39	0.059872	5.15	0.838	6.24	0.101479	3.53	0.13	599	108	623	21	-4.03
40	7280	0.24	0.065542	5.04	1.109	6.29	0.122676	3.76	0.93	792	102	746	26	5.79
41	infinite	0.00	0.220056	0.96	17.769	1.26	0.585626	0.81	0.95	2981	15	2972	19	0.32
43	infinite	0.00	0.078284	1.05	2.115	1.64	0.195968	1.26	0.94	1154	21	1154	13	0.04
44	20877	0.08	0.065432	1.92	1.100	2.22	0.121928	1.11	0.92	788	40	742	8	5.91
46	1913	0.89	0.071581	5.53	1.693	6.68	0.171580	3.75	0.87	974	109	1021	35	-4.80
47	infinite	0.00	0.071376	0.98	1.684	1.25	0.171086	0.77	0.84	968	20	1018	7	-5.15
~~48~~	~~303~~	~~5.83~~	~~0.064750~~	~~5.94~~	~~0.905~~	~~6.40~~	~~0.101321~~	~~2.38~~	~~0.30~~	~~766~~	~~120~~	~~622~~	~~14~~	~~18.81~~
~~49~~	~~1228~~	~~1.36~~	~~0.117627~~	~~8.69~~	~~3.380~~	~~11.54~~	~~0.208385~~	~~7.60~~	~~0.97~~	~~1920~~	~~148~~	~~1220~~	~~84~~	~~36.46~~
50	19281	0.09	0.074552	3.73	1.880	3.83	0.182914	0.85	0.83	1056	73	1083	8	-2.50
51	5916	0.30	0.065697	3.64	1.160	4.49	0.128076	2.62	0.34	797	75	777	19	2.49
52	11278	0.15	0.073603	5.84	1.755	7.17	0.172909	4.15	0.91	1031	114	1028	39	0.24
53	9121	0.19	0.064736	3.81	1.142	4.73	0.127965	2.81	0.59	766	78	776	21	-1.37
54	8881	0.18	0.118302	7.09	5.047	8.59	0.309436	4.84	0.74	1931	122	1738	73	9.99
55	67269	0.02	0.119612	2.10	5.520	2.23	0.334700	0.76	0.91	1950	37	1861	12	4.58
56	72420	0.02	0.169968	2.82	11.388	2.92	0.485941	0.77	0.93	2557	46	2553	16	0.17
57	25963	0.06	0.125009	2.89	6.088	3.03	0.353212	0.89	0.95	2029	50	1950	15	3.89
59	1768	0.96	0.071569	4.63	1.684	5.71	0.170692	3.34	0.79	974	92	1016	31	-4.34
~~60~~	~~549~~	~~3.14~~	~~0.077039~~	~~10.24~~	~~1.574~~	~~12.15~~	~~0.148213~~	~~6.54~~	~~0.48~~	~~1122~~	~~192~~	~~891~~	~~54~~	~~20.61~~
61	infinite	0.00	0.073453	1.01	1.766	1.44	0.174372	1.02	0.89	1026	20	1036	10	-0.94
62	infinite	0.00	0.238796	0.95	21.153	1.23	0.642449	0.78	0.95	3112	15	3199	20	-2.79
63	41450	0.04	0.073453	2.53	1.832	2.71	0.180909	0.97	0.93	1026	50	1072	10	-4.43
64	16282	0.11	0.067539	5.67	1.359	6.97	0.145903	4.05	0.93	854	114	878	33	-2.75
65	8505	0.18	0.108742	4.54	4.962	5.88	0.330966	3.74	0.97	1778	81	1843	60	-3.63
66	94820	0.02	0.075760	3.26	1.893	3.36	0.181252	0.82	0.85	1089	64	1074	8	1.37
71	14993	0.11	0.102533	6.94	4.165	8.65	0.294607	5.17	0.95	1670	123	1665	75	0.36
72	2997	0.58	0.064196	6.32	1.135	7.64	0.128239	4.29	0.25	748	128	778	31	-3.97
73	13431	0.10	0.203673	2.23	16.150	2.39	0.575109	0.87	0.94	2856	36	2929	20	-2.55
~~75~~	~~2081~~	~~0.75~~	~~0.118306~~	~~7.63~~	~~5.017~~	~~9.35~~	~~0.307561~~	~~5.40~~	~~0.83~~	~~1931~~	~~131~~	~~1729~~	~~81~~	~~10.47~~
76	6236	0.28	0.067719	3.65	1.271	4.39	0.136129	2.44	0.94	860	74	823	19	4.33
77	6203	0.28	0.068576	3.50	1.416	4.35	0.149783	2.59	0.58	886	71	900	22	-1.55
78	259838	0.01	0.093538	0.96	3.282	1.21	0.254487	0.73	0.86	1499	18	1462	10	2.48
~~79~~	~~3203~~	~~0.55~~	~~0.057340~~	~~2.59~~	~~0.860~~	~~3.20~~	~~0.108780~~	~~1.88~~	~~0.62~~	~~505~~	~~56~~	~~666~~	~~12~~	~~-31.91~~
80	5354	0.33	0.062780	2.67	0.940	3.18	0.108640	1.73	0.23	701	56	665	11	5.13
81	2604	0.58	0.120935	5.62	6.262	6.93	0.375553	4.04	0.83	1970	97	2055	71	-4.34
82	infinite	0.00	0.063322	0.98	1.004	1.21	0.114944	0.71	0.69	719	21	701	5	2.45
83	infinite	0.00	0.073984	0.98	1.873	1.31	0.183586	0.87	0.88	1041	20	1087	9	-4.37

Table 5.10 – U-Pb LAM-ICP-MS data of the sample SS-2

Grain	$^{206}Pb/^{204}Pb$	f_{206} %	Ratios							Ages				
			$^{207}Pb/^{206}Pb$	±	$^{207}Pb/^{235}U$	±	$^{206}Pb/^{238}U$	±	Rho	$^{207}Pb/^{206}Pb$	±	$^{206}Pb/^{238}U$	±	Disc. %
1	14872	0.10	0.130061	2.29	6.756	2.81	0.376748	1.63	0.87	2099	40	2061	29	1.80
2	15198	0.09	0.178141	2.53	11.133	3.46	0.453269	2.36	0.90	2636	41	2410	47	8.57
~~4~~	~~370~~	~~4.67~~	~~0.113486~~	~~20.13~~	~~2.215~~	~~24.68~~	~~0.141569~~	~~14.29~~	~~0.94~~	~~1856~~	~~325~~	~~854~~	~~113~~	~~54.01~~
5	6117	0.25	0.136250	3.87	7.081	4.76	0.376906	2.77	0.90	2180	66	2062	49	5.42
6	18594	0.08	0.123455	2.45	5.875	3.38	0.345146	2.33	0.87	2007	43	1911	38	4.75
~~8~~	~~2116~~	~~0.84~~	~~0.056819~~	~~3.10~~	~~0.786~~	~~3.77~~	~~0.100312~~	~~2.15~~	~~0.39~~	~~485~~	~~67~~	~~616~~	~~13~~	~~-27.18~~
~~9~~	~~3435~~	~~0.52~~	~~0.056410~~	~~4.11~~	~~0.761~~	~~5.04~~	~~0.097905~~	~~2.92~~	~~0.68~~	~~469~~	~~88~~	~~602~~	~~17~~	~~-28.51~~

SS-2 (continued)

			Ratios							Ages				
Grain	$^{206}Pb/^{204}Pb$	f_{206} %	$^{207}Pb/^{206}Pb$	±	$^{207}Pb/^{235}U$	±	$^{206}Pb/^{238}U$	±	Rho	$^{207}Pb/^{206}Pb$	±	$^{206}Pb/^{238}U$	±	Disc. %
10	6636	0.23	0.118813	3.44	5.589	4.19	0.341195	2.40	0.77	1938	60	1892	39	2.37
11	13624	0.12	0.104140	6.65	4.167	8.17	0.290174	4.74	0.94	1699	118	1642	68	3.34
12	103317	0.02	0.109670	4.17	4.505	5.86	0.297947	4.11	0.96	1794	74	1681	61	6.29
14	24000	0.05	0.215670	2.18	17.492	2.95	0.588217	1.99	0.90	2949	35	2982	47	-1.14
15	12596	0.11	0.173374	2.66	11.617	3.24	0.485970	1.85	0.87	2590	44	2553	39	1.44
16	21738	0.08	0.064174	2.46	1.157	3.34	0.130716	2.26	0.84	747	51	792	17	-5.96
~~17~~	~~27675~~	~~0.05~~	~~0.227137~~	~~7.20~~	~~16.440~~	~~10.17~~	~~0.524938~~	~~7.19~~	~~0.90~~	~~3032~~	~~111~~	~~2720~~	~~158~~	~~10.29~~
18	12326	0.13	0.105054	2.72	4.389	3.37	0.302999	1.98	0.89	1715	49	1706	30	0.53
19	24729	0.07	0.071331	3.16	1.555	4.40	0.158059	3.07	0.84	967	63	946	27	2.17
20	infinite	0.00	0.176953	0.97	11.948	1.64	0.489704	1.33	0.82	2625	16	2569	28	2.10
21	142977	0.01	0.108661	0.96	4.783	2.54	0.319240	2.35	0.86	1777	17	1786	37	-0.50
22	1041	1.70	0.061038	5.97	0.880	7.38	0.104575	4.33	0.18	641	123	641	26	-0.09
23	8395	0.18	0.125485	8.05	6.497	9.89	0.375500	5.74	0.92	2036	136	2055	100	-0.96
24	2583	0.62	0.102192	3.08	4.033	3.83	0.286192	2.28	0.84	1664	56	1622	33	2.51
25	3183	0.55	0.065138	4.88	1.191	6.02	0.132599	3.53	0.85	779	99	803	27	-3.07
26	infinite	0.00	0.198471	1.00	15.073	2.90	0.550822	2.72	0.87	2814	16	2829	62	-0.53
27	3074	0.50	0.121337	7.51	5.776	9.17	0.345245	5.27	0.68	1976	128	1912	87	3.25
28	infinite	0.00	0.106955	0.99	4.584	4.26	0.310868	4.15	0.86	1748	18	1745	63	0.18
30	4890	0.31	0.114167	6.77	5.407	8.32	0.343490	4.83	0.94	1867	117	1903	79	-1.96
~~31~~	~~infinite~~	~~0.00~~	~~0.066287~~	~~1.31~~	~~0.988~~	~~2.83~~	~~0.108086~~	~~2.51~~	~~0.72~~	~~815~~	~~27~~	~~662~~	~~16~~	~~18.87~~
32	40520	0.04	0.068746	2.25	1.313	3.01	0.138545	2.00	0.66	891	46	836	16	6.14
33	206901	0.01	0.071731	0.98	1.636	1.68	0.165400	1.36	0.59	978	20	987	12	-0.86
35	15885	0.10	0.088717	2.92	2.957	3.56	0.241777	2.05	0.89	1398	55	1396	26	0.15
~~36~~	~~2716~~	~~0.64~~	~~0.062979~~	~~4.12~~	~~1.135~~	~~5.10~~	~~0.130741~~	~~3.00~~	~~0.66~~	~~708~~	~~85~~	~~792~~	~~22~~	~~-11.95~~
37	infinite	0.00	0.176731	0.96	12.332	2.27	0.506099	2.05	0.90	2622	16	2640	44	-0.67
38	infinite	0.00	0.126452	0.98	6.610	2.09	0.379143	1.85	0.76	2049	17	2072	33	-1.13
39	infinite	0.00	0.129729	0.97	6.991	2.85	0.390860	2.68	0.69	2094	17	2127	48	-1.55
40	13752	0.11	0.114771	3.86	5.494	4.74	0.347180	2.76	0.62	1876	68	1921	46	-2.39
41	infinite	0.00	0.170237	0.97	10.956	6.41	0.466772	6.34	0.90	2560	16	2469	129	3.54
42	infinite	0.00	0.062434	1.05	0.946	2.63	0.109934	2.41	0.26	689	22	672	15	2.41
~~43~~	~~3810~~	~~0.47~~	~~0.056417~~	~~2.87~~	~~0.755~~	~~3.48~~	~~0.097003~~	~~1.97~~	~~0.30~~	~~469~~	~~62~~	~~597~~	~~11~~	~~-27.30~~
44	infinite	0.00	0.171070	0.96	11.075	1.45	0.469541	1.09	0.93	2568	16	2482	22	3.37
45	infinite	0.00	0.186797	0.96	13.358	2.05	0.518662	1.81	0.85	2714	16	2694	40	0.76
45	infinite	0.00	0.186797	0.96	13.358	2.05	0.518662	1.81	0.85	2714	16	2694	40	0.76
~~46~~	~~infinite~~	~~0.00~~	~~0.063758~~	~~1.37~~	~~0.912~~	~~1.79~~	~~0.103699~~	~~1.15~~	~~0.14~~	~~734~~	~~29~~	~~636~~	~~7~~	~~13.30~~
47	infinite	0.00	0.134954	0.95	7.463	1.88	0.401087	1.62	0.86	2163	17	2174	30	-0.49
48	infinite	0.00	0.119957	0.98	5.836	5.92	0.352843	5.83	0.76	1956	17	1948	97	0.38
50	infinite	0.00	0.095951	0.95	3.642	3.85	0.275315	3.73	0.79	1547	18	1568	52	-1.35
51	4808	0.31	0.124276	5.20	6.256	6.38	0.365096	3.70	0.85	2019	89	2006	64	0.61
52	infinite	0.00	0.060307	1.04	0.822	2.44	0.098898	2.21	0.88	615	22	608	13	1.08
~~53~~	~~1758~~	~~0.98~~	~~0.094220~~	~~2.62~~	~~1.856~~	~~3.21~~	~~0.142838~~	~~1.86~~	~~0.89~~	~~1513~~	~~49~~	~~861~~	~~15~~	~~43.10~~
54	infinite	0.00	0.131527	0.96	7.026	5.88	0.387446	5.80	0.88	2118	17	2111	104	0.35
55	25078	0.06	0.175959	3.29	11.725	4.53	0.483269	3.11	0.87	2615	54	2541	65	2.82
56	8355	0.19	0.102835	2.03	3.839	2.59	0.270721	1.60	0.96	1676	37	1544	22	7.84
57	5631	0.26	0.129334	9.66	6.973	11.81	0.391037	6.80	0.54	2089	161	2128	122	-1.85
60	1219	1.42	0.069231	2.97	1.298	3.56	0.136014	1.96	0.87	906	60	822	15	9.23
61	infinite	0.00	0.074254	0.96	1.842	1.32	0.179888	0.91	0.40	1048	19	1066	9	-1.71
64	infinite	0.00	0.184576	0.97	13.095	2.58	0.514550	2.39	0.90	2694	16	2676	52	0.68
~~66~~	~~1179~~	~~1.47~~	~~0.082485~~	~~3.80~~	~~1.596~~	~~4.75~~	~~0.140291~~	~~2.86~~	~~0.82~~	~~1257~~	~~72~~	~~846~~	~~23~~	~~32.68~~
67	infinite	0.00	0.134960	0.97	7.943	1.69	0.426841	1.38	0.82	2163	17	2291	27	-5.91
68	infinite	0.00	0.060914	1.06	0.894	2.54	0.106430	2.30	0.68	636	23	652	14	-2.48
69	infinite	0.00	0.068383	1.07	1.239	1.71	0.131386	1.33	0.62	880	22	796	10	9.59
~~71~~	~~8694~~	~~0.20~~	~~0.088295~~	~~2.10~~	~~1.853~~	~~2.60~~	~~0.152202~~	~~1.53~~	~~0.92~~	~~1389~~	~~40~~	~~913~~	~~13~~	~~34.24~~
72	8613	0.17	0.125264	4.13	6.439	5.08	0.372787	2.97	0.86	2033	71	2042	52	-0.49
75	infinite	0.00	0.129706	0.95	7.077	1.75	0.395696	1.47	0.77	2094	17	2149	27	-2.64

Capítulo 6 – CONCLUSÕES

Nos capítulos anteriores foram apresentados e discutidos individualmente os dados isotópicos produzidos para os grupos Vazante, Canastra, Ibiá e Bambuí, além da Formação Jequitaí. Neste capítulo pretende-se apresentar um quadro geral dos dados e suas interpretações.

6.1 - IDADE DE DEPOSIÇÃO

6.1.1 – Grupo Canastra

Dentre as unidades estudadas, somente o Grupo Canastra não apresentou zircões neoproterozóicos. Distintos padrões de idades foram encontrados nas diferentes formações, no entanto houve certa constância nos valores das idades dos grãos mais jovens, que forneceram valores próximos a 1,03 Ga. Desta forma esta idade limite ente o Meso e o Neoproterozoico é interpretada como a idade máxima de deposição para o Grupo Canastra. Os novos dados Sm-Nd reiteram a semelhança entre os padrões de idades modelo apresentados pelos grupos Canastra e Paranoá, conforme salientado por Pimentel et al., 2001.

6.1.2 – Grupo Vazante

Embora a ampla maioria dos grãos de zircão do Grupo Vazante apresentem idades U-Pb Paleo- e Mesoproterozóicas, uma pequena, porém não desprezível, população neoproterozóica foi encontrada. Os zircões jovens foram identificados em amostras das formações basais Santo Antônio do Bonito e Rocinha. O grão mais jovem forneceu a idade concordante de 935±14 Ma, que é tida como a idade máxima para a deposição do grupo. O limite mínimo da deposição ainda permanece um tanto impreciso, sendo limitado somente pela idade do pico metamórfico da Faixa Brasília de ca. 630 Ma.

Embora morfologicamente similares, os cristais de zircão do tonalito (amostra UNAI-19) forneceram dois grupos de idades bastante distintos. Os dados do grupo mais jovem permitiram calcular a *concordia age* de 785 ± 17 Ma (Fig. 3.9) que é interpretada como a idade de cristalização do corpo; já o grupo mais velho é formado por cristais de ~2,1 Ga, interpretados como herança. É interessante ressaltar que as amostras de sedimentos do Grupo Vazante da região de Unaí apresentaram um padrão único de idade U-Pb (Fig. 3.2), em um

intervalo sempre próximo a 2,1 Ga, o que permite aventar que a fonte do magma que originou o tonalito pode ter sido a mesma fonte dos sedimentos do grupo.

6.1.3 –Grupo Ibiá

A idade máxima de deposição da Formação Rio Verde é dada pelo conjunto de idades do grupo de zircões mais jovens, que indicam a idade de 640 Ma. Uma vez que um contato gradual é descrito entre as formações do Grupo Ibiá (Pereira, 1992, Pereira *et al*., 1994), a idade máxima para a deposição da Formação Rio Verde é interpretada aqui também como a idade limite para a deposição do grupo, apesar do significativo contraste entre as idades dos grãos mais jovens das formações Cubatão (936 Ma) e Rio Verde (636 Ma).

6.1.4 – Grupo Bambuí

Os zircões mais jovens de um nível pelítico da segunda seqüência deposicional da Formação Sete Lagoas forneceram o limite máximo de deposição da unidade. As idades deste grupo de 5 grãos de zircão apresentaram dados concordantes em cerca de 610 Ma. Grãos com idades similares também foram identificados em amostras das demais formações estudadas. A sensível diferença entre a idade máxima de deposição indicada pelos zircões detríticos da seqüência deposicional de topo da Formação Sete Lagoas e a idade isocrônica Pb-Pb de boa qualidade encontrada em rochas carbonáticas da primeira seqüência (Babinski *et al*., 2007) reforçaram a sugestão, baseada em dados sísmicos (Zálan & Romeiro-Silva, 2007), de que ambas representem unidades distintas.

6.1.5 –Formação Jequitaí

Dentre as amostras estudadas, na proveniente da região de Jequitaí foi identificado o grupo mais jovem de zircões, que forneceram o limite máximo de deposição da unidade em 880 Ma.

6.2 – FONTES DOS SEDIMENTOS E IMPLICAÇÕES TECTÔNICAS

Embora as unidades tenham sido estudadas apenas em escala regional, os dados permitiram identificar significativas variações de fontes ao longo das diferentes bacias. De maneira geral foi observada pequena contribuição de terrenos arqueanos nos sedimentos estudados. O Cráton São Francisco, como era de se esperar, mostrou-se um importante

fornecedor de detritos, especialmente para os grupos Canastra e Vazante. Os dados dos grupos Ibiá e Bambuí evidenciaram a considerável presença de rochas da Faixa Brasília no suprimento de sedimentos. A Tabela 6.1 apresenta possíveis fontes para os zircões dos diferentes intervalos de idades identificados nos diversos grupos.

Intervalo Aproximado (Ma)	**Possíveis Terrenos Fonte**
600-800	• Arco Magmático de Goiás e rochas ígneas associadas à Faixa Brasília (Pimentel *et al.*, 1997, 1999, Ebert *et al.*, 1996, Rodrigues *et al.*, 1999, Campos Neto and Caby, 1999, Piuzana *et al.*, 2003a,b, Laux *et al.*, 2004, 2005, Oliveira *et al.*, 2004, entre outros)
900-1050	• Suíte Granítica Salto da Divisa (Silva *et al.*, 2008) • Diques máficos intrusivos no Supergrupo Espinhaço (Machado *et al.* 1989) • Rochas dos grupos Zadinian e Mayumbian, no oeste africano (Tack *et al.*, 2001) • Rochas graníticas associadas ao Cinturão Kibaran (Kokonyangi et al, 2004)
~1200	• Complexos Máfico-Ultramáficos de Goiás (Moraes *et al.*, 2006, Pimentel *et al.*, 2004, Correia *et al.*, 1999); • Domínio Nova Aurora – Faixa Brasília (Klein, 2008); • Cinturão Kibaran, no Cráton do Congo (Hanson *et al.*, 1988, Tack *et al.*, 1994, Ring *et al.*, 1999)
1800	• Granitos estaníferos de Goiás e vulcanismo associado ao Grupo Arai (Pimentel *et al* 1991b) • Magmatismo associado ao Rifte Espinhaço (Cordani *et al.*, 1992, Schobbenhaus *et al.*, 1994, Pimentel *et al.*,1994).
2100	• Cinturão Mineiro (Noce et al., 1998, 1999, 2007b, Ávila et al., 2005). • Complexos Mantiqueira and Juiz de Fora (Noce *et al.*, 2007a, Silva et al., 2002b, Heilbron et al., 2001), • Rochas intrusivas no Cinturão Salvador-Curaçá (Oliveira et al, 2002, Carvalho & Oliveira, 2003, D'el Rey et al., 2007, Rios et al., 2007).
2860-2712	• Complexo Belo Horizonte (Teixeira *et al.*, 1996)

Tabela 6.1 – Lista de algumas possíveis fontes para os sedimentos estudados.

6.2.1 – Grupos Canastra

As formações do Grupo Canastra apresentaram largo espectro de idades com padrões bastante distintos entre si. Terrenos rhyacianos (~2.1 Ga) foram os principais fornecedores dos detritos das formações Serra do Landin e Chapada dos Pilões, em ambos os casos seguidos por fontes secundárias de ~1.8 Ga. Já a Formação Paracatu revelou importantes contribuições de terrenos de idade ectasiana (~1,2 Ga). Da mesma forma que os dados U-Pb, as análises Sm-Nd sugerem que os sedimentos do Grupo Canastra sofreram pouca influência

de fontes juvenis Neoproterozóicas, já que a maioria de suas amostras apresenta valores de T_{DM} superiores a 1.9 Ga. Esta associação de dados reforça a hipótese de que o Grupo Canastra tenha sido depositado em um ambiente de margem continental passiva ao longo da margem oeste do continente São Francisco-Congo (Pimentel *et al.*, 2001).

6.2.2 – Grupo Vazante

As formações do Grupo Vazante forneceram padrões variados de idade U-Pb de zircões detríticos, por vezes com largo intervalo de idade e em outros casos com padrões bastante simples. De maneira geral terrenos de ~2,1 Ga constituem a principal fonte de sedimentos de boa parte das formações. Da base para o topo a primeira grande mudança observada no espectro de idades dos zircões detríticos é a ausência de grãos neoproterozóicos na formação Lagamar e demais formações que se sobrepõem. Ao que parece, ou de alguma forma esta fonte neoproterozóica, identificada nas formações Santo Antônio do Bonito e Rocinha, foi isolada da bacia e não voltou a contribuir com material detrítico, ou existem descontinuidades tectônicas internas ainda não identificadas. No entanto dados Sm-Nd, que são influenciados também pelos componentes pelíticos, revelam a participação de terrenos jovens em diferentes intensidades praticamente em todo o grupo. Tanto os dados U-Pb como os Sm-Nd da Formação Serra do Garrote revelaram a predominância de material paleoproterozóico em suas fontes; nesta formação são encontradas as idades modelo Sm-Nd mais velhas do grupo, superiores a 2,2 Ga.

A segunda alteração significativa no padrão das fontes ocorre no topo da bacia, onde nas formações Morro do Calcário e Lapa, os terrenos rhyacianos passam a contribuir minimamente com sedimentos e fontes mesoproterozóicas de ~1,2 Ga passam a ser praticamente as únicas fornecedoras de detritos. Apesar dos zircões das formações Morro do Calcário e Lapa apresentarem padrões de idades U-Pb praticamente idênticos, suas idades modelo Sm-Nd são distintas e indicam que ou a Formação Lapa recebeu considerável componente pelítico juvenil Neoproterozóico em seus depósitos ou deixou de receber contribuições paleoproterozóicas e/ou arqueanas. Estas marcantes mudanças de padrão refletem expressivas alterações na paleogeografia e/ou paleocorrentes atuantes na bacia, o que pode representar a aproximação de terrenos, especialmente mesoproterozóicos fornecedores de zircão e talvez neoproterozóicos que influenciariam as composições de Sm-Nd.

Embora não tenha sido possível restringir significativamente o período de deposição dos grupos Canastra e Vazante, de forma abrangente o Grupo Vazante apresenta resultados U-

Pb e Sm-Nd mais jovens que o Grupo Canastra, o que pode sugerir também que pelo menos parte de suas rochas podem ser mais jovens que as do Grupo Canastra.

A ocorrência de zircões de ~1.2 Ga nos grupo Canastra e Vazante chama a atenção, já que a origem destes zircões não é óbvia. Sabe-se que há pouco registro de magmas ectasianos no Cráton São Francisco-Congo (atualmente praticamente restritos ao *Kibaran Belt* – Hanson *et al*., 1988, Tack et *al*., 1994, Ring et *al*., 1999), embora outras ocorrências possam estar sob as imensas áreas cratônicas que estão atualmente recobertas por sedimentos neoproterozóicos e fanerozóicos. Na Faixa Brasília são reconhecidos terrenos com idades similares, entre eles o terreno alóctone que encerra os Complexos Máfico-Ultamáfico Acamadados (Moraes *et al*., 2006, Pimentel *et al*., 2004, Correia *et al*., 1999). A cerca de 60 Km a oeste do Grupo Canastra, recentemente foi identificado um terreno mesoproterozóico de ~1,2 Ga, de extensão ainda incerta (Klein, 2008). Este terreno denominado Domínio Nova Aurora é constituído de rochas granitóides com composição geoquímica similar a rochas de arco de ilha e interpretado por Klein (2008) também como um terreno alóctone.

6.2.3 – Grupo Ibiá

As duas amostras analisadas para U-Pb do Grupo Ibiá forneceram padrões completamente diferentes de idades U-Pb. A Formação Cubatão não apresenta zircões mais jovens que 930 Ma, ao passo que a maioria dos zircões da amostra da Formação Rio Verde são mais jovens que 900 Ma. Os dados Sm-Nd revelam que apesar de não possuir zircões jovens, a matriz do diamictito da Formação Cubatão já apresenta componentes juvenis, com valores similares aos encontrados nos sedimentos da Formação Rio Verde. Os dados sugerem que durante a sedimentação da Formação Cubatão ocorreu o aporte de material oriundo do Cráton São Francisco, porém com alguma contribuição distal de terrenos da própria Faixa Brasília. Já durante a sedimentação dos depósitos da Formação Rio Verde, o provimento de detritos parece ter sido principalmente a partir da Faixa Brasília. A associação dos dados permite interpretar que as rochas do Grupo Ibiá representem um depósito do tipo *fore-arc*. É interessante notar a grande diferença entre os padrões de idades U-Pb e Sm-Nd do Grupo Ibiá e de suas unidades vizinhas Canastra e Vazante. As importantes fontes de ~2,1 e 1, 2 Ga dos grupos vizinhos só são identificadas como fontes secundárias na Formação Cubatão e se quer foram encontradas na amostra da Formação Rio Verde. Por outro lado tanto os dados U-Pb como Sm-Nd da Formação Rio Verde são muito parecidos (Fig. 4.13) com os encontrados em amostra do Grupo Araxá (Piuzana *et al*., 2003a), o que permite afirmar que ambas as unidades tanto possuem fontes similares, como elas contribuiram em proporções semelhantes.

6.2.4 – Formação Jequitaí

As amostras da Formação Jequitaí mostraram a predominância de fontes paleoproterozoicas, e secundariamente contribuições arqueanas e mesoproterozóicas. A fonte neoproterozóica (Toniano) somente foi identificada na amostra da região de Jequitaí. Este conjunto de dados sugere fontes provavelmente localizadas no Cráton São Francisco-Congo (Tabela 6.1).

6.2.5 – Grupo Bambuí

Os espectros de idades U-Pb das amostras do Grupo Bambuí mostraram-se bastante variados entre as formações e ao longo da bacia. Entretanto de forma geral é possível observar a forte influência de terrenos neoproterozóicos no fornecimento de sedimentos (Fig. 5.4). A única exceção foi identificada na amostra do conglomerado Carrancas, que apresentou idades U-Pb de zircão e monazita idênticas às encontradas em rochas do Complexo Belo Horizonte (Teixeira *et al.*, 1996), localizado imediatamente a sul do ponto de amostragem. Este resultado indica que o conglomerado provavelmente é um depósito associado a uma pequena bacia com aporte local de detritos.

A origem mais provável dos zircões neoproterozóicos encontrados em todo o Grupo Bambuí é a Faixa Brasília, localizada a oeste e a sul da bacia. As amostras estudadas oriundas da região da Serra de São Domingos (MG) apresentaram, além de fontes neoproterozóicas, um volume considerável de detritos gerados a partir de fontes meso-paleoproterozóicas e arqueanas (Fig. 5.4), o que revela a importância de sedimentos provenientes do Cráton São Francisco-Congo nesta região da bacia.

Por outro lado, as amostras das formações Sete Lagoas (7L-1) e Três Marias coletadas na porção meridional do grupo revelaram o aporte praticamente único de material neoproterozóico, embora tenham sido depositadas em ambientes sedimentares distintos. Enquanto o nível pelítico da Formação Sete Lagoas é interpretado como um depósito de ambiente marinho profundo e anóxico (Vieira *et al.*, 2007), a Formação Três Marias é considerada um depósito aluvial a marinho raso (Chiavegatto, 1992).

A ausência de grãos meso e paleoproterozóicos na amostra 7L-1 pode representar um período em que o nível do mar recobriu a porção sul da área cratônica, impedindo o aporte de material.

Exceto a Formação Sete Lagoas, que revelou um comportamento bimodal, as idades modelo Sm-Nd das rochas do Grupo Bambuí mostram crescente contribuição de terrenos

juvenis, culminando em valores de T_{DM} de 1,53 a 1,87 Ga para amostras das formações Serra da Saudade e Três Marias.

Tantos os dados U-Pb como Sm-Nd indicam que desde sua fase inicial de deposição, o Grupo Bambuí recebeu o aporte de sedimentos neoproterozóicos (Faixa Brasília) em sua bacia. Considerando a idade máxima de deposição sugerida para o grupo (~610 Ma), é possível afirmar que a deformação impressa no grupo não é cronocorrelata ao pico metamórfico da Faixa Brasília, identificado por volta de 630 Ma.

6.3 – CONSIDERAÇÕES FINAIS

Um modelo evolutivo interpretativo e simplificado para o segmento centro-sul da Faixa Brasília é mostrado na Figura 6.1. Apesar do Grupo Paranoá não ter sido estudado neste trabalho, as semelhanças litológicas e isotópicas (idades modelo Sm-Nd) permitem supor que sua evolução tenha sido contemporânea à do Grupo Canastra e que ambos representem os primeiros depósitos da margem passiva do continente São Francisco-Congo, possivelmente formados no início do Neoproterozóico. A identificação dos componentes distais desta bacia ainda é incerta e talvez estejam representados por parte do que hoje é chamado de Grupo Araxá. Os dados Sm-Nd do Grupo Vazante revelam alguma contribuição mais jovem, quando comparados aos dados dos grupos Canastra e Paranoá, o que pode sugerir a contribuição de algum terreno distal juvenil, possivelmente Neoproterozóico. O período de deposição do Grupo Vazante ainda permanece impreciso, mas especulativamente no modelo apresentado ele é posicionado por volta de 0,74 Ga, contemporâneo aos depósitos carbonáticos que têm sido interpretados como a base do Grupo Bambuí. Os dados desta tese em conjunto com outros previamente publicados conduzem à individualização destas rochas carbonáticas, que são aqui denominadas informalmente de Seqüência Sambra. Em um estágio posterior, por volta de 640 Ma, são depositados sedimentos hoje classificados como os grupos Araxá e Ibiá. A partir deste momento fica clara a participação de terrenos da própria Faixa Brasília no fornecimento de material detrítico, evidenciada pela presença de zircões mais jovens que 660 Ma e idades modelo bastante jovens, de 1,1-1,3 Ga. Por volta de 630 Ma a Faixa Brasíla passava pelo seu pico metamórfico (Pimentel et al., 1999) e neste período boa parte de seus sedimentos foi envolvido por processos deformacionais e metamórficos, chegando localmente a atingir fácies granulito (Anápolis-Itauçu). Sobre a área cratônica e parte da Faixa Brasília,

em cerca de 600 Ma estavam sendo depositados os sedimentos incluídos no Grupo Bambuí, culminando com os depósitos molássicos da Formação Três Marias.

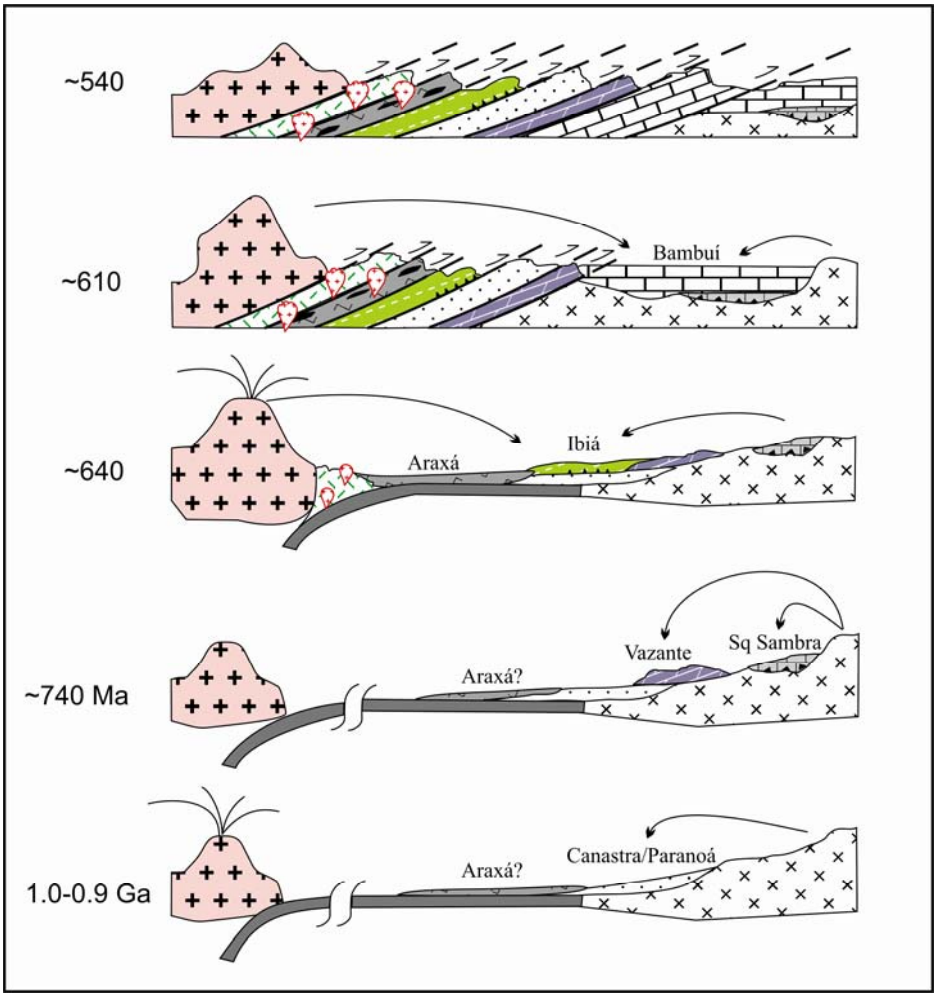

Figura 6.1 – Modelo evolutivo simplificado para o segmento centro-sul da Faixa Brasília.

Referências Bibliográficas

Almeida, F.F.M. 1969. Diferenciação tectônica da Plataforma Brasileira. *In:* Congresso Brasileiro de Geologia, 13, Anais... Salvador, pp.29-46.

Alvarenga, C.J.S. 1978. Geologia e Prospecção geoquímica dos grupos Bambuí e Paranoá na Serra de São Domingos – MG. Dissertação de Mestrado, IG-UnB

Araújo Filho, J.O. 2000. The Pirineus Syntaxis: An example of the Intersection of two Brasiliano Fold-Thrust Belts in Central Brazil and its Implications for the Tectonic Evolution of Western Gondwana. *Revista Brasileira de Geociências*, 30(1):144-148.

Ávila, C.A., Valença, J.G., Teixeira, W., Barrueto, H., R., Cordani, U.G., Moura, C.A.V., Pereira, R.M., Martins, V.T. 2005. Geocronologia U-Pb e Pb-Pb da Suíte Serrinha: Implicações para a evolução Paleoproterozóica da margem sul do Cráton São Francisco. In: III Simpósio de Vulcanismo e Ambients Associados, Cabo Frio, Rio de Janeiro.

Azmy, K., Kendall, B., Creaser, R.A., Heaman, L., Oliveira, T.F., 2008. Global correlation of the Vazante Group, São Francisco Basin, Brazil: Re-Os and U-Pb radiometric age constraints, *Precambrian Research*, 164(3-4):160-172.

Azmy, K.; Kaufman, A.J.; Misi, A.; Oliveira, T.F. - 2006 - Isotope stratigraphy of the Lapa Fomation, São Francisco Basin, Brazil: Implications for Late Neoproterozoic glacial events in South America. *Precambrian Research*, (3-4):231-248.

Azmy, K., Kaufman, A.J.; Misi, A.; Kimura, H.; Oliveira, T.F. 2005. Chemostratigraphy of Neoproterozoic sequences of the Vazante Group, São Francisco Basin, Brazil: New data and a review. *In:* III Simp. São Francisco Craton – Short Papers, pp. 269-273. Salvador, BA, Brazil.

Azmy, K., Veizer, J., Misi, A., Oliveira, T.F., Sanches, A.L., Dardenne, M.A., 2001. Dolomitization and isotope stratigraphy of the Vazante Formation, São Francisco Basin, Brazil. *Precambrian Research* 112, 303–329.

Babinski, M., Vieira, L.C., Trindade, R.I.F. 2007. Direct dating of the Sete Lagoas cap carbonate (Bambuí Group, Brazil) and implications for the Neoprotezoic glacial events. *Terra Nova*, v. 19, p. 401-406.

Babinski, M.; Monteiro, L.V.S.; Fetter, A.H.; Bettencourt, J.S.; Oliveira, T.F. 2005. Isotope geochemistry of the mafic dikes from the Vazante nonsulfide zinc deposit, Brazil. *Journal of South American Earth Sciences*, 18(2005):293-304.

Babinski, M. & Kaufman, A.J. 2003. Fist direct dating of a Neoproterozoic pos-glacial cap carbonate. *In:* South American Symposium on Isotope Geology, 4, Salvador, Brazil. Short Papers, vol. I, pp. 321-323.

Babinski, M.; Van Schmus, W.R.; Chemale, J.R.F. 1999. Pb-Pb dating and Pb isotope geochemistry of Neoproterozoic carbonate rocks from the São Francisco basin, Brazil: implications for the mobility of Pb isotopes during tectonism and metamorphism. *Chemical Geology*, 160:175-199.

Babinski, M.; Schmus, W. R. V.; Chemale Jr, F.; Kawashita, K. 1993. Evolução geológica da porção sul da Bacia do São Francisco baseada na geoquímica isotópica de Pb em rochas carbonáticas. *In:* Simpósio sobre o Cráton do São Francisco, 2, Salvador, BA. Anais. p. 182-185.

Barbosa, O. 1955. Guia das Excursões do IX Congresso Brasileiro de Geologia, Notic. Soc. Bras. Geol., São Paulo, (3):3-5.

Barbosa, O. 1963. Geologia Econômica e Aplicada a uma Parte do Planalto Central Brasileiro. DNPM/PROSPEC, Goiânia, 70 p.

Barbosa, O.; Braun, O.P.G.; Dyer, R.C.; Cunha, C.A.B.R. 1970. Geologia da região do Triângulo Mineiro. DNPM/DFPM. 140p. (Boletim 136).

Bizzi, L. A.; Schobbenhaus, C. Gonçalves, J.H.; Baars, F.J.; Delgado, I.M.; Abram, M.B.; Leão Neto, R.; Matos, G.M.M.; Santos, J.O.S. 2001. Geologia, Tectônica e Recursos Minerais do Brasil: Sistema de Informações Geográficas – SIG e Mapas na Escala 1:2.500.000. Brasília: CPRM, 2001.

Bonhomme, M.G.; Cordani, U.G.; Kawashita, K., Macedo, M.H.F.; Thomaz Filho, A. 1982. Radiochronological age and correlation of Proterozoic sediments in Brazil. *Precambrian Research*, 18, 103-118.

Braun O.P.G. 1970. Geologia da Folha de Ipameri. *In:* Resumo do 24° Congresso Brasileiro de Geologia, Brasília.

Braun, O.P.G. & Batista, M.B. 1976. Considerações sobre a geologia Pré-Cambriana da região Sudoeste e parte da região Centro-Oeste. *In:* 29º Congresso Brasileiro de Geologia. Resumo dos Trabalhos, Ouro Preto, pp 27-28.

Braun, O.P.G. 1968. Contribuição à estratigrafia do Grupo Bambuí. *In:* Anais do XXII Congresso Brasileiro de Geologia, pp. 155-166, Belo Horizonte.

Brody, K.B.; Kaufman, A.J.; Eigenbrode, J.L.; Cody, G.D. 2004 Biomarker Geochemistry of a Post-glacial Neoproterozoic succession in Brazil. *In:* Geological Society of America - Annual Meeting, Denve, CO, November, 2004. Abstract.

Bühn, B., Pimentel, M.M., Matteini, M., Dantas, E.L. (*in press*) High spatial resolution analysis of Pb and U isotopes for geochronology by lases ablation multi-collector inductively coupled plasma mass spectrometry (LA-MC-IC-MS). Anais da Academia Brasileira de Ciências...

Campos Neto, M.C. 1984. Litoestratigrafia e evolução paleogeográfica dos Grupos Canastra e Paranoá (região Vazante-Lagamar, MG). *Revista Brasileira de Geociências* 14 (2): 81-91.

Campos Neto, M.C., Caby, R., 1999. Neoproterozoic high-pressure metamorphism and tectonic constraint from the nappe system south f the São Francisco Craton, southeast Brazil. *Precambrian Research* 97, 3–26.

Carvalho, M.J. & Oliveira, E.P. 2003. Geologia do tonalito Itareru, Bloco Serrinha, Bahia: Uma intrusão sin-tectônica do início da colisão continental no segmento norte do Orógeno Itabuna-Salvador-Curaça. *Revista Brasileira de Geociências*, 33(1-Suplemento):55-68.

Castro, P.T.A. & Dardenne, M.A. 1996 O conglomerado Samburá (Grupo Bambuí, Neoproterozóico) e rochas sedimentares associadas no flanco leste da Serra da Pimente, SW de Minas Gerais: Um sistema de Fan-Delta. Geonomos, 3(2):35-41.

Chang, H.K. 1997. Isótopos Estáveis (C,H,O) e $^{87}Sr/^{86}Sr$ – Implicações na Estratigrafia e na Paleocirculação de Fluidos na Bacia do São Francisco. Tese de Livre Docência, USP, 129p.

Chang, H.K., Kawashita, K., Alkimin, F.F., Moreira, M.Z. 1993. Considerações sobre a estratigrafia isotópica do Grupo Bambuí. In Anais do II Simpósio do Cráton São Francisco, 195-196

Chiavegatto, J.R.S. 1992. Análise estratigráfica das seqüências tempestíticas da Formação Três Marias (Proterozóico Superior), na porção meridional da Bacia do São Francisco. Dissertação de Mestrado. Departamento de Geologia da Escola de Minas, Universidade Federal de Ouro Preto. 216 p.

Cloud, P.E., Dardenne, M.A., 1973. Proterozoic age of the Bambuí Group in Brazil. *Geological Society of America Bulletin* 84, 1673–1676.

Coelho, J.C.C., Martins-Neto, M.A., Pedrosa-Soares, A.C., Nelson, D. Marinho, M.S. (unpublished). Integração dos dados de superfície, sub-superfície, litogeoquímica Sm-Nd e datações U-Pb SHRIMP na borda oeste da Bacia do São Francisco, Minas Gerais. Boletim de Geociências da Petrobrás.

Cordani, U.G., Iyer, S.S., Taylor, P.N., Kawashita, K., Sato, K., McReath, I. 1992. Pb-Pb, Rb-Sr and K-Ar systematics of the Lagoa Real uranium province (south-central Bahia, Brazil) and the Espinhaço Cycle (ca. 1.5-1.0 Ga). Journal of South American Earth-Science, 5(1):33-46.

Correia, C.T., Jost, H., Tassinari, C.C.G., Girardi, V.A.V., Kinni, P.D., 1999. Ectasian Mesoproterozoic U–Pb ages (SHRIMP II) for the metavolcanosedimentary sequence of Juscelaˆndia and Indaianópolis and for high grade metamorphosed rocks of Barro Alto stratiform igneous Complex, Goiás State, central Brazil. *In*: Second South American Symposium on Isotope Geology. Abstract, Cordoba, pp. 31–33.

Costa, L.A.M.; Angeiras, A.G.; Valença, J.G.; Stevenazzi, V. 1970. Novos conceitos sobre o Grupo Bambuí e sua divisão em tectonogrupos. Bol. Geol. do Inst. Geoc., 5:3-34. UFRJ, Rio de Janeiro.

Costa, M.T. & Branco, J.J.R. 1961. Roteiro de Excursão Belo Horizonte-Brasília. In: XIV Congresso Brasileiro de Geologia, V. 15: 9-25. Belo Horizonte.

Cruz, E. L. C. C. ; Kuyumjian, R. M. ; Hagemann, S. ; Mcnaughton, N. 2000. Paleoproterozoic U-Pb SHRIMP ages of low- and high-Al low-K granitoids in the Brasília Fold Belt basement. *In:* 31 International Geological Congress, Rio de Janeiro, 2000. CR-ROM - 31 International Geological Congress, Rio de Janeiro.

Cuckov, N. 1999. A glaciação neoproterozóica na porção sul do Cráton do São Francisco e suas litofácies nas regiões de Jequitaí-MG e Cristalina-GO. Dissertação de Mestrado. Universidade de Brasília, 256 p.

D'agrella-Filho, M.S.; Babinski, M.; Trindade, R.I.F.; Van Schmus, W.R.; Ernesto, M. 2000. Simultaneous remagnetization and U-Pb isotope resetting in Neoproterozoic carbonates of the São Francisco Craton, Brazil. Precambrian Research, 99(2000):179-196.

D'el Rey Silva, L.J.H., Dantas, E.L., Teixeira, J.B.G.; Laux, J.H., Silva, M.G. 2007. U-Pb and Sm-Nd geochronology of amphibolites from the Curaçá Belt, São Francisco Craton, Brazil: Tectonic implications. *Gondwana Research., 12(4):454-467.*

Dardenne, M.A., Pimentel, M.M., Alvarenga, C.J.S. 2003. Provenance of conglomerates of the Bambuí, Jequitaí, Vazante and Ibiá Groups: Implications for the evolution of The Brasília Belt *In:* Boletim de Resumos, IX Simpósio Nacional de Estudos Tectônicos, pp. 47-49.

Dardenne, M.A. 2000. The Brasília Fold Belt. *In:* Cordani, U.G.; Milani, E.J.; Tomas Filho, A. and CAMPOS, D.A., Editors, 2000. Tectonic Evolution of South America. *Proceedings of the XXXI International Geological Congress (Rio de Janeiro), pp.231-263*

Dardenne, M.A.; Freitas-Silva, F.H., Souza, J.C.F., Campos, J.E.G. 1998. Evolução tectono-sedimentar do Grupo Vazante no contexto da Faixa de Dobramentos Brasília. *Congresso Brasileiro Geologia 40*, Belo Horizonte. Resumos, SBG, 26.

Dardenne, M.A.; Freitas-Silva, F.H., Nogueira, G.S.M.; Souza, J.C.F. 1997. Depósitos de fosfato de Rochinha e Lagamar, Minas Gerais. *In*: Schobbenhaus, C.; Queiroz, E.T.; Coelho, C.E.S. (cords); Principais Depósitos Minerais do Brasil, DNPM/CPRM, pp. 113-122.

Dardenne, M.A. 1981. Os grupos Paranoá e Bambuí na Faixa Dobrada Brasília. *In:* SIMPÓSIO SOBRE O CRÁTON SÃO FRANCISCO E SUAS FAIXAS MARGINAIS, 1, Salvador, 1981. *Anais...*Salvador, SBG/SME, p. 140-157.

Dardenne, M.A., 1979. Les minéralisations de Plomb, Zinc, Flúor du Protérozoıque Supérieur dans le Brésil Central. *Thesis*, University of Paris VI, 251 p.

Dardenne, M.A. 1978. Geologia do Grupo Bambuí no vale do Rio Paraná (Goiás). *In:* XXX Congresso Brasileiro de Geologia (Recife). Anais... Vol. 2, pp. 611-621.

De Paolo, D.J., 1981. A neodymium and strontium isotopic study of the Mesozoic calc-alkaline granitic batholiths of the Sierra Nevada and Peninsular Ranges, California. Journal of Geophysical Research 86, 10470–10488.

Ebert, H.D., Chemale, F. Jr., Babinski, M., Artur, A.C., Van Schmus, W.R., 1996. Tectonic setting and U–Pb zircon dating of the plutonic Socorro- Guaxupé complex in the Transpressive Rio Paraíba do Sul shear belt, SE Brazil. *Tectonics* 15, 688–699.

Freitas-Silva, F.H. & Dardenne, M.A. 1994. Proposta de subdivisão estratigráfica formal para o grupo Canastra no oeste de Minas Gerais e leste de Goiás. *In:* Simp. Geol. Centro Oeste, 4, Brasília, 1991. Anais... Brasília, SBG-DF/CO, p. 164-165.

Freitas-Silva, F.H. 1991. Enquadramento litoestratigáfico e estrutural do depósito de ouro do Morro do Ouro, Paracatu (MG). *Dissertação de Mestrado*, IG-UnB. Brasília. 151p.

Fuck, R.A., Pimentel, M.M.; Del'rey-Silva, L.J.H. 1994. Compartimentação Tectônica da Porção Oriental da Província Tocantins. *In:* Cong. Brás. Geol., 38. Boletim de Resumos Expandidos, V.1, p.215-216.

Gioia, S.M.C.L., Hollanda, M.H.B.M., Pimentel, M.M. 1999. Uso de resinas RE-Spec e Sr-Spe em Geoquímica Isotópica. *In:* VII Congresso Brasileiro de Geoquímica. Porto Seguro, Bahia, Brazil.

Gioia, S.M.C.L., Pimentel, M.M., 2000. The Sm-Nd isotopic method in the Geochronology Laboratory of the University of Brasília. *Anais da. Academia Brasília de Ciências*, 72(2):219-245.

Gonzaga, G. 2001 – Glaciação Samburá (Neoproterozóico-Vendiano?) como possível agente transportador de diamantes no estado de Minas Gerais. *Revista Brasileira de Geociências*, 31(4):597-604.

Guimarães, E.M. 1997. Estudos de proveniência e diagênese com ênfase na caracterização dos filossilicatos dos grupos Paranoá e Bambuí, na região de Bezerras-Cabeceiras (GO). Tese de Doutorado. IG-UnB, 270p.

Halverson, G.P.; Dudás, F.Ö, Maloof, A.C., Bowring, S.A. 2007. Evolution of the $^{87}Sr/^{86}Sr$ composition of Neoproterozoic seawater. *Palaeogeography, Palaeoclimatology, Palaeoecology* 256 (2007) 103–129.

Halverson, G.P.; Hoffman, P.F., Schrag, D.P.; Maloof, A.C.; Rice, A.H.N. 2005 Toward a Neoproterozoic composite carbon-isotope record. *Geological Society of America Bulletin*, 117 (2005) 1181–1207.

Hanson, R.E.; Wilson, T.J.; Brueckner, H.K.; Onstott, T.C.; Wardlaw, M.S.; Johnd, C.C.; Hardcastle, K.C. 1988. Reconnaissance geochronology, tectonothermal evolution, and regional significance of the Middle Proterozoic Choma-Kalomo Block, Southern Zambia. *Precambrian Research*, 42(1-2):39-61.

Heilbron, M., Machado, N., Duarte, B.P. 2001. Evolution of the Paleoproterozoic Transamazonian Orogen in Southeastern Brazil: a view from the Neoproterozoic Ribeira Belt. *In:* Abstracts, GAC-MAC. Joint Annual Meeting. St Jonhs, Canada, Vol. 26, p. 61.

Heineck, C.A., Vieira, V.S., Drumond J.B.V., Leite, C.A.L., Lacerda Filho, J.V., Valente, C.R., Lopes, R.C., Malouf, R.F., Oliveira, I.W.B., Oliveira, C.C., Sachs, L.L.B., Paes, V.J.C., Junqueira, P.A., Netto, C. 2004. Folha SE.23 – Belo Horizonte. *In:* Schobbenhaus, C., Gonçalves, J.H., Santos, J.O.S., Abram, M.B., Leão Neto, R., Matos, G.M.M., Vidotti, R.M., Ramos, M.A.B., Jesus, J.D.A. (eds). Carta Geológica do Brasil ao Milionésimo, Sistema de Informações Geográficas. Programa Geologia do Brasil. CPRM.. Brasília, CD-ROM.

Hoffmann, K.H.; Condon, D.J.; Bowring, S.A.; Crowley, J.L. 2004. U–Pb zircon date from the Neoproterozoic Ghaub Formation, Namibia: constraints on Marinoan glaciation, *Geology*, 32 (2004) 817–820.

Hoffman, P.F., Schrag, D.P., 2002. The Snowball Earth hypothesis: testing the limits of global change. *Terra Nova* 14, 129–155.

Hoffman, P.F., Kaufman, A. J., Halverson, G.P. 1998. A Neoproterozoic Snowball Earth. *Science* 281, 1342-1346.

Hyde, W.T., Crowley, T.J., Baum, S.K., Peltier, R.W., 2000. Neoproterozoic 'Snowball Earth' simulations with a coupled climate/ice-sheet model. *Nature* 405, 425–429.

Iyer, S.S.; Babinski, M.; Krouse, H.R.; Chemale, F. 1995. Highly 13C enriched carbonate and organic matter in the Neoproterozoic sediments of the Bambuí Group, Brazil. *Precambrian Research*, 73, 271-282.

Karfunkl, J.; Hoppe, A. 1988. Late Proterozoic glaciation in central-eastern Brazil: Syntesis and model. *Palaeogeography, Palaeoclimatology, Palaeoecology, 65:1-21.*

Kawashita, K. ; Mizusaki, A M ; Kiang, C H. 1987. Razões $^{87}Sr/^{86}Sr$ em sedimentos carbonáticos do Grupo Bambuí (MG). *In*: I Brasilian Congress of Geochemistry, V. 1. p. 133-137.

Kennedy, M.J., Runnegar, B., Prave, A.R., Hoffmann, K-H, Arthur, M.A. 1998. Two or four Neoproterozoic glaciations? *Geology* 26:1059-1063.

Klein, P.B.W. 2008. Geoquímica de Rocha Total, Geocronologia de U-Pb e Geologia Isotópica de Sm-Nd das Rochas Ortognáissicas e Unidades Litológicas Associadas da Região Ipameri – Catalão (Goiás). Unpublished *PhD Thesis*, University of Brasília, Brazil, 154p.

Kokonyangi, J., Armstrong, R., Kampunzu, A.B.; Yoshida, M., Okidaira, T. 2004. U–Pb zircon geochronology and petrology of granitoids from Mitwaba (Katanga, Congo): implications for the evolution of the Mesoproterozoic Kibaran belt. *Precambrian Research* 132, 79-106.

Laranjeira, N.P., 1992. A plataforma mista de siliciclásticos e carbonatos do Grupo Paranoá na região de Unaí, Minas Gerais. *MSc Thesis*, University of Brasília, 167p.

Laux, J.H., Pimentel, M.M., Dantas, E.L., Armstrong, R., Armele, A., Nilson, A.A. 2004. Mafic magmatism associated with the Goiás magmatic arc in the Anincuns region, Goiás, central Brazil: Sm-Nd isotopoes and new ID-TIMS and SHRIMP U-Pb data. *Journal of South American Earth Sciences*, 16(7): 599-614

Laux, J.H., Pimentel, M.M., Dantas, E.L., Armstrong, R., Junges, S.L. 2005. Two Neoproterozoic crustal accretion events in the Brasília belt, central Brazil. *Journal of South American Earth Sciences*, 18(2):183-198.

Lima, O.N.B & Uhlein, A. 2005 – Estratigrafia e sistemas deposicionais do Grupo Bambuí no Alto Rio São Francisco. *In:* III Simp. São Francisco Craton, Short Papers, pp. 279-282. Salvador, Brazil.

Lima, S.A.A.; Martins Neto, M.A.; Pedrosa Soares, A.C.; Cordani, U.G.; Nutman, A. 2002. A Formação Salinas na área-tipo, NE de Minas Gerais: uma proposta de revisão da estratigrafia da Faixa Araçuaí com base em evidências sedimentares, metamórficas e idades U-Pb SHRIMP. *Revista Brasileira de Geociências*, 32(4), 491-500.

Ludwing, K.R., 2003. Isoplot 3.00 – A Geochronological Tollkit for Microsoft Excel. *Berkeley Geochronology Center, Special Publication Nº 4.*

Ludwig, K.R. 2000. SQUID 1.00, A User's Manual; Berkeley Geochronology Center, Special Publication, No 2, 2455 Ridge Road, Berkeley, CA. 18p.

Machado, N., Schrank, A., Abreu, F.R. Knauer, L.G., Almeirda-Abreu, P.A. 1989. Resultados preliminares da geocronologia U-Pb na Serra do Espinhaço Meridional. In: SBG, Simpósio de Geologia de Minas Gerais, 5, Belo Horizonte, Anais, 171-174.

Madalosso, A. 1980. Considerações sobre a paleogeografia do Grupo Bambuí na região de Paracatu – Morro Agudo (MG). *In:* 31º Congresso Brasileiro de Geologia, Anais... (2):772-785.

Madalosso, A. & Valle, C.R.O. 1978. Considerações sobre a estratigrafia e sedimentologia do Grupo Bambuí na região de Paracatu-Morro Agudo (MG). *In:* Congresso Brasileiro de Geologia 30, pp.622-631.

Marini, J.O.; Fuck, R.A.; Danni, J.C.M.; Dardenne, M.A.; Loguércio, S.O.C.; Ramalho, R. 1984a. As Faixas de Dobramentos Brasília, Uruaçu e Paraguai-Araguaia e o Maciço Mediano de Goiás. *In*: Schobbenhaus, C.; Diogenes, A.C.; Derge, G.R; Asmos, M.E. (coord.) Geologia do Brasil; Texto Explicativo do Mapa Geológico do Brasil e Área Oceânica Adjacente, Incluindo Depósitos Minerais, Escala 1:2.500.000. DNPM. 501p.

Marini, J.O.. Fuck, R.A.; Dardenne, M.A.; Danni, J.C.M. 1984b. Província Tocantins. Setores Central e Sudeste. *In:* Almeida, F.F.M. & Hasui, Y., Editores, 1984. O Pré-Cambriano do Brasil, Edgard Blücher, São Paulo, pp.205-264.

Martins, M. – 1999 – Análise estratigráfica das seqüências Mesoproterozóicas (borda oeste) e Neoproterozóicas da Bacia do São Francisco. Unpublished Master Dissertation, Universidade Federal do Rio Grande do Sul, Porto Alegre, pp. 247.

Martins-Neto, M.A.; Alkmim, F.F. 2001. Estratigrafia e evolução tectônica das bacias neoproterozóicas do paleocontinente São Francisco e suas margens: Registro da quebra de Rodínia e colagem de Gondwana. *In:* Pinto, C.P., Martins-Neto, M.A. (ed.) Bacia do São Francisco: Geologia e Recursos Naturais, SBG/Núcleo MG, 31-54.

Misi, A., Kaufman, A.J., Veizer, J., Powis, K., Azmy, K., Boggiani, P.C., Gaucher, C., Teixeira, J.B.G., Sanches, A.L., Iyer, S.S.S. 2007. Chemostratigraphic correlation of Neoproterozoic successions in South América. *Chemical Geology* 237 (2007) 143–167

Misi, A.; Sanches, A.L., Kaufman, A.J., Veizer, J., Azmy, K., Powis, K., Teixeira, J.B.G. 2005. Phosphorites and the chemostratigraphic correlation of the Neoproterozoic sequences of the São Francisco Craton and the Brasília Fold Belt. *In:* III Simp. São Francisco Craton, Short Papers, 291-294. Salvador, BA, Brazil.

Moraes, R., Fuck, R.A., Pimentel, M.M., Gioia, S.M.C.L., Hollanda, H.B.M., Armstrong, R. 2006. The bimodal rift-related Juscelândia volcanosedimentary sequence in central Brazil: Mesoproterozoic

extension and Neoproterozoic metamorphism. *Journal of South American Earth Sciences*, 20(4):287-301.

Noce, C.M., Machado, N., Teixeira, W. 1998. U-Pb geochronology of gneisses and granitoids in the Quadrilátero Ferrífero (Southern São Francisco Craton): age, constraints for Archean and Paloproterozoic magmatism and metamorphism. Revista Brasileira de Geociências, 28(1):95-102.

Noce, C.M, Teixeira, W., Quémeneur, J.J.G., Martins, V.T.S and Bolzachini, E. 2000. Isotopic signatures of Paleoproterozoic granitoids from the southern São Francisco Craton and implications for the evolution of the Transamazonian Orogeny. Journal of South America Earth Sciences, 13(3):225-239.

Noce, C.M., Pedrosa-Soares, A.C., Silva, L.C., Armstrong, R., Piuzana, D. 2007a. Evolution of polycyclic basement complexes in the Araçuaí Orogen, based on U–Pb SHRIMP data: Implications for Brazil–Africa links in Paleoproterozoic time. *Precambrian Research*, 159(1-2): 60-78.

Noce, C.M., Tassinari, C.C.G., Lobato, L.M.. 2007b. Geochronological framework of the Quadrilátero Ferrífero, with emphasis on the age of gold mineralization hosted in Archean greenstone belts. *Ore Geology Reviews*, 32(3-4):500-510

Nogueira, G.S.M. 1993. Enquadramento litoestratigráfico, sedimentologia e evolução geoquímica do depósito fostático de Lagamar (MG), Formação Vazante. *MSc Thesis*, University of Brasília, 165 p.

Olcott, A.N.; Sessions, A.L.; Corsetti, F.A.; Kaufman, A.J.; Oliveira, T.F. 2005. Biomarker Evidence for Photosynthesis During Neoproterozoic Glaciation. Science, 310 (21): 471-474.

Oliveira, C.G., Pimentel, M.M., Melo, L.V., Fuck, R.A. 2004. The cooper-gold and gold deposits fo the Neoproterozoic Mara Rosa magmatic arc, Central Brazil. Ore Geology Reviews, 25 (3-4):285-299.

Oliveira, E.P., Mello, E.F., McNaughton, N. 2002. Reconnaissance U-Pb geochronology of Precambrian quartizites from the Caldeirão belt and their basement, NE São Francisco Craton, Bahia, Brazil: implication for the early evolution of the Paleoproterozoic Itabuna-Salvador-Curaçá orogen. Journal of South American Earth Sciences, 15(3):349-362.

Oliveira, L.L., Rios, D.C., Burgos, C.M.G. Conceição, H., Macambira, M.J.B., Santos, C.G.P., Scheller, T., 1999. Geochronology of Cansanção Massif by 207Pb/206Pb Evaporation Method – Northeastern of Bahia State – Brazil. *In:* II International Symposium on Granites and Associated Mineralizations, 234-237.

Oliveira, M.A. 1967. Contribuição à geologia da parte sul da Bacia do São Francisco e áreas adjacentes. *Coletâneas de Relatórios de Exploração, 1: 71-105. DEPIN/CENPES/PETROBRAS.*

Parenti Couto, J.G.; Cordani, U.G.; Kawashita, K. Iyer, S.S.; Moraes, N.M.P. 1981. Considerações sobre a idade do Grupo Bambuí com base em análises isotópicas de Sr e Pb. Revista Brasileira de Geociências, 11, 5-16.

Pedrosa-Soares, A.C., Cordani, U.G., Nutman, A. 2000. Constraining the age of the Neoproterozoic Glaciation in Eastern Brazil: First U-Pb (SHRIMP) data of detrital zircons. Revista Brasileira de Geociências, 30: 58-61.

Pereira, L. 1992. Relações Tectono-Estratigráficas entre as Unidades Canastra e Ibiá na Região de Coromandel e Guarda-Mor. MG. Dissertação de Mestrado. IG-UnB, 73p.

Pereira, L.; Dardenne, M.A.; Rosière, C.A.; Pedrosa-Soares, A.C. 1994. Evolução Geológica dos Grupos Canastra e Ibiá na região entre Coromandel e Guarda-Mor, MG. Geonomos, 2(1):22-32.

Pimentel, M.M., Alvarenga, C.J.S., Armstrong, R., Cukrov, N., 2002. Proveniência da Formação Jequitaí. Brasil Central, com base em dados de U–Pb SHRIMP em zircões detríticos. *In:* Congresso Brasileiro de Geologia, 41, João Pessoa. Anais, 503.

Pimentel, M.M., Ferreira Filho, C.F., Armstrong, R.A., 2004. SHRIMP U–Pb and Sm–Nd ages of the Niquelândia layered complex: Meso- (1.25 Ga) and Neoproterozoic (0.79 Ga) extensional events in central Brazil. *Precambrian Research* 132, 133–153.

Pimentel, M.M.; Dardenne, M.A.; Fuck, R.A.; Viana, M.G.; Junges, S.L.; Fischel, D.P.; Seer, H.; Dantas, E.L. 2001. Nd Isotopes and the Provenance of Detrital Sediments of the Neoproterozoic Brasília Belt, Central Brazil. *Jour. South Am. Ear. Sci.*, 14(6):571-585.

Pimentel, M.M., Fuck, R.A., Botelho, N.F. 1999. Granites and the geodynamic history of the Brasília Belt, central Brazil: a review. *Lithos* 46, 463-483.

Pimentel, M.M., Whitehouse, M.J., Viana, M.G., Fuck, R.A., Machado, N., 1997. The Mara Rosa arc in the Tocantins Province: further evidence for Neoproterozoic crustal accretion in Central Brazil. Precambrian Research 81, 299–310.

Pimentel, M.M., Machado, N., Lobato, L.M. 1994. Geocronologia U-Pb de rochas graníticas e gnássicas da região de Lagoa Real, Bahia, e implicações para a idade da mineralização de Urânio. *In:* SBG, Congresso Brasileiro de Geologia, 38, Balneário Camboriú. Anais, 2:389-390.

Pimentel M.M. & Fuck R.A. (1992) Neoproterozoic crustal accretion in Central Brazil. *Geology*, 20:375 – 379.

Pimentel, M.M., Heaman, L., Fuck, R.A., 1991a. U–Pb zircon and sphene geochronology of late Proterozoic volcanic arc rock units from southwestern Goiás, Central Brazil. *Journal of South America Earth Science*, 4: 329–339.

Pimentel, M.M., Heaman, L., Fuck, R.A., Marini, O.J. 1991b. U-Pb zircon geochronology of Precambrian tin-bearing continental-type acid magmatism in central Brazil. Precambrian Research, 52(3-4):321-335.

Pinho, J.M.M. 1990. Evolução Tectônica da Mineralização de zinco de Vazante, MG. *MSc Thesis*, University of Brasília, 115p.

Piuzana, D., Pimentel, M.M., Fuck, R.A., Armstrong, R. 2003a. SHRIMP U–Pb and Sm–Nd data for the Araxá Group and associated magmatic rocks: constraints for the age of sedimentation and geodynamic context of the southern Brasília Belt, central Brazil. *Precambrian Research* 125 (2003) 139–160

Piuzana, D., Pimentel, M.M., Armstrong, R., Fuck, R.A., 2003b. Neoproterozoic granulite facies metamorphism and coeval granitic magmatism in the Brasilia Belt, Central Brazil: regional implications of new SHRIMP U–Pb and Sm–Nd data. *Precambrian Research* 125 (2003) 245–273

Piuzana, D.; Pimentel, M. M. ; Fuck, R. A. ; Armstrong, R. A. 2001. U-Pb SHRIMP and Sm-Nd geochronology of the Silvânia Volcanics and Jurubatuba Granite: juvenile Paleoproterozoic crust in the basement of the Neoproterozoic Brasília Belt, Goiás, central Brazil. *Anais da Academia Brasileira de Ciências*, Rio de Janeiro, v. 73, n. 3, p. 445-460.

Rigobello, A.E., Branquinho, J.A., Dantas, M.G.S., Oliveria, T.F., Neves Filho, W., 1988. Mina de Zinco de Vazante. *In*: Schobbenhaus, C., Coelho, C.E.S. (Coords.), Principais Depósitos Minerais do Brasil. DNPM 3, pp. 101–110.

Rimann, E.T. 1917. A kimberlita no Brasil. *In:* Anais da Escola de Minas, Ouro Preto (15):27-32.

Ring, U.; Kröner, A.; Layer, P.; Buchwaldt, R.; Toulkeredis, T. 1999. Deformed A-type granites in northern Malawi, east-central Africa: pre- or syntectonic. *Journal Geological Society of. London*, 156, 695–714.

Rios, D.C., Conceição, H., Davis, D.W., Plá Cid, J., Rosa, M.L.S., Macambira, M.J.B., Mcreath, I., Marinho, M.M., Davis, W.J., 2007. Paleoproterozoic potassic-ultrapotassic magmatism: Morro do Afonso Syenite Pluton, Bahia, Brazil. *Precambrian Research*, 154(1-2):1-30.

Rodrigues, J.B., Gioia, S.M.L.C., Pimentel, M.M. 1999. Geocronologia e Geoquímica de Ortognaisses da Região de Iporá e Firminópolis: Implicações para Evolução do Arco Magmático de Goiás.. *Revista Brasileira de Geociências*, 29 (2):207-216.

Santos, R.V.; Alvarenga, C.J.S.; Babinski, M.; Ramos, M.L.S.; Cukrov, A.N.; Fonseca, M.A.; Sial, A.N.; Dardenne, M.A.; Noce, C.M. 2004. Carbon isotopes of Mesoproterozoic–Neoproterozoic sequences from Southern Sa˜o Francisco craton and Araçuaı´ Belt, Brazil: Paleographic implications *Journal of South American Earth Sciences* 18 (2004) 27–39

Santos, R.V.; Alvarenga, C.J.S.; Dardenne, M.A.; Sial, A.N.; Ferreira, V.P. 2000. Carbon and oxigen isotope profiles across Meso-Neoproterozoic limestones from central Brazil: Bambuí and Paranoá groups. *Precambrian Research*, 104(2000):107-122.

Schobbenhaus, C., Hoppe, A., Baumann, A., Lork, A. 1994. Idade U-Pb do vulcanismo Rio dos Remédios, Chapada Diamantina, Bahia. *In:* SBG, Congresso Brasileiro de Geologia, 38, Balneário Camboriú. Anais, 2:397-399.

Seer, H.J. 1999. Evolução Tectônica dos Grupos Araxá, Ibiá e Canastra na Sinforma de Araxá, Minas Gerais. *Tese de Doutorado*. Igc-USP, 149p.

Seer H.J., Brod J.A., Valeriano C.M., Fuck R.A. (2005) – Leucogranitos intrusivos no Grupo Araxá: Registro de um evento magmático durante colisão neoproterozóica na porção meridional da Faixa Brasília. *Revista Brasileira de Geociências*, 35(1):33-42.

Silva, C.H. 2003. Evolução geológica da Faixa Brasília na região de Tapira, sudoeste de Minas Gerais. *Tese de Doutoramento*, IGCE-UNESP, 102p

Silva, C.H.; Simões, L.A.; Krymsky, R.; Macambira, M. 2006. Proveniência e idade do metamorfismo das rochas da Faixa Brasília na região de Tapira (Sudoeste de Minas Gerais). *In:* Anais do XLIII Congresso Brasileiro de Geologia, ST08-AO485, Maceió.

Silva, L.C.; Pedrosa-Soars, A.C.; Teixeira, L.R.; Armstrong, R. 2008. Tonian rift-related, A-type continental plutonism in the Araçuaí Orogen, eastern Brazil: New evidence for the breakup stage of the São Francisco–Congo Paleocontinent. *Gondwana Research*, 13 (2008) 527–537.

Silva, L.C.; Armstrong, R., Delgado, I.M., Pimentel, M.M., Arcanjo, J.B.A.; Melo, R.C., Teixeira, L., Jost, H., Cardoso Filho, J.M., Pereira, J.H.M., 2002a. Reavaliação da Evolução Geológica em Terrenos Pré-cambrianos com base em novos dados U-Pb SHRIMP. Parte I: Limite centro-oriental do Cráton São Francisco. *Revista Brasileira de Geociências*, 32(4):501-512.

Silva, L.C.; Armstrong, R., Noce, C.M., Carneiro, M.A., Pimentel, Pedrosa-Soares, A.C., Leite, C.A, Vieira, V.S. Silva, M.A., Paes, V.J.C., Cardoso Filho, J.M., Pereira, J.H.M., 2002b. Reavaliação da Evolução Geológica em Terrenos Pré-cambrianos com base em novos dados U-Pb SHRIMP. Parte II: Orógeno Araçuaí, Cinturão Mineiro e Cráton São Francisco Meridional. Revista Brasileira de Geociências, 32(4):513-528.

Souza, J.C.F. 1997. Litoestratigrafia e sedimentologia da Formação Vazante na região de Coromandel (MG). *MSc Thesis*, University of Brasília, 75p.

Stacey, J.S.& Kramers, J.D. 1975. Approximation of terrestrial lead isotope evolution by a two-stage model. *Earth and Planetary Science Letters, 26:207-221.*

Stern, R.J., Abigad, D., Miller, N.R., Beyth, M., 2006. Evidence for the Snowball Earth hypothesis in the Arabian–Nubian Shield and the East African Orogen. Journal of African Earth Sciences 44, 1–20.

Tack, L, Wingate, M.T.D., Liégeos, J.P., Fernandes Alonso, M., Deblond, A., 2001. Early Neoproterozoic magmatism (100–900 Ma) of the Zadinian and Mayumbian goups (Bas Congo): onset of the Rodinia rifting at the west edge of Congo Craton. *Precambrian Research* 110, 277–306.

Tack, L.; Liégeois, J.P.; Deblond, A.; Duchesne, J.C. 1994. Kibaran A-type granitoids and mafic rocks generated by two mantle sources in a late orogenic setting (Burundi). *Precambrian Research*, 68 (3/4), 323–356.

Teixeira, W., Carneiro, M.A., Noce, C.M., Machado, N., Sato, K., Taylor, P.T. 1996. Pb, Sr and Nd isotope constraints on the Archaean evolution of gneissic-granitoid complexes in the southern São Francisco Craton, Brazil. *Precambrian Research* 78 (1996) 151-164

Thomas Filho, A. , Kawashita, K., Cordani, U.G., 1998. A Origem do Grupo Bambuí no Contexto da Evolução Geotectônica e de Idades Radiométricas. *Anais Academia Brasileira Ciências*, 70(3):527-548.

Uhlein, A., Trompette, R., Egydio-Silva, M. 1998. Proterozoic rifting and closure SE, border São Francisco Craton, Brazil. *Journal of South American Earth Sciences*, 11(2):191-203.

Uhlein, A., Trompette, R, Alvarenga, C.J. 1994. Late Proterozoic gravitational sedimentation on a continental margin under glacial influence: The Jequitaí-Macaúbas sequence (Minas Gerais, Brazil). *In:* 14th International Sedimentalogy Congress. Abstract. G85-86. Recife, Brazil.

Uhlein, A. 1991. Transição Cráton-Faixa dobrada: exemplo do Cráton do São Francisco e da Faixa Araçuaí (Ciclo Brasiliano) no Estado de Minas Gerais. Aspectos estratigráficos e estruturais. *Ph. D. Thesis*,Universidade de São Paulo, 295 (unpublished).

Valeriano, C.M.; Machado, N.; Simonetti, A.; Valladares, C.S.; Seer, H.J.; Simões, L.S.A. 2004a. U-Pb Geochronology of the Southern Brasília Belt (SE-BRAZIL): Sedimentary Provenance, Neoproterozoic Orogeny and Assemblegy of West Gondwana. *Precambrian Research.*, 130(2004):27-55.

Valeriano, C.M., Dardenne, M.A.; Fonseca, M.A.; Simões, L.S.A.; Seer, H.J. 2004b. A evolução tectônica da Faixa Brasília. *In:* MANTESSO-NETO, V. (org.) 2004. Geologia do continente sul-americano: Evolução da obra de Fernando Flávio Marques de Almeida. São Paulo. 647p.

Vieira, L.C., Trindade, R.I.F., Nogueira, A.C.R., Ader, M. 2007a – Identification of a Sturtian cap carbonate in the Neoproterozoic Sete Lagoas carbonate platform, Bambuí Group, Brazil. *Comptes Rendus- Geoscience*, 339(3-4):240-258.

Williams, I.S. 1998. U-Th-Pb Geochronology by Ion Microprobe, pp. 1-46. *In:* Applications of Microanalytical Techniques to Understanding Mineralizing Processes. Eds. McKibben, M.A. & Shanks III, W.C. Reviews in Economic Geology, Society of Economic Geologists, 7.

Williams, I.S., Meyer, C., 1998. U–Pb geochronology of zircons from lunar breccia 73217 using a sensitive high mass-resolution ion microprobe. *Journal Geophysical Research*, 89, B525–B534.

Zalán, P. V. & Romeiro-Silva, P.C. 2007. Proposta de mudança significativa na coluna estratigráfica da Bacia do São Francisco. In: 14º. Simpósio de Geologia de Minas Gerais e 10º Simpósio de Geologia do Sudeste, pp. 79.